frontiers | Research Topics

The endocrine role of the musculoskeletal system

Edited by
Giuseppina Storlino and Sandeep Kumar

Coordinated by
Siyi Zhu

Published in
Frontiers in Endocrinology

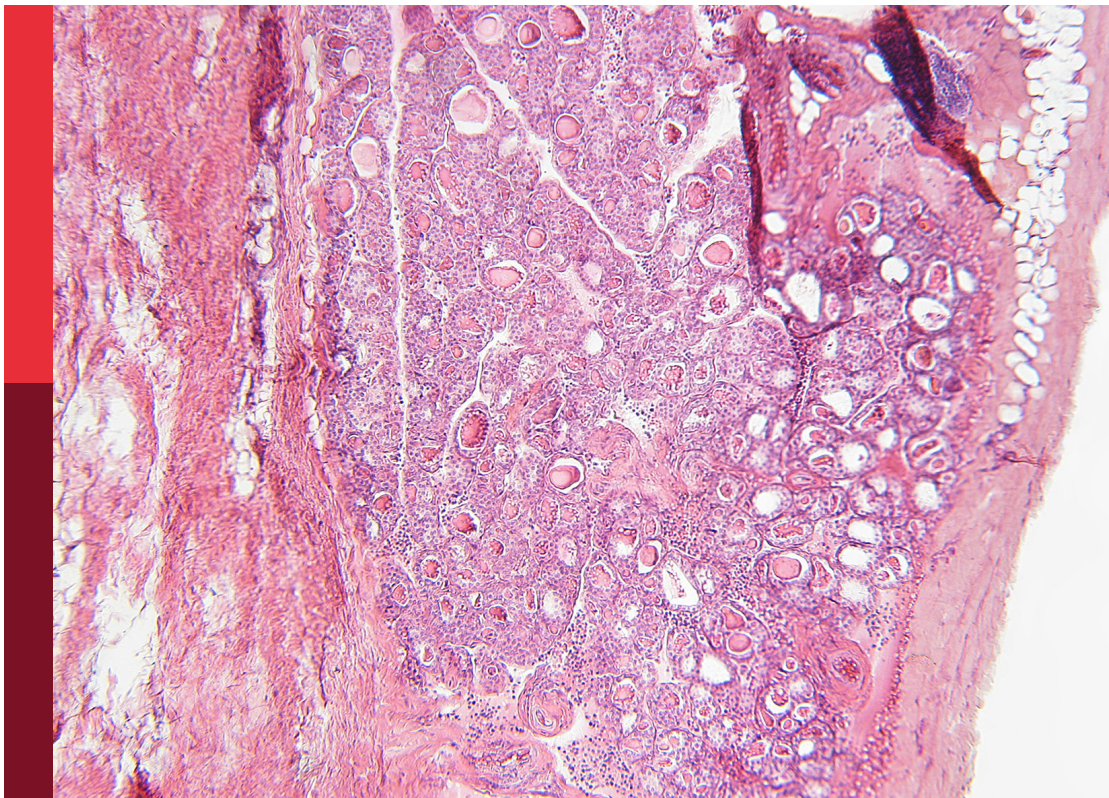

ISSN 1664-8714
ISBN 978-2-8325-5970-3
DOI 10.3389/978-2-8325-5970-3

About Frontiers

Frontiers is more than just an open access publisher of scholarly articles: it is a pioneering approach to the world of academia, radically improving the way scholarly research is managed. The grand vision of Frontiers is a world where all people have an equal opportunity to seek, share and generate knowledge. Frontiers provides immediate and permanent online open access to all its publications, but this alone is not enough to realize our grand goals.

Frontiers journal series

The Frontiers journal series is a multi-tier and interdisciplinary set of open-access, online journals, promising a paradigm shift from the current review, selection and dissemination processes in academic publishing. All Frontiers journals are driven by researchers for researchers; therefore, they constitute a service to the scholarly community. At the same time, the *Frontiers journal series* operates on a revolutionary invention, the tiered publishing system, initially addressing specific communities of scholars, and gradually climbing up to broader public understanding, thus serving the interests of the lay society, too.

Dedication to quality

Each Frontiers article is a landmark of the highest quality, thanks to genuinely collaborative interactions between authors and review editors, who include some of the world's best academicians. Research must be certified by peers before entering a stream of knowledge that may eventually reach the public - and shape society; therefore, Frontiers only applies the most rigorous and unbiased reviews. Frontiers revolutionizes research publishing by freely delivering the most outstanding research, evaluated with no bias from both the academic and social point of view. By applying the most advanced information technologies, Frontiers is catapulting scholarly publishing into a new generation.

What are Frontiers Research Topics?

Frontiers Research Topics are very popular trademarks of the *Frontiers journals series*: they are collections of at least ten articles, all centered on a particular subject. With their unique mix of varied contributions from Original Research to Review Articles, Frontiers Research Topics unify the most influential researchers, the latest key findings and historical advances in a hot research area.

Find out more on how to host your own Frontiers Research Topic or contribute to one as an author by contacting the Frontiers editorial office: frontiersin.org/about/contact

The endocrine role of the musculoskeletal system

Topic editors
Giuseppina Storlino — University of Foggia, Italy
Sandeep Kumar — University of Alabama at Birmingham, United States

Topic coordinator
Siyi Zhu — Sichuan University, China

Citation
Storlino, G., Kumar, S., Zhu, S., eds. (2025). *The endocrine role of the musculoskeletal system*. Lausanne: Frontiers Media SA.
doi: 10.3389/978-2-8325-5970-3

Table of contents

frontiers | Frontiers in Endocrinology

TYPE Editorial
PUBLISHED 23 January 2025
DOI 10.3389/fendo.2025.1552950

OPEN ACCESS

EDITED AND REVIEWED BY
Jonathan H Tobias,
University of Bristol, United Kingdom

*CORRESPONDENCE
Sandeep Kumar
sschaudhary55@gmail.com
Siyi Zhu
hxkfzsy@scu.edu.cn

RECEIVED 29 December 2024
ACCEPTED 09 January 2025
PUBLISHED 23 January 2025

CITATION
Zhu S, Storlino G and Kumar S (2025) Editorial: The endocrine role of the musculoskeletal system. *Front. Endocrinol.* 16:1552950. doi: 10.3389/fendo.2025.1552950

Editorial: The endocrine role of the musculoskeletal system

Siyi Zhu[1,2]*, Giuseppina Storlino[3] and Sandeep Kumar[4]*

[1]Rehabilitation Medicine Center and Institute of Rehabilitation Medicine, West China Hospital, Sichuan University, Chengdu, China, [2]Key Laboratory of Rehabilitation Medicine in Sichuan Province, West China Hospital, Sichuan University, Chengdu, China, [3]Department of Clinical and Experimental Medicine, University of Foggia, Foggia, Italy, [4]Department of Genetics, University of Alabama at Birmingham, Birmingham, AL, United States

KEYWORDS

musculoskeletal endocrinology, bone-muscle crosstalk, myokines and osteokines, systemic homeostasis, metabolic bone diseases

Editorial on the Research Topic
The endocrine role of the musculoskeletal system

The musculoskeletal system's dual role as a structural framework and an endocrine organ has unveiled a new frontier in understanding its systemic influence (1–3). This Research Topic focuses on the endocrine crosstalk between bone and muscle, emphasizing the production and regulation of myokines and osteokines, and their roles in maintaining systemic homeostasis (2–5). The collected studies explore how the musculoskeletal system contributes to both physiological and pathological conditions, enriching the field of endocrinology with innovative insights.

MicroRNAs in bone loss and diabetes

Daamouch et al. examine the role of microRNAs in Type 1 diabetes-induced bone loss, identifying key dysregulated miRNAs in serum and bone tissues. This study highlights miR-136-3p and miR-206-3p as pivotal biomarkers and their links to pathways like TGF-beta and osteoclast differentiation, advancing potential diagnostics for bone fragility.

Vitamin B12's role in musculoskeletal health

Zhao et al. investigate the impact of Vitamin B12 and its biomarkers on musculoskeletal health, revealing significant associations with bone mineral density (BMD) and muscle strength in older adults. These findings underscore the potential of Vitamin B12 as a critical determinant of aging-related musculoskeletal integrity.

Sclerostin levels and metabolic disorders

Alramah et al. analyze sclerostin levels in a multiethnic population with obesity and Type 2 diabetes, uncovering significant gender and ethnic differences. Elevated sclerostin correlated with metabolic markers and bone health, emphasizing its role as a potential biomarker for metabolic bone diseases.

Glucocorticoid receptor in bone marrow adipocytes

Schill et al. investigate the effects of glucocorticoid receptor deficiency in bone marrow adipocytes, revealing mild impacts on bone and hematopoiesis but no influence on marrow adiposity expansion under caloric restriction. This study adds nuance to our understanding of marrow adipose tissue's endocrine function.

Fatty acids and adolescent bone health

Wang et al. link dietary fatty acids to bone mineral density in adolescents, finding that saturated fatty acids enhance BMD while polyunsaturated fats have a negative effect. This study highlights the importance of dietary balance in adolescent skeletal development.

Lead exposure and bone density

Wang et al. reveal a significant negative correlation between urinary lead levels and BMD, emphasizing the toxicological impact of environmental lead on bone health. This study calls for heightened public health initiatives targeting heavy metal exposure.

Sarcopenia and rotator cuff tears

Yang et al. establish a genetic link between sarcopenia-related traits and rotator cuff tears using Mendelian randomization, providing evidence-based insights for optimizing clinical management of these conditions.

FGF21 and osteoporosis

Liu et al. explore the causal effects of FGF21 overexpression on bone health, demonstrating its role in reducing BMD and increasing osteoporosis risk. This study identifies FGF21 as a potential therapeutic target for bone-related metabolic disorders.

Vascular and lymphatic networks in bone health

Huang et al. review the interplay between vascular and lymphatic systems in bone and joint homeostasis, highlighting their co-regulatory roles and potential therapeutic implications for inflammatory joint diseases.

Acupuncture and lumbar disc herniation

Yan et al. compare acupuncture to traditional rehabilitation in lumbar disc herniation, finding superior long-term benefits in muscle restoration and pain relief. This research underscores acupuncture's potential as an integrative therapy.

Conclusion

Collectively, these studies enhance our understanding of the musculoskeletal system's endocrine roles and its systemic interactions. We thank the authors for their valuable contributions, advancing both fundamental and clinical endocrinology. Their work lays a robust foundation for future interdisciplinary research.

Author contributions

SZ: Funding acquisition, Writing – original draft, Writing – review & editing. GS: Writing – original draft, Writing – review & editing. SK: Validation, Writing – original draft, Writing – review & editing.

Funding

The author(s) declare financial support was received for the research, authorship, and/or publication of this article. This study was supported by the National Natural Science Foundation of China (82272599), Natural Science Foundation of Sichuan Province (2024NSFSC0533), Sichuan University "Research Special Project on the Comprehensive Reform of Innovative Educational Practices Enabled by Artificial Intelligence" (2024-44), 1.3.5 project for disciplines of excellence, West China Hospital, Sichuan University (ZYGD23014), Sichuan University West China School of Medicine Graduate Education Reform Project (HXYJS202415) and Science and Technology Bureau of Deyang City (Deyang Clinical Research Center for Rehabilitation Medicine, Mianzhu People's Hospital, 2023-64). The funders played no role in the design, conduct, or reporting of this study.

Acknowledgments

We appreciate all authors, reviewers, and journal editors who have contributed to this Research Topic.

Conflict of interest

The authors declare that the research was conducted in the absence of any commercial or financial relationships that could be construed as a potential conflict of interest.

The author declared that they were an editorial board member of Frontiers, at the time of submission. This had no impact on the peer review process and the final decision.

Publisher's note

References

1. DiGirolamo DJ, Clemens TL, Kousteni S. The skeleton as an endocrine organ. *Nat Rev Rheumatol.* (2012) 8:674–83. doi: 10.1038/nrrheum.2012.157

2. Van Gastel N, Carmeliet G. Metabolic regulation of skeletal cell fate and function in physiology and disease. *Nat Metab.* (2021) 3:11–20. doi: 10.1038/s42255-020-00321-3

3. Zhou R, Guo Q, Xiao Y, Guo Q, Huang Y, Li C, et al. Endocrine role of bone in the regulation of energy metabolism. *Bone Res.* (2021) 9:25. doi: 10.1038/s41413-021-00142-4

4. Gomarasca M, Banfi G, Lombardi G. Myokines: The endocrine coupling of skeletal muscle and bone. *Adv Clin Chem.* (2020) 94:155–218. doi: 10.1016/bs.acc.2019.07.010

5. Wan M, Gray-Gaillard EF, Elisseeff JH. Cellular senescence in musculoskeletal homeostasis, diseases, and regeneration. *Bone Res.* (2021) 9:41. doi: 10.1038/s41413-021-00164-y

frontiers | Frontiers in Endocrinology

TYPE Original Research
PUBLISHED 22 April 2024
DOI 10.3389/fendo.2024.1392675

OPEN ACCESS

EDITED BY
Sandeep Kumar,
Oklahoma University Health Science Center, United States

REVIEWED BY
Surbhi Gahlot,
University of Texas Southwestern Medical Center, United States
Priyanka Sharma,
Rutgers, The State University of New Jersey, United States

*CORRESPONDENCE
Jehad Abubaker
jehad.abubakr@dasmaninstitute.org
Fahd Al-Mulla
fahd.almulla@dasmaninstitute.org

†These authors have contributed equally to this work

RECEIVED 27 February 2024
ACCEPTED 09 April 2024
PUBLISHED 22 April 2024

CITATION
Alramah T, Cherian P, Al-Khairi I, Abu-Farha M, Thanaraj TA, Albatineh AN, Safadi F, Ali H, Abdul-Ghani M, Tuomilehto J, Koistinen HA, Al-Mulla F and Abubaker J (2024) Evaluating the correlation of sclerostin levels with obesity and type 2 diabetes in a multiethnic population living in Kuwait. *Front. Endocrinol.* 15:1392675. doi: 10.3389/fendo.2024.1392675

Evaluating the correlation of sclerostin levels with obesity and type 2 diabetes in a multiethnic population living in Kuwait

Tahani Alramah[1†], Preethi Cherian[1†], Irina Al-Khairi[1†], Mohamed Abu-Farha[1,2†], Thangavel Alphonse Thanaraj[3], Ahmed N. Albatineh[4], Fayez Safadi[5,6], Hamad Ali[7], Muhammad Abdul-Ghani[2,8], Jaakko Tuomilehto[9,10,11], Heikki A. Koistinen[9,12,13], Fahd Al-Mulla[2,3*] and Jehad Abubaker[1*]

[1]Department of Biochemistry and Molecular Biology, Dasman Diabetes Institute, Dasman, Kuwait, [2]Department of Translational Research, Dasman Diabetes Institute, Dasman, Kuwait, [3]Genetics and Bioinformatics Department, Dasman Diabetes Institute, Dasman, Kuwait, [4]Faculty of Medicine, Kuwait University, Kuwait City, Kuwait, [5]Department of Anatomy and Neurobiology, Northeast Ohio Medical University, Rootstown, OH, United States, [6]Rebecca D. Considine Research Institute, Akron Children Hospital, Akron, OH, United States, [7]Department of Medical Laboratory Sciences, Faculty of Allied Health Sciences, Health Sciences Center, Kuwait University, Jabriya, Kuwait, [8]Division of Diabetes, University of Texas Health Science Center, San Antonio, TX, United States, [9]Department of Public Health and Welfare, Finnish Institute for Health and Welfare, Helsinki, Finland, [10]Department of Public Health, University of Helsinki, Helsinki, Finland, [11]Saudi Diabetes Research Group, King Abdulaziz University, Jeddah, Saudi Arabia, [12]Internal Medicine and Endocrinology, Minerva Foundation Institute for Medical Research, Helsinki, Finland, [13]Department of Medicine, University of Helsinki and Helsinki University Hospital, Helsinki, Finland

Obesity and Type 2 Diabetes Mellitus (T2DM) are intricate metabolic disorders with a multifactorial etiology, often leading to a spectrum of complications. Recent research has highlighted the impact of these conditions on bone health, with a particular focus on the role of sclerostin (SOST), a protein molecule integral to bone metabolism. Elevated circulating levels of SOST have been observed in patients with T2DM compared to healthy individuals. This study aims to examine the circulating levels of SOST in a multiethnic population living in Kuwait and to elucidate the relationship between SOST levels, obesity, T2DM, and ethnic background. The study is a cross-sectional analysis of a large cohort of 2083 individuals living in Kuwait. The plasma level of SOST was measured using a bone panel multiplex assay. The study found a significant increase in SOST levels in individuals with T2DM (1008.3 pg/mL, IQR-648) compared to non-diabetic individuals (710.6 pg/mL, IQR-479). There was a significant gender difference in median SOST levels, with males exhibiting higher levels than females across various covariates (diabetes, IR, age, weight, and ethnicity). Notably, SOST levels varied significantly with ethnicity: Arabs (677.4 pg/mL, IQR-481.7), South Asians (914.6 pg/mL, IQR-515), and Southeast Asians (695.2 pg/mL, IQR-436.8). Furthermore, SOST levels showed a significant positive correlation with gender, age, waist circumference, systolic and diastolic blood pressure, fasting blood glucose, HbA1c, insulin, total cholesterol, triglycerides, HDL, LDL, ALT, and AST (p-Value $\geq$0.05). South Asian participants, who exhibited the highest SOST levels, demonstrated the most pronounced associations, even after adjusting for

age, gender, BMI, and diabetes status (p-Value ≥0.05). The observed correlations of SOST with various clinical parameters suggest its significant role in the diabetic milieu, particularly pronounced in the South Asian population compared to other ethnic groups.

KEYWORDS

SOST, gender, T2DM, obesity, ethnicity, bone metabolism

1 Introduction

Obesity and diabetes are known metabolic diseases that result due to disturbance in the lipid and glucose metabolism leading to imbalance in energy homeostasis (1, 2). The prevalence of obesity has been continuously increasing in most countries since 1980, as per the report by the Global Burden of Disease Group in 2017 (3). Obesity is defined by a body mass index (BMI) of more than or equal to 30 kg/m2, which occurs due to the imbalance between energy intake and expenditure, resulting in excess accumulation of body fat (WHO and CDC). Another metabolic disease characterized by hyperglycemia and is increasing in prevalence is diabetes mellitus (DM), particularly T2DM, which accounts for 90–95% of all patients with diabetes and is expected to increase to 439 million by 2030 (4, 5). Both obesity and T2DM are complex metabolic disorders of multifaceted etiology accompanied by a series of complications, including macrovascular diseases (hypertension, hyperlipidemia, heart attacks, coronary artery disease, strokes, cerebral vascular disease, and peripheral vascular disease), microvascular diseases (retinopathy, nephropathy, and neuropathy), and cancers (6). Recently, studies have shown that bone health is also compromised in people with obesity and T2DM (7).

The skeletal system is highly dynamic and constantly undergoes repair and remodeling (8). Normal bone remodeling is necessary for fracture healing and skeleton adaptation to mechanical use. A disruption in the equilibrium between bone formation and resorption processes can result in bone-related diseases such as osteoporosis (9). Recently, bone has been recognized as an endocrine organ capable of synthesizing and secreting a variety of bioactive compounds that regulate bone remodeling and affect the metabolic processes throughout the body (9, 10). The endocrine function of bone is mediated through the secretion of several hormones, such as osteocalcin (OC), fibroblast growth factor 23 (FGF23), lipocalin 2 (Lcn2), and sclerostin (SOST) (11, 12).

SOST is a glycoprotein with a molecular weight of27 kDa, which is crucial in regulating bone metabolism (13). Encoded by the SOST gene, it is predominantly synthesized by osteocytes and is vital in maintaining bone homeostasis (14). SOST influences both bone formation and remodeling processes by acting as an inhibitory agent in the Wnt/β-catenin signaling pathway via binding to LDL receptor-related proteins 5/6 (LRP5/6) thereby negatively regulating bone formation (15, 16). Mutations in the SOST gene, leading to a deficiency of SOST, can give rise to two uncommon autosomal recessive bone-hardening conditions: Sclerosteosis and van Buchem disease (17).

Circulating SOST levels have been found to be altered in individuals with T2DM (18, 19). Patients with T2DM show higher circulating levels of SOST compared with healthy individuals. Since SOST is mainly produced by osteocytes this indicates that fluctuations in glucose levels could significantly impact the primary cells responsible for bone health. Specifically, when blood glucose levels vary considerably from the standard 80–140 mg/dL range it may negatively affect osteocytes (20). This is inferred from the observation that T2DM patients often display disrupted bone metabolism, making them more susceptible to fractures and other bone-related issues (12, 21). Notably, the risk of fractures in T2DM patients is nearly double that of healthy individuals, even if their bone mineral density (BMD) is normal or elevated (11). This points to potential issues with bone quality, possibly affecting its strength or micro-architecture. Moreover, Daniele et al. reported an increase in blood SOST levels, which was significantly associated with insulin resistance in skeletal muscle, liver, and adipose tissue in patients with diabetes (22). Additionally, in a study done on Indian male individuals who have been diagnosed with T2DM, the authors observed a notable increase in the levels of circulating SOST when compared to the healthy male control group (23). This finding was consistent with the expression levels of SOST mRNA. Furthermore, in a study done on SOST knockout mice the author showed that these mice exhibit increased bone mass, decreased fat mass, and increased insulin sensitivity (24). The authors also demonstrated that treatment with anti-SOST antibodies decreased fat mass in wild-type mice and enhanced differentiation of adipocytes.

Abbreviations: ALT, Alanine Aminotransferase; AST, Aspartate Aminotransferase; BMD, Bone Mineral Density; BMI, Body Mass Index; CDC, Centers for Disease Control and Prevention; DM, Diabetes Mellitus; FBG, Fasting Blood Glucose; FPG, Fasting Plasma Glucose; HDL, High-Density Lipoprotein; HOMA-IR, Homeostatic Model Assessment for Insulin Resistance; HbA1c, Hemoglobin A1c; IQR, Interquartile Range; KDEP, Kuwait Diabetes Epidemiological Program; LDL, Low-Density Lipoprotein; SOST, Sclerostin; T2DM, Type 2 Diabetes Mellitus; TC, Total Cholesterol; TG, Triglycerides; WC, Waist Circumference; WHO, World Health Organization.

The role of SOST in obesity and diabetes is well documented. We hypothesize that Individuals with obesity and T2DM will have higher circulating levels of SOST compared to healthy individuals. Additionally, we predict that ethnic variations within the population residing in Kuwait may influence SOST plasma levels due to the high prevalence of obesity and T2DM. This study aims to investigate the circulating level of SOST in the population living in Kuwait. Also, since the Kuwaiti population is comprised of people from different ethnic backgrounds, the impact of ethnic variation in relationships between SOST and obesity/diabetes was explored. Furthermore, the objective of this study is to identify the factors that may be associated with SOST levels and their possible health implications.

2 Materials and methods

2.1 Participants and the study design

Kuwait Diabetes Epidemiological Program (KDEP) was a cross-sectional, population-based study conducted between 2011 and 2014 at the Dasman Diabetes Institute (DDI). The study protocol was approved by the Ethics Review Committee at DDI under the reference RA2011-003, and done in accordance with the principles of the Declaration of Helsinki and good clinical practice guidelines. Participants were recruited using a stratified random sampling method designed to ensure a balanced representation across all seven governorates of Kuwait. The primary criteria for exclusion from the study were refusal to sign the consent form, being younger than 21, or suffering from an ongoing infection. This method of participant selection aimed to ensure a diverse and representative sample of the adult population as previously described (25–27).

2.2 Anthropometric and vital signs measurements

Anthropometric measurements were recorded, including body weight, height, and waist circumference (WC). Height and weight measurements were conducted using calibrated scales and fixed height bars while participants wore light clothing and were barefoot. The waist circumference was measured using a tension tape at the iliac crest and mid-axillary line after a normal exhalation with relaxed arms. BMI was calculated using the standard formula: weight in kilograms divided by height in meters squared. Blood pressure was measured with an Omron HEM-907XL Digital sphygmomanometer, taking three separate readings with 5–10 minute rests between them and the final values were averaged from these readings.

2.3 Laboratory measurements

Blood samples were collected from each participant after an overnight fasting. The samples were used to measure fasting plasma glucose (FPG), hemoglobin A1c (HbA1c), fasting insulin, triglycerides (TG), total cholesterol (TC), low-density lipoprotein (LDL), and high-density lipoprotein (HDL). The Siemens Dimension RXL chemistry analyzer (Diamond Diagnostics, Holliston, MA) was used for all measurements except for HbA1c, which was measured using the VariantTM device (BioRad, Hercules, CA).

The insulin levels were quantified using the Access Insulin Assay (Beckman Coulter, Brea, CA). The Homeostatic Model Assessment for Insulin Resistance (HOMA-IR) was used to calculate insulin resistance using the following formula: (FBG in mmol/L) × (fasting insulin in mU/L)/22.5.

SOST plasma levels were measured using an R&D custom multiplexing assay following the kit instructions for the Luminex custom-made panel (cat #LXSAHM, R&D, CA, USA). Plasma levels of inflammatory markers were assessed with the multiplexing immunobead array using the Data analyzed with Bio-Plex manager software version 6 (Bio-Rad, Hercules, CA), and the results were calculated using a 5-PL nonlinear standard curve setting in the Bio-Plex manager software version 6.0. Intra-assay coefficients of variation ranged from 1.2% to 3.8%, whereas inter-assay coefficients ranged from 6.8% to 10.2%. The sensitivity of the Luminex assay for SOST is 7.0 pg.ml as per R&D technical specifications, while SOST antibody used for these assays show< 0.5% cross-reactivity with available related molecules and < 50% cross-species reactivity observed with tested species.

2.4 Statistical analysis

The analysis was performed on data from a total of 2,083 subjects. Descriptive statistics on population characteristics were carried out and presented as medians (interquartile ranges: IQR). A Pearson chi-squared test, a Fisher's exact test, and a Wilcoxon rank sum test were used to determine whether there were significant differences between groups. The association between various clinical parameters and SOST was assessed using Spearman's correlation. Furthermore, subjects were grouped according to the tertiles (two points that divide an ordered distribution into three parts) of markers of interest. Statistical significance was determined by a p-value of 0.05. All statistical analyses were performed using R statistical software (R Core Team, 2020).

3 Results

3.1 Descriptive analysis of the population

Descriptive statistics revealed that the majority of the cohort were male (54.7% Table 1), non-Kuwaiti (70.2%), with a median age of 45 years (Interquartile Range, IQR=16), and 36% of the participants were under the age of 40. In terms of ethnicity, 46.6% of the participants were of Arab descent. With respect to the health status, 30.8% of the sample were diagnosed with diabetes, 40.2% were classified as overweight, and 38.7% fell into the obese

10.3389/fendo.2024.1392675

TABLE 1 Demographic characteristics of 2,083 participants.

Characteristics	(%) or median (IQR)
Gender, n (%)	
Male	1161 (55.7%)
Female	922 (44.3%)
Age, n(%)	
< 40	750 (36.0%)
40-50	680 (32.7%)
> 50	653 (31.3%)
Ethnicity, n(%)	
Arab	899 (46.6%)
South Asian	666 (34.5%)
Southeast Asian	364 (18.9%)
Diabetes status, n (%)	
Non-Diabetic	1425 (69.2%)
Diabetic	633 (30.8%)
BMI, n (%)	
Normal BMI	441 (21.2%)
Overweight	837 (40.2%)
Obese	805 (38.6)%
HOMA-IR, n (%)	
HOMA-IR ≤ 2	969 (50.3%)
HOMA-IR > 2	958 (49.7%)
Hip Circumference, median (IQR)	102.3 (13)
Waist Circumference, median (IQR)	95 (15)
SBP, median (IQR)	131 (26)
DBP, median (IQR)	80 (16)
FBG, median (IQR)	5.3 (1.7)
Insulin, median (IQR)	7.9 (6.7)
TSH, median (IQR)	1.53 (1.14)
FT4, median (IQR)	11.78 (3.43)
FT3, median (IQR)	4.76 (0.78)
HbA1c, median (IQR)	5.8 (1.2)
TC, median IQR)	5.1 (1.33)
AST, median (IQR)	21 (8)
CRP, median (IQR)	3 (2)

IQR, interquartile range; n, number; BMI, body mass index; HOMA-IR, Homeostatic Model Assessment for Insulin Resistance; SBP, systolic blood pressure; DBP, diastolic blood pressure; FBG, fasting blood Glucose; TSH, thyroid stimulating hormone; FT4, free Thyroxine; FT3, free triiodothyronine; HbA1c, glycated haemoglobin; TC, total cholesterol; AST, aspartate aminotransferase; CRP, c-reactive protein.

category. The distributions of the main outcome SOST across several covariates are presented in (Figures 1, 2). Results indicated that males have significantly higher median SOST compared to females (889.3 (554.6), and 634.8 (418.4), pg/ml (IQR) respectively) (Figure 1A). There was a significant difference in median SOST across age groups with a dose-response relationship [age: >40 = 655.0 (438.8), 40-50 = 765.5 (464.5), and > 50 = 959.9 (669.1), pg/ml (IQR)] (Figure 1B). There were significant differences in median SOST across ethnicity with the South Asians having the highest median SOST [Ethnicity: Arab = 677.4 (481.7), South Asian = 914.6 (515.0), and South East Asian = 695.2 (436.8) pg/ml (IQR)] (Figure 1C).

T2DM patients have significantly higher median SOST [1008.3 (648), pg/ml (IQR)) compared to non-diabetic (710.6 (479) pg/ml (IQR)] with $p < 0.001$ (Figure 2A). Similarly, a significant difference was observed with increased insulin resistance [HOMA-IR score: Normal ≤ 2 = 714.7 (478), and IR > 2 = 825.0 (585) pg/ml (IQR)] (Figure 2B). Finally, no significant difference was observed in median level of SOST across the different BMI categories [BMI: > 24.99 (Normal) = 710.1 (495.0), 25-29.9 (Overweight) = 786.5 (484), ≥ 30 (Obese) = 752.3 (563.0), pg/ml (IQR)].

3.2 Gender based analysis of the level of SOST

To understand the impact of gender on the circulating level of SOST various parameters were examined stratifying them into male and female categories.

The distributions of the main outcome SOST across several covariates are presented in Figures 3, 4. Results indicated that Males have significantly higher median SOST compared to females in both non-diabetic and T2D groups (non-diabetic: Male 833.5 (503.9), and Female 616.4 (390), pg/ml (IQR), in T2D: Male 1168.4 (636.1) and Female 805.8 (487.3), pg/ml) (Figure 3A). There was a significant difference in median SOST in both the normal and IR groups (Normal: Male 853.4 (527.4), and Female 622.4 (413.4), pg/ml (IQR), in IR: Male 953.4 (578.4) and Female 656.2 (458), pg/ml) (Figure 3B). There were significant differences in median SOST across ethnicity with the South Asians having the highest median SOST [Arab: Male 817.2 (607.2), and Female 591.3 (385), pg/ml (IQR) South Asian: Male 953.4 (519.6), and Female 765.9 (486.4), pg/ml (IQR) and South East Asian: Male 881.9 (469.8), and Female 635.2 (373.4), pg/ml (IQR)] (Figure 4A). When the data was categorized on the basis of BMI significant difference was observed in median level of SOST between male and female [Normal: Male 874.5 (598.0), and Female 578.1 (386), pg/ml (IQR). Overweight: Male 868.5 (510), and Female 651.4 (424.9), pg/ml (IQR). Obese: Male 925.2 (608.7), and Female 648.1 (442.8), pg/ml (IQR)] (Figure 4B). Finally, when the male and female were further categorized by age the results again showed significant difference among male when compared to female (Age < 40: Male 792.3 (434.8), and Female 532.1 (321.1), pg/ml (IQR). Age 40-50: Male 883.6 (526.7), and Female 666.3 (398.7), pg/ml (IQR). Age 50 <: Male 1093.5 (683.9), and Female 828.8 (518.3), pg/ml (IQR) (Figure 4C).

3.3 Correlation of SOST level with various clinical parameters

The correlation analysis was performed on all population as presented in Table 2. The results show significant positive correlation between SOST level and gender (Male), age, waist circumference, SBP, DBP, insulin, TG, TC, LDL, ALT, AST, FBG, HbA1c,. A significant negative correlation was observed with HDL.

To better understand the correlation between SOST and the other clinical covariates the data was stratified based on diabetes

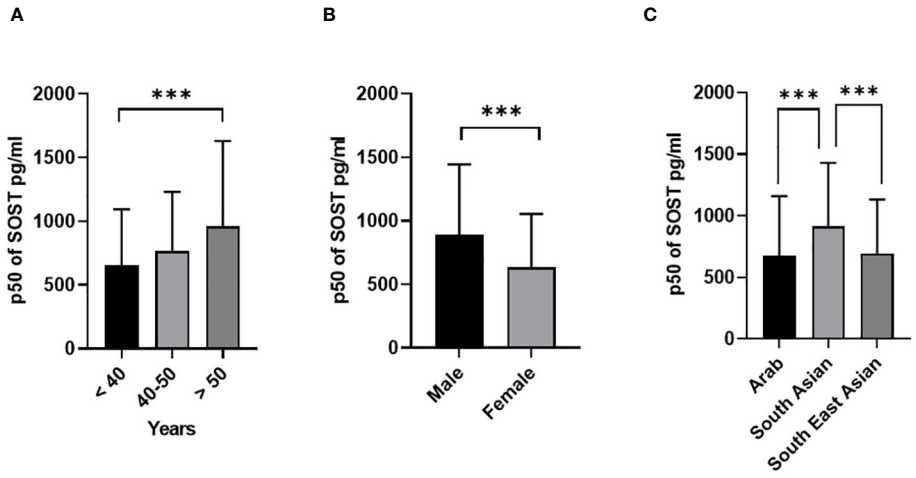

FIGURE 1
Sclerostin (SOST) level in plasma in all population (n = 2083). The population was stratified based on gender (Male and Female) **(A)**, Age (>40, 40-50, and > 50 years) **(B)**, and Ethnicity (Arab, South Asian, and Southeast Asian) **(C)**. The level of SOST in plasma was determined using a multiplex bone panel. Statistical assessment was 2-sided and considered statistically significant at ***p < 0.001.

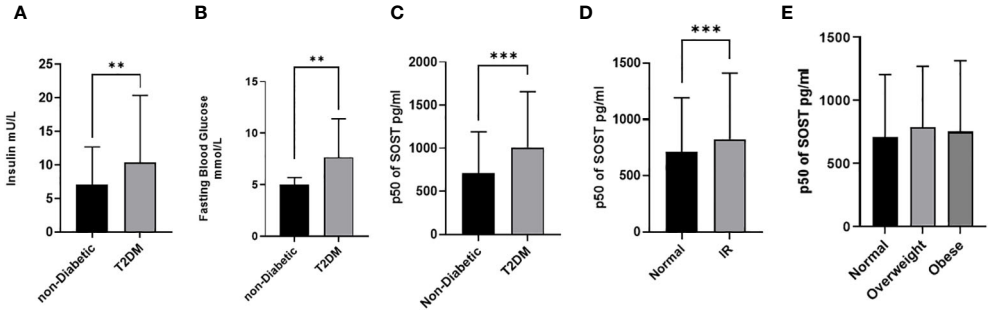

FIGURE 2
Sclerostin (SOST) level in plasma in all population (n = 2083). The population was stratified based on insulin level **(A)**, Fasting blood glucose (Non-diabetic and T2DM) **(B)**, diabetic status **(C)**, Insulin resistance (HOMA score: ≤ 2 (Normal) and > 2 (IR)) **(D)**, and BMI (BMI: > 24.99 (Normal), 25-29.9 (Overweight), ≥ 30 (Obese)) **(E)**. The level of SOST in plasma was determined using a multiplex bone panel. Statistical assessment was 2-sided and considered statistically significant at **p < 0.001.

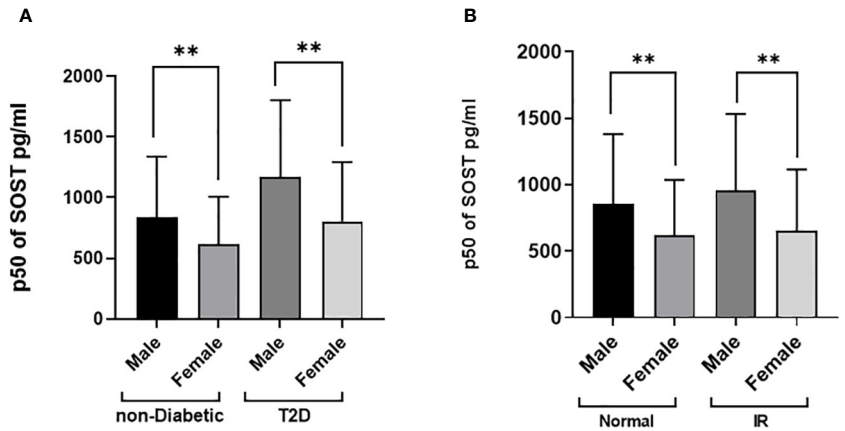

FIGURE 3
Sclerostin (SOST) level in plasma in the population stratified based on gender (Male and Female). **(A)** Diabetes Status (Non-diabetic and T2DM) **(B)** Insulin resistance [HOMA score: ≤ 2 (Normal) and > 2 (IR)]. The level of SOST in plasma was determined using a multiplex bone panel. Statistical assessment was 2-sided and considered statistically significant at **p < 0.001.

10.3389/fendo.2024.1392675

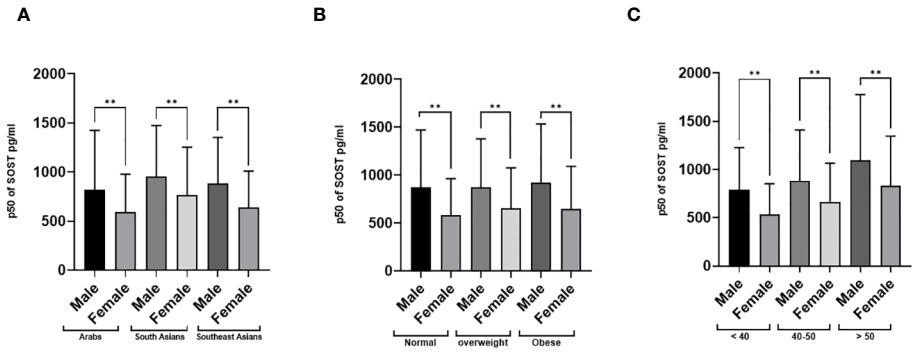

FIGURE 4
Sclerostin (SOST) level in plasma in the population stratified based on gender (Male and Female). **(A)** Ethnicity (Arab, South Asian, and Southeast Asian) **(B)** BMI [BMI: > 24.99 (Normal), 25-29.9 (Overweight), ≥ 30 (Obese)] **(C)** Age (>40, 40-50, and > 50 years). The level of SOST in plasma was determined using a multiplex bone panel. Statistical assessment was 2-sided and considered statistically significant at **p < 0.001.

status and the correlations were estimated in the nondiabetic population Table 3. Within the non-diabetic patients, the point biserial correlation indicated that males tend to have significantly higher SOST compared to females. Furthermore, other covariates like age, HbA1c, SBP, ALT and AST showed higher and significant correlations compared to other covariates.

To quantify and test the effect of each covariate on the SOST, univariate and adjusted estimates were produced along with their 95% confidence intervals with quantile regression results presented in Table 4. Univariate quantile regression results indicated that gender, age, ethnicity, diabetes status, and HbA1c were independently and significantly associated with SOST as presented in Table 4.

Results from the adjusted model indicated that males have a higher median SOST by 176 units (96%CI: 137.3, 215.4) compared to females. For a one-unit increase in age, the median SOST increases by 8.9 units (95%CI: 6.8, 10.9). Compared to Arabs, South Asians have a higher median SOST of 224.1 units (95%CI: 169.7, 278.6) while Southeast Asians have a higher median SOST of 112.4 units (95%CI: 73.6, 151.1). Furthermore, patients with diabetes have a higher median SOST of 113.7 units (95%CI: 33.0, 194.4), while for a one-unit increase in HbA1c, the median SOST increases by 31.7 units (95%CI: 14.2, 49.2). Results showed that BMI was not significantly associated with SOST.

It is worth noting that when age was categorized using tertile values and BMI was categorized according to the WHO recommendations for obesity, the results were consistent with modeling age and BMI as continuous covariates which indicates the reliability of the results.

4 Discussion

This large cross-sectional study provides insight into the potential factors affecting circulating SOST levels in a multiethnic population. The data presented in the current study showed that diabetes status, HbA1c, age, gender, and ethnicity are the major factors associated with circulating SOST levels. This observation was further confirmed by quantile regression analysis where the associations were independent and remained significant even after adjusting for

TABLE 2 Correlations between SOST and other covariates and metabolic traits (N=2,083).

Covariate	SOST	Covariate	SOST
Gender	0.256[a] (<0.001)	Insulin	0.097[b] (<0.001)
Age	0.300[b] (<0.001)	TC	0.092[b] (<0.001)
BMI	0.037[b] (0.125)	TG	0.152[b] (<0.001)
Hip Circumference	0.014[b] (0.571)	HDL	-0.137[b] (<0.001)
Waist Circumference	0.144[b] (<0.001)	LDL	0.085[b] (<0.001)
SBP	0.277[b] (<0.001)	ALT	0.225[b] (<0.001)
DBP	0.150[b] (<0.001)	AST	0.182[b] (<0.001)
FBG	0.185[b] (<0.001)	CRP	-0.010[b] (0.702)
HbA1c	0.309[b] (<0.001)		

[a]Point biserial correlation.
[b]Spearman correlation coefficient, P-value in parenthesis.

TABLE 3 Correlations between SOST and other covariates for non-diabetic patients (N=1425).

Covariate	SOST	Covariate	SOST
Gender[a]	0.250 (<0.001)	Insulin	0.041 (0.142)
Age	0.250 (<0.001)	TC	0.153 (<0.001)
BMI	0.015 (0.572)	TG	0.164 (<0.001)
Hip Circumference	-0.017 (0.545)	HDL	-0.105 (<0.001)
Waist Circumference	0.094 (<0.001)	LDL	0.142 (<0.001)
SBP	0.212 (<0.001)	ALT	0.198 (<0.001)
DBP	0.175 (<0.001)	AST	0.209 (<0.001)
FBG	0.071 (0.009)	CRP	-0.018 (0.523)
HbA1c	0.214 (<0.001)		

[a]point biserial correlation and others by Spearman correlation coefficient, P-value in parenthesis.

10.3389/fendo.2024.1392675

TABLE 4 Associations between SOST and other demographic and clinical traits using quantile (median) regression analysis (N=2,083).

Covariate	Univariate Median Regression β (95%CI) (p-value)	Adjusted Median Regression β (95%CI) (p-value)
Gender Female Male	 Ref 254.4 (217.8, 291.0) (<0.001)	 Ref 181.3 (140.8, 221.8) (<0.001)
Age, years	12.2 (9.8, 14.5) (<0.001)	8.8 (6.4, 11.3) (<0.001)
Ethnicity Arab South Asian Southeast Asian	 Ref 237.4 (190.6, 284.2) (<0.001) 18.1 (-31.1, 67.4) (0.471)	 Ref 225.4 (169.7, 281.0) (<0.001) 121.9 (77.4, 166.4) (<0.001)
Diabetes Status Non-Diabetic Diabetic	 Ref 297.7 (200.8, 394.7) (<0.001)	 Ref 91.5 (15.7, 167.3) (0.018)
HbA1c	98.3 (82.3, 114.2) (<0.001)	44.2 (10.5, 77.9) (0.010)
BMI	-1.08 (-4.0, 1.85) (0.469)	1.41 (-1.61, 4.42) (0.361)

confounders. We also showed that obesity does not affect circulating SOST levels, as shown by the lack of correlation and the results of the quantile regression.

Patients with T2DM exhibited significantly higher SOST levels compared to their non-diabetic counterparts. Moreover, we observed strong correlations between SOST and HbA1c, FBG, and HOMA-IR, which are measures of long-term blood sugar control, blood sugar level, and insulin sensitivity, respectively. Among these variables, HbA1c showed the highest correlation with SOST, suggesting that SOST may reflect the chronic effects of hyperglycemia on bone health. Furthermore, the adjusted model highlighted the independent associations of SOST with diabetes and HbA1c. Our findings are in accord with previous reports (18, 19, 23, 28). In addition, Pacicca and colleagues conducted an *in vitro* study using the IDG-SW3 osteocyte-like cell line. When cultured under high glucose conditions, these cells exhibited a significant increase in SOST mRNA (by 100-fold) and SOST protein (by 5000-fold) compared to cells in control media. These findings indicate that glucose levels directly influence osteocyte function via SOST expression, shedding light on a potential mechanism by which high glucose/diabetes adversely affects bone quality. While the exact mechanism by which glucose homeostasis influences SOST levels is not fully understood, it is believed to involve the Wnt signaling pathway. A number of studies have demonstrated that activation of the Wnt signaling pathway enhances glucose metabolism (29, 30). Wnt7b has been shown to affect glucose uptake, GLUT expression, and Akt activation during osteoclastogenesis (31). Additionally, Wnt3a may boost mitochondrial oxygen consumption (32), elevate energy output by augmenting glutamine use in the TCA cycle (33), and activate the mTORC2 and protein kinase B (Akt) pathways, leading to the upregulation of essential glycolytic enzymes (34).

The age-associated increase of circulating levels of SOST in this study is in line with most previous investigations (35–37). Possibly, this is due to the natural aging process, which is known to affect bone turnover and remodeling (9, 38). SOST inhibits osteoblast activity, making it a potential biomarker for bone formation. The fact that the amount of SOST in our bodies increases as we age indicates that its increased production may reflect bone structure rather than size.

Moreover, there was a significant gender difference in median SOST levels, with males exhibiting higher levels compared to females. Gender disparities were observed across various factors, including diabetes status, insulin resistance (IR), body weight classifications, age brackets, and ethnicities (as illustrated in Figures 3, 4). For example, a notable rise in SOST levels was evident among men compared to women within the diabetes cohort, a pattern consistent among non-diabetics, those with normal glucose tolerance, individuals with insulin resistance, and participants across different body weight categories (normal, overweight, obese), age groups, and ethnic backgrounds (Arab, South Asian, Southeast Asian). Our study findings underscore the significant role of gender in the variability of SOST levels. This observation aligns with previous studies that have reported gender-based differences in circulating SOST (36, 39, 40). Moreover, In a study conducted by MÖdder et al. involving 362 women and 318 men from a population-based cohort, it was observed that men consistently had higher serum SOST levels than women regardless of age (41). The exact reasons for this difference remain uncertain. However, one hypothesis the authors suggested was that the higher SOST levels in men could be attributed to their larger skeletal mass, which might produce and release more SOST into the bloodstream. In a second interventional study, the authors assessed the effect of estrogen on circulating SOST levels in both genders (37). They used two distinct direct intervention study methodologies (estrogen treatment and estrogen withdrawal) and found that estrogen treatment leads to a decrease in serum SOST levels, while estrogen withdrawal causes an increase in SOST levels. This evidence strongly suggests that estrogen has a regulatory effect on circulating SOST levels and, potentially, the production of SOST by osteocytes in the bone. Apparently, both hormonal and bone mass differences between genders might play a role in influencing circulating SOST levels. However, the exact mechanisms underlying these differences need further investigation.

The influence of ethnicity on SOST levels has not been comprehensively investigated. While several studies have examined the ethnic impact on SOST levels (23, 42, 43), there is still a need for a more detailed understanding. The study we present is one of the few that examines ethnic differences in the levels of circulating SOST. Our findings suggest distinct ethnic-specific variations in circulating SOST levels among Arabs, South Asians, and Southeast Asians. Notably, South Asian participants exhibited the most pronounced association, even when accounting for factors like age, gender, BMI, and diabetes status. This is in agreement with the observation of Janssen L. et al. who observed elevated plasma SOST levels in South Asians compared to white Caucasians (44). While their comparison was with an ethnic group different from the groups examined in our study, it underscores the unique metabolic

challenges faced by the South Asian population (45, 46). Another study, focusing on 138 healthy pre-menopausal and post-menopausal women, included Chinese American and white Caucasian participants to identify ethnic variation in serum SOST levels (42). Their findings showed no significant ethnic-specific variations in SOST levels. However, they did note that post-menopausal women had higher SOST levels than pre-menopausal women across both racial categories. It is worth noting that the first important difference between our study and the other is that our study compared South Asians and Southeast Asians with Arabs rather than Caucasians; secondly, we included both genders, whereas their study included only women, and lastly, our larger sample size enhances the robustness of our results.

The relationship between obesity and circulating SOST levels is unclear in the literature. While some studies indicate a rise in serum SOST levels with obesity (35, 47, 48), others have not identified such a link (30, 43). In our study, we used three different anthropometric measurements to evaluate obesity, BMI, WC, and HC. We did not find any significant correlation between SOST and BMI or HC, but we found a weak correlation between SOST and WC. This suggests that obesity may not be a major determinant of SOST levels, and that other factors may have more influence. Our result is more reliable than previous studies, as we used a large sample size (n=2083) that increased the statistical power and reduced the sampling error.

Although our study controlled for age, gender, diabetes status, and BMI, we did not include assessments for Metabolic Associated Fatty Liver Disease (MAFLD). This omission limits our understanding of the full impact of metabolic comorbidities on SOST. Future research should consider incorporating a wider range of metabolic conditions, including MAFLD, to provide a more comprehensive view of how obesity and related disorders influence SOST levels. We also did not assess bone mineral density (BMD) in our study. We acknowledge the significance of BMD as a key marker of bone health, particularly in relation to sclerostin levels. Such data could enrich our research findings and implications. We hope to explore this in future work, including a comprehensive bone health assessment. We believe that our study's findings lay the groundwork for such investigations.

In conclusion, the study confirms that circulating level of SOST is impacted by diabetes. The positive association between the level of SOST and various blood markers that are related to different metabolic complications implies that it plays a detrimental role in the individual's wellbeing. As for the ethnicity, South Asian participants had the highest levels of SOST across the three groups and exhibited the most pronounced association, even when accounting for factors like age, gender, BMI, and diabetes status. This shows that the level of SOST may have a stronger impact on health conditions among people of specific ethnic background. This also sheds light on the importance of personalized medicine to address the development of medications taking into consideration the ethnic background.

Data availability statement

The raw data supporting the conclusions of this article will be made available by the authors, without undue reservation.

Ethics statement

The study protocol was approved by the Ethics Review Committee at Dasman Diabetes Institute under the reference RA2011-003, and done in accordance with the principles of the Declaration of Helsinki and good clinical practice guidelines. The studies were conducted in accordance with the local legislation and institutional requirements. The participants provided their written informed consent to participate in this study.

Author contributions

TA: Writing – review & editing, Writing – original draft, Methodology, Investigation, Formal analysis. PC: Writing – review & editing, Methodology, Investigation, Data curation. IA-K: Writing – review & editing, Methodology, Investigation, Data curation. MA-F: Writing – review & editing, Writing – original draft, Supervision, Investigation, Formal analysis, Conceptualization. TT: Writing – review & editing, Methodology, Investigation, Formal analysis. AA: Writing – review & editing, Software, Methodology, Formal analysis. FS: Writing – review & editing, Methodology, Investigation, Formal analysis. HA: Writing – review & editing, Methodology, Investigation, Formal analysis. MA-G: Writing – review & editing, Methodology, Investigation, Formal analysis. JT: Writing – review & editing, Methodology, Investigation, Formal analysis. HK: Writing – review & editing, Methodology, Investigation, Formal analysis. FA-M: Writing – review & editing, Writing – original draft, Resources, Investigation, Formal analysis. JA: Writing – review & editing, Writing – original draft, Supervision, Methodology, Investigation, Formal analysis, Data curation, Conceptualization.

Funding

The author(s) declare financial support was received for the research, authorship, and/or publication of this article. This work was supported by the Kuwait Foundation for the Advancement of Sciences (KFAS) under projects (RAHM-2019-030).

Conflict of interest

The authors declare that the research was conducted in the absence of any commercial or financial relationships that could be construed as a potential conflict of interest.

The author(s) declared that they were an editorial board member of Frontiers, at the time of submission. This had no impact on the peer review process and the final decision.

Publisher's note

All claims expressed in this article are solely those of the authors and do not necessarily represent those of their affiliated organizations, or those of the publisher, the editors and the reviewers. Any product that may be evaluated in this article, or claim that may be made by its manufacturer, is not guaranteed or endorsed by the publisher.

Supplementary material

The Supplementary Material for this article can be found online at: https://www.frontiersin.org/articles/10.3389/fendo.2024.1392675/full#supplementary-material

References

1. Leitner DR, Frühbeck G, Yumuk V, Schindler K, Micic D, Woodward E, et al. Obesity and type 2 diabetes: Two diseases with a need for combined treatment strategies - EASO can lead the way. *Obes Facts*. (2017) 10:483–92. doi: 10.1159/000480525

2. Lingvay I, Sumithran P, Cohen RV, le Roux CW. Obesity management as a primary treatment goal for type 2 diabetes: time to reframe the conversation. *Lancet*. (2022) 399:394–405. doi: 10.1016/S0140-6736(21)01919-X

3. Collaborators G 2015 O, Afshin A, Forouzanfar MH, Reitsma MB, Sur P, Estep K, et al. Health effects of overweight and obesity in 195 countries over 25 years. *N Engl J Med*. (2017) 377:13–27. doi: 10.1056/NEJMoa1614362

4. Banday MZ, Sameer AS, Nissar S. Pathophysiology of diabetes: An overview. *Avicenna J Med*. (2020) 10:174–88. doi: 10.4103/ajm.ajm_53_20

5. Ye J, Wu Y, Yang S, Zhu D, Chen F, Chen J, et al. The global, regional and national burden of type 2 diabetes mellitus in the past, present and future: a systematic analysis of the Global Burden of Disease Study 2019. *Front Endocrinol (Lausanne)*. (2023) 14:1–12. doi: 10.3389/fendo.2023.1192629

6. Banerjee S, Talukdar I, Banerjee A, Gupta A, Balaji A, Aduri R. Type II diabetes mellitus and obesity: Common links, existing therapeutics and future developments. *J Biosci*. (2019) 44:1–13. doi: 10.1007/s12038-019-9962-7

7. Bathina S, Armamento-Villareal R. The complex pathophysiology of bone fragility in obesity and type 2 diabetes mellitus: therapeutic targets to promote osteogenesis. *Front Endocrinol (Lausanne)*. (2023) 14:1–10. doi: 10.3389/fendo.2023.1168687

8. Datta HK, Ng WF, Walker JA, Tuck SP, Varanasi SS. The cell biology of bone metabolism. *J Clin Pathol*. (2008) 61:577–87. doi: 10.1136/jcp.2007.048868

9. Florencio-Silva R, Sasso GRDS, Sasso-Cerri E, Simões MJ, Cerri PS. Biology of bone tissue: structure, function, and factors that influence bone cells. *BioMed Res Int*. (2015) 2015:421746. doi: 10.1155/2015/421746

10. Zhou R, Guo Q, Xiao Y, Guo Q, Huang Y, Li C, et al. Endocrine role of bone in the regulation of energy metabolism. *Bone Res*. (2021) 9:25. doi: 10.1038/s41413-021-00142-4

11. Russo GT, Giandalia A, Romeo EL, Nunziata M, Muscianisi M, Ruffo MC, et al. Fracture risk in type 2 diabetes: current perspectives and gender differences. *Int J Endocrinol*. (2016) 2016:1615735. doi: 10.1155/2016/1615735

12. Conte C, Epstein S, Napoli N. Insulin resistance and bone: a biological partnership. *Acta Diabetol*. (2018) 55:305–14. doi: 10.1007/s00592-018-1101-7

13. Dreyer TJ, Keen JA, Wells LM, Roberts SJ. Novel insights on the effect of sclerostin on bone and other organs. *J Endocrinol*. (2023) 257:257. doi: 10.1530/JOE-22-0209

14. Balemans W, Ebeling M, Patel N, Van HE, Olson P, Dioszegi M, et al. Increased bone density in sclerosteosis is due to the deficiency of a novel secreted protein (SOST). *Hum Mol Genet*. (2001) 10(5):537–44. doi: 10.1093/hmg/10.5.537

15. Holdsworth G, Roberts SJ, Ke HZ. Novel actions of sclerostin on bone. *J Mol Endocrinol*. (2019) 62:R167–85. doi: 10.1530/JME-18-0176

16. Delgado-Calle J, Sato AY, Bellido T. Role and mechanism of action of sclerostin in bone. *Bone*. (2017) 96:29–37. doi: 10.1016/j.bone.2016.10.007

17. Sebastian A, Loots GG. Genetics of Sost/SOST in sclerosteosis and van Buchem disease animal models. *Metabolism*. (2018) 80:38–47. doi: 10.1016/j.metabol.2017.10.005

18. Gennari L, Merlotti D, Valenti R, Ceccarelli E, Ruvio M, Pietrini MG, et al. Circulating Sclerostin levels and bone turnover in type 1 and type 2 diabetes. *J Clin Endocrinol Metab*. (2012) 97:1737–44. doi: 10.1210/jc.2011-2958

19. García-Martín A, Rozas-Moreno P, Reyes-García R, Morales-Santana S, García-Fontana B, García-Salcedo JA, et al. Circulating levels of sclerostin are increased in patients with type 2 diabetes mellitus. *J Clin Endocrinol Metab*. (2012) 97:234–41. doi: 10.1210/jc.2011-2186

20. Pacicca DM, Brown T, Watkins D, Kover K, Yan Y, Prideaux M, et al. Elevated glucose acts directly on osteocytes to increase sclerostin expression in diabetes. *Sci Rep*. (2019) 9:1–11. doi: 10.1038/s41598-019-52224-3

21. Sanches CP, Vianna AGD, Barreto FDC. The impact of type 2 diabetes on bone metabolism. *Diabetol Metab Syndr*. (2017) 9:1–7. doi: 10.1186/s13098-017-0278-1

22. Daniele G, Winnier D, Mari A, Bruder J, Fourcaudot M, Pengou Z, et al. Sclerostin and insulin resistance in prediabetes: Evidence of a cross talk between bone and glucose metabolism. *Diabetes Care*. (2015) 38:1509–17. doi: 10.2337/dc14-2989

23. Singh PK, Naithani M, Pathania M, Mirza AA, Saha S. An insight into the association of sclerostin with insulin sensitivity and glycemic parameters in male Indian prediabetic and diabetic population. *Cureus*. (2022) 14:1–9. doi: 10.7759/cureus.27123

24. Kim SP, Frey JL, Li Z, Kushwaha P, Zoch ML, Tomlinson RE, et al. Sclerostin influences body composition by regulating catabolic and anabolic metabolism in adipocytes. *Proc Natl Acad Sci U S A*. (2017) 114:E11238–47. doi: 10.1073/pnas.1707876115

25. Abu-Farha M, Abubaker J, Noronha F, Al-Khairi I, Cherian P, Alarouj M, et al. Lack of associations between betatrophin/ANGPTL8 level and C-peptide in type 2 diabetic subjects. *Cardiovasc Diabetol*. (2015) 14:1–9. doi: 10.1186/s12933-015-0277-1

26. Abu-Farha M, Abubaker J, Al-Khairi I, Cherian P, Noronha F, Hu FB, et al. Higher plasma betatrophin/ANGPTL8 level in Type 2 Diabetes subjects does not correlate with blood glucose or insulin resistance. *Sci Rep*. (2015) 5:1–8. doi: 10.1038/srep10949

27. Alkandari A, Alarouj M, Elkum N, Sharma P, Devarajan S, Abu-Farha M, et al. Adult diabetes and prediabetes prevalence in Kuwait: Data from the cross-sectional Kuwait diabetes epidemiology program. *J Clin Med*. (2020) 9:1–12. doi: 10.3390/jcm9113420

28. Guo H, An Z, Wang N, Ge S, Cai J, Yu S, et al. Diabetes mellitus type 2 patients with abdominal obesity are prone to osteodysfunction: A cross-sectional study. *J Diabetes Res*. (2023) 2023:3872126. doi: 10.1155/2023/3872126

29. Balatsky VV, Sowka A, Dobrzyn P, Piven OO. 2023-WNTβ-catenin pathway is a key regulator of cardiac function and energetic metabolism.pdf. *Acta Physiol*. (2023) 237(3):e13912. doi: 10.1111/apha.13912

30. Cisternas P, Salazar P, Silva-Álvarez C, Barros LF, Inestrosa NC. Activation of Wnt signaling in cortical neurons enhances glucose utilization through glycolysis. *J Biol Chem*. (2016) 291:25950–64. doi: 10.1074/jbc.M116.735373

31. Wu F, Li B, Hu X, Yu F, Shi Y, Ye L. Wnt7b inhibits osteoclastogenesis *via* AKT activation and glucose metabolic rewiring. *Front Cell Dev Biol*. (2021) 9:1–13. doi: 10.3389/fcell.2021.771336

32. Smith CO, Eliseev RA. Energy metabolism during osteogenic differentiation: the role of akt. *Stem Cells Dev*. (2021) 30:149–62. doi: 10.1089/scd.2020.0141

33. Glatz JFC, Luiken JJFP, Bonen A. Membrane fatty acid transporters as regulators of lipid metabolism: Implications for metabolic disease. *Physiol Rev*. (2010) 90:367–417. doi: 10.1152/physrev.00003.2009

34. Esen E, Chen J, Karner CM, Okunade AL, Patterson BW, Long F. WNT-LRP5 signaling induces warburg effect through mTORC2 activation during osteoblast differentiation. *Cell Metab*. (2013) 17:745–55. doi: 10.1016/j.cmet.2013.03.017

35. Kerschan-Schindl K, Föger-Samwald U, Gleiss A, Kudlacek S, Wallwitz J, Pietschmann P. Circulating bioactive sclerostin levels in an Austrian population-based cohort. *Wien Klin Wochenschr*. (2022) 134:39–44. doi: 10.1007/s00508-021-01815-0

36. Xu Y, Gao C, He J, Gu W, Yi C, Chen B, et al. Sclerostin and its associations with bone metabolism markers and sex hormones in healthy community-dwelling elderly individuals and adolescents. *Front Cell Dev Biol*. (2020) 8:1–7. doi: 10.3389/fcell.2020.00057

37. Mödder U, Clowes JA, Hoey K, Peterson JM, McCready L, Oursler MJ, et al. Regulation of circulating sclerostin levels by sex steroids in women and in men. *J Bone Miner Res*. (2011) 26:27–34. doi: 10.1002/jbmr.128

38. Fang H, Deng Z, Liu J, Chen S, Deng Z, Li W. The mechanism of bone remodeling after bone aging. *Clin Interv Aging*. (2022) 17:405–15. doi: 10.2147/CIA.S349604

39. Kirmani S, Amin S, McCready LK, Atkinson EJ, Melton LJ, Müller R, et al. Sclerostin levels during growth in children. *Osteoporos Int*. (2012) 23:1123–30. doi: 10.1007/s00198-011-1669-z

40. Catalano A, Pintaudi B, Morabito N, Di Vieste G, Giunta L, Lucia Bruno M, et al. Gender differences in sclerostin and clinical characteristics in type 1 diabetes mellitus. *Eur J Endocrinol*. (2014) 171:293–300. doi: 10.1530/EJE-14-0106

41. Mödder UI, Hoey KA, Amin S, McCready LK, Achenbach SJ, Riggs BL, et al. Relation of age, gender, and bone mass to circulating sclerostin levels in women and men. *J Bone Miner Res*. (2011) 26:373–9. doi: 10.1002/jbmr.217

42. Costa AG, Walker MD, Zhang CA, Cremers S, Dworakowski E, McMahon DJ, et al. Circulating sclerostin levels and markers of bone turnover in chinese-american and white women. *J Clin Endocrinol Metab*. (2013) 98:4736–43. doi: 10.1210/jc.2013-2106

43. Umekwe N, Owei I, Stentz F, Dagogo-Jack S. Plasma FGF-21 and sclerostin levels, glycemia, adiposity, and insulin sensitivity in normoglycemic black and white adults. *J Endocr Soc*. (2022) 6:1–6. doi: 10.1210/jendso/bvab183

44. Janssen LGM, van Dam AD, Hanssen MJW, Kooijman S, Nahon KJ, Reinders H, et al. Higher plasma sclerostin and lower Wnt signaling gene expression in white adipose tissue of prediabetic South Asian men compared with white Caucasian men. *Diabetes Metab J*. (2019) 43:326–35. doi: 10.4093/dmj.2019.0031

45. Haldar S, Chia SC, Henry CJ. Body Composition in Asians and Caucasians: Comparative Analyses and Influences on Cardiometabolic Outcomes [Internet]. In: *Advances in Food and Nutrition Research*. Berkeley, CA, USA: Elsevier Inc (2015). p. 97–154. doi: 10.1016/bs.afnr.2015.07.001

46. Meeks KAC, Freitas-Da-Silva D, Adeyemo A, Beune EJAJ, Modesti PA, Stronks K, et al. Disparities in type 2 diabetes prevalence among ethnic minority groups resident in Europe: a systematic review and meta-analysis. *Intern Emerg Med*. (2016) 11:327–40. doi: 10.1007/s11739-015-1302-9

47. Kalem MN, Kalem Z, Akgun N, Bakırarar B. The relationship between postmenopausal women's sclerostin levels and their bone density, age, body mass index, hormonal status, and smoking and consumption of coffee and dairy products. *Arch Gynecol Obstet*. (2017) 295:785–93. doi: 10.1007/s00404-017-4288-x

48. Amrein K, Amrein S, Drexler C, Dimai HP, Dobnig H, Pfeifer K, et al. Sclerostin and its association with physical activity, age, gender, body composition, and bone mineral content in healthy adults. *J Clin Endocrinol Metab*. (2012) 97:148–54. doi: 10.1210/jc.2011-2152

frontiers | Frontiers in Endocrinology

TYPE Original Research
PUBLISHED 14 May 2024
DOI 10.3389/fendo.2024.1387035

OPEN ACCESS

EDITED BY
Antonino Catalano,
University of Messina, Italy

REVIEWED BY
Norliza Muhammad,
Universiti Kebangsaan Malaysia Medical Center (UKMMC), Malaysia
Carol Johnston,
Arizona State University, United States
Alexander Johannes Michels,
Oregon State University, United States

*CORRESPONDENCE
Xianfeng Zhang
zhangxianfeng2018@qq.com

†These authors have contributed equally to this work and share first authorship

RECEIVED 16 February 2024
ACCEPTED 30 April 2024
PUBLISHED 14 May 2024

CITATION
Zhao J, Lu Q and Zhang X (2024) Associations of serum vitamin B12 and its biomarkers with musculoskeletal health in middle-aged and older adults.
Front. Endocrinol. 15:1387035.
doi: 10.3389/fendo.2024.1387035

Associations of serum vitamin B12 and its biomarkers with musculoskeletal health in middle-aged and older adults

Jiao Zhao[1†], Qi Lu[2†] and Xianfeng Zhang[3*]

[1]Zhejiang University School of Medicine, Hangzhou, Zhejiang, China, [2]Shanghai Clinical Research Center of Bone Disease, Department of Osteoporosis and Bone Disease, Shanghai Jiaotong University Affiliated Sixth People's Hospital, Shanghai, China, [3]Department of Endocrinology, Affiliated Hangzhou First People's Hospital, School of Medicine, Westlake University, Hangzhou, Zhejiang, China

Introduction: The effects of vitamin B12 metabolism on musculoskeletal health and the exact mechanism have not been fully determined. Our study aimed to assess the association of vitamin B12 and its biomarkers with musculoskeletal health in middle-aged and older adults.

Methods: The data from the National Health and Nutrition Examination Survey 2001–2002 were used to investigate the effects of serum vitamin B12 and its biomarkers (homocysteine and methylmalonic acid) on skeletal muscle health. Bone mineral density (BMD), lean mass, gait speed and knee extensor strength were used as indicators for musculoskeletal health.

Results: Serum vitamin B12 level was positively correlated with the total and appendicular lean mass (β = 584.83, *P* = 0.044; β = 291.65, *P* = 0.043) in older adults over 65 years of age. In the full population, plasma homocysteine was associated with total lean mass, appendicular lean mass, gait speed, and knee extensor strength (all *P* < 0.05). Among older adults over 65 years of age, homocysteine level was significantly negatively correlated with gait speed and knee extensor strength (β = -12.75, *P* = 0.019; β = -0.06, *P* <0.001). Plasma methylmalonic acid was negatively associated with total BMD and femur BMD in the full population (β = -0.01, *P* = 0.018; β = -0.01, *P* = 0.004). In older adults, methylmalonic acid significantly affected total BMD, femur BMD and knee extensor strength (β = -0.01, *P* = 0.048; β = -0.01, *P* = 0.025; β = -7.53, *P* = 0.015).

Conclusions: Vitamin B12 and its biomarkers are closely related to BMD, body composition, muscle strength and physical function in middle-aged and older adults. Vitamin B12 may be an important indicator of musculoskeletal health in the elderly.

KEYWORDS

bone mineral density, osteoporosis, sarcopenia, vitamin B12, hyperhomocysteinemia

10.3389/fendo.2024.1387035

1 Introduction

Vitamin B12 as a member of the B vitamins, is a hydrosoluble vitamin. It cannot be synthesized by the human body and must be taken up in food or synthesized by the gut microbiota (1). Vitamin B12 is an important cofactor of methionine synthase and L-methylmalonyl-CoA mutase, which are involved in homocysteine and methylmalonic acid metabolism (MMA) (2). Figure 1 shows the metabolic pathways of vitamin B12, homocysteine and MMA. Low levels of vitamin B12 are associated with homocysteine and MMA. Therefore, these two factors are considered as two functional biomarkers of vitamin B12 deficiency (3). Vitamin B12 deficiency is a fairly common public health problem, occurring mainly in pregnant women and the elderly (4). In addition, recent studies have suggested that vitamin B12 deficiency is associated with a variety of chronic diseases, especially stroke (5), osteoporosis (6), cognitive impairment (7) and physical dysfunction (8, 9). That is why there has been interest in the effects of vitamin B12 on musculoskeletal health. Although studies have shown that vitamin B12 is closely associated with the musculoskeletal system (10), however, the effects of vitamin B12 metabolism on musculoskeletal health and the precise mechanisms remain unclear (11, 12).

Clarke (13) et al. investigated the relationship between B vitamins and bone mineral density (BMD) in patients with celiac disease aged 20 years and older. The study showed a significant association between serum vitamin B12 and BMD in the hip and femur neck, but this protective effect on bone was found only in men (13). In a study of postmenopausal women by Bozkurt (14) et al., low BMD in the femur neck and vertebrae were associated with a significant reduction in serum vitamin B12 levels. In addition, women with osteoporosis had higher levels of homocysteine compared with healthy or osteopenia women (14).The Framingham Study showed that vitamin B12 levels were inversely associated with hip fracture risk, but after controlling for covariates such as BMD, vitamin D and homocysteine levels in a multivariate analysis, this negative correlation was attenuated (15). An analysis by Morris et al. (16) on 1550 participants showed a positive association between serum vitamin B12 concentrations and hip BMD, and this relationship was a dose-response fashion. At the same time, participants with hyperhomocysteinemia had lower BMD than those with normal homocysteine levels (16). According to the Hordaland Homocysteine Study, high homocysteine levels in middle-aged and elderly women were associated with decreased BMD, whereas this association did not exist in men (17). A meta-analysis revealed a 4% reduction in fracture risk for every 50 pmol/L increase in vitamin B12 concentration, whereas a 4% increase in fracture risk for every 1 µmol/L increase in homocysteine concentration (18). A study by Herrmann et al. has shown that B-vitamin supplementation in osteoporosis patients with high homocysteine levels, leading to an increase in lumbar spine BMD and a decrease in bone turnover markers (19). However, Rumbak et al. noted that in healthy women aged 45–65 years, neither vitamin B12, folate, nor homocysteine levels were significantly associated with BMD (20). Furthermore, Holstein et al. found no association between serum levels of vitamin B12 and trabecular thickness, thus questioning the true role of vitamin B12 in bone turnover (21). In a study by Bailey et al., serum vitamin B12 levels were not directly associated with BMD, but their main functional markers, MMA and homocysteine levels, were significantly associated with the risk of developing osteoporosis (22). A randomized controlled trial by Green et al. showed that vitamin B12 supplementation had no effect on bone turnover in healthy older adults (23). Analysis of the HOPE-2 Trial also showed that vitamin B12 supplementation did not reduce fracture risk in a high-cardiovascular-risk population (24).

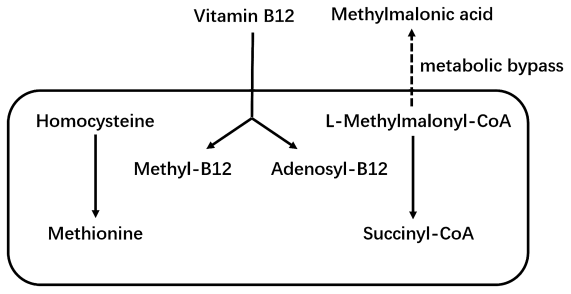

FIGURE 1
Metabolic pathway of vitamin B12, homocysteine and methylmalonic acid.

Many studies have reported the effect of vitamin B12 deficiency on many geriatric syndromes, but to date, only a few cross-sectional studies have investigated the association of vitamin B12 with sarcopenia (25). The study by Mithal et al. suggested that vitamin B12 deficiency may impair muscle function in a homocysteine dependent manner, manifested in reduced gait speed and muscle strength (8). A cross-sectional study by Matteini et al. showed that decreased serum vitamin B12 concentration, increased in MMA concentration, and increased in homocysteine concentration all resulted in decreased muscle mass and impaired physical function in subjects (26). In addition, studies have shown that increased homocysteine concentrations were associated with decreased quadriceps strength and gait speed (27). In contrast, Swart et al. showed that hyperhomocysteinemia was not associated with muscle mass (28). Consistently, no association was observed between low vitamin B12 levels or high homocysteine levels and recurrent falls in the LASA study (6). In a randomized controlled trial study of stroke patients, vitamin B12 was found to have no statistically significant effect on fall rates (29).

At present, studies on the relationship between vitamin B12 and its metabolic markers and musculoskeletal health are still insufficient, and further large cohort studies are needed. Assessment of musculoskeletal system health should include multiple dimensions such as BMD, muscle mass, and function (30). In view of this, this study used data from the National Health and Nutrition Examination Survey (NHANES) to explore the relationship between serum vitamin B12 and its biomarkers (homocysteine and MMA) with BMD, body composition, muscle strength and physical function.

2 Materials and methods

2.1 Population

The NHANES is a cross-sectional study sponsored annually by the National Center for Health Statistics at the Centers for Disease Control and Prevention (CDC). The study used a nationally representative sample to assess the health and nutritional status of the U.S. civilian population. The NHANES data is released to the public every 2 years and includes standardized physical exams and health-related interviews. All NHANES surveys collect data through household interviews and direct standardized medical examinations at specially equipped mobile examination centers. Details of investigation and the NHANES methodology used can be found in the CDC website (http://www.cdc.gov/nchs/nhanes.htm). The NHANES study is in line with the Declaration of Helsinki and the protocols were approved by the National Center for Health Statistics Ethics Review Board.

We studied individuals enrolled in the NHANES 2001–2002. Vitamin B12 and its metabolic markers, parameters of the musculoskeletal health, along with other information such as demographic, lifestyle, and laboratory test data were measured and recorded. The NHANES 2001–2002 included a total of 11,039 participants, of whom 8390 had their serum vitamin B12 concentrations measured. The NHANES exclusion criteria for dual-energy X-ray absorptiometry (DXA) scans include weight over 136 kg or height over 196 cm, pregnancy, nuclear medicine studies in the past 3 days or a history of contrast agent use (barium) in the past 7 days (31). As a result, a total of 7,126 participants underwent DXA scans. It is important to note that NHANES 2001–2002 only assessed muscle strength and physical function in participants who were older than 50 years old, so only this subset of participants was included in this study. In addition, participants who had a history of brain aneurysm or stroke, severe back pain, a history of myocardial infarction in the past 6 weeks, knee surgery or knee replacement, or chest or abdominal surgery in the past 3 weeks were unable to undergo strength testing and were excluded from this study (32). In the end, out of 7,126 participants, we included only 1,466 participants who completed DXA scans (BMD and body composition), as well as muscle strength and physical function tests. Given that musculoskeletal health is strongly associated with age, we also performed a subgroup analysis of participants over 65 years of age.

2.2 Measurement of serum vitamin B12 and its biomarkers

Serum vitamin B12 concentration was measured using Bio-Rad Laboratories "Quantaphase II Folate/vitamin B12" radioassay kit (Bio-Rad Laboratories, 1993) (33). Serum samples were determined in combination with ^{57}Co-vitamin B12 in a solution containing dithiothreitol (DTT) and cyanide (33). More detailed information about vitamin B12 concentration measurement can be found on the NHANES website (33). For NHANES 2001, the levels of plasma total homocysteine were determined using the "Abbott Homocysteine IMX (HCY) assay" (34). For NHANES 2002, the plasma total homocysteine concentration was determined by the "Abbott Axsym system" (34). Both methods use fully automated fluorescence polarization immunoassay (FPIA) (34). The FPIA method has been shown to have excellent accuracy (coefficient of variation ≤5%) compared to high-performance liquid chromatography (35). More detailed information on the measurement of plasma total homocysteine levels can be found on the NHANES website (34). MMA was extracted from plasma using strong anion exchange resin and added to internal standard (36). The extracted acid was subsequently derived from cyclohexanol to form dicyclohexyl ester (36). The derivatization samples were injected into gas chromatography to separate the other components (36). The mass selective detector using selected ion monitoring was used to monitor the effluent of the gas chromatograph (36). Results were quantified by using the peak area ratios of MMA and internal calibration of internal standards (36). More detailed information on MMA concentration measurement can be found on the NHANES website (36).

2.3 BMD and body composition

DXA scanning was performed on the QDR 4500A fan beam densitometer (Hologic, Inc., Bedford, MA) in accordance with the manufacturer's guidelines (31). Participants were asked to remove any jewelry or metal objects that might affect the scan results and change into gowns (31). We used available data on total and regional BMD (g/cm^2), fat mass (g), total and appendicular lean mass (g), and percent body fat (%). Based on the results of the analysis of QDR 4500A DXA data, NHANES adjusted lean mass and fat mass, reducing lean mass by 5% and increasing fat mass by the equivalent weight (31). Further details of the DXA data acquisition protocol are described on the NHANES website (31).

2.4 Muscle strength and physical function

The muscle strength and physical function tests were done on participants who were middle–aged and older adults (≥50 years). The average peak force of the knee extensor muscle was measured using the Kin Com Isokinetic Dynamometer (Chattanooga group, Inc., Chattanooga, TN), which required multiple tests (32) (37). Participants did not have to exert their best efforts in the first 3 tests, which were used to learn movements and warm up (32). In the latter 3 trials, muscle strength was measured with maximum effort (32). If the participant completed 4–6 trials, the maximum peak force value was selected. When fewer than 4 trials were completed, the highest values of the remaining trials were used for analysis. The final test result was the peak force (Newton) of the quadriceps at one speed (60 degrees/second) (32). The gait speed test required participants to complete a timed 20 foot (6.1 m) walk at a normal pace (32). Participants could use canes or walkers if needed. The gait speed was then converted to meters per second (m/s) and used

for our analysis. The full information for these procedures is available on the NHANES website (32).

2.5 Covariates

The demographic and lifestyle characteristics of the participants were collected using a standardized questionnaire during the interview. Information on alcohol consumption, weight and height was obtained during physical examinations at a mobile examination center. Races was categorized as "Mexican American", "Other Hispanic", "non-Hispanic White", "non-Hispanic Black", and "other race" Educational attainment was classified as "less than high school", "high school graduate/general education development", and "more than high school". The family income to poverty ratio (PIR) is based on the ratio of household income to the poverty level set by the U.S. Department of Health and Human Services (37). PIR was classified as 0–1.0, 1.01–4.99 and 5.0, with higher PIR values indicating higher household income. Body mass index (BMI) values were obtained by calculating height and weight data from physical examination. Alcohol intake habits were based on the answer of "In the past 12 months, how often did you drink any type of alcoholic beverage?", and the participants were sorted into "never", "1–2 times", "3–10 times" and ">10 times". Smoking status was based on the answer of "Have you smoked at least 100 cigarettes in your entire life?" And "Do you now smoke cigarettes?". Participants were classified as "non-smoker", "former smoker" and "current smoker". "Non-smokers" were participants who had never smoked 100 cigarettes in their lives. "Former smokers" were defined as people who have smoked at least 100 cigarettes in their lifetime, but not currently smoking. "Current smokers" were defined as participants who had smoked at least 100 cigarettes in their lifetime and were still smoking. Physical activity was categorized on the answer of "Moderate activity over past 30 days?" Histories of hypertension, diabetes, renal impairment, liver impairment and cancer were defined as "yes" to the following questions: "Have you ever been told by a doctor or other health professional that you had hypertension, also called high blood pressure?", "Have you ever been told by a doctor or other health professional that you had diabetes or sugar diabetes?", "Have you ever been told by a doctor or other health professional that you had weak or failing kidneys?", "Has a doctor or other health professional ever told you that you had any kind of liver condition?" And "Have you ever been told by a doctor or other health professional that you had cancer or a malignancy of any kind?" Cardiovascular disease (CVD) is based on the answer of these questions: "Has a doctor or other health professional ever told you that you had congestive heart failure?", "Has a doctor or other health professional ever told you that you had coronary heart disease?", "Has a doctor or other health professional ever told you that you had angina, also called angina pectoris?" and "Has a doctor or other health professional ever told you that you had a heart attack (also called myocardial infarction)?" If the answer to any of these questions is "yes," the participant was judged as had CVD. Total vitamin B12 intake and vitamin K intake (μg/day) was measured through in-person dietary intake interviews conducted by trained visitors for the first 24 and 48 hours, and then averaged as final inclusion data. The family history of osteoporosis was based on the answer of "Including living and deceased, were any of your biological that is, blood relatives including grandparents, parents, brothers, sisters ever told by a health professional that they had osteoporosis or brittle bones?". Total serum calcium was determined using o-cresolphthalein complexone, which reacted with calcium in the presence of 8-hydroxyquinoline to form chromophore. The intensity of the color reaction was proportional to the amount of calcium in the sample. Serum 25-hydroxyvitamin D [25(OH) D] data from NHANES 2001–2002 have been converted by using regression to equivalent 25(OH) D measurements from standardized liquid chromatography-tandem mass spectrometry methods, and used for subsequent analysis. Serum folate concentration was measured using Bio-Rad Laboratories "Quantaphase II Folate/vitamin B12" radioassay kit (Bio-Rad Laboratories, 1993), same as serum vitamin B12. Details of Demographics Data (38), Dietary Data (39), Laboratory Data (40) and Questionnaire Data (41) can be obtained from the NHANES website.

2.6 Statistical methods

According to the analysis guidelines developed by NHANES (42), all analyses include sample weights to account for the complex survey design. All analyses were performed using R software (version 4.0.3, available at https://www.R-project.org). P value < 0.05 was considered statistically significant. Categorical variables are presented as frequency [percent (%)], while continuous variables are presented as median [interquartile range (IQR)]. Serum vitamin B12 and its biomarkers (homocysteine and MMA) were used as exposure. The musculoskeletal health was assessed using the following parameters: total BMD (g/cm^2), lumbar spine BMD (g/cm^2), femoral BMD (g/cm^2), total lean mass (g), appendicular lean mass (g), gait speed (m/s), and knee extensor strength (Newton). After evaluating the visual inspection of residuals of these data, we found that the linear regression fit was better when these exposures were logarithmically transformed. In the multivariate linear regression analysis, we established three models. Model 1 was an unadjusted model, and Model 2 was adjusted for age and sex. Model 3 was a fully adjusted model using variables selected according to the current literature. These variables included age, sex, race, alcohol consumption, smoking status, height, fat mass (%), physical activity, CVD, diabetes, cancer, liver impairment, kidney impairment, serum folate, serum 25(OH) D, total serum calcium and vitamin K intake. In 1999–2004, approximately 21% of NHANES participants eligible for DXA screening had all or part of their DXA data missing (43). The amount of missing DXA data is larger than other data files, and the missing data appear to have a systematic, non-random pattern. Therefore, the missing DXA data were imputed using the sequential regression imputation method, and a further description can be found in the NHANES document (43). All analyses were repeated in the full population and in a subgroup of older adults (≥65 years).

3 Results

3.1 Participant characteristics

The median age of participants was 64 (IQR: 56–73) years, with an equal distribution between males and females (50.48% and 49.52%, respectively). Table 1 shows the characteristics of participants in the full population (≥50 years of age) and the subgroup of older adults (≥65 years of age). The median serum vitamin B12 concentration was 352.76(263.65–467.70) pmol/L in the full population, and 353.13(260.51–471.95) pmol/L in the older adults subgroup. There was no significant difference in vitamin B12 and MMA concentrations between the subgroup and the full population (*P* values were 0.230 and 0.365, respectively), but the homocysteine levels in the elderly individuals were significantly higher than that in the full population ($P < 0.001$)). Except lumbar spine BMD, the total BMD, femur BMD, total lean mass, appendicular lean mass, gait speed and knee extensor strength of the elderly were lower than those of the full population ($P < 0.001$).

3.2 Associations between the serum vitamin B12 concentration and potential confounders

Supplementary Table 1 shows a univariate analysis of the association between serum vitamin B12 concentration and potential confounders (demographic, lifestyle, and clinical factors) in the full population. As expected, vitamin B12 levels were inversely correlated with the levels of homocysteine and MMA. Serum vitamin B12 concentration was associated with sex, race, height, weight, BMI, smoking status, vitamin B12 intake, total serum calcium, serum 25(OH)D, total fat mass, as well as certain diseases. Serum vitamin B12 concentrations were negatively correlated with height, weight, and BMI, and positively correlated with vitamin B12 intake, total serum calcium, serum 25(OH)D and total fat mass. In addition, vitamin B12 concentrations were higher in women, Mexican Americans, and non-smokers, and lower in participants with cancer and CVD.

TABLE 1 Participant characteristics in the full population (≥ 50 years) and older adults (≥ 65 years).

Variable	Full population (≥ 50 years)	Older adults (≥ 65 years)	*P* value
Vitamin B12 (pmol/L)	352.76 (263.65–467.70)	353.13 (260.51–471.95)	0.230
Homocysteine (μmol/L)	9.15 (7.59–11.26)	9.84 (8.17–12.15)	**<0.001**
Methylmalonic acid (μmol/L)	0.14 (0.11–0.19)	0.16 (0.12–0.21)	0.365
Total BMD (g/cm2)	1.09 (1.00–1.19)	1.05 (0.95–1.16)	**<0.001**
Lumbar Spine BMD (g/cm2)	0.99 (0.88–1.12)	0.97 (0.85–1.12)	0.142
Femur BMD (g/cm2)	1.14 (1.02–1.26)	1.10 (0.97–1.24)	**<0.001**
Total lean mass (g)	47600 (39163–57532)	45134 (37817–53979)	**<0.001**
Appendicular lean mass (g)	20366 (16115–24968)	19094 (15377–23236)	**<0.001**
Knee extensor strength (N)	253.6 (196.8–318.6)	224.6 (175.6–282.6)	**<0.001**
Gait speed (m/s)	1.02 (0.87–1.18)	0.96 (0.80–1.10)	**<0.001**

BMD, bone mineral density. P values were obtained by inter group comparison between the fall population and the older adults subgroup. Bolded values statistically significant.

3.3 Associations between the serum vitamin B12 concentration and outcome measures

Serum vitamin B12 concentration was associated with lumbar spine BMD, femur BMD, total lean mass, appendicular lean mass, and knee extensor strength (all *P* values < 0.05; Table 2). After adjusting for age and sex, serum vitamin B12 concentration was only associated with total lean mass and appendicular lean mass. According to the fully adjusted model, there was no significant correlation between serum vitamin B12 concentration and outcomes in the full population. In the subgroup analysis of older adults over 65 years, the association between serum vitamin B12 and total lean mass, appendicular lean mass remained in the fully adjusted model (β = 584.83, 95%CI 14.84, 1154.73, $P = 0.044$; β = 291.65,95% CI 8.68,574.60, $P = 0.043$) (Table 3). As for bone outcomes, there was no significant association between serum vitamin B12 concentration and total BMD, lumbar spine BMD, or femur BMD in the fully adjusted model.

3.4 Associations between plasma homocysteine levels and outcome measures

In the full population, homocysteine levels were inversely associated with total lean mass, appendicular lean mass, gait speed, and knee extensor strength after full adjustment for covariates (all *P* values < 0.05) (Table 4). According to the results of the subgroup analysis of older adults, homocysteine concentrations were associated with gait speed and knee extensor strength in the fully adjusted model (β = -0.06, 95% CI -0.10, -0.03, P <0.001; β = -12.75, 95%CI-23.17, -2.35, $P = 0.019$) (Table 5). In addition, there were no significant correlations between homocysteine levels and BMD in the full population and subgroup of older adults.

3.5 Associations between the plasma MMA concentration and outcome measures

According to the fully adjusted model, MMA concentration was negatively correlated with total BMD and femur BMD (β = -0.01, 95%CI -0.02, -0.00, $P = 0.018$; β = -0.01, 95%CI -0.02, -0.00, P = 0.004) (Table 6). The associations between MMA and total BMD,

10.3389/fendo.2024.1387035

TABLE 2 Multivariate associations between vitamin B12 concentrations and outcome measures in the full population (≥ 50 years).

Variable	Model 1		Model 2		Model 3	
	β [95% CI]	*P* value	β [95% CI]	*P* value	β [95% CI]	*P* value
Total BMD (g/cm2)	0.01 [-0.00, 0.02]	0.115	0.00 [-0.01, 0.01]	0.659	0.00 [-0.01, 0.01]	0.705
Lumbar Spine BMD (g/cm2)	0.02 [0.01, 0.03]	**0.009**	0.01 [-0.00, 0.03]	0.091	0.01 [-0.01, 0.02]	0.210
Femur BMD (g/cm2)	0.02 [0.00, 0.03]	**0.014**	0.00 [-0.01, 0.01]	0.866	0.00 [-0.01, 0.01]	0.668
Total lean mass (g)	1957.45 [1142.74,2771.75]	**<0.001**	788.89 [264.61,1313.16]	**0.003**	229.03 [-193.06,651.15]	0.285
Appendicular lean mass (g)	889.45 [483.92, 1294.97]	**<0.001**	320.98 [57.76, 584.21]	**0.017**	98.02 [-118.78,314.79]	0.376
Knee extensor strength (N)	6.51 [0.05, 12.98]	**0.048**	1.15 [-3.98, 6.28]	0.660	2.00 [-3.36, 7.37]	0.468
Gait speed (m/s)	0.00 [-0.02, 0.02]	0.785	0.00 [-0.01, 0.02]	0.776	-0.00 [-0.02, 0.02]	0.912

BMD, bone mineral density. The coefficient (β) with 95% CI represents the percentage difference in the variable as vitamin B12 increases for 1-fold. Model 1, unadjusted; Model 2, adjusted for age and sex. Model 3, age, sex, race, smoking status, alcohol intake, height, fat mass (%), physical activity, cardiovascular disease, diabetes, cancer, liver impairment, renal impairment, serum folate, serum 25(OH) D, total serum calcium and vitamin K intake. All regressions were also accounted for complex survey design using the sampling weights provided. Bolded values statistically significant.

femur BMD and knee extensor strength were maintained in a fully adjusted model of subgroup analysis of older adults (β = -0.01,95% CI -0.02, 0.00, *P* = 0.048; β = -0.01,95% CI -0.03, -0.00, *P* = 0.025; β = -7.53,95% CI-14.10, -0.14, *P* = 0.015) (Table 7).

4 Discussion

In this study, we found that the association between serum vitamin B12 concentration and musculoskeletal health was only present in older adults. In people over 60 years of age, vitamin B12 was associated with total and appendicular lean mass. Homocysteine levels were inversely associated with muscle strength and physical function, total and appendicular lean mass. A similar association was observed in our subgroup analysis of older adults over 65 years of age. The MMA levels were negatively correlated with total BMD and femur BMD in the full population. In the elderly population, MMA was inversely associated with total BMD, femur BMD and knee extensor strength. Notably, this is the first study to report the

TABLE 3 Multivariate associations between vitamin B12 concentrations and outcome measures in older adults (≥ 65 years).

Variable	Model 1		Model 2		Model 3	
	β [95% CI]	*P* value	β [95% CI]	*P* value	β [95% CI]	*P* value
Total BMD (g/cm2)	-0.01 [-0.03, 0.00]	0.153	0.01 [-0.00, 0.02]	0.167	0.01 [-0.01, 0.02]	0.293
Lumbar Spine BMD (g/cm2)	-0.02 [-0.04, 0.00]	0.0616	-0.00 [-0.02, 0.02]	0.753	0.01 [-0.02, 0.03]	0.603
Femur BMD (g/cm2)	-0.02 [-0.04, -0.00]	**0.0197**	0.01 [-0.01, 0.02]	0.344	0.01 [-0.01, 0.02]	0.348
Total lean mass (g)	2459.49 [1391.87, 3527.08]	**<0.001**	832.94 [137.78, 1528.10]	**0.019**	584.83 [14.84, 1154.73]	**0.044**
Appendicular lean mass (g)	1111.74 [588.49, 1634.97]	**<0.001**	331.48 [-13.07, 676.04]	**0.050**	291.65 [8.68, 574.60]	**0.043**
Knee extensor strength (N)	9.17 [1.25, 17.09]	**0.023**	2.89 [-3.75, 9.53]	0.393	5.90 [-1.01, 12.85]	0.089
Gait speed (m/s)	0.00 [-0.02, 0.03]	0.813	-0.00 [-0.03, 0.02]	0.839	0.01 [-0.01, 0.03]	0.380

BMD, bone mineral density. The coefficient (β) with 95% CI represents the percentage difference in the variable as vitamin B12 increases for 1-fold. Model 1, unadjusted; Model 2, adjusted for age and sex; Model 3, age, sex, race, smoking status, alcohol intake, height, fat mass (%), physical activity, cardiovascular disease, diabetes, cancer, liver impairment, renal impairment, serum folate, serum 25(OH) D, total serum calcium and vitamin K intake. All regressions were also accounted for complex survey design using sampling weights provided. Bolded values statistically significant.

10.3389/fendo.2024.1387035

TABLE 4 Multivariate associations between homocysteine levels and outcome measures in the full population (≥ 50 years).

Variable	Model 1		Model 2		Model3	
	β [95% CI]	*P* value	β [95% CI]	*P* value	β [95% CI]	*P* value
Total BMD (g/cm2)	0.01 [-0.01, 0.02]	0.267	0.00 [-0.01, 0.01]	0.920	-0.01 [-0.02, 0.01]	0.435
Lumbar Spine BMD (g/cm2)	0.03 [0.01, 0.05]	**0.002**	0.02 [-0.00, 0.04]	0.071	0.00 [-0.02, 0.03]	0.789
Femur BMD (g/cm2)	0.02 [0.01, 0.04]	**0.010**	-0.00 [-0.02, 0.01]	0.652	-0.01 [-0.03, 0.00]	0.090
Total lean mass (g)	2518.41 [1308.60, 3728.29]	**<0.001**	570.28 [-265.93, 1406.49]	0.181	-860.15 [-1535.85, -184.45]	**0.015**
Appendicular lean mass (g)	1126.36 [524.00, 1728.69]	**<0.001**	281.67 [-137.61, 700.94]	0.188	-442.82 [-789.92, -95.67]	**0.013**
Knee extensor strength (N)	-17.59 [-27.15, -8.04]	**<0.001**	-14.08 [-22.21, -5.95]	**<0.001**	-9.65 [-18.28, -1.03]	**0.028**
Gait speed (m/s)	-0.13 [-0.16, -0.11]	**<0.001**	-0.08 [-0.11, -0.06]	**<0.001**	-0.06 [-0.08, -0.03]	**<0.001**

BMD, bone mineral density. The coefficient (β) with 95% CI represents the percentage difference in the variable as vitamin B12 increases for 1-fold. Model 1, unadjusted; Model 2, adjusted for age and sex; Model 3, age, sex, race, smoking status, alcohol intake, height, fat mass (%), physical activity, cardiovascular disease, diabetes, cancer, liver impairment, renal impairment, serum folate, serum 25 (OH) D, total serum calcium and vitamin K intake. All regressions were also accounted for complex survey design using sampling weights provided. Bolded values statistically significant.

relationship between vitamin B12 and its biomarkers and musculoskeletal health in the same cohort.

Ates Bulut et al. conducted a prospective study and found that lean mass, total bone mass and skeletal muscle mass index in the vitamin B12 insufficient group were lower than those in the vitamin B12 sufficient group in the elderly over 60 years of age (44). A study of 2325 adults aged 70–84 years by Chae et al. found that vitamin B12 deficiency was associated with decreased muscle mass, but not with the incidence of sarcopenia and decreased physical function (45). Our study also found an association between B12 deficiency and lower lean mass. However, sarcopenia is characterized not only by low muscle mass, but also by decreased muscle strength and function. Whether there is a direct relationship between vitamin B12 and sarcopenia incidence remains controversial. A case-control study by Verlaan et al. showed that serum vitamin B12 levels were 15% lower in patients with sarcopenia than those in the control group, but the causal relationship remained unclear (25). In a study of 427 hospitalized older adults aged ≥80 years, Tao et al. found that serum vitamin B12 levels had no effect on the incidence of sarcopenia (46). Another study of 731 community-dwelling adults aged ≥65 years investigated the impact of nutritional factors on sarcopenia, and found no correlation between vitamin B12 and muscle mass (47). Singh et al. found that changes in vitamin B12 metabolism generally have little impact on muscle mass and function compared to bone (48). The relationship between vitamin B12 and sarcopenia, including muscle mass and muscle function, is not well understood. Our population-based study provides evidence that vitamin B12 levels affect lean mass. However, further studies are needed to more fully and thoroughly investigate the effects of vitamin B12 on the development of sarcopenia.

Our study found that homocysteine levels were negatively correlated with muscle strength, body function, total lean mass and appendicular lean mass. There are several possible explanations for the differences in muscle strength and physical function associated with hyperhomocysteinemia. Firstly, hyperhomocysteinemia may disrupt the structural integrity of elastin, collagen and proteoglycans, leading to decreased muscle strength (18). In addition, hyperhomocysteinemia may cause angiotoxicity and atherosclerosis by targeting vascular smooth muscle, endothelial cells and thrombocytes, leading to muscle atrophy and decreased muscle strength (27). Secondly, hyperhomocysteinemia can increase

TABLE 5 Multivariate associations between homocysteine levels and outcome measures in older adults (≥ 65 years).

Variable	Model 1		Model 2		Model3	
	β [95% CI]	*P* value	β [95% CI]	*P* value	β [95% CI]	*P* value
Total BMD (g/cm2)	0.02 [-0.01, 0.04]	0.132	-0.00 [-0.02, 0.01]	0.673	-0.01 [-0.03, 0.01]	0.352
Lumbar Spine BMD (g/cm2)	0.05 [0.02, 0.08]	**0.002**	-0.02 [-0.01, 0.04]	0.319	-0.00 [-0.03, 0.03]	0.996
Femur BMD (g/cm2)	0.03 [-0.00, 0.05]	0.058	-0.01 [-0.03, 0.01]	0.419	-0.02 [-0.04, 0.00]	0.097
Total lean mass (g)	2206.98 [687.32, 3727.32]	**0.004**	534.65 [-490.06, 1559.35]	0.306	-763.95 [-1619.90, 92.12]	0.083
Appendicular lean mass (g)	1016.99 [273.02, 1760.92]	**0.007**	268.45 [-238.31, -775.21]	0.299	-377.65 [-815.07, 59.81]	0.095
Knee extensor strength (N)	-14.34 [-25.52, -3.16]	**0.012**	-13.51 [-23.22, -3.79]	**0.007**	-12.75 [-23.17, -2.35]	**0.019**
Gait speed (m/s)	-0.11 [-0.14, -0.07]	**<0.001**	-0.08 [-0.12, -0.05]	**<0.001**	-0.06 [-0.10, -0.03]	**<0.001**

BMD, bone mineral density. The coefficient (β) with 95% CI represents the percentage difference in the variable as vitamin B12 increases for 1-fold. Model 1, unadjusted; Model 2, adjusted for age and sex; Model 3, age, sex, race, smoking status, alcohol intake, height, fat mass (%), physical activity, cardiovascular disease, diabetes, cancer, liver impairment, renal impairment, serum folate, serum 25 (OH) D, total serum calcium and vitamin K intake. All regressions were also accounted for complex survey design using sampling weights provided. Bolded values statistically significant.

10.3389/fendo.2024.1387035

TABLE 6 Multivariate associations between methylmalonic acid levels and outcome measures in the full population (≥ 50 years).

Variable	Model 1		Model 2		Model3	
	β [95% CI]	*P* value	β [95% CI]	*P* value	β [95% CI]	*P* value
Total BMD (g/cm2)	-0.02 [-0.03, -0.01]	**<0.001**	-0.01 [-0.02, -0.00]	**0.008**	-0.01 [-0.02, -0.00]	**0.018**
Lumbar Spine BMD (g/cm2)	-0.00 [-0.02, 0.01]	0.829	0.00 [-0.01, 0.01]	0.972	0.00 [-0.01, 0.02]	0.873
Femur BMD (g/cm2)	-0.02 [-0.03, -0.01]	**<0.001**	-0.01 [-0.02, -0.00]	**0.007**	-0.01 [-0.02, -0.00]	**0.004**
Total lean mass (g)	-674.16 [-1505.59, 157.30]	0.112	8.61 [-549.94, 567.16]	0.976	-197.17 [-646.12, 252.05]	0.392
Appendicular lean mass (g)	-477.86 [-890.89, -64.84]	**0.0234**	-79.78 [-359.84, 200.28]	0.576	-133.35 [-363.85, 97.17]	0.255
Knee extensor strength (N)	-19.49 [-25.97, -13.01]	**<0.001**	-6.07 [-11.50, -0.64]	**0.028**	-4.96 [-10.67, 0.74]	0.095
Gait speed (m/s)	-0.06 [-0.08, -0.05]	**<0.001**	-0.02 [-0.04, -0.00]	**0.019**	-0.02 [-0.03, 0.00]	0.089

BMD, bone mineral density. The coefficient (β) with 95% CI represents the percentage difference in the variable as vitamin B12 increases for 1-fold. Model 1, unadjusted; Model 2, adjusted for age and sex; Model 3, age, sex, race, smoking status, alcohol intake, height, fat mass (%), physical activity, cardiovascular disease, diabetes, cancer, liver impairment, renal impairment, serum folate, serum 25(OH) D, total serum calcium and vitamin K intake. All regressions were also accounted for complex survey design using sampling weights provided. Bolded values statistically significant.

the release of reactive oxygen species, which may lead to mitochondrial damage and subsequent inflammation (49). Hyperhomocysteinemia reduces nitric oxide bioavailability and blood flow to muscle cells, which may also contribute to muscle mass (50). In fact, several clinical studies have shown a negative effect of hyperhomocysteinemia on muscle mass and physical function. In the Baltimore Longitudinal Study of Aging, homocysteine levels in healthy women over 50 years of age were negatively correlated with grip strength and gait speed (51). Kirk et al. also reported negative effect of homocysteine on lower limb muscle strength and physical function, and can further cause falls and fractures (52).

Sarcopenia is defined as a geriatric syndrome associated with decreased muscle mass, muscle strength, and/or physical function (53). The main parameters currently available for diagnosis and assessment of sarcopenia are lean mass, muscle strength, and physical function. To date, it has been unclear whether vitamin B12 and its biomarkers are associated with specific components of sarcopenia. Our study suggested that vitamin B12 and its biomarkers were associated with different aspects of sarcopenia, possibly because homocysteine and MMA can affect muscle health in ways independent of vitamin B12. Further studies can use magnetic resonance imaging or high-resolution computed tomography to directly measure the muscle mass/volume to get more accurate conclusions.

In our study, we found that MMA levels were primarily associated with BMD. In the full population and elderly subgroup analysis, we found a negative association between MMA concentration and total BMD and femur BMD. At present, the exact relationship between vitamin B12 metabolism and bone health is not fully established. The results of preclinical studies on the effects of vitamin B12 on bone are also inconsistent. Decreased vitamin B12 concentration and subsequent increased levels of homocysteine and MMA have different effects on multiple intracellular pathways (54). A study by Bailey et al. have shown that vitamin B12 can have an impact on bone health through multiple pathways, including increasing osteoclast formation, altering osteoblast function, and regulating collagen crosslinking (55). Roman-Garcia et al. reported that vitamin B12 deficiency caused stunted growth and decreased bone mass in mice, and that this phenomenon was not due to the accumulation of MMA or homocysteine (54). The authors speculate that it was down-regulated due to the production of other vitamin B12 dependent

TABLE 7 Multivariate associations between methylmalonic acid levels and outcome measures in older adults (≥ 65 years).

Variable	Model 1		Model 2		Model3	
	β [95% CI]	*P* value	β [95% CI]	*P* value	β [95% CI]	*P* value
Total BMD (g/cm2)	-0.01 [-0.03, 0.00]	0.090	-0.01 [-0.02, 0.00]	0.064	-0.01 [-0.02, 0.00]	**0.048**
Lumbar Spine BMD (g/cm2)	0.01 [-0.01, 0.03]	0.196	0.01 [-0.01, 0.02]	0.617	0.00 [-0.02, 0.02]	0.683
Femur BMD (g/cm2)	-0.01 [-0.03, 0.01]	0.174	-0.01 [-0.02, 0.00]	0.056	-0.01 [-0.03, -0.00]	**0.025**
Total lean mass (g)	-136.20 [-1106.79, 834.34]	0.783	33.43 [-605.30, 672.16]	0.918	-296.73 [-830.35, 237.09]	0.289
Appendicular lean mass (g)	-169.82 [-644.58, 304.89]	0.483	-58.08 [-374.22, 258.07]	0.718	-245.63 [-518.03, 26.85]	0.083
Knee extensor strength (N)	-14.08 [-21.14, -7.01]	**<0.001**	-8.00 [-14.06, -1.95]	**0.010**	-7.53 [-14.10, -0.14]	**0.015**
Gait speed (m/s)	-0.04 [-0.07, -0.02]	**<0.001**	-0.02 [-0.04, -0.00]	**0.042**	-0.02 [-0.04, 0.00]	0.237

BMD, bone mineral density. The coefficient (β) with 95% CI represents the percentage difference in the variable as vitamin B12 increases for 1-fold. Model 1, unadjusted; Model 2, adjusted for age and sex; Model 3, age, sex, race, smoking status, alcohol intake, height, fat mass (%), physical activity, cardiovascular disease, diabetes, cancer, liver impairment, renal impairment, serum folate, serum 25(OH) D, total serum calcium and vitamin K intake. All regressions were also accounted for complex survey design using sampling weights provided. Bolded values statistically significant.

downstream metabolites (54). Kim et al. used vitamin B12 to stimulate two osteosarcoma cell lines and found functional and dose-dependent proliferative responses, suggesting that vitamin B12 can directly inhibit osteoblast activity (56). In a model of mouse fracture healing, vitamin B12 deficiency, although causing hyperhomocysteinemia, had no effect on fracture repair (57). Singh et al. noted that in mouse models, vitamin B12 deficiency affected parameters including thickness, number and connectivity of trabeculae, as well as cortical thickness and porosity (48). The structural deterioration of cortical and trabecular bone led to a substantial decrease in the density and content of bone minerals in the whole body, further leading to a decline in the biomechanical properties of long bone (48). A Study by Herrmann et al. showed that vitamin B12 deficiency stimulated osteoclasts in a homocysteine-dependent manner, but did not affect osteoblasts (58). However, the authors also found that prolonged vitamin B12 deficiency induced significant homocysteine accumulation in healthy rats, and that these metabolic changes had no adverse effects on bone (58). At present, there is no clear conclusion on the exact relationship between vitamin B12 and bone metabolism, and there are few studies on the relationship between MMA and musculoskeletal health. Our study showed that MMA is inversely associated with total BMD and femur BMD. Some studies have shown that increased MMA concentrations were more strongly associated with poor functional performance than serum vitamin B12 (59). NHANES has also been aware of this problem and, in a roundtable, clarified that MMA concentrations were more reflective of early vitamin B12 status and marginal vitamin B12 deficiency than serum vitamin B12 (60). This could also explain why MMA concentrations were significantly negatively associated with BMD, while vitamin B12 levels were not.

This study has some advantages and limitations. The data for this study came from NHANES, which underwent robust quality assurance and control procedures. The NHANES study included a large representative sample, so there is less potential for sampling bias. In addition, our analysis took into account various factors known to influence vitamin B12 and its metabolic markers and musculoskeletal health. Therefore, our study can better eliminate confounding factors that may appear in multiple regression models. Moreover, this study included 1,466 participants and was more capable of produce meaningful results due to the large sample size provided by NHANES. The main limit of this study is that cross-sectional studies cannot explain causality, and follow-up prospective cohort studies should be conducted to verify these findings. Second, there are residual confounding factors that cannot be eliminated in population-based studies. Finally, current evaluation parameters for musculoskeletal health are still not specific enough, and more accurate measurements of muscle mass/function and bone structure are needed to strengthen our ability to examine the relationship between vitamin B12 and musculoskeletal health.

In this nationally representative sample of middle-aged and older adults, we found that vitamin B12 was associated with total and appendicular lean mass in adults over 60 years of age. Homocysteine levels were inversely associated with muscle strength/physical function, total lean mass, and appendicular lean mass. The MMA concentrations were negatively correlated with total BMD and femur BMD. In general, vitamin B12 and its biomarkers are closely related to musculoskeletal status in middle-aged and elderly people. These three indicators may reflect different changes in BMD, body composition and physical function, respectively, and can be used as important indicators of musculoskeletal health status in elderly people. Further researches are needed to determine the possible mechanisms behind this phenomenon. In addition, more prospective studies are needed to investigate the relationship between vitamin B12 and BMD, muscle strength, and physical function.

Data availability statement

The original contributions presented in the study are included in the article/Supplementary Material. Further inquiries can be directed to the corresponding author.

Ethics statement

The institutional review board approved the NHANES protocol of the Centers for Disease Control and Prevention (CDC). The studies were conducted in accordance with the local legislation and institutional requirements. The participants provided their written informed consent to participate in this study.

Author contributions

JZ: Data curation, Investigation, Writing – original draft. QL: Formal analysis, Methodology, Writing – original draft. XZ: Funding acquisition, Supervision, Writing – review & editing.

Funding

The author(s) declare that financial support was received for the research, authorship, and/or publication of this article. This research was funded by the Science and Technology Development Project of Hangzhou, grant number 20191203B83.

Acknowledgments

The authors acknowledge the NHANES. The NHANES survey data are available publicly. The institutional review board approved the NHANES protocol of the Centers for Disease Control and Prevention (CDC), and each participant provided written informed consent.

Conflict of interest

The authors declare that the research was conducted in the absence of any commercial or financial relationships that could be construed as a potential conflict of interest.

Publisher's note

All claims expressed in this article are solely those of the authors and do not necessarily represent those of their affiliated organizations, or those of the publisher, the editors and the reviewers. Any product that may be evaluated in this article, or claim that may be made by its manufacturer, is not guaranteed or endorsed by the publisher.

Supplementary material

The Supplementary Material for this article can be found online at: https://www.frontiersin.org/articles/10.3389/fendo.2024.1387035/full#supplementary-material

References

1. Hughes CF, Ward M, Hoey L, McNulty H. Vitamin B12 and ageing: current issues and interaction with folate. *Ann Clin Biochem*. (2013) 50:315–29. doi: 10.1177/0004563212473279

2. Hoey L, Strain JJ, McNulty H. Studies of biomarker responses to intervention with vitamin B-12: a systematic review of randomized controlled trials. *Am J Clin Nutr*. (2009) 89:1981s–96s. doi: 10.3945/ajcn.2009.27230C

3. Chatthanawaree W. Biomarkers of cobalamin (vitamin B12) deficiency and its application. *J Nutr Health Aging*. (2011) 15:227–31. doi: 10.1007/s12603-010-0280-x

4. Yajnik CS, Deshmukh US. Fetal programming: maternal nutrition and role of one-carbon metabolism. *Rev Endocr Metab Disord*. (2012) 13:121–7. doi: 10.1007/s11154-012-9214-8

5. Rafnsson SB, Saravanan P, Bhopal RS, Yajnik CS. Is a low blood level of vitamin B12 a cardiovascular and diabetes risk factor? A systematic review of cohort studies. *Eur J Nutr*. (2011) 50:97–106. doi: 10.1007/s00394-010-0119-6

6. Dhonukshe-Rutten RA, Pluijm SM, de Groot LC, Lips P, Smit JH, van Staveren WA. Homocysteine and vitamin B12 status relate to bone turnover markers, broadband ultrasound attenuation, and fractures in healthy elderly people. *J Bone Miner Res*. (2005) 20:921–9. doi: 10.1359/JBMR.050202

7. Clarke R, Birks J, Nexo E, Ueland PM, Schneede J, Scott J, et al. Low vitamin B-12 status and risk of cognitive decline in older adults. *Am J Clin Nutr*. (2007) 86:1384–91. doi: 10.1093/ajcn/86.5.1384

8. Mithal A, Bonjour JP, Boonen S, Burckhardt P, Degens H, El Hajj Fuleihan G, et al. Impact of nutrition on muscle mass, strength, and performance in older adults. *Osteoporos Int*. (2013) 24:1555–66. doi: 10.1007/s00198-012-2236-y

9. van Schoor NM, Swart KM, Pluijm SM, Visser M, Simsek S, Smulders Y, et al. Cross-sectional and longitudinal association between homocysteine, vitamin B12 and physical performance in older persons. *Eur J Clin Nutr*. (2012) 66:174–81. doi: 10.1038/ejcn.2011.151

10. Dai Z, Koh WP. B-vitamins and bone health–a review of the current evidence. *Nutrients*. (2015) 7:3322–46. doi: 10.3390/nu7053322

11. Gjesdal CG, Vollset SE, Ueland PM, Refsum H, Meyer HE, Tell GS. Plasma homocysteine, folate, and vitamin B 12 and the risk of hip fracture: the hordaland homocysteine study. *J Bone Miner Res*. (2007) 22:747–56. doi: 10.1359/jbmr.070210

12. Gerdhem P, Ivaska KK, Isaksson A, Pettersson K, Väänänen HK, Obrant KJ, et al. Associations between homocysteine, bone turnover, BMD, mortality, and fracture risk in elderly women. *J Bone Miner Res*. (2007) 22:127–34. doi: 10.1359/jbmr.061003

13. Clarke M, Ward M, Dickey W, Hoey L, Molloy AM, Waldron L, et al. B-vitamin status in relation to bone mineral density in treated celiac disease patients. *Scand J Gastroenterol*. (2015) 50:975–84. doi: 10.3109/00365521.2015.1015603

14. Bozkurt N, Erdem M, Yilmaz E, Erdem A, Biri A, Kubatova A, et al. The relationship of homocyteine, B12 and folic acid with the bone mineral density of the femur and lumbar spine in Turkish postmenopausal women. *Arch Gynecol Obstet*. (2009) 280:381–7. doi: 10.1007/s00404-009-0936-0

15. McLean RR, Jacques PF, Selhub J, Fredman L, Tucker KL, Samelson EJ, et al. Plasma B vitamins, homocysteine, and their relation with bone loss and hip fracture in elderly men and women. *J Clin Endocrinol Metab*. (2008) 93:2206–12. doi: 10.1210/jc.2007-2710

16. Morris MS, Jacques PF, Selhub J. Relation between homocysteine and B-vitamin status indicators and bone mineral density in older Americans. *Bone*. (2005) 37:234–42. doi: 10.1016/j.bone.2005.04.017

17. Gjesdal CG, Vollset SE, Ueland PM, Refsum H, Drevon CA, Gjessing HK, et al. Plasma total homocysteine level and bone mineral density: the Hordaland Homocysteine Study. *Arch Intern Med*. (2006) 166:88–94. doi: 10.1001/archinte.166.1.88

18. van Wijngaarden JP, Doets EL, Szczecińska A, Souverein OW, Duffy ME, Dullemeijer C, et al. Vitamin B12, folate, homocysteine, and bone health in adults and elderly people: a systematic review with meta-analyses. *J Nutr Metab*. (2013) 2013:486186. doi: 10.1155/2013/486186

19. Herrmann M, Umanskaya N, Traber L, Schmidt-Gayk H, Menke W, Lanzer G, et al. The effect of B-vitamins on biochemical bone turnover markers and bone mineral density in osteoporotic patients: a 1-year double blind placebo controlled trial. *Clin Chem Lab Med*. (2007) 45:1785–92. doi: 10.1515/CCLM.2007.352

20. Rumbak I, Zižić V, Sokolić L, Cvijetić S, Kajfež R, Colić Barić I. Bone mineral density is not associated with homocysteine level, folate and vitamin B12 status. *Arch Gynecol Obstet*. (2012) 285:991–1000. doi: 10.1007/s00404-011-2079-3

21. Holstein JH, Herrmann M, Splett C, Herrmann W, Garcia P, Histing T, et al. Low serum folate and vitamin B-6 are associated with an altered cancellous bone structure in humans. *Am J Clin Nutr*. (2009) 90:1440–5. doi: 10.3945/ajcn.2009.28116

22. Bailey RL, Looker AC, Lu Z, Fan R, Eicher-Miller HA, Fakhouri TH, et al. B-vitamin status and bone mineral density and risk of lumbar osteoporosis in older females in the United States. *Am J Clin Nutr*. (2015) 102:687–94. doi: 10.3945/ajcn.115.108787

23. Green TJ, McMahon JA, Skeaff CM, Williams SM, Whiting SJ. Lowering homocysteine with B vitamins has no effect on biomarkers of bone turnover in older persons: a 2-y randomized controlled trial. *Am J Clin Nutr*. (2007) 85:460–4. doi: 10.1093/ajcn/85.2.460

24. Sawka AM, Ray JG, Yi Q, Josse RG, Lonn E. Randomized clinical trial of homocysteine level lowering therapy and fractures. *Arch Intern Med*. (2007) 167:2136–9. doi: 10.1001/archinte.167.19.2136

25. Verlaan S, Aspray TJ, Bauer JM, Cederholm T, Hemsworth J, Hill TR, et al. Nutritional status, body composition, and quality of life in community-dwelling sarcopenic and non-sarcopenic older adults: A case-control study. *Clin Nutr*. (2017) 36:267–74. doi: 10.1016/j.clnu.2015.11.013

26. Matteini AM, Walston JD, Fallin MD, Bandeen-Roche K, Kao WH, Semba RD, et al. Markers of B-vitamin deficiency and frailty in older women. *J Nutr Health Aging*. (2008) 12:303–8. doi: 10.1007/BF02982659

27. Kuo HK, Liao KC, Leveille SG, Bean JF, Yen CJ, Chen JH, et al. Relationship of homocysteine levels to quadriceps strength, gait speed, and late-life disability in older adults. *J Gerontol A Biol Sci Med Sci*. (2007) 62:434–9. doi: 10.1093/gerona/62.4.434

28. Swart KM, van Schoor NM, Heymans MW, Schaap LA, den Heijer M, Lips P. Elevated homocysteine levels are associated with low muscle strength and functional limitations in older persons. *J Nutr Health Aging*. (2013) 17:578–84. doi: 10.1007/s12603-013-0047-2

29. Swart KM, van Schoor NM, Lips P. Vitamin B12, folic acid, and bone. *Curr osteoporosis Rep*. (2013) 11:213–8. doi: 10.1007/s11914-013-0155-2

30. Kirk B, Duque G. Muscle and bone: an indissoluble union. *J Bone Miner Res*. (2022) 37:1211–12. doi: 10.1002/jbmr.4626

31. Dual-energy X-ray absorptiometry (2023). Available online at: https://wwwn.cdc.gov/nchs/nhanes/dxa/dxa.aspx.

32. Muscle strength (2023). Available online at: https://wwwn.cdc.gov/Nchs/Nhanes/2001–2002/MSX_B.htm.

33. Folate/vitamin B12 in serum and whole blood (2023). Available online at: https://wwwn.cdc.gov/nchs/data/nhanes/2001–2002/labmethods/l06_b_met_folate_b12.pdf.

34. Total homocysteine in plasma (2023). Available online at: https://wwwn.cdc.gov/nchs/data/nhanes/2001–2002/labmethods/l06_b_met_homocysteine_axsym.pdf.

35. Lonati S, Novembrino C, Ippolito S, Accinni R, Galli C, Troonen H, et al. Analytical performance and method comparison study of the total homocysteine

fluorescence polarization immunoassay (FPIA) on the AxSYM analyzer. *Clin Chem Lab Med*. (2004) 42:228–34. doi: 10.1515/CCLM.2004.041

36. Methylmalonic acid (MMA) in Plasma or Serum. (2023). Available online at: https://wwwn.cdc.gov/nchs/data/nhanes/2001–2002/labmethods/l06_b_met_methylmalonic_acid.pdf.

37. Smith J, Jain N, Normington J, Holschuh N, Zhu Y. Associations of ready-to-eat cereal consumption and income with dietary outcomes: results from the national health and nutrition examination survey 2015–2018. *Front Nutr*. (2022) 9:816548. doi: 10.3389/fnut.2022.816548

38. Demographics data (2023). Available online at: https://wwwn.cdc.gov/nchs/nhanes/search/datapage.aspx?Component=Demographics&CycleBeginYear=2001.

39. Dietary data (2023). Available online at: https://wwwn.cdc.gov/nchs/nhanes/search/datapage.aspx?Component=Dietary&CycleBeginYear=2001.

40. Laboratory data . Available online at: https://wwwn.cdc.gov/nchs/nhanes/search/datapage.aspx?Component=Laboratory&CycleBeginYear=2001.

41. Questionnaire Data. (2023). Available online at: https://wwwn.cdc.gov/nchs/nhanes/search/datapage.aspx?Component=Questionnaire&CycleBeginYear=2001.

42. Weighting (2023). Available online at: https://wwwn.cdc.gov/nchs/nhanes/tutorials/module3.aspx.

43. Schenker N, Borrud LG, Burt VL, Curtin LR, Flegal KM, Hughes J, et al. Multiple imputation of missing dual-energy X-ray absorptiometry data in the National Health and Nutrition Examination Survey. *Stat Med*. (2011) 30:260–76. doi: 10.1002/sim.4080

44. Ates Bulut E, Soysal P, Aydin AE, Dokuzlar O, Kocyigit SE, Isik AT. Vitamin B12 deficiency might be related to sarcopenia in older adults. *Exp Gerontol*. (2017) 95:136–40. doi: 10.1016/j.exger.2017.05.017

45. Chae SA, Kim HS, Lee JH, Yun DH, Chon J, Yoo MC, et al. Impact of vitamin B12 insufficiency on sarcopenia in community-dwelling older korean adults. *Int J Environ Res Public Health*. (2021) 18:12433. doi: 10.3390/ijerph182312433

46. Tao J, Ke YY, Zhang Z, Zhang Y, Wang YY, Ren CX, et al. Comparison of the value of malnutrition and sarcopenia for predicting mortality in hospitalized old adults over 80 years. *Exp Gerontol*. (2020) 138:111007. doi: 10.1016/j.exger.2020.111007

47. Kuo YH, Wang TF, Liu LK, Lee WJ, Peng LN, Chen LK. Epidemiology of sarcopenia and factors associated with it among community-dwelling older adults in Taiwan. *Am J Med Sci*. (2019) 357:124–33. doi: 10.1016/j.amjms.2018.11.008

48. Singh P, Telnova S, Zhou B, Mohamed AD, Mello V, Wackerhage H, et al. Maternal vitamin B(12) in mice positively regulates bone, but not muscle mass and strength in post-weaning and mature offspring. *Am J Physiol Regul Integr Comp Physiol*. (2021) 320:R984–r93. doi: 10.1152/ajpregu.00355.2020

49. Kaplan P, Tatarkova Z, Sivonova MK, Racay P, Lehotsky J. Homocysteine and mitochondria in cardiovascular and cerebrovascular systems. *Int J Mol Sci*. (2020) 21:7698. doi: 10.3390/ijms21207698

50. Veeranki S, Tyagi SC. Defective homocysteine metabolism: potential implications for skeletal muscle malfunction. *Int J Mol Sci*. (2013) 14:15074–91. doi: 10.3390/ijms140715074

51. Vidoni ML, Pettee Gabriel K, Luo ST, Simonsick EM, Day RS. Relationship between homocysteine and muscle strength decline: the baltimore longitudinal study of aging. *J Gerontol A Biol Sci Med Sci*. (2018) 73:546–51. doi: 10.1093/gerona/glx161

52. Kirk B, Zanker J, Bani Hassan E, Bird S, Brennan-Olsen S, Duque G. Sarcopenia definitions and outcomes consortium (SDOC) criteria are strongly associated with malnutrition, depression, falls, and fractures in high-risk older persons. *J Am Med Dir Assoc*. (2021) 22:741–45. doi: 10.1016/j.jamda.2020.06.050

53. Cruz-Jentoft AJ, Baeyens JP, Bauer JM, Boirie Y, Cederholm T, Landi F, et al. Sarcopenia: European consensus on definition and diagnosis: Report of the European Working Group on Sarcopenia in Older People. *Age Ageing*. (2010) 39:412–23. doi: 10.1093/ageing/afq034

54. Roman-Garcia P, Quiros-Gonzalez I, Mottram L, Lieben L, Sharan K, Wangwiwatsin A, et al. Vitamin B_{12}-dependent taurine synthesis regulates growth and bone mass. *J Clin Invest*. (2014) 124:2988–3002. doi: 10.1172/JCI72606

55. Bailey RL, van Wijngaarden JP. The role of B-vitamins in bone health and disease in older adults. *Curr osteoporosis Rep*. (2015) 13:256–61. doi: 10.1007/s11914-015-0273-0

56. Kim GS, Kim CH, Park JY, Lee KU, Park CS. Effects of vitamin B12 on cell proliferation and cellular alkaline phosphatase activity in human bone marrow stromal osteoprogenitor cells and UMR106 osteoblastic cells. *Metabolism*. (1996) 45:1443–6. doi: 10.1016/S0026-0495(96)90171-7

57. Holstein JH, Herrmann M, Schmalenbach J, Obeid R, Olkü I, Klein M, et al. Deficiencies of folate and vitamin B12 do not affect fracture healing in mice. *Bone*. (2010) 47:151–5. doi: 10.1016/j.bone.2010.04.592

58. Herrmann M, Schmidt J, Umanskaya N, Colaianni G, Al Marrawi F, Widmann T, et al. Stimulation of osteoclast activity by low B-vitamin concentrations. *Bone*. (2007) 41:584–91. doi: 10.1016/j.bone.2007.06.005

59. Wolffenbuttel BHR, Wouters H, de Jong WHA, Huls G, van der Klauw MM. Association of vitamin B12, methylmalonic acid, and functional parameters. *Neth J Med*. (2020) 78:10–24.

60. Yetley EA, Pfeiffer CM, Phinney KW, Bailey RL, Blackmore S, Bock JL, et al. Biomarkers of vitamin B-12 status in NHANES: a roundtable summary. *Am J Clin Nutr*. (2011) 94:313s–21s. doi: 10.3945/ajcn.111.013243

frontiers | Frontiers in Endocrinology

TYPE Original Research
PUBLISHED 03 June 2024
DOI 10.3389/fendo.2024.1397081

OPEN ACCESS

EDITED BY
Giuseppina Storlino,
University of Foggia, Italy

REVIEWED BY
Biagio Palmisano,
Sapienza University of Rome, Italy
Robert Brommage,
BoneGenomics, United States

*CORRESPONDENCE
Ormond A. MacDougald
macdouga@umich.edu

RECEIVED 06 March 2024
ACCEPTED 14 May 2024
PUBLISHED 03 June 2024

CITATION
Schill RL, Visser J, Ashby ML, Li Z, Lewis KT, Morales-Hernandez A, Hoose KS, Maung JN, Uranga RM, Hariri H, Hermsmeyer IDK, Mori H and MacDougald OA (2024) Deficiency of glucocorticoid receptor in bone marrow adipocytes has mild effects on bone and hematopoiesis but does not influence expansion of marrow adiposity with caloric restriction. *Front. Endocrinol.* 15:1397081. doi: 10.3389/fendo.2024.1397081

Deficiency of glucocorticoid receptor in bone marrow adipocytes has mild effects on bone and hematopoiesis but does not influence expansion of marrow adiposity with caloric restriction

Rebecca L. Schill[1], Jack Visser[1], Mariah L. Ashby[1], Ziru Li[1], Kenneth T. Lewis[1], Antonio Morales-Hernandez[2], Keegan S. Hoose[1], Jessica N. Maung[1], Romina M. Uranga[1], Hadla Hariri[1], Isabel D. K. Hermsmeyer[1], Hiroyuki Mori[1] and Ormond A. MacDougald[1,3]*

[1]Department of Molecular & Integrative Physiology, University of Michigan, Ann Arbor, MI, United States, [2]Department of Periodontics and Oral Medicine, University of Michigan School of Dentistry, Ann Arbor, MI, United States, [3]Department of Internal Medicine, University of Michigan, Ann Arbor, MI, United States

Introduction: Unlike white adipose tissue depots, bone marrow adipose tissue (BMAT) expands during caloric restriction (CR). Although mechanisms for BMAT expansion remain unclear, prior research suggested an intermediary role for increased circulating glucocorticoids.

Methods: In this study, we utilized a recently described mouse model (*BMAd-Cre*) to exclusively target bone marrow adipocytes (BMAds) for elimination of the glucocorticoid receptor (GR) (i.e. *Nr3c1*) whilst maintaining GR expression in other adipose depots.

Results: Mice lacking GR in BMAds (*BMAd-Nr3c1*$^{-/-}$) and control mice (*BMAd-Nr3c1*$^{+/+}$) were fed *ad libitum* or placed on a 30% CR diet for six weeks. On a normal chow diet, tibiae of female *BMAd-Nr3c1*$^{-/-}$ mice had slightly elevated proximal trabecular metaphyseal bone volume fraction and thickness. Both control and *BMAd-Nr3c1*$^{-/-}$ mice had increased circulating glucocorticoids and elevated numbers of BMAds in the proximal tibia following CR. However, no significant differences in trabecular and cortical bone were observed, and quantification with osmium tetroxide and μCT revealed no difference in BMAT accumulation between control or *BMAd-Nr3c1*$^{-/-}$ mice. Differences in BMAd size

10.3389/fendo.2024.1397081

were not observed between *BMAd-Nr3c1*$^{-/-}$ and control mice. Interestingly, *BMAd-Nr3c1*$^{-/-}$ mice had decreased circulating white blood cell counts 4 h into the light cycle.

Discussion: In conclusion, our data suggest that eliminating GR from BMAd has minor effects on bone and hematopoiesis, and does not impair BMAT accumulation during CR.

KEYWORDS

glucocorticoids (GC), glucocorticoid receptor (GR), bone marrow adipose tissue (BMAT), caloric restriction (CR), bone, hematopoiesis

Introduction

Adipocytes are widely distributed throughout the human body, and their physiological functions differ depending on location. Bone marrow adipose tissue (BMAT) is a unique adipocyte depot located within the medullary cavity of bones. While the presence of BMAT has been known since the late 19th century, the physiological importance of BMAT remains incompletely understood. Humans are born with very little BMAT, but it gradually expands with age, and by adulthood, BMAT constitutes about 50-70% of total marrow volume (1). Two types of BMAT have previously been described (2). Constitutive BMAT (cBMAT) is located within the distal region of long bones and in caudal vertebrae, and as suggested by the name, remains constitutively present despite a wide variety of physiological interventions. Alternatively, regulated BMAT (rBMAT) is in proximal tibia and distal femur. rBMAT is typically seen as single cells or in small clusters of adipocytes interspersed with hematopoietic cellularity. rBMAT volume changes under a variety of physiological and pathological conditions. For example, cold exposure, acute myeloid leukemia, exercise, and lactation lead to decreased rBMAT volume (3). Alternatively, expansion of rBMAT is observed with type 1 and type 2 diabetes, obesity, growth hormone deficiencies, impaired hematopoiesis, osteoporosis, as well as caloric restriction (CR) (3). BMAT also functions to influence bone and hematopoiesis by serving as an endocrine organ, contributing to circulating concentrations of adiponectin, stem-cell factor, leptin, and receptor activator for NF-κB (RANK) ligand (4–6).

Bone is a dynamic organ that responds to local and systemic stimuli to regulate resorption and formation of bone. Most human and mouse data suggest an inverse relationship between bone marrow adiposity and bone mineral density (7); however, this is not always the case. In C57Bl/6J mice, long-term high fat diet leads to increased BMAT with variable loss to trabecular and cortical bone mass (8, 9). Following bariatric surgery in mice, there is a dramatic loss of BMAT, in addition to a loss trabecular and cortical bone mass (10). Recent work demonstrates that BMAT has a negative effect on bone mass, although, under conditions of energy deficit, BMAT lipolysis helps to maintain bone mass (11). BMAds arise from skeletal stem cells, which also give rise to osteoblasts. Fate determination is controlled by several key transcription factors including runt-related transcription factor 2 (Runx2) and osterix (Osx), which promote osteoblastogenesis (12, 13) and proliferator-activated receptor gamma (PPARγ) and CCAAT/enhancer-binding protein alpha (C/EBPα), which promote adipogenesis (14). The bone marrow microenvironment is complex. In addition to impacting bone health, BMAds have also been shown to influence hematopoiesis. Several studies have suggested that BMAds are a negative regulator of hematopoiesis (15, 16). However, other studies suggest that BMAds support the function of hematopoietic cells (11, 17, 18). Thus, interactions between BMAT and other cell types within the marrow are complex and remain poorly understood.

CR has been shown to increase lifespan and improve overall metabolic health (19). Unlike white adipose tissue (WAT), BMAT paradoxically increases during CR (20), suggesting that BMAT and WAT are metabolically and functionally distinct. The physiological purpose for increased BMAT with CR is unknown; however, a recent study from *Li et al.* demonstrates that lipolysis of BMAds helps to fuel the bone and myelopoiesis during times of CR (11). M olecular signals that lead to these changes in BMAT volume remain poorly understood. Previous hypotheses have included potential roles for leptin, estradiol, fibroblast growth factor 21, ghrelin, and cortisol (21–25). Previously, *Cawthorn et al.* (26) showed that CR in female mice leads to BMAT increase, without changes in circulating leptin concentrations. Using mice and rabbits, these studies also showed that BMAT expansion was observed only when circulating corticosterone concentrations were elevated, implying a potential role for glucocorticoids in BMAT expansion following CR.

Glucocorticoids (GC) are corticosteroids that are essential for vertebrate biology. Due to their anti-inflammatory effects, they are widely used to treat a variety of inflammatory diseases. Glucocorticoids are mainly synthesized by the cortex of the adrenal gland. Production of GCs is regulated by the hypothalamic-pituitary-adrenal axis. Mechanisms of action by GCs are also tightly regulated by enzymatic conversion between active and inactive forms. Two

enzymes regulate the conversion between active and inactive GCs. 11β-hydroxysteroid dehydrogenase 1 (11β-HSD1) catalyzes the conversion of inactive cortisone (11-dehydrocorticosterone in mice) to active cortisol (corticosterone in mice), while 11β-HSD2 performs the opposite conversion (27, 28). GCs bind to the glucocorticoid receptor (GR, gene name *Nr3c1)*, a member of the nuclear receptor family. This receptor functions to regulate GC-responsive genes. Furthermore, activation of GRs is regulated by its subcellular distribution. When unbound, GR resides in the cytosol as a monomer, stabilized by several heat shock proteins. Once bound by a GC, a conformation change occurs, leading to exposure of two nuclear localization signals, at which point GR is transported to the nucleus. Once nuclear, GR directly binds DNA through GC-response elements. The effects of GC on adipose tissue are complex. Under most circumstances, GC stimulates fatty acid uptake and lipolysis in adipocytes (29, 30). Chronic GC treatment leads to metabolic impacts such as insulin resistance, dyslipidemia, and obesity (31). GC are present in almost all adipocyte differentiation protocols (32). In particular, the use of dexamethasone, a synthetic GR ligand, is common. Several groups have used adipocyte GR-knockout models with mixed results (31). Most studies demonstrate that GR is not required for development or maintenance of adipose depots (33–35). However, some studies suggest it may play an important role during high-fat diet feeding (36). Importantly, none of these studies have investigated the impact of adipocyte GR on bone biology.

To investigate the role of GC in BMAT expansion, we utilized a previously described BMAd-specific Cre mouse model to knock out GRs in BMAds (11). Female *BMAd-Nr3c1*$^{-/-}$ mice had a small but significant increase in trabecular bone volume fraction (Tb. BV/TV), trabecular thickness, and distal tibial bone volume (BV). Male *BMAd-Nr3c1*$^{-/-}$ mice did not show changes in bone parameters. Loss of GR in BMAds did not alter the response of young or adult male mice to CR. However, *BMAd-Nr3c1*$^{-/-}$ mice had decreased circulating white blood cells in the light cycle without changes to hematopoietic progenitor populations, suggesting that GRs in BMAds may play a regulatory role in hematopoiesis.

Materials and methods

Mouse generation, care, and housing

Generation and validation of the BMAd-specific Cre model were performed as previously described (11). By monitoring the conversion of cell membrane-localized tdTomato to cell membrane-localized EGFP, Cre efficiency was determined to be ~80% in both male and female mice over 16 weeks of age with one Cre allele, and over 90% with two Cre alleles (11). To generate *BMAd-Nr3c1*$^{-/-}$ mice, BMAd-specific Cre mice (11) were crossed to mice containing *loxP* sites flanking exon 3 of the *Nr3c1* gene (Jax Strain #: 021021. ID: B6. Cg-*Nr3c1*$^{tm1.1Jda/J}$ (37)). Control *BMAd-Nr3c1*$^{+/+}$ mice contain *Osterix-Flpo* and *Flp-activated adiponectin-CRE* but not the floxed *Nr3c1*. Since *BMAd-Cre* and *Nr3c1*$^{-/-}$ mice were initially obtained on mixed genetic backgrounds, and because a systematic breeding to congenicity was not performed, we monitored the background strain of *BMAd-Nr3c1*$^{-/-}$ (n=5; Transnetyx Inc, Cordova, TN). Our results demonstrated that these mice have an average observed frequency of the following sub-strains: 63.9% C57BL/6J, 13.2% C57BL/6NJ, and 33.4% C57BL/6. Three of the five mice demonstrated an observed frequency average of 17.6% 129S strain, with two mice showing nonsignificant amounts of the 129S strain. Together, these data indicate that mice used in these studies had a predominately C57BL/6 background. Control mice used in these studies are *BMAd-Cre* mice lacking *loxP* sites in the *Nr3c1* gene. The presence of *loxP* sites and confirmation of recombination in BMAds was determined by PCR (see Genotyping and PCR). Mice were housed in a 12 h light/dark cycle in the Unit of Laboratory Animal Medicine at the University of Michigan, with free access to water. Unless indicated, mice were fed a normal chow diet (NCD) *ad libitum* (LabDiet 5LOD PicoLab). All procedures were approved by the University of Michigan Committee on the Use and Care of Animals.

Genotyping and PCR

The presence of flanking *loxP* sites on exon 3 of the mouse *Nr3c1* gene was determined using PCR and the following primers:

Forward primer (Fwd): ATGCCTGCTAGGCAAATGAT

Reverse primer #1 (R1): TTCCAGGGCTATAGGAAGCA

Recombination and removal of exon 3 of the mouse *Nr3c1* gene was determined using PCR and the following primers:

Forward primer (Fwd): ATGCCTGCTAGGCAAATGAT

Reverse primer #2 (R2): TTAAGACAGTCGTCTGGAATTCC

Caloric restriction

After acclimation to single housing and the control diet (D17110202; Research Diets) for two weeks, food intake was determined by giving a defined amount of food and weighing the remainder daily for 2 weeks. Individual adult male mice (starting age of 28-35 weeks, body weights of 26.5 g to 35.2 g) consumed approximately 2.42 g of food per day. As such, we provided 1.70 g of the nutrient-matched CR diet (D19051601; Research Diets) to mice daily to ensure 30% CR. Female mice consumed approximately 2.27 g of food per day and were therefore provided 1.59 g of the CR diet. Mice on CR consumed all the food provided and food was provided at ~2 pm daily.

Histology

Tissue histology was performed as previously described (10). Briefly, soft tissues were fixed in 10% formalin for 24 hours and embedded in paraffin for sectioning. Bones were fixed in formalin for 24 hours, decalcified in 14% EDTA for a minimum of 2 weeks, with fresh EDTA provided every 48 hours. Following decalcification, bones were fixed an additional 24 hours with 10% formalin. Bones were then embedded in paraffin and sectioned to 5

μm. After staining with hematoxylin and eosin (H&E), sectioned tissue was imaged on an Olympus BX52 microscope.

μCT analysis

Tibial bone parameters were measured using μCT as previously described (11, 38). Briefly, the entire tibia was scanned using a μCT system (μCT100 Scanco Medical, Bassersdorf, Switzerland). The following parameters were used: voxel size 12 μm, 70 kVp, 114 μA, 0.5 mm AL filter, and integration time 500 ms. Mid-cortical bone: a total of 30 slices (360 μm) were analyzed. The starting slice number was determined using the following equation: *Starting slice = [(Tib/fib junction slice #) – (growth plate slice #)] x 0.7 + (growth plate slice #).* Trabecular bone: a total of 50 slices (600 μm) were analyzed, initiated 5 slices distal to the proximal tibial growth plate. Distal cortical bone: slices were analyzed starting at the junction of the tibia and fibula and continuing to the distal end of the cortical bone, where distal trabecular bone is first observed (~450 slices, ~5.4 mm). Schematic of tibial bone locations use for μCT is present within relevant figures.

Osmium tetroxide staining and BMAd quantification

Mouse tibiae were fixed for 24 hours in formalin, then decalcified using 14% EDTA as previously described (10). Osmium tetroxide staining and μCT was performed as previously described (2, 38).

Circulating corticosterone measurements

Immediately following euthanasia, blood was harvested via cardiac punction, allowed to clot on ice for 2 hours and the serum was collected and stored at -80°C. To measure circulating corticosterone concentrations, an ELISA was performed per the manufacturer's recommended protocols (Cayman Chemical, 501320, Ann Arbor, MI).

Complete blood count

Blood was harvested from the tail of *BMAd-Nr3c1*$^{-/-}$ and *BMAd-Nr3c1*$^{+/+}$ mice and a complete blood count was performed by the University of Michigan Unit for Laboratory Animal Medicine Pathology Core using a Heska Element HT5 Veterinary Hematology Analyzer (Loveland, CO). Blood draws were performed at zeitgeber time 5 (ZT5; 10 am) and ZT17 (10 pm).

Bone marrow cellular quantification

Bone marrow was extracted from the femurs and tibiae of *BMAd-Nr3c1*$^{-/-}$ and *BMAd-Nr3c1*$^{+/+}$ mice. Bones were crushed and incubated in Red Blood Cell lysis buffer (Sigma-Aldrich St. Louis, MO) for five minutes on ice. Bone marrow compartments were visualized by flow cytometry after staining with the following antibodies: LT-HSC/ST-HSC/MPP2/MPP3/MPP4 [B220-PerCP (RA3-6B2), CD3-PerCP (145-2C11), CD4-PerCP (GK1.5), CD8-PerCP (53-6.7), CD19-PerCP (6D5), Gr-1-PerCP (RB6-8C5), Ter119-PerCP (TER-119), Sca-1-PerCP-Cy5.5 (E13-161.7), c-Kit-APC-780 (2B8), CD150-PE-Cy7 (TC15-12F12.2), CD48-Alexa Fluor 700 (HM48-1), and Flt3-PE (A2F10.1)]; CMP/GMP/MEP [B220-PerCP (RA3-6B2), CD3-PerCP (145-2C11), CD4-PerCP (GK1.5), CD8-PerCP (53-6.7), CD19-PerCP (6D5), Gr-1-PerCP (RB6-Ter119-PerCP (TER-119), Sca-1-PerCP-Cy5.5 (E13-161.7), c-Kit-APC-780 (2B8), FcR II/III-Alexa Fluor 700 (93), CD34-FITC (RAM34), and IL-7R-PE-Cy7 (A7R34)]. All antibodies were used at 1:200 dilution except for CD34-FITC, which was used at 1:50 dilution. Populations were identified according to the following gating strategy: LT-HSC [Lineage-Sca1+cKit+ (LSK)CD48-CD150+Flt3-]; ST-HSC (LSK, CD48-CD150-Flt3-); MPP2 (LSK, CD48+CD150+Flt3-); MPP3 (LSK, CD48+CD150-Flt3-); MPP4 (LSK, CD48+CD150-Flt3+); CMP (Lineage-Sca1-cKit+CD34+ FcR II/IIImed); GMP (Lineage-Sca1-cKit+CD34+ FcR II/IIIhigh); MEP (Lineage-Sca1-cKit+CD34- FcR II/III-); CLP (Lineage-Sca1medcKitmedIL-7R+). DAPI (Sigma-Aldrich, St. Louis, MO) was used for dead cell exclusion. Data collection was performed using a Northern Lights (Cytek) flow cytometer. Data analyses were performed with FlowJo version 10 (LLC, Ashland, OR).

Statistics

Significant differences between groups were assessed using a two-sample *t*-test or ANOVA with post-tests as appropriate: one-way ANOVA with Tukey's multiple comparisons test or two-way ANOVA with Sidak's multiple comparisons test. All analyses were conducted using the GraphPad Prism version 9. All graphical presentations are mean ± SD. For statistical comparisons, a *P*-value of <0.05 was considered significant.

Results

Deletion of the GR in BMAds does not alter BMAT but slightly increases bone mass of proximal and distal tibia of female mice

To determine the roles of GR in BMAds we sought to selectively eliminate GR from BMAds while avoiding loss of GR in white adipocytes and osteoblasts. To do this, we utilized a recently described BMAd-specific Cre model (11). We crossed this *BMAd-Cre* line to mice containing *loxP* sites flanking exon 3 of the mouse GR gene (*Nr3c1*) (Figure 1A). We confirmed that recombination in *BMAd-Nr3c1*$^{-/-}$ mice occurred in caudal vertebrae and tibial bone marrow, where high amounts of BMAds are present (Figure 1B). No recombination was observed in subcutaneous WAT (sWAT), epididymal WAT (eWAT), or liver. In addition, RNA was isolated, converted to cDNA, and sequenced to confirm the presence of a product lacking exon 3 (not shown).

10.3389/fendo.2024.1397081

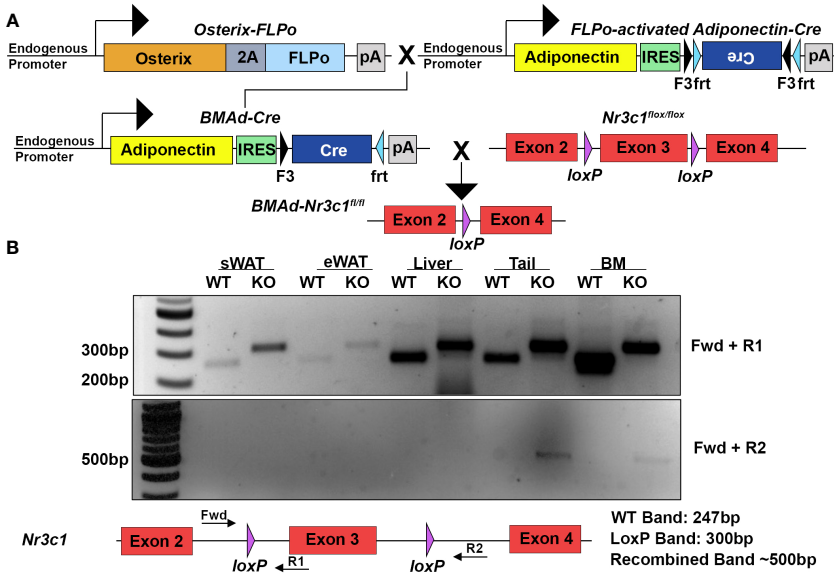

FIGURE 1
Deletion of GR specifically in BMAds using the BMAd-Cre mouse model. **(A)** Breeding strategy for generation of *BMAd-Nr3c1*$^{-/-}$ mice. **(B)** PCR amplification was used to detect the presence of loxP sites flanking exon 3 of *Nr3c1* (top panel, primers Fwd + R1). PCR products demonstrate presence of a band lacking exon 3 (bottom panel, primers Fwd + R2) in tail and bone marrow (BM) of *BMAd-Nr3c1*$^{-/-}$ (KO) mice but not in subcutaneous WAT (sWAT), epididymal (eWAT), or liver. Recombination was not detected in *BMAd-Nr3c1*$^{+/+}$ mice (WT).

We next investigated whether loss of GR in BMAds alters BMAT volume and/or tibial bone variables. Female *BMAd-Nr3c1*$^{+/+}$ and *BMAd-Nr3c1*$^{-/-}$ mice (31-39 weeks old) on a NCD were euthanized and a necropsy performed. As expected, no significant differences were observed in body weight (Supplementary Figure 1A) or tissue weights of the sWAT, periovarian WAT (poWAT), liver, or spleen of *BMAd-Nr3c1*$^{-/-}$ mice compared to controls (Supplementary Figure 1B). We also did not observe histological changes to the WAT (Supplementary Figure 1C). Next, we determined if loss of GR in BMAds alters BMAT volume. Histological analyses showed no observable differences in BMAT histology in the tibiae or caudal vertebrae of *BMAd-Nr3c1*$^{-/-}$ mice compared to controls (Figure 2A). Qualitative histological analysis suggested a slight reduction in the proximal trabecular metaphyseal bone in the femur of female *BMAd-Nr3c1*$^{-/-}$ mice. To determine quantitatively whether the lack of GR in BMAds alters bone parameters, we performed μCT on the tibiae of *BMAd-Nr3c1*$^{+/+}$ and *BMAd-Nr3c1*$^{-/-}$ mice. Female *BMAd-Nr3c1*$^{-/-}$ mice had a small but significant increase in proximal trabecular metaphyseal bone volume fraction and trabecular thickness (Figure 2B). No differences were observed in the mid-cortical region of the tibiae, where few BMAds are typically present (Figure 2C). Female *BMAd-Nr3c1*$^{-/-}$ mice also had a small but significant increase in cortical bone volume in the distal tibiae (Figure 2D). Although histological analysis suggested a slight reduction in trabecular bone in distal femur, male *BMAd-Nr3c1*$^{-/-}$ mice did not have differences in bone histology in tibiae or caudal vertebrae (Supplementary Figure 2A). Consistent with histological results, μCT did not reveal differences in b one parameters (Supplementary Figures 2B-D). These data indicate that at baseline, GR plays a dispensable role in size and number of BMAds and a minor role in inhibiting tibial bone mass in female but not male mice.

Deletion of Nr3c1 in BMAds does not alter BMAT accumulation with CR

In addition to increased BMAT volume, circulating concentrations of GC are elevated with CR in mice (26). We next sought to determine if GR is required for BMAT expansion following CR. Developing (10-16 weeks old) male *BMAd-Nr3c1*$^{+/+}$ and *BMAd-Nr3c1*$^{-/-}$ mice were fed *ad libitum* or were provided a 30% CR diet for 6 weeks. Because no significant changes in BMAT were observed in male *BMAd-Nr3c1*$^{-/-}$ mice at baseline (Supplementary Figure 2), all *BMAd-Nr3c1*$^{-/-}$ mice were placed on a 30% CR diet. As expected, CR mice had significant decreases in body and tissue weights (Figures 3A, B). CR mice also had significant decreases in length of tibiae and femurs (Figures 3C, D), with an increase in trabecular connective density (Figure 3E). Changes in the mid- or distal cortical bone were not observed (Figures 3F, G).

Due to decreased length of both the tibia and femur with CR, we concluded that CR blunts development of bone in growing mice. Therefore, we performed an additional CR study using adult male mice (34-41 weeks old) (Figure 4). CR mice lost ~26% of their body weight (Figure 4A) and had reductions in sWAT, eWAT, liver, and spleen mass (Supplementary Figure 3A). Importantly, we observed that CR induced a 7-fold increase in circulating corticosterone concentrations in both *BMAd-Nr3c1*$^{+/+}$ and *BMAd-Nr3c1*$^{-/-}$ adult mice (Figure 4B). Histological analysis showed CR leads to an increase in the number of BMAds in tibiae and femurs of mice placed on CR (Figure 4C), but differences in BMAT volume were not observed between *BMAd-*

10.3389/fendo.2024.1397081

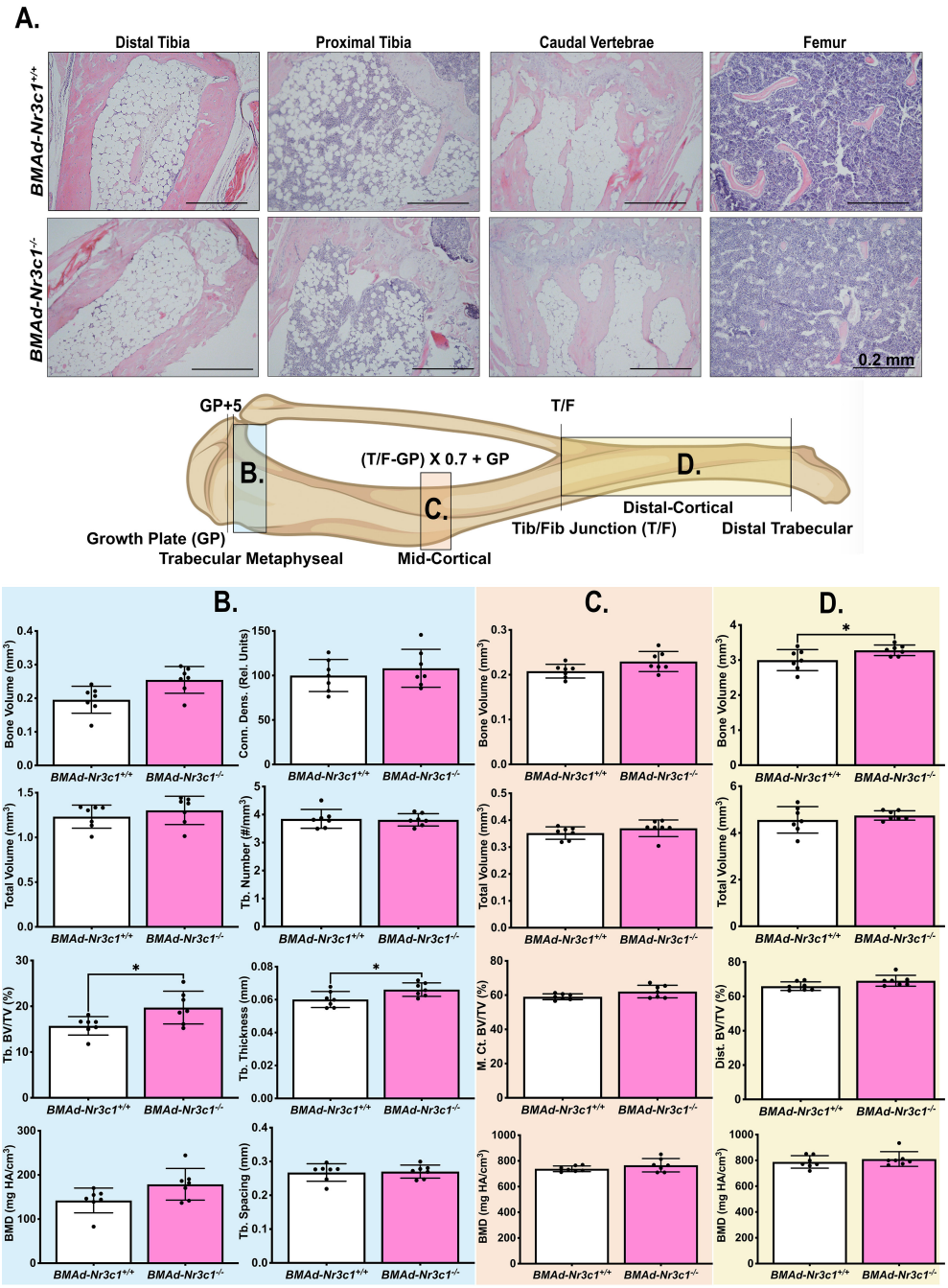

FIGURE 2
Female *BMAd-Nr3c1*$^{-/-}$ mice have slightly elevated tibial bone variables. **(A)** Female mice at 31–39 weeks of age were euthanized. Tibiae, tail, and femurs were decalcified, embedded, paraffin-sectioned, and stained with H&E. Representative photos are shown. Scale bar: 0.22 mm. **(B–D)** A schematic of the tibia illustrating locations of μCT slices. Tibiae were analyzed by μCT for **(B)** proximal trabecular metaphyseal, **(C)** mid-cortical, and **(D)** distal cortical bone variables. Tb: Trabecular, BV: Bone Volume, TV: Total Volume, Conn. Dens.: Connective Density, M. Ct.: Mid-Cortical, Dist., Ct.: Distal Cortical. Statistical analysis was performed using an unpaired t-test. *p<0.05.

Nr3c1$^{+/+}$ and *BMAd-Nr3c1*$^{-/-}$ mice on CR. There were also no significant differences in adipocyte size in tibiae from *BMAd-Nr3c1*$^{+/+}{}_{CR}$ and *BMAd-Nr3c1*$^{-/-}{}_{CR}$ mice (Figures 4D, E). Quantification of BMAT volume using osmium tetroxide and μCT demonstrated a significant increase in proximal tibial BMAT with CR (Figures 4F–H). Neither CR nor the loss of GR in BMAds altered tibial bone parameters quantified by μCT (Supplementary Figures 3B-D).

Deletion of Nr3c1 in BMAds alters circulating white blood cell counts

In addition to impacting bone biology, BMAds and GC have independent effects on hematopoiesis (39–42). To determine if loss of GR in BMAds impacts hematopoiesis, we measured complete blood counts from male and female *BMAd-Nr3c1*$^{+/+}$ and *BMAd-*

10.3389/fendo.2024.1397081

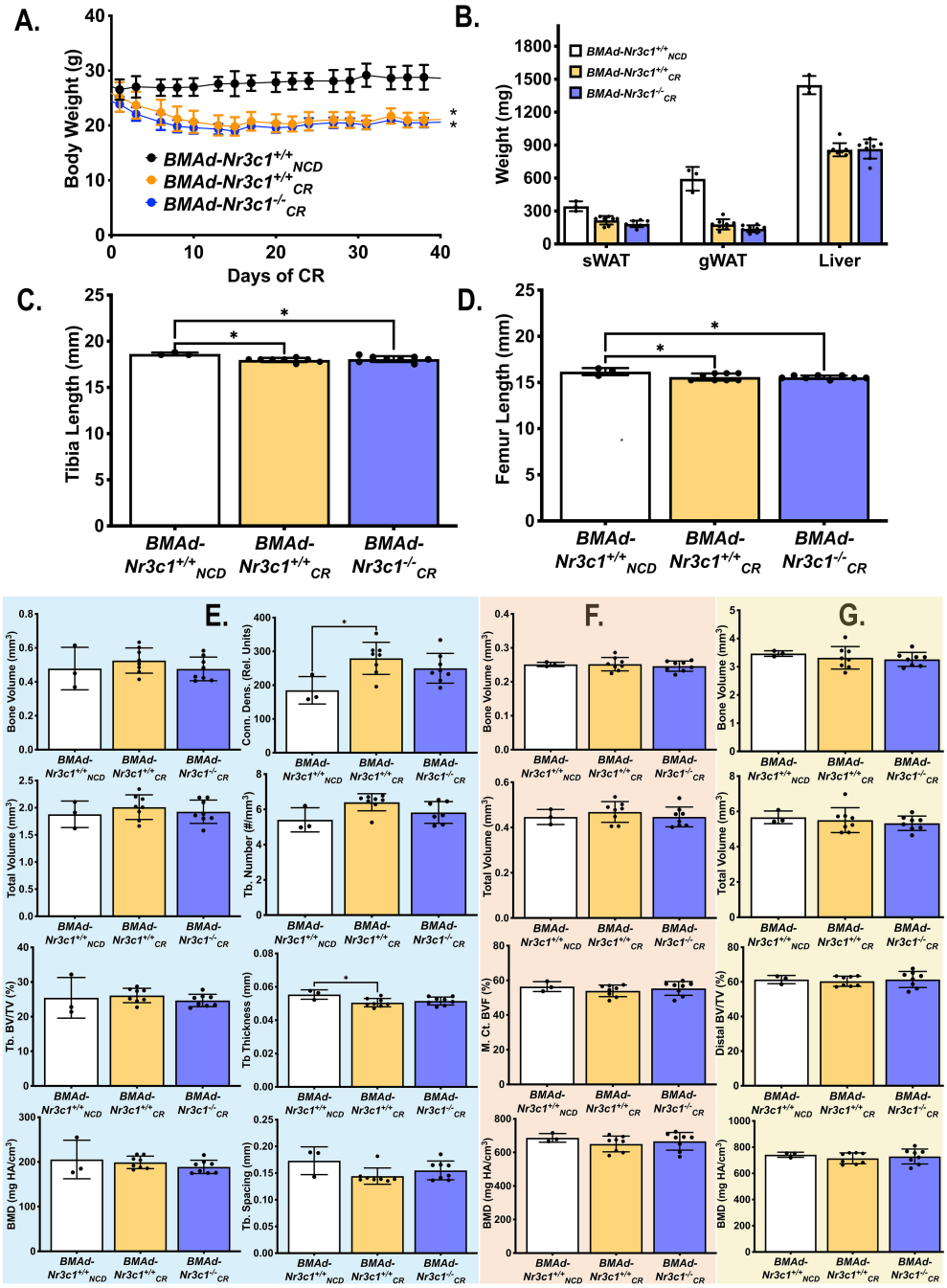

FIGURE 3
CR leads to decreased bone length in developing male mice independent of GR in BMAd. Male mice (10-16 weeks old) were fed *ad libitum* (NCD) or placed on a 30% CR diet for 6 weeks. **(A)** B ody weights of mice were measured throughout the experiment. Statistical analysis was performed using a two-way ANOVA. *p<0.05 compared to *BMAd-Nr3c1*$^{+/+}{}_{NCD}$. **(B)** At the time of euthanasia, tissue weights of sWAT, eWAT, and liver were measured. **(C, D)** Following necropsy, the length of the tibia **(C)** and femur **(D)** were measured. Tibiae were analyzed by µCT for **(E)** proximal trabecular metaphyseal, **(F)** mid-cortical, and **(G)** distal cortical bone variables. Tb: Trabecular, BV: Bone Volume, TV: Total Volume, Conn. Dens.: Connective Density, M. Ct.: Mid-Cortical, Dist. Ct.: Distal Cortical. Statistical analysis was performed using a one-way ANOVA with a Tukey multiple comparison *post hoc* test. *p<0.05.

Nr3c1$^{-/-}$ mice. Previous reports have shown that both GC and blood cell concentrations vary greatly with time of day (43, 44). Therefore, we measured blood cell parameters during the day (ZT5) and in the evening (ZT17). As expected, all blood cell populations were lower during the evening (Figures 5A–H). Our results demonstrated that both male and female *BMAd-Nr3c1*$^{-/-}$ mice have reduced white blood cell counts compared to *BMAd-Nr3c1*$^{+/+}$ mice (Figures 5A, E). Specifically, female *BMAd-Nr3c1*$^{-/-}$ mice showed a significant reduction in numbers of circulating lymphocytes (Figure 5B), whereas male mice showed a significant reduction in circulating monocytes (Figure 5H). Loss of GR in BMAds did not alter red blood cell parameters or platelets (Supplementary Figure 4). After

10.3389/fendo.2024.1397081

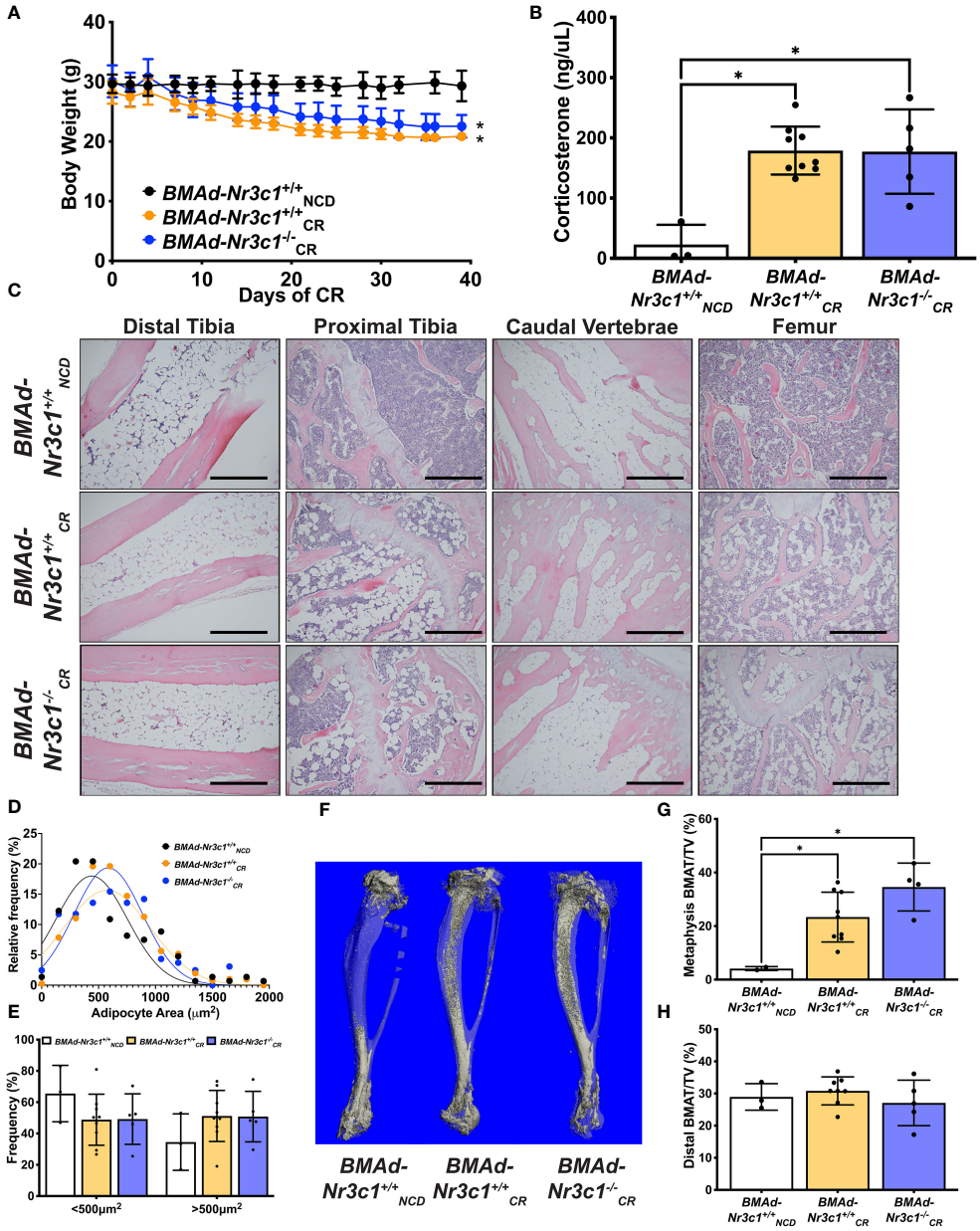

FIGURE 4
Loss of GR in BMAds of male mice does not alter BMAT responses to CR. Male mice (34-41 weeks old) were fed *ad libitum* or placed on a 30% CR diet for 6 weeks. **(A)** Body weight of mice was measured throughout the experiment. Statistical analysis was performed using a two-way ANOVA. *p<0.05 compared to *BMAd-Nr3c1*$^{+/+}_{NCD}$. **(B)** At the time of euthanasia, blood was isolated, and circulating corticosterone concentrations were measured. **(C)** Tibiae, caudal vertebrae, and femurs were decalcified, embedded, paraffin-sectioned, and stained with H&E. Representative photos are shown. Scale bar: 0.22 mm. **(D, E)** BMAd size was calculated using MetaMorph. **(F)** Using osmium tetroxide and μCT, a three-dimensional reconstruction of tibial BMAT was generated. BMAT volume in tibial **(G)** metaphasis and **(H)** distal cortical regions was determined.Statistical analysis was performed using a one-way ANOVA with a Tukey multiple comparison *post hoc* test. *p<0.05.

observing changes to circulating blood cell populations, we next investigated whether this observation could be a result of changes to the bone marrow cell composition. Therefore, we measured hematopoietic progenitor cell populations within bone marrow compartments of femurs and tibiae. Our results demonstrated that *BMAd-Nr3c1*$^{-/-}$ mice had fewer short-term reconstituting hematopoietic stem cells (ST-HSC) in the femur. However, we did not observe changes in common myeloid progenitors (CMP) or common lymphoid progenitors (CLP). We also did not observe altered frequencies of progenitor cell populations in the tibia of *BMAd-Nr3c1*$^{-/-}$ mice compared to control (Figures 5I, J).

Discussion

BMAds are a unique group of adipocytes residing within the bone marrow microenvironment. rBMAT volume expands under a variety of physiological and pathological conditions including CR

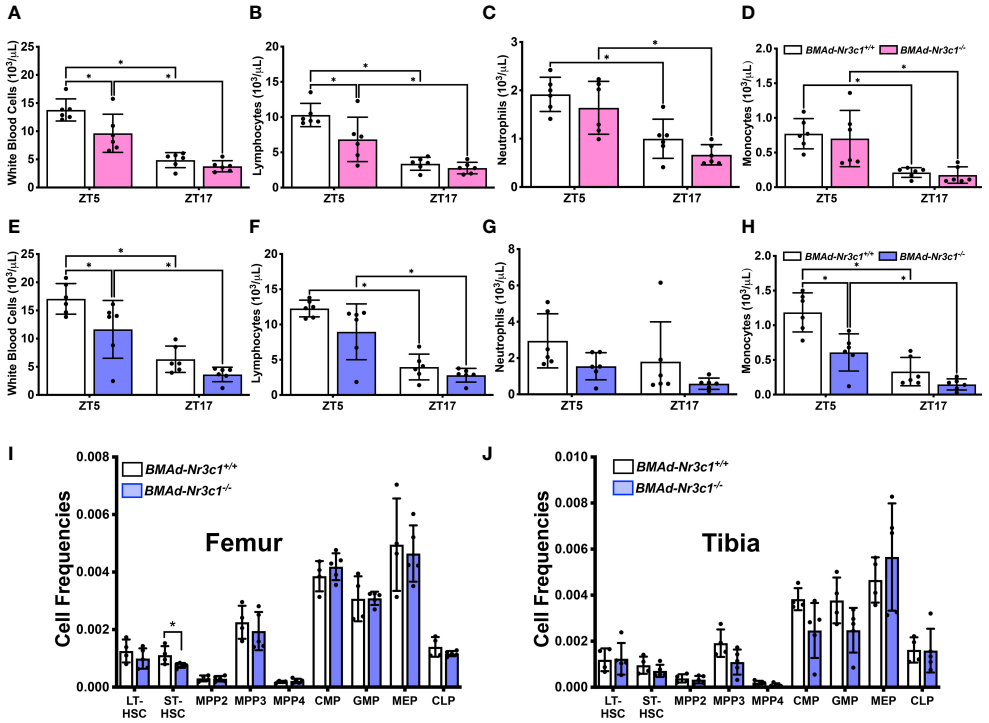

FIGURE 5
Loss of GR in BMAds reduces circulating white blood cell counts in female and male mice during the light cycle. Circulating blood cell populations were measured in **(A–D)** female and **(E–H)** male *BMAd-Nr3c1*$^{-/-}$ and control mice at ZT5 and, following a 48-hour recovery period, at ZT17. Statistical analyses of panels A-H were performed using a two-way ANOVA with a Sidak's multiple comparison's *post hoc* test. *p<0.05. Hematopoietic progenitor cell populations were measured in bone marrow isolated from the **(I)** femur and **(J)** tibia of *BMAd-Nr3c1*$^{-/-}$ or control mice. Statistical analysis of panels I and J was performed using an unpaired t-test. *p<0.05.

(20) and anorexia nervosa (4, 45, 46). The molecular mechanisms during CR leading to increased BMAT are unknown. Previous studies using mouse models have shown that BMAT expansion occurs when circulating GC are elevated (26). Both excess synthetic and endogenous GCs are known to cause bone loss (47). In general, an inverse relationship exists between BMAT volume and bone mass, including in patients with anorexia nervosa (48–50). Together these results suggest that excess GC during CR may lead to increased BMAT and subsequent bone loss (51, 52). Indeed, work from *Pierce et al.* have shown that GR-deficiency in *Osx*-expressing cells led to loss of cortical and trabecular bone mass in mice fed *ad libitum* or CR (53). However, previous studies using adipocyte-specific deletion of GR have not investigated changes to bone mass (31, 33–35). Indeed, in these studies, the direct effects of GR in BMAd would not be distinguishable from potential indirect effects caused by the deletion of GR in other adipose depots.

In this study, our results suggest that GRs in BMAds are not required for the expansion of BMAT with CR. One explanation is that GR plays an important role in the early differentiation of BMAds, and the *BMAd-Cre* model used in these studies targets only mature BMAds (11). Another possibility is that the loss of GR in BMAds is compensated by other GC-responsive proteins such as the mineralocorticoid receptor (MR), which can also directly bind to GC. However, evidence for robust compensation by MR has not been observed in adipocyte-specific GR-KO models (33, 54). In the current studies, we also did not observe significant changes to MR expression levels in *BMAd-Nr3c1*$^{-/-}$ mice (data not shown). Several groups have targeted GC activity through knock-out of the enzymes involved in their activation, such as 11β-HSD1, a major regulator of the tissue-specific effects of GC (55, 56). Previous work has shown that global deletion of 11β-HSD1 produces a favorable metabolic state (57–59); however, the impact of 11β-HSD1-deficiency in BMAds has not been evaluated. With the recent invention of genetic tools like the *BMAd-Cre* mouse (11), future experiments can investigate this hypothesis that 11β-HSD1 is important for BMAT responses to GC. It is possible that GR in BMAds is important with other stressors that lead to BMAT expansion such as aging or obesity (60). Alternatively, it may be that elevated GC and BMAd-GR do not contribute to BMAT expansion following CR.

Whereas our results did not suggest a critical role for GR in BMAd in expansion of BMAT during CR, we did observe a small but significant increase in trabecular bone volume fraction and thickness as well as distal cortical bone volume in the tibiae of adult female *BMAd-Nr3c1*$^{-/-}$ mice at baseline. Sex-specific differences in bone parameters are well documented (61, 62), and 6 weeks of 30% CR did not lead to loss of tibial bone mass in adult male mice. Indeed, the clinical data surrounding bone loss from CR is variable. One study showed that six months of CR in young adults does not lead to significant bone loss (63). However, similar studies in adults

show a significant reduction in bone following CR (64, 65). Amongst these conflicting findings, one consensus is that patients with anorexia nervosa are at an increased fracture risk due to bone loss (66–69). Of note, anorexia nervosa is a condition of more severe caloric deficiency than that achieved in most CR studies. In mouse and rabbit models, results have also been mixed. One common observation is that CR results in stunted bone growth and low bone mass in some regions of the skeleton of young mice (21) and rabbits (26). Indeed, our studies support this finding, which is why we then chose to investigate CR in adult mice (34+ weeks). In adult animals, most studies suggest that CR leads to bone loss (21, 70). However, results have been variable both in terms of the severity of bone loss and the location of bone loss within the skeleton (21, 70). One study showed that bone loss occurs with 6 weeks of CR, even when performed in combination with exercise (71), which typically positively supports bone health (72). Interestingly, some studies suggest that long-term CR may protect against or delay age-related bone loss (73, 74). Several factors could influence the impact of CR on bone mass including sex, age, length of CR, strain of mice, and region of the skeleton being investigated. While our CR diet includes micronutrient supplementation, in other dietary restriction studies (21), the availability of calcium and other essential minerals is of concern.

Due to its location within the marrow niche, as well as its endocrine functions, many studies have aimed to investigate the roles of BMAd on hematopoiesis. Several studies suggest an inverse relationship between BMAT and hematopoiesis (10, 15, 16, 18). However, others suggest a supportive role for BMAds in hematopoiesis (11, 18, 75). In our study, loss of GR from BMAds led to a significant decrease in circulating white blood cells. Female *BMAd-Nr3c1*$^{-/-}$ mice showed a decrease in lymphocytes, while male mice showed a significant reduction in monocytes. These changes were only significant when the blood draw was performed during the day (ZT5). Confirming previous studies showing that hematopoiesis is circadian (43), nearly all blood cell populations were reduced when the blood draw was performed at night (ZT17). We did not observe changes in circulating red blood cells in *BMAd-Nr3c1*$^{-/-}$ mice. While GR has previously been shown to mediate stress erythropoiesis (41), we hypothesize that the lack of changes in circulating red blood cells in *BMAd-Nr3c1*$^{-/-}$ mice is because this process mostly occurs in the spleen (76). In WAT, adipocyte GR suppresses the immune system, maintaining immune homeostasis (77, 78). While circulating white blood cells were decreased during the day in *BMAd-Nr3c1*$^{-/-}$ mice, we did not observe differences in the abundance of bone marrow progenitor cell populations in the tibiae of *BMAd-Nr3c1*$^{-/-}$ mice. We observed a subtle but significant change in ST-HSCs in the femur of *BMAd-Nr3c1*$^{-/-}$ mice, but the frequency of CMP or CLP populations was not different. BMAds locally interact with hematopoietic cells and contribute to whole-body metabolism through the secretion of adipokines (79, 80). Lipodystrophic A-ZIP/F1 mice, which lack BMAT, have delayed hematopoietic regeneration in the long bones following irradiation (5), a process that involves the secretion of stem cell factor (SCF) from BMAds (5, 80, 81). Loss of SCF from BMAT reduces the bone marrow cellularity, hematopoietic stem and progenitor cells, common myeloid progenitors, megakaryocyte-erythrocyte progenitors, and granulocyte-monocyte progenitors (81). Supporting this hypothesis, there is a depletion of BMAT accompanied by a decrease in bone marrow erythroid cells and anemia following bariatric surgery (10). Our data suggests that loss of GR from BMAd lowers circulating white blood cells without altering bone marrow hematopoietic progenitor cell populations.

Our experiments demonstrate that loss of GR in BMAd of female mice led to a small but significant increase in trabecular bone volume fraction and trabecular thickness. Loss of GR in BMAd of male mice showed no changes to bone parameters. CR in young mice resulted in a decrease in tibial and femur lengths as sufficient caloric intake is important for growth in developing bones. CR studies in both young and adult male mice demonstrated that GR in BMAd is not required for BMAT expansion following CR. This study has several limitations. One caveat to the *BMAd- Cre* mouse model is that the insertion of a flipped Cre gene in the 3' untranslated region of adiponectin leads to a small, but significant, decrease in circulating adiponectin concentrations (11). To confirm that excess GC do not work directly on BMAds to promote BMAT expansion during CR, future mouse models should target other aspects of the GC pathway, such as deletion of MR or 11β-HSD1. It is also highly likely that GC induce BMAT expansion by promoting the differentiation of new adipocytes, and the *BMAd-Cre* model used herein targets mature adipocytes. In conclusion, our data suggest that BMAd-GR is not required for BMAT expansion following CR.

Data availability statement

The raw data supporting the conclusions of this article will be made available by the authors, without undue reservation.

Ethics statement

The animal study was approved by Institutional Animal Care & Use Committee University of Michigan. The study was conducted in accordance with the local legislation and institutional requirements.

Author contributions

RS: Conceptualization, Data curation, Formal analysis, Funding acquisition, Investigation, Writing – original draft, Writing – review & editing. JV: Data curation, Writing – review & editing. MA: Data curation, Writing – review & editing. ZL: Data curation, Writing – review & editing. KL: Data curation, Writing – review & editing. AM-H: Data curation, Writing – review & editing. KH: Data curation, Writing – review & editing. JM: Data curation, Writing – review & editing. RU: Data curation, Writing – review & editing. HH: Data curation, Writing – review & editing. IH: Data curation, Writing – review & editing. HM: Data curation, Writing – review & editing. OM: Writing – original draft, Writing – review & editing.

Funding

The author(s) declare financial support was received for the research, authorship, and/or publication of this article. The work was supported by grants from the NIH to OAM (AG069795; DK121759, DK137798), RLS (T32 DK101357; F32 DK123887), KTL (T32 DK071212, F32 DK122654), JNM (T32 HD007505, F31 DK135181) and by a grant from the American Diabetes Association to ZL (1-18-PDF-087).

Acknowledgments

The authors would like to thank Drs. William Cawthorn (University of Edinburgh) and Clifford Rosen (Maine Medical Center) for their scientific guidance. This research was also supported by core facilities at the University of Michigan including the Unit for Laboratory Animal Medicine Pathology, the University of Michigan School of Dentistry MicroCT Core, and the MNORC Adipose Tissue Core (P30 DK089503). We would also like to thank Tanu Soni (University of Michigan, Computational Medicine and Bioinformatics) and the University of Michigan's Consulting for Statistics, Computing, & Analytics Research Office for support and guidance on statistical analysis.

Conflict of interest

The authors declare that the research was conducted in the absence of any commercial or financial relationships that could be construed as a potential conflict of interest.

Publisher's note

All claims expressed in this article are solely those of the authors and do not necessarily represent those of their affiliated organizations, or those of the publisher, the editors and the reviewers. Any product that may be evaluated in this article, or claim that may be made by its manufacturer, is not guaranteed or endorsed by the publisher.

Supplementary material

The Supplementary Material for this article can be found online at: https://www.frontiersin.org/articles/10.3389/fendo.2024.1397081/full#supplementary-material

References

1. Nandy A, Rendina-Ruedy E. Bone marrow adipocytes - Good, bad, or just different? *Best Pract Res Clin Endocrinol Metab*. (2021) 35:101550. doi: 10.1016/j.beem.2021.101550

2. Scheller EL, Doucette CR, Learman BS, Cawthorn WP, Khandaker S, Schell B, et al. Region-specific variation in the properties of skeletal adipocytes reveals regulated and constitutive marrow adipose tissues. *Nat Commun*. (2015) 6:7808. doi: 10.1038/ncomms8808

3. Li Z, Hardij J, Bagchi DP, Scheller EL, MacDougald OA. Development, regulation, metabolism and function of bone marrow adipose tissues. *Bone*. (2018) 110:134–40. doi: 10.1016/j.bone.2018.01.008

4. Cawthorn WP, Scheller EL, Learman BS, Parlee SD, Simon BR, Mori H, et al. Bone marrow adipose tissue is an endocrine organ that contributes to increased circulating adiponectin during caloric restriction. *Cell Metab*. (2014) 20:368–75. doi: 10.1016/j.cmet.2014.06.003

5. Zhou BO, Yu H, Yue R, Zhao Z, Rios JJ, Naveiras O, et al. Bone marrow adipocytes promote the regeneration of stem cells and haematopoiesis by secreting SCF. *Nat Cell Biol*. (2017) 19:891–903. doi: 10.1038/ncb3570

6. Takeshita S, Fumoto T, Naoe Y, Ikeda K. Age-related marrow adipogenesis is linked to increased expression of RANKL. *J Biol Chem*. (2014) 289:16699–710. doi: 10.1074/jbc.M114.547919

7. Fazeli PK, Horowitz MC, MacDougald OA, Scheller EL, Rodeheffer MS, Rosen CJ, et al. Marrow fat and bone–new perspectives. *J Clin Endocrinol Metab*. (2013) 98:935–45. doi: 10.1210/jc.2012-3634

8. Doucette CR, Horowitz MC, Berry R, MacDougald OA, Anunciado-Koza R, Koza RA, et al. A high fat diet increases bone marrow adipose tissue (MAT) but does not alter trabecular or cortical bone mass in C57BL/6J mice. *J Cell Physiol*. (2015) 230:2032–7. doi: 10.1002/jcp.24954

9. Scheller EL, Khoury B, Moller KL, Wee NK, Khandaker S, Kozloff KM, et al. Changes in Skeletal Integrity and Marrow Adiposity during High-Fat Diet and after Weight Loss. *Front Endocrinol (Lausanne)*. (2016) 7:102. doi: 10.3389/fendo.2016.00102

10. Li Z, Hardij J, Evers SS, Hutch CR, Choi SM, Shao Y, et al. G-CSF partially mediates effects of sleeve gastrectomy on the bone marrow niche. *J Clin Invest*. (2019) 129:2404–16. doi: 10.1172/JCI126173

11. Li Z, Bowers E, Zhu J, Yu H, Hardij J, Bagchi DP, et al. Lipolysis of bone marrow adipocytes is required to fuel bone and the marrow niche during energy deficits. *Elife*. (2022) 11. doi: 10.7554/eLife.78496

12. Komori T. Regulation of osteoblast differentiation by Runx2. *Adv Exp Med Biol*. (2010) 658:43–9. doi: 10.1007/978-1-4419-1050-9_5

13. Liu Q, Li M, Wang S, Xiao Z, Xiong Y, Wang G. Recent advances of osterix transcription factor in osteoblast differentiation and bone formation. *Front Cell Dev Biol*. (2020) 8:601224. doi: 10.3389/fcell.2020.601224

14. Rosen ED, Walkey CJ, Puigserver P, Spiegelman BM. Transcriptional regulation of adipogenesis. *Genes Dev*. (2000) 14:1293–307. doi: 10.1101/gad.14.11.1293

15. Naveiras O, Nardi V, Wenzel PL, Hauschka PV, Fahey F, Daley GQ. Bone-marrow adipocytes as negative regulators of the haematopoietic microenvironment. *Nature*. (2009) 460:259–63. doi: 10.1038/nature08099

16. Polineni S, Resulaj M, Faje AT, Meenaghan E, Bredella MA, Bouxsein M, et al. Red and white blood cell counts are associated with bone marrow adipose tissue, bone mineral density, and bone microarchitecture in premenopausal women. *J Bone Miner Res*. (2020) 35:1031–9. doi: 10.1002/jbmr.3986

17. Boyd AL, Reid JC, Salci KR, Aslostovar L, Benoit YD, Shapovalova Z, et al. Acute myeloid leukaemia disrupts endogenous myelo-erythropoiesis by compromising the adipocyte bone marrow niche. *Nat Cell Biol*. (2017) 19:1336–47. doi: 10.1038/ncb3625

18. Li Z, Bagchi DP, Zhu J, Bowers E, Yu H, Hardij J, et al. Constitutive bone marrow adipocytes suppress local bone formation. *JCI Insight*. (2022) 7. doi: 10.1172/jci.insight.160915

19. Bales CW, Kraus WE. Caloric restriction: implications for human cardiometabolic health. *J Cardiopulm Rehabil Prev*. (2013) 33:201–8. doi: 10.1097/HCR.0b013e318295019e

20. Devlin MJ. Why does starvation make bones fat? *Am J Hum Biol*. (2011) 23:577–85. doi: 10.1002/ajhb.21202

21. Devlin MJ, Cloutier AM, Thomas NA, Panus DA, Lotinun S, Pinz I, et al. Caloric restriction leads to high marrow adiposity and low bone mass in growing mice. *J Bone Miner Res*. (2010) 25:2078–88. doi: 10.1002/jbmr.82

22. Nedvidkova J, Krykorkova I, Bartak V, Papezova H, Gold PW, Alesci S, et al. Loss of meal-induced decrease in plasma ghrelin levels in patients with anorexia nervosa. *J Clin Endocrinol Metab*. (2003) 88:1678–82. doi: 10.1210/jc.2002-021669

23. Misra M, Miller KK, Cord J, Prabhakaran R, Herzog DB, Goldstein M, et al. Relationships between serum adipokines, insulin levels, and bone density in girls with anorexia nervosa. *J Clin Endocrinol Metab*. (2007) 92:2046–52. doi: 10.1210/jc.2006-2855

24. Inagaki T, Dutchak P, Zhao G, Ding X, Gautron L, Parameswara V, et al. Endocrine regulation of the fasting response by PPARalpha-mediated induction of

fibroblast growth factor 21. *Cell Metab*. (2007) 5:415–25. doi: 10.1016/j.cmet.2007.05.003

25. Cangemi R, Friedmann AJ, Holloszy JO, Fontana L. Long-term effects of calorie restriction on serum sex-hormone concentrations in men. *Aging Cell*. (2010) 9:236–42. doi: 10.1111/j.1474-9726.2010.00553.x

26. Cawthorn WP, Scheller EL, Parlee SD, Pham HA, Learman BS, Redshaw CM, et al. Expansion of bone marrow adipose tissue during caloric restriction is associated with increased circulating glucocorticoids and not with hypoleptinemia. *Endocrinology*. (2016) 157:508–21. doi: 10.1210/en.2015-1477

27. Monder C, Shackleton CH. 11 beta-Hydroxysteroid dehydrogenase: fact or fancy? *Steroids*. (1984) 44:383–417. doi: 10.1016/S0039-128X(84)80001-X

28. Albiston AL, Obeyesekere VR, Smith RE, Krozowski ZS. Cloning and tissue distribution of the human 11 beta-hydroxysteroid dehydrogenase type 2 enzyme. *Mol Cell Endocrinol*. (1994) 105:R11–7. doi: 10.1016/0303-7207(94)90176-7

29. Slavin BG, Ong JM, Kern PA. Hormonal regulation of hormone-sensitive lipase activity and mRNA levels in isolated rat adipocytes. *J Lipid Res*. (1994) 35:1535–41. doi: 10.1016/S0022-2275(20)41151-4

30. Villena JA, Roy S, Sarkadi-Nagy E, Kim KH, Sul HS. Desnutrin, an adipocyte gene encoding a novel patatin domain-containing protein, is induced by fasting and glucocorticoids: ectopic expression of desnutrin increases triglyceride hydrolysis. *J Biol Chem*. (2004) 279:47066–75. doi: 10.1074/jbc.M403855200

31. Lee RA, Harris CA, Wang JC. Glucocorticoid receptor and adipocyte biology. *Nucl Receptor Res*. (2018) 5. doi: 10.32527/2018/101373

32. Zhao X, Hu H, Wang C, Bai L, Wang Y, Wang W, et al. A comparison of methods for effective differentiation of the frozen-thawed 3T3-L1 cells. *Anal Biochem*. (2019) 568:57–64. doi: 10.1016/j.ab.2018.12.020

33. Desarzens S, Faresse N. Adipocyte glucocorticoid receptor has a minor contribution in adipose tissue growth. *J Endocrinol*. (2016) 230:1–11. doi: 10.1530/JOE-16-0121

34. Park YK, Ge K. Glucocorticoid Receptor Accelerates, but Is Dispensable for, Adipogenesis. *Mol Cell Biol*. (2017) 37:e00260-16. doi: 10.1128/MCB.00260-16

35. Bauerle KT, Hutson I, Scheller EL, Harris CA. Glucocorticoid receptor signaling is not required for *in vivo* adipogenesis. *Endocrinology*. (2018) 159:2050–61. doi: 10.1210/en.2018-00118

36. Mueller KM, Hartmann K, Kaltenecker D, Vettorazzi S, Bauer M, Mauser L, et al. Adipocyte glucocorticoid receptor deficiency attenuates aging- and HFD-induced obesity and impairs the feeding-fasting transition. *Diabetes*. (2017) 66:272–86. doi: 10.2337/db16-0381

37. Mittelstadt PR, Monteiro JP, Ashwell JD. Thymocyte responsiveness to endogenous glucocorticoids is required for immunological fitness. *J Clin Invest*. (2012) 122:2384–94. doi: 10.1172/JCI63067

38. Scheller EL, Troiano N, Vanhoutan JN, Bouxsein MA, Fretz JA, Xi Y, et al. Use of osmium tetroxide staining with microcomputerized tomography to visualize and quantify bone marrow adipose tissue *in vivo*. *Methods Enzymol*. (2014) 537:123–39. doi: 10.1016/B978-0-12-411619-1.00007-0

39. Ambrosi TH, Scialdone A, Graja A, Gohlke S, Jank AM, Bocian C, et al. Adipocyte accumulation in the bone marrow during obesity and aging impairs stem cell-based hematopoietic and bone regeneration. *Cell Stem Cell*. (2017) 20:771–84 e6. doi: 10.1016/j.stem.2017.02.009

40. von Lindern M, Zauner W, Mellitzer G, Steinlein P, Fritsch G, Huber K, et al. The glucocorticoid receptor cooperates with the erythropoietin receptor and c-Kit to enhance and sustain proliferation of erythroid progenitors in vitro. *Blood*. (1999) 94:550–9. doi: 10.1182/blood.V94.2.550.414k39_550_559

41. Bauer A, Tronche F, Wessely O, Kellendonk C, Reichardt HM, Steinlein P, et al. The glucocorticoid receptor is required for stress erythropoiesis. *Genes Dev*. (1999) 13:2996–3002. doi: 10.1101/gad.13.22.2996

42. Quatrini L, Tumino N, Besi F, Ciancaglini C, Galaverna F, Grasso AG, et al. Glucocorticoids inhibit human hematopoietic stem cell differentiation toward a common ILC precursor. *J Allergy Clin Immunol*. (2022) 149:1772–85. doi: 10.1016/j.jaci.2021.10.012

43. Mendez-, Chow A, Merad M, Frenette PS. Circadian rhythms influence hematopoietic stem cells. *Curr Opin Hematol*. (2009) 16:235–42. doi: 10.1097/MOH.0b013e32832bd0f5

44. Lightman SL, Wiles CC, Atkinson HC, Henley DE, Russell GM, Leendertz JA, et al. The significance of glucocorticoid pulsatility. *Eur J Pharmacol*. (2008) 583:255–62. doi: 10.1016/j.ejphar.2007.11.073

45. Bredella MA, Fazeli PK, Miller KK, Misra M, Torriani M, Thomas BJ, et al. Increased bone marrow fat in anorexia nervosa. *J Clin Endocrinol Metab*. (2009) 94:2129–36. doi: 10.1210/jc.2008-2532

46. Fazeli PK, Klibanski A. The paradox of marrow adipose tissue in anorexia nervosa. *Bone*. (2019) 118:47–52. doi: 10.1016/j.bone.2018.02.013

47. Canalis E, Delany AM. Mechanisms of glucocorticoid action in bone. *Ann N Y Acad Sci*. (2002) 966:73–81. doi: 10.1111/j.1749-6632.2002.tb04204.x

48. Beresford JN, Bennett JH, Devlin C, Leboy PS, Owen ME. Evidence for an inverse relationship between the differentiation of adipocytic and osteogenic cells in rat marrow stromal cell cultures. *J Cell Sci*. (1992) 102:341–51. doi: 10.1242/jcs.102.2.341

49. Meunier P, Aaron J, Edouard C, Vignon G. Osteoporosis and the replacement of cell populations of the marrow by adipose tissue. A quantitative study of 84 iliac bone biopsies. *Clin Orthop Relat Res*. (1971) 80:147–54. doi: 10.1097/00003086-197110000-00021

50. Di Iorgi N, Rosol M, Mittelman SD, Gilsanz V. Reciprocal relation between marrow adiposity and the amount of bone in the axial and appendicular skeleton of young adults. *J Clin Endocrinol Metab*. (2008) 93:2281–6. doi: 10.1210/jc.2007-2691

51. Bensreti H, Alhamad DW, Gonzalez AM, Pizarro-Mondesir M, Bollag WB, Isales CM, et al. Update on the role of glucocorticoid signaling in osteoblasts and bone marrow adipocytes during aging. *Curr Osteoporos Rep*. (2023) 21:32–44. doi: 10.1007/s11914-022-00772-5

52. Sharma AK, Shi X, Isales CM, McGee-Lawrence ME. Endogenous glucocorticoid signaling in the regulation of bone and marrow adiposity: Lessons from metabolism and cross talk in other tissues. *Curr Osteoporos Rep*. (2019) 17:438–45. doi: 10.1007/s11914-019-00554-6

53. Pierce JL, Sharma AK, Roberts RL, Yu K, Irsik DL, Choudhary V, et al. The glucocorticoid receptor in osterix-expressing cells regulates bone mass, bone marrow adipose tissue, and systemic metabolism in female mice during aging. *J Bone Miner Res*. (2022) 37:285–302. doi: 10.1002/jbmr.4468

54. Shen Y, Roh HC, Kumari M, Rosen ED. Adipocyte glucocorticoid receptor is important in lipolysis and insulin resistance due to exogenous steroids, but not insulin resistance caused by high fat feeding. *Mol Metab*. (2017) 6:1150–60. doi: 10.1016/j.molmet.2017.06.013

55. Morgan SA, McCabe EL, Gathercole LL, Hassan-Smith ZK, Larner DP, Bujalska IJ, et al. 11beta-HSD1 is the major regulator of the tissue-specific effects of circulating glucocorticoid excess. *Proc Natl Acad Sci U.S.A*. (2014) 111:E2482–91. doi: 10.1073/pnas.1323681111

56. Chapman K, Holmes M, Seckl J. 11beta-hydroxysteroid dehydrogenases: intracellular gate-keepers of tissue glucocorticoid action. *Physiol Rev*. (2013) 93:1139–206. doi: 10.1152/physrev.00020.2012

57. Kotelevtsev Y, Holmes MC, Burchell A, Houston PM, Schmoll D, Jamieson P, et al. 11beta-hydroxysteroid dehydrogenase type 1 knockout mice show attenuated glucocorticoid-inducible responses and resist hyperglycemia on obesity or stress. *Proc Natl Acad Sci U.S.A*. (1997) 94:14924–9. doi: 10.1073/pnas.94.26.14924

58. Morton NM, Holmes MC, Fievet C, Staels B, Tailleux A, Mullins JJ, et al. Improved lipid and lipoprotein profile, hepatic insulin sensitivity, and glucose tolerance in 11beta-hydroxysteroid dehydrogenase type 1 null mice. *J Biol Chem*. (2001) 276:41293–300. doi: 10.1074/jbc.M103676200

59. Morton NM, Paterson JM, Masuzaki H, Holmes MC, Staels B, Fievet C, et al. Novel adipose tissue-mediated resistance to diet-induced visceral obesity in 11 beta-hydroxysteroid dehydrogenase type 1-deficient mice. *Diabetes*. (2004) 53:931–8. doi: 10.2337/diabetes.53.4.931

60. Horton JA, Beck-Cormier S, van Wijnen AJ. Editorial: Bone marrow adiposity - contributions to bone, aging and beyond. *Front Endocrinol (Lausanne)*. (2023) 14:1144163. doi: 10.3389/fendo.2023.1144163

61. Hogler W, Blimkie CJ, Cowell CT, Inglis D, Rauch F, Kemp AF, et al. Sex-specific developmental changes in muscle size and bone geometry at the femoral shaft. *Bone*. (2008) 42:982–9. doi: 10.1016/j.bone.2008.01.008

62. Choi KH, Lee JH, Lee DG. Sex-related differences in bone metabolism in osteoporosis observational study. *Med (Baltimore)*. (2021) 100:e26153. doi: 10.1097/MD.0000000000026153

63. Villareal DT, Fontana L, Das SK, Redman L, Smith SR, Saltzman E, et al. Effect of two-year caloric restriction on bone metabolism and bone mineral density in non-obese younger adults: A randomized clinical trial. *J Bone Miner Res*. (2016) 31:40–51. doi: 10.1002/jbmr.2701

64. Villareal DT, Fontana L, Weiss EP, Racette SB, Steger-May K, Schechtman KB, et al. Bone mineral density response to caloric restriction-induced weight loss or exercise-induced weight loss: a randomized controlled trial. *Arch Intern Med*. (2006) 166:2502–10. doi: 10.1001/archinte.166.22.2502

65. Sukumar D, Ambia-Sobhan H, Zurfluh R, Schlussel Y, Stahl TJ, Gordon CL, et al. Areal and volumetric bone mineral density and geometry at two levels of protein intake during caloric restriction: a randomized, controlled trial. *J Bone Miner Res*. (2011) 26:1339–48. doi: 10.1002/jbmr.318

66. Lawson EA, Miller KK, Bredella MA, Phan C, Misra M, Meenaghan E, et al. Hormone predictors of abnormal bone microarchitecture in women with anorexia nervosa. *Bone*. (2010) 46:458–63. doi: 10.1016/j.bone.2009.09.005

67. Mika C, Holtkamp K, Heer M, Gunther RW, Herpertz-Dahlmann B. A 2-year prospective study of bone metabolism and bone mineral density in adolescents with anorexia nervosa. *J Neural Transm (Vienna)*. (2007) 114:1611–8. doi: 10.1007/s00702-007-0787-4

68. Clarke J, Peyre H, Alison M, Bargiacchi A, Stordeur C, Boizeau P, et al. Abnormal bone mineral density and content in girls with early-onset anorexia nervosa. *J Eat Disord*. (2021) 9:9. doi: 10.1186/s40337-020-00365-6

69. Lucas AR, Melton LJ 3rd, Crowson CS, O'Fallon WM. Long-term fracture risk among women with anorexia nervosa: a population-based cohort study. *Mayo Clin Proc*. (1999) 74:972–7. doi: 10.4065/74.10.972

70. Devlin MJ, Brooks DJ, Conlon C, Vliet M, Louis L, Rosen CJ, et al. Daily leptin blunts marrow fat but does not impact bone mass in calorie-restricted mice. *J Endocrinol*. (2016) 229:295–306. doi: 10.1530/JOE-15-0473

71. McGrath C, Sankaran JS, Misaghian-Xanthos N, Sen B, Xie Z, Styner MA, et al. Exercise degrades bone in caloric restriction, despite suppression of marrow adipose tissue (MAT). *J Bone Miner Res*. (2020) 35:106–15. doi: 10.1002/jbmr.3872

72. Benedetti MG, Furlini G, Zati A, Letizia Mauro G. The effectiveness of physical exercise on bone density in osteoporotic patients. *BioMed Res Int*. (2018) 2018:4840531. doi: 10.1155/2018/4840531

73. Behrendt AK, Kuhla A, Osterberg A, Polley C, Herlyn P, Fischer DC, et al. Dietary restriction-induced alterations in bone phenotype: Effects of lifelong versus short-term caloric restriction on femoral and vertebral bone in C57BL/6 mice. *J Bone Miner Res*. (2016) 31:852–63. doi: 10.1002/jbmr.2745

74. Hamrick MW, Ding KH, Ponnala S, Ferrari SL, Isales CM. Caloric restriction decreases cortical bone mass but spares trabecular bone in the mouse skeleton: implications for the regulation of bone mass by body weight. *J Bone Miner Res*. (2008) 23:870–8. doi: 10.1359/jbmr.080213

75. Mattiucci D, Maurizi G, Izzi V, Cenci L, Ciarlantini M, Mancini S, et al. Bone marrow adipocytes support hematopoietic stem cell survival. *J Cell Physiol*. (2018) 233:1500–11. doi: 10.1002/jcp.26037

76. Broudy VC, Lin NL, Priestley GV, Nocka K, Wolf NS. Interaction of stem cell factor and its receptor c-kit mediates lodgment and acute expansion of hematopoietic cells in the murine spleen. *Blood*. (1996) 88:75–81. doi: 10.1182/blood.V88.1.75.75

77. Amatya S, Tietje-Mckinney D, Mueller S, Petrillo MG, Woolard MD, Bharrhan S, et al. Adipocyte glucocorticoid receptor inhibits immune regulatory genes to maintain immune cell homeostasis in adipose tissue. *Endocrinology*. (2023) 164. doi: 10.1210/endocr/bqad143

78. Rocamora-Reverte L, Villunger A, Wiegers GJ. Cell-specific immune regulation by glucocorticoids in murine models of infection and inflammation. *Cells*. (2022) 11:2126. doi: 10.3390/cells11142126

79. Herrmann M. Marrow fat-secreted factors as biomarkers for osteoporosis. *Curr Osteoporos Rep*. (2019) 17:429–37. doi: 10.1007/s11914-019-00550-w

80. Li Z, MacDougald OA. Stem cell factor: the bridge between bone marrow adipocytes and hematopoietic cells. *Haematologica*. (2019) 104:1689–91. doi: 10.3324/haematol.2019.224188

81. Zhang Z, Huang Z, Ong B, Sahu C, Zeng H, Ruan HB. Bone marrow adipose tissue-derived stem cell factor mediates metabolic regulation of hematopoiesis. *Haematologica*. (2019) 104:1731–43. doi: 10.3324/haematol.2018.205856

frontiers | Frontiers in Endocrinology

TYPE Original Research
PUBLISHED 09 July 2024
DOI 10.3389/fendo.2024.1402937

OPEN ACCESS

EDITED BY
Sandeep Kumar,
University of Alabama at Birmingham, United States

REVIEWED BY
Surbhi Gahlot,
University of Texas Southwestern Medical Center, United States
Shivmurat Yadav,
University of Oklahoma Health Sciences Center, United States
Sonal Kale,
National Institute of Allergy and Infectious Diseases (NIH), United States
Sanjukta Majumder,
Connecticut Children's Medical Center, United States

*CORRESPONDENCE
Xiao-Li Xie
13826553075@163.com

RECEIVED 18 March 2024
ACCEPTED 26 June 2024
PUBLISHED 09 July 2024

CITATION
Wang Z-G, Fang Z-B and Xie X-L (2024) Association between fatty acids intake and bone mineral density in adolescents aged 12-19: NHANES 2011–2018.
Front. Endocrinol. 15:1402937.
doi: 10.3389/fendo.2024.1402937

Association between fatty acids intake and bone mineral density in adolescents aged 12-19: NHANES 2011–2018

Zhi-Gang Wang[1], Ze-Bin Fang[2] and Xiao-Li Xie[1*]

[1]Department of Emergency, Beijing University of Chinese Medicine Shenzhen Hospital (Long gang), Shenzhen, China, [2]The First School of Clinical Medicine, Guangzhou University of Chinese Medicine, Guangzhou, China

Background: The relationship between the intake of dietary fatty acids (FA) and bone mineral density (BMD) has been the subject of prior investigations. However, the outcomes of these studies remain contentious. The objective of this research is to examine the link between dietary FA consumption among adolescents and BMD.

Methods: This study utilized high-quality data from the National Health and Nutrition Examination Survey database, spanning 2011 to 2018, to explore the association between dietary fatty acids and bone health indicators in adolescents, including BMD and bone mineral content (BMC). Analyses were performed using weighted multivariate linear regression models, incorporating detailed subgroup analysis.

Results: The study included 3440 participants. Analysis demonstrated that intake of saturated fatty acids (SFA) was positively correlated with total BMD, left arm BMD, total BMC, and left arm BMC. Monounsaturated fatty acid (MUFA) intake was positively correlated with BMC across most body parts, though it showed no correlation with BMD. Intake of polyunsaturated fatty acids (PUFA) was significantly inversely correlated with both BMD and BMC in most body parts. Additionally, subgroup analysis indicated that variables such as sex, age, standing height, and race significantly influenced the correlation between FA intake and BMD.

Conclusions: Our study indicates that dietary intake of SFA may benefit to BMD in adolescents, in contrast to PUFA and MUFA. Therefore, we recommend that adolescents maintain a balanced intake of SFA to promote optimal bone mass development while preserving metabolic health.

KEYWORDS

bone mineral density, saturated fatty acids, monounsaturated fatty acids, polyunsaturated fatty acids, adolescent, NHANES

1 Introduction

Osteoporosis (OP), a systemic disease affecting the musculoskeletal framework, is characterized by reduced bone density, degeneration of bone tissue structure, increased susceptibility to fractures, and enhanced fragility (1, 2). Given the aging population and increased life expectancy, the World Health Organization has recognized OP as one of the most pressing global public health issues. In recent years, there has been noticeable increase in the incidence of OP. A study by the International Society for Clinical Densitometry and the International Osteoporosis Foundation projects that by 2030, osteoporosis will affect over 70 million individuals in America, a condition marked by decreased bone mineral density (BMD) (3). Statistics indicate that osteoporosis-related fractures result in an estimated annual direct economic loss of 17 billion US dollars worldwide, posing a significant economic burden on healthcare systems across various countries (4). Currently, the clinical diagnosis and assessment of OP rely on BMD measurements, a method proven reliable and effective in numerous studies (5–7). Consequently, the early detection, intervention, and management of OP have attracted increasing interest among researchers.

In recent years, adolescent dietary patterns in economically developed countries have increasingly shifted towards processed and calorie-dense foods (8). From 2009 to 2019, there was a significant increase in the proportion of U.S. teenagers-across all genders and racial demographics-consuming fruit or 100% juice less than once daily (9). Similarly, the daily vegetable consumption among teenagers has notably declined. Insufficient intake of fruits and vegetables correlates with deficiencies in vital nutrients essential for bone health and development. Specifically, essential nutrients for bone health, such as calcium, vitamin D, and protein, are primarily derived from dairy products, green leafy vegetables, and other nutrient-rich sources. Inadequate intake of calcium and vitamin D is linked to lower bone density and a heightened fracture risk among adolescents (10). Furthermore, while protein supports bone growth, excessive intake can adversely affect bone health, particularly if not balanced with adequate calcium (10). Furthermore, a plethora of other nutrients are integral to bone health. Essential trace elements such as zinc, copper, manganese, and boron, in conjunction with critical vitamins like vitamin K and vitamin C, significantly influence bone structure and integrity (11, 12). Emerging research further delineates dietary fat as an instrumental regulatory element in the preservation of musculoskeletal structure and functionality (13–18). Fatty acids (FA) have garnered increasing attention due to their significant significance as a crucial constituent of dietary fat and their potential regulatory role in metabolic disorders. FA are classified into three distinct groups based on the saturation level of their hydrocarbon chains: saturated fatty acids (SFA), which contain no double bonds; monounsaturated fatty acids (MUFA), characterized by the presence of a single double bond; and polyunsaturated fatty acids (PUFA), which possess multiple double bonds (16). This categorization reflects the structural differences and physiochemical properties attributable to the degree of saturation within the hydrocarbon chains of fatty acids.

Recent research into dietary fatty acids' influence on bone mineral density presents varied and often contradictory outcomes (19–23). Such discrepancies likely arise from small sample sizes, varied survey methodologies, and inherent selection biases. Alarmingly, few studies have assessed fatty acids' effects on bone health in adolescents. Given that adolescence is a crucial period for bone development, ensuring optimal nutrition is imperative to foster peak bone density and quality, which are essential for long-term health. We hypothesize that dietary FA intake is associated with BMD in adolescents; however, this association is likely non-linear and modulated by variables including age, gender, and ethnicity. Thus, it is vital to further investigate the link between fatty acids and bone health during adolescence. This study utilizes data from the National Health and Nutrition Examination Survey (NHANES) to delve into how dietary fatty acids influence adolescent bone health and to develop novel clinical intervention strategies.

2 Methods

2.1 Data source and study population

NHANES is designed to assess the health and nutritional status of the American population across a broad age spectrum. The study stands out due to its distinctive integration of questionnaires and physical evaluations. The survey is administered on an annual schedule, utilizing a sample that is representative of the entire nation and consisting of roughly 5,000 individuals. These individuals are situated in various counties throughout the whole country, performing visits to a total of 15 counties annually. The NHANES interviews encompassed a range of inquiries about demographics, socioeconomic status, dietary habits, and health-related factors. Skilled medical professionals undertake a battery of diagnostic tests, including physical, dental, and physiological evaluations, as well as laboratory analysis. The primary purpose of utilizing the data collected from this survey is to facilitate epidemiological and health science research. The objective of NHANES is to support the development of comprehensive public health policies and promote health education across the broader population (24).

Our cross-sectional study examined 39,156 NHENAS participants from 2011 to 2018. This study examined the correlation between dietary fatty acids and adolescent bone health, focusing on BMD and BMC in individuals aged 12-19. Recognizing that regional bone properties may be influenced by distinct factors, we conducted a comprehensive analysis that incorporated BMD and BMC measurements from various anatomical sites and assessed multiple classes of FA. Consequently, participants under 12 years of age (11,324 individuals) and those older than 19 years (22,617 individuals) were excluded. Additionally, individuals lacking fatty acid intake data (1,166 participants), total BMD measurements (531 participants), or other BMD data (78 participants) were also excluded. Following the completion of this screening process, a

cumulative total of 3440 people were deemed eligible for inclusion in the study (Figure 1).

2.2 Ethics statement

Prior to their involvement in the survey, participants received detailed explanations about the nature and specifics of the study, following which they executed a consent agreement. This process of informed consent received approval from the National Center for Health Statistics' Ethics Review Board. After the process of formal anonymization is concluded, the entirety of the data is released to the public to optimize the utilization of these resources. The accessibility of these statistics is contingent upon adherence to the NHANES database restrictions and a commitment to statistical analysis. All experimental research conducted using this data must adhere to the relevant laws and legislation.

2.3 Covariates

Daily FAs consumption was the independent variable in this study. All participants in the NHANES underwent two 24-hour food recall interviews, both of which were administered by proficient dietary interviewers who were fluent in both Spanish and English. The initial in-person interviews took place within designated private rooms at the Mobile Examination Centre (MEC), wherein a standardized collection of measuring guides was utilized. The subsequent 24-hour dietary recall interview is conducted via telephone, often within a time frame of 3 to 10 days following the MEC diet assessment. Furthermore, this study used categorical variables, including gender, ethnicity, and moderate physical activity. Continuous variables include the ratio of family income to poverty, body mass index (BMI), standing height, alkaline phosphatase (ALP), serum calcium (Ca), serum phosphorus (P), serum uric acid (UA), total cholesterol (TC), triglycerides (TG), glycohemoglobin, blood urea nitrogen (BUN), serum creatinine (Scr), urinary albumin-creatinine ratio (UACR), total protein (TP), vitamin D (VitD) intake, alcohol intake, energy intake, carbohydrate intake, protein intake, cholesterol intake, as well as BMD (lumbar spine, left arm, left leg, head, trunk, thoracic, pelvis, and left rib), and BMC (total, lumbar spine, left arm, left leg, head, thoracic, trunk, pelvis, and left rib). At www.cdc.gov/nchs/nhanes/, you can find out more about the collection of covariates and the 24-hour dietary recall interview.

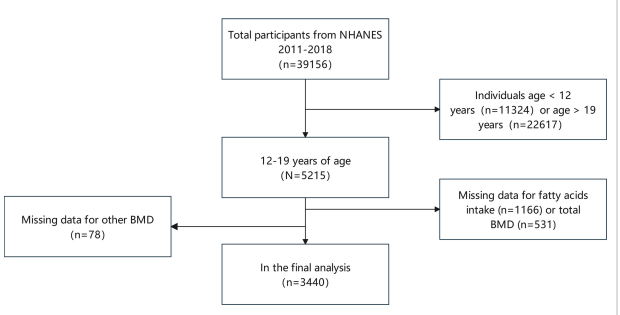

FIGURE 1
Participant selection flow chart. NHANES, National Health and Nutrition Examination Survey; BMD, bone mineral density.

2.4 Outcome variable

Dual-energy X-ray absorptiometry (DXA) is a highly prevalent technique for assessing body composition due to its rapidity, user-friendliness, and minimal radiation exposure (25). DXA detection results are often used for osteoporotic fractures, fracture risk prediction, and drug efficacy evaluation. The Hologic Discovery A is a bone densitometer that utilizes fan-beam X-ray technology. Manufactured by Hologic, Inc. in Bedford, Massachusetts, this device uses an energy tube to generate two distinct energy levels. These energy levels are then used to determine BMC and BMD. All DXA scans are performed by a certified radiographer. Additional information regarding the operational mechanisms of the DXA examination can be found on the official website of the NHANES, which offers a comprehensive body composition manual.

2.5 Statistical analysis

Statistical analyses were conducted using EmpowerStats2 (http://www.empowerstats.com) and R software (version 3.4.4), considering *P*-values below 0.05 as statistically significant. Sample sizes were weighted. Continuous variables were described as mean ± standard deviation, and categorical variables as percentages for baseline comparison. *P*-values for continuous and categorical variables were derived using weighted linear regression and chi-square tests, respectively. Furthermore, weighted multiple regression models assessed the association between dietary FA intake and BMD metrics (total, lumbar spine, and left arm), with adjustments for covariates outlined in Table 1. Linear trend tests were employed to analyze effect size trends. To enhance data utilization, subgroup analyses were stratified by gender, age, standing height, and race, enriching our insights into the relationships between FA intake and BMD.

3 Results

3.1 Characteristics of participants

Table 1 displays the weighted sociodemographic and physiological characteristics of the participants. Following stratification of total BMD into quartiles, we observed significant differences across multiple variables: age, gender, race, the ratio of family income to poverty, BMI, standing height, and moderate activity. Biochemical parameters such as ALP, Ca, P, UA, BUN, Scr, UACR, TP also varied significantly. Additionally, intakes of VitD, alcohol, energy, carbohydrate, protein, cholesterol, total SFA, total MUFA, total PUFA were distinct among the quartiles. BMD at various sites including lumbar spine, left arm, left leg, head, trunk,

10.3389/fendo.2024.1402937

TABLE 1 Weighted characteristics of the study sample.

Quartiles of total bone mineral density (g/cm2)	Lowest quartiles	2nd	3rd	4th	*P* value
Age (years)	13.53 ± 1.77	15.26 ± 2.13	16.12 ± 1.96	17.11 ± 1.60	< 0.001
Gender (%)					< 0.001
male	53.14	43.53	44.74	66.67	
female	46.86	56.47	55.26	33.33	
Race/ethnicity (%)					< 0.001
White people	55.47	57.85	53.54	43.13	
Black people	6.27	10.08	14.57	24.44	
Mexican American	17.96	13.75	15.29	18.05	
Other race	20.3	18.33	16.59	14.38	
Ratio of family income to poverty (%)	2.52 ± 1.58	2.45 ± 1.58	2.31 ± 1.57	2.29 ± 1.60	0.006
Body mass index (kg/m2)	21.29 ± 4.94	22.95 ± 5.31	25.24 ± 6.13	26.57 ± 6.34	< 0.001
Standing height(cm)	158.67 ± 8.33	164.62 ± 8.23	167.38 ± 8.79	171.52 ± 8.39	< 0.001
Moderate activities (%)					< 0.001
No	29.1	25.52	25.39	28.54	
Yes	50.43	57.09	57.83	60.78	
Don't know	20.48	17.39	16.78	10.69	
Alkaline phosphatase (u/L)	201.34 ± 102.64	138.16 ± 87.04	107.94 ± 62.79	91.19 ± 39.60	< 0.001
Serum calcium (mmol/L)	2.41 ± 0.08	2.40 ± 0.07	2.39 ± 0.07	2.40 ± 0.07	< 0.001
Serum phosphorus (mmol/L)	1.52 ± 0.19	1.40 ± 0.21	1.36 ± 0.18	1.32 ± 0.16	< 0.001
Serum uric acid (umol/L)	283.70 ± 61.65	294.17 ± 67.50	303.01 ± 71.78	322.51 ± 70.76	< 0.001
Total cholesterol (mmol/L)	4.07 ± 0.71	4.08 ± 0.71	4.04 ± 0.76	4.08 ± 0.75	0.582
Triglycerides (mmol/L)	1.11 ± 0.65	1.12 ± 0.72	1.16 ± 0.76	1.12 ± 0.71	0.561
Glycohemoglobin (%)	5.27 ± 0.41	5.25 ± 0.44	5.24 ± 0.31	5.23 ± 0.31	0.093
Blood urea nitrogen (mmol/L)	3.99 ± 1.21	3.90 ± 1.13	4.12 ± 1.20	4.22 ± 1.13	< 0.001
Serum creatinine (umol/L)	54.44 ± 11.41	61.34 ± 11.47	66.04 ± 12.54	74.46 ± 13.08	< 0.001
Urinary albumin creatinine ratio (mg/g)	35.13 ± 124.55	24.06 ± 85.26	22.06 ± 87.35	14.87 ± 38.19	< 0.001
Total protein (g/L)	72.07 ± 3.98	72.58 ± 3.83	72.68 ± 3.87	72.69 ± 4.06	0.003
Vitamin D intake (mcg/d)	5.39 ± 4.67	4.50 ± 3.60	4.62 ± 4.12	5.18 ± 4.70	< 0.001
Alcohol intake (g/d)	0.07 ± 1.05	0.49 ± 3.75	0.63 ± 5.56	1.28 ± 6.58	< 0.001
Energy intake (kcal/d)	1921.21 ± 655.70	1868.20 ± 704.25	1915.88 ± 744.43	2207.70 ± 854.88	< 0.001
Carbohydrate intake (g/d)	248.87 ± 91.16	243.11 ± 88.67	242.51 ± 95.98	274.64 ± 110.90	< 0.001
Protein intake (g/d)	71.54 ± 27.98	69.57 ± 34.39	74.46 ± 40.84	86.33 ± 41.35	< 0.001
Cholesterol intake (mg/d)	224.37 ± 139.31	222.59 ± 167.22	246.20 ± 201.71	285.22 ± 186.41	< 0.001
Total saturated fatty acids intake (g/d)	25.67 ± 11.83	23.72 ± 11.59	25.01 ± 12.61	29.10 ± 14.04	< 0.001
Total monounsaturated fatty acids intake (g/d)	24.74 ± 10.60	23.83 ± 11.66	24.94 ± 12.21	29.79 ± 15.09	< 0.001
Total Polyunsaturated fatty acids intake (g/d)	16.26 ± 7.80	16.70 ± 9.04	16.85 ± 9.17	19.36 ± 9.94	< 0.001
Lumbar Spine Bone Mineral Density (g/cm2)	0.80 ± 0.11	0.94 ± 0.09	1.03 ± 0.10	1.12 ± 0.12	< 0.001
Left Arm Bone Mineral Density (g/cm2)	0.61 ± 0.05	0.68 ± 0.04	0.73 ± 0.05	0.81 ± 0.07	< 0.001

(Continued)

TABLE 1 Continued

Quartiles of total bone mineral density (g/cm2)	Lowest quartiles	2nd	3rd	4th	*P* value
Left Leg Bone Mineral Density (g/cm2)	0.94 ± 0.08	1.05 ± 0.06	1.14 ± 0.06	1.27 ± 0.10	< 0.001
Head Bone Mineral Density (g/cm2)	1.48 ± 0.19	1.75 ± 0.20	1.94 ± 0.24	2.16 ± 0.26	< 0.001
Trunk Bone Mineral Density (g/cm2)	0.71 ± 0.06	0.82 ± 0.04	0.90 ± 0.05	1.01 ± 0.08	< 0.001
Thoracic Bone Mineral Density (g/cm2)	0.62 ± 0.07	0.72 ± 0.05	0.78 ± 0.06	0.86 ± 0.08	< 0.001
Pelvis Bone Mineral Density (g/cm2)	0.99 ± 0.11	1.13 ± 0.09	1.24 ± 0.10	1.38 ± 0.14	<0.001
Left Rib Bone Mineral Density (g/cm2)	0.53 ± 0.05	0.60 ± 0.04	0.64 ± 0.04	0.72 ± 0.07	< 0.001
Total Bone Mineral Content(g)	1507.12 ± 233.25	1887.45 ± 202.25	2179.48 ± 236.61	2616.33 ± 332.20	< 0.001
Lumbar Spine Bone Mineral Content (g)	35.52 ± 9.43	48.38 ± 8.84	54.47 ± 9.20	63.56 ± 11.37	< 0.001
Left Arm Bone Mineral Content (g)	99.08 ± 21.40	130.23 ± 22.98	153.10 ± 27.52	189.37 ± 35.78	< 0.001
Left Leg Bone Mineral Content (g)	295.04 ± 55.00	360.79 ± 56.08	413.12 ± 65.78	500.52 ± 83.86	< 0.001
Head Bone Mineral Content (g)	327.88 ± 46.81	393.24 ± 48.31	442.50 ± 56.81	509.54 ± 69.27	< 0.001
Thoracic Bone Mineral Content (g)	69.77 ± 17.62	91.58 ± 16.45	105.66 ± 18.52	119.29 ± 20.12	< 0.001
Trunk Bone Mineral Content (g)	382.05 ± 76.76	500.39 ± 67.96	589.33 ± 79.43	709.34 ± 107.80	< 0.001
Pelvis Bone Mineral Content (g)	163.23 ± 38.08	220.72 ± 38.06	270.03 ± 45.82	340.38 ± 68.99	< 0.001
Left Rib Bone Mineral Content (g)	57.59 ± 12.30	70.86 ± 11.31	80.58 ± 13.52	94.72 ± 15.93	< 0.001

Continuous variables are presented as Mean ± SD, P-value was calculated by a weighted linear regression model. Categorical variables are presented as %, P-value was calculated by the chi-square test.

thoracic, pelvis, left rib, along with bone mineral content (BMC) at these locations, showed significant variances. In contrast, no significant differences were observed in glycohemoglobin, TC, and TG. These findings suggest that BMD is potentially influenced by demographic characteristics, dietary habits, and physical activity levels.

3.2 Association between total SFAs intake, BMD, and BMC

Figure 2 illustrates the association between total SFA intake and both BMD (Figure 2A) and BMC (Figure 2B). Positive correlations were observed between the overall intake of SFA and both total and left arm BMD, with *P*-values of 0.0197 and 0.0011, respectively. Similarly, positive correlations persisted for both total and left arm BMC, with *P*-values of 0.0270 and 0.0016, respectively. Three weighted multivariate linear regression models of total SFA intake versus total BMD, lumbar spine BMD, and left arm BMD are shown in Table 2. Adjustments were made for all factors. The stratification variable was not adjusted for in the subgroup analysis.

The lowest quartiles of total SFA were used as a control group in the weighted multiple linear regression model of total BMD and total SFA intake. In the highest quartile of total SFA, a positive association with total BMD was identified, exhibiting statistical significance ($P < 0.05$), with the trend's P value also reaching a notable level of significance ($P = 0.007$). In the process of performing subgroup analysis based on gender, age, and race, it was shown that in male and Mexican Americans, there existed a positive association between total SFA intake and total BMD ($P < 0.05$). We also stratified the standing height, with 132.9-160.2 cm as Q1, 160.3-168.7 cm as Q2, and 168.8-190.9 cm as Q3, and only in Q3, there was a positive association between total SFA intake and total BMD. This phenomenon could be attributed to the generally larger bone size and greater bone mass observed in men, with testosterone significantly contributing to the preservation of bone density. Moreover, taller individuals typically exhibit elevated levels of growth and sex hormones, which are associated with enhanced bone growth and density. These hormonal effects may be further influenced by biomechanical stimulation, genetic factors, among other determinants. Furthermore, dietary preferences among Mexicans, which often include high-calcium foods, might also play a role in influencing bone density.

In the model of lumbar spine BMD and total SFA intake, when SFA intake was stratified by quartiles, with the lowest quartiles as the reference, the 2nd quartile of total SFA was negatively correlated with total BMD ($P < 0.05$). Nonetheless, the trend across quartiles did not reach statistical significance ($P = 0.172$). Further subgroup analysis, which was categorized by gender, age, standing height, and race, revealed a significant positive correlation between dietary SFA and lumbar spine BMD exclusively in adolescents aged 13 and in Mexican American individuals ($P < 0.01$). After accounting for confounding factors, the overall correlation between SFA intake and BMD may be obscured (Figure 2). However, this correlation might become significant when analyses are conducted separately for particular subgroups, suggesting unique relationships within these populations.

The measurement of BMD in the left arm provides valuable insights for the young population, particularly in evaluating overall

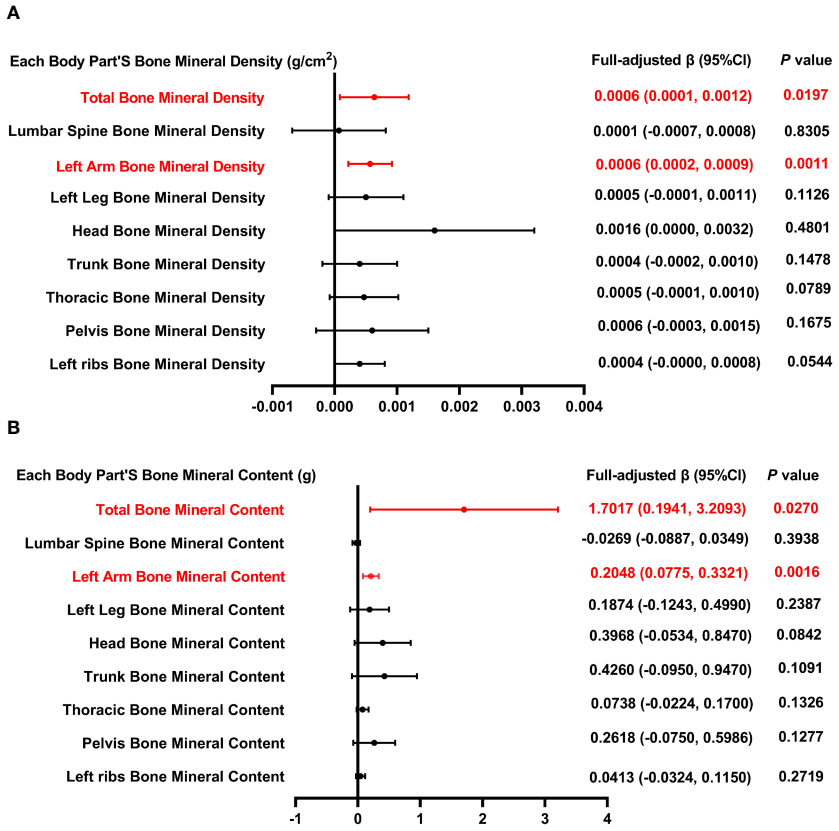

FIGURE 2
Forest plot of the relationship between total SFA intake and BMD and BMC for each body part. **(A)** Correlation between BMD and total SFA intake in each body part. **(B)** Correlation between BMC and total SFA intake in each body part. SFA, saturated fatty acids intake; BMD, bone mineral density; BMC, bone mineral content.

TABLE 2 Association between total saturated fatty acids intake (g/d) and bone mineral density (g/cm^2).

Exposure	Total BMD β, 95%CI, *P* value	Lumbar Spine BMD β, 95%CI, *P* value	Left Arm BMD β, 95%CI, *P* value
Quartiles of total polyunsaturated fatty acids intake (g/d)			
Lowest quartiles (2.00-16.29)	reference	reference	reference
2nd (16.30-23.24)	-0.0079 (-0.0163, 0.0004)	-0.0126 (-0.0242, -0.0011)*	-0.0101 (-0.0156, -0.0046)***
3rd (23.25-31.64)	0.0048 (-0.0048, 0.0145)	0.0043 (-0.0091, 0.0177)	-0.0025 (-0.0088, 0.0038)
4th (31.65-116.23)	0.0170 (0.0035, 0.0305)*	0.0073 (-0.0114, 0.0260)	0.0031 (-0.0057, 0.0120)
P *for* trend	0.007	0.172	0.341
Stratified by gender			
Male	0.0009 (0.0002, 0.0016)*	0.0004 (-0.0005, 0.0014)	0.0007 (0.0002, 0.0012)**
Female	0.0003 (-0.0006, 0.0011)	-0.0007 (-0.0019, 0.0006)	0.0005 (-0.0000, 0.0009)
Stratified by age (years old)			
12	0.0013 (-0.0002, 0.0028)	0.0002 (-0.0018, 0.0023)	0.0007 (-0.0003, 0.0017)
13	0.0014 (-0.0002, 0.0029)	0.0029 (0.0008, 0.0050) **	0.0008 (-0.0003, 0.0018)
14	-0.0004 (-0.0019, 0.0011)	-0.0007 (-0.0026, 0.0012)	0.0004 (-0.0005, 0.0013)
15	0.0014 (-0.0004, 0.0032)	0.0013 (-0.0012, 0.0037)	0.0005 (-0.0007, 0.0016)

(Continued)

TABLE 2 Continued

Exposure	Total BMD β, 95%CI, *P* value	Lumbar Spine BMD β, 95%CI, *P* value	Left Arm BMD β, 95%CI, *P* value
Stratified by age (years old)			
16	0.0007 (-0.0008, 0.0022)	-0.0007 (-0.0028, 0.0015)	0.0002 (-0.0008, 0.0012)
17	0.0010 (-0.0006, 0.0026)	0.0010 (-0.0013, 0.0034)	0.0014 (0.0005, 0.0024) **
18	-0.0007 (-0.0024, 0.0009)	-0.0007 (-0.0030, 0.0015)	0.0003 (-0.0008, 0.0013)
19	0.0011 (-0.0004, 0.0027)	0.0012 (-0.0010, 0.0034)	0.0008 (-0.0003, 0.0019)
Stratified by standing height (cm)			
Q1 (132.9-160.2)	0.0004 (-0.0006, 0.0014)	0.0002 (-0.0013, 0.0017)	0.0001 (-0.0005, 0.0008)
Q2 (160.3-168.7)	0.0007 (-0.0003, 0.0017)	-0.0001 (-0.0014, 0.0013)	0.0007 (0.0001, 0.0013)*
Q3 (168.8-190.9)	0.0010 (0.0001, 0.0019)*	0.0004 (-0.0009, 0.0016)	0.0010 (0.0004, 0.0016)**
Stratified by race			
White people	0.0009 (-0.0001, 0.0019)	-0.0003 (-0.0017, 0.0011)	0.0008 (0.0002, 0.0015)*
Black people	0.0003 (-0.0010, 0.0015)	-0.0001 (-0.0019, 0.0017)	0.0005 (-0.0003, 0.0012)
Mexican American	0.0016 (0.0002, 0.0029)*	0.0023 (0.0006, 0.0041)**	0.0006 (-0.0003, 0.0015)
Other race	-0.0010 (-0.0020, 0.0001)	-0.0008 (-0.0023, 0.0006)	-0.0002 (-0.0009, 0.0005)

All factors were adjusted. In the subgroup analysis, not adjusted for the stratification variable itself. *P < 0.05, **P < 0.01, ***P < 0.001.

bone health and estimating the risk of fractures. As illustrated in Figure 2, a positive correlation exists between dietary SFA intake and BMD. In the analysis concerning the relationship between left arm BMD and overall SFA consumption, segmentation of SFA intake into quartiles revealed a negative association between the second quartile of SFA intake and left arm BMD ($P < 0.001$). Nonetheless, the trend across quartiles did not achieve statistical significance ($P = 0.341$). In the subgroup analysis stratified by gender, age, and race, a significant positive association between dietary SFA and BMD in the left arm was observed exclusively in males, 17-year-olds, and white people. In subgroups stratified by standing height, dietary SFA intake was positively related to left arm BMD in Q2 and Q3, with significance levels of $P < 0.05$ and $P < 0.01$, respectively.

3.3 Association between total MUFA intake, BMD, and BMC

Figure 3 illustrates the correlation between total MUFA and both BMD and BMC. Figure 3B illustrates that BMC measurements across multiple anatomical regions—including the total body, lumbar spine, left leg, trunk, pelvis, and left ribs—demonstrate a positive relationship with overall MUFA intake. However, the association between MUFA intake and BMD across these regions did not reach statistical significance ($P > 0.05$).

Table 3 outlines three models that examine the relationship between MUFA consumption and BMD, with adjustments made for all pertinent variables. The analysis of total BMD in relation to MUFA intake, categorized by quartiles, reveals a negative correlation in the 2nd quartile with total BMD ($P < 0.01$), without a significant trend across quartiles ($P = 0.850$). Furthermore, when dissecting the data by gender, age, standing height, and race, a significant negative relationship between total MUFA intake and total BMD was observed exclusively in the "other race" category ($P < 0.05$). In the model of lumbar spine BMD and total dietary MUFA. When categorized by gender, age, standing height, and race, positive correlations between dietary MUFA and lumbar spine BMD and MUFA were found only in female, 16-year-olds, and white people ($P < 0.05$); however, in 13-year-olds, lumbar spine BMD was negatively correlated with total MUFA intake. In the analysis of the left arm BMD model, stratification of MUFA across quartiles revealed that MUFA levels within the second and third quartiles exhibited a significant inverse relationship with BMD, as evidenced by *P*-values of <0.001 and <0.01, respectively; the *P* for trend was 0.034. When analyses were stratified by gender, age, standing height, and race, total MUFA intake and left arm BMD were negatively associated only in subgroups of 12 and 17 years, Q1, and other race.

3.4 Association between total PUFA intake, BMD, and BMC

Figure 4 presents the association between the intake of dietary PUFA and each body part's BMD as well as BMC. The analysis reveals a consistent inverse relationship across various BMD parameters, including total BMD, BMD of the left arm, left leg, head, trunk, pelvis, thoracic region, and left rib, with the intake of total PUFA. Similarly, this inverse association extends to BMC measurements, encompassing total BMC, BMC of the left arm, left leg, head, trunk, pelvis, and left rib, further supporting the negative

10.3389/fendo.2024.1402937

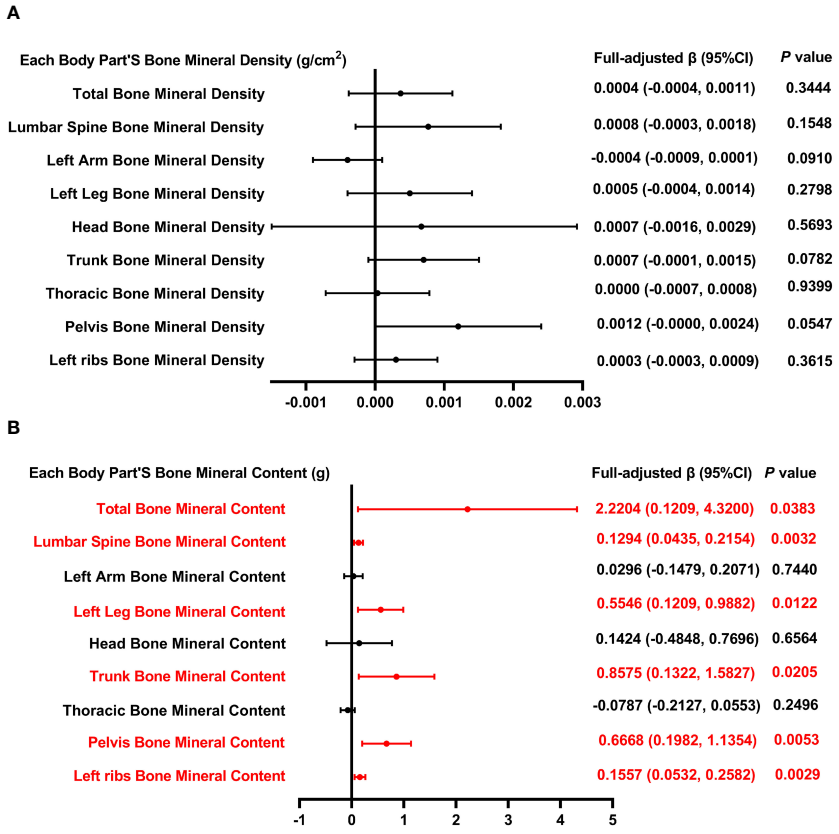

FIGURE 3
Forest plot of the relationship between total MUFA intake and BMD and BMC for each body part. **(A)** Correlation between BMD and total SFA intake in each body part. **(B)** Correlation between BMC and total SFA intake in each body part. MUFA, monounsaturated fatty acids intake; BMD, bone mineral density; BMC, bone mineral content.

TABLE 3 Association between total monounsaturated fatty acids intake (g/d) and bone mineral density (g/cm^2).

Exposure	Total BMD β, 95%CI, *P* value	Lumbar Spine BMD β, 95%CI, *P* value	Left Arm BMD β, 95%CI, *P* value
Quartiles of total monounsaturated fatty acids intake (g/d)			
Lowest quartiles (2.44-16.79)	reference	reference	reference
2nd (16.80-23.49)	-0.0132 (-0.0217, -0.0047)**	-0.0110 (-0.0228, 0.0008)	-0.0121 (-0.0176, -0.0065)***
3rd (23.491-32.06)	-0.0065 (-0.0164, 0.0035)	0.0021 (-0.0116, 0.0158)	-0.0100 (-0.0165, -0.0035)**
4th (32.062-118.49)	0.0042 (-0.0104, 0.0187)	0.0053 (-0.0149, 0.0254)	-0.0095 (-0.0190, 0.0000)
P for trend	0.850	0.412	0.034
Stratified by gender			
Male	0.0003 (-0.0007, 0.0012)	0.0005 (-0.0008, 0.0018)	-0.0003 (-0.0010, 0.0004)
Female	0.0010 (-0.0002, 0.0022)	0.0019 (0.0001, 0.0037)*	-0.0006 (-0.0013, 0.0001)
Stratified by age (years old)			
12	-0.0014 (-0.0034, 0.0007)	0.0016 (-0.0012, 0.0045)	-0.0014 (-0.0027, -0.0001)*
13	-0.0018 (-0.0038, 0.0003)	-0.0035 (-0.0064, -0.0006)*	-0.0010 (-0.0025, 0.0005)
14	0.0002 (-0.0022, 0.0026)	-0.0001 (-0.0031, 0.0029)	-0.0013 (-0.0027, 0.0001)
15	0.0011 (-0.0015, 0.0036)	0.0015 (-0.0020, 0.0050)	0.0008 (-0.0009, 0.0024)

(Continued)

TABLE 3 Continued

Exposure	Total BMD β, 95%CI, *P* value	Lumbar Spine BMD β, 95%CI, *P* value	Left Arm BMD β, 95%CI, *P* value
Stratified by age (years old)			
16	0.0006 (-0.0019, 0.0031)	0.0040 (0.0005, 0.0074)*	0.0003 (-0.0014, 0.0019)
17	-0.0005 (-0.0028, 0.0018)	-0.0034 (-0.0068, 0.0000)	-0.0019 (-0.0033, -0.0005)**
18	0.0007 (-0.0012, 0.0025)	-0.0002 (-0.0028, 0.0023)	-0.0004 (-0.0015, 0.0008)
19	0.0019 (-0.0009, 0.0048)	0.0014 (-0.0027, 0.0054)	0.0003 (-0.0016, 0.0023)
Stratified by standing height (cm)			
Q1 (132.9-160.2)	-0.0010 (-0.0024, 0.0005)	0.0008 (-0.0014, 0.0030)	-0.0015 (-0.0025, -0.0006)**
Q2 (160.3-168.7)	0.0000 (-0.0015, 0.0015)	-0.0003 (-0.0023, 0.0016)	-0.0009 (-0.0018, 0.0000)
Q3 (168.8-190.9)	0.0004 (-0.0007, 0.0016)	0.0007 (-0.0009, 0.0023)	-0.0004 (-0.0012, 0.0004)
Stratified by race			
White people	0.0011 (-0.0002, 0.0024)	0.0021 (0.0002, 0.0039)*	-0.0001 (-0.0009, 0.0008)
Black people	-0.0016 (-0.0037, 0.0005)	-0.0026 (-0.0056, 0.0003)	-0.0012 (-0.0024, 0.0001)
Mexican American	0.0012 (-0.0008, 0.0031)	0.0010 (-0.0015, 0.0034)	0.0003 (-0.0009, 0.0015)
Other race	-0.0020 (-0.0035, -0.0005)*	-0.0020 (-0.0040, 0.0000)	-0.0019 (-0.0029, -0.0009)***

All factors were adjusted. In the subgroup analysis, not adjusted for the stratification variable itself. *P < 0.05, **P < 0.01, ***P < 0.001.

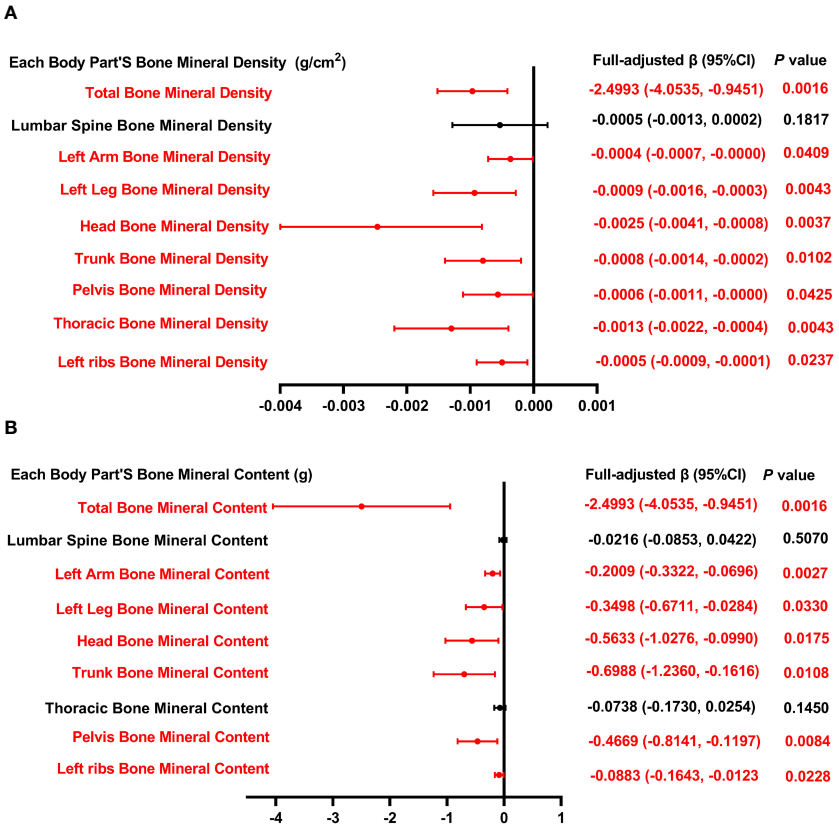

FIGURE 4
Forest plot of the relationship between total PUFA intake and BMD and BMC for each body part. **(A)** Correlation between BMD and total SFA intake in each body part. **(B)** Correlation between BMC and total SFA intake in each body part. PUFA, monounsaturated fatty acids intake; BMD, bone mineral density; BMC, bone mineral content.

association between dietary polyunsaturated fatty acid intake and bone health.

In Table 4, we investigate the relationship between overall PUFA consumption and BMD at various anatomical locations. This analysis examines the link between PUFA consumption and BMD, highlighting the influence of factors including gender, age, height, and ethnicity. Specifically, in the context of PUFA consumption and total BMD, a negative correlation is observed among males aged 15 and 19, Q3, and within white people and Mexican American cohorts. Conversely, a significant positive correlation is noted across other ethnic groups. This nuanced examination underscores the complex interplay between dietary PUFA and bone health, contingent upon demographic factors. In models of PUFA and lumbar spine BMD, when PUFA intake was divided into quartiles, there was a positive correlation in the 2nd quartile (P <0.05), and the P for trend was 0.376. In subgroup analysis, PUFA was significantly inversely associated with lumbar spine BMD only in males, 15-year-olds, and Mexican Americans (P <0.05). In the analysis of total PUFA intake and left arm BMD, dividing PUFA intake into quartiles did not reveal a statistically significant trend (P = 0.426). Stratifying by gender, age, height, and race, PUFA intake showed a negative correlation with left arm BMD in male, 17-year-olds, Q3, and white people, whereas it exhibited a positive correlation in individuals of other races. The above findings indicate that PUFA could potentially influence BMD negatively.

TABLE 4 Association between total polyunsaturated fatty acids intake (g/d) and bone mineral density (g/cm^2).

Exposure	Total BMD β, 95%CI, *P* value	Lumbar Spine BMD β, 95%CI, *P* value	Left Arm BMD β, 95%CI, *P* value
Quartiles of total polyunsaturated fatty acids intake (g/d)			
Lowest quartiles (1.29-10.66)	reference	reference	reference
2nd (10.669-15.516)	0.0057 (-0.0024, 0.0139)	0.0135 (0.0023, 0.0247)*	0.0023 (-0.0030, 0.0076)
3rd (15.519-24.66)	-0.0044 (-0.0134, 0.0046)	0.0090 (-0.0034, 0.0215)	-0.0015 (-0.0074, 0.0044)
4th (24.96-51.87)	-0.0073 (-0.0189, 0.0043)	0.0091 (-0.0069, 0.0252)	-0.0017 (-0.0093, 0.0059)
P for trend	0.076	0.376	0.426
Stratified by gender			
Male	-0.0012 (-0.0019, -0.0004)**	-0.0010 (-0.0019, -0.0000)*	-0.0005 (-0.0010, -0.0000)*
Female	-0.0008 (-0.0017, 0.0000)	0.0001 (-0.0012, 0.0014)	-0.0003 (-0.0008, 0.0002)
Stratified by age (years old)			
12	-0.0013 (-0.0028, 0.0003)	-0.0012 (-0.0034, 0.0010)	-0.0003 (-0.0013, 0.0008)
13	0.0008 (-0.0007, 0.0024)	0.0006 (-0.0016, 0.0028)	0.0005 (-0.0006, 0.0016)
14	0.0001 (-0.0013, 0.0015)	0.0005 (-0.0012, 0.0023)	-0.0000 (-0.0009, 0.0008)
15	-0.0022 (-0.0039, -0.0005)*	-0.0029 (-0.0052, -0.0005)*	-0.0010 (-0.0021, 0.0002)
16	-0.0012 (-0.0028, 0.0003)	-0.0006 (-0.0028, 0.0015)	-0.0004 (-0.0014, 0.0006)
17	-0.0014 (-0.0031, 0.0003)	-0.0016 (-0.0041, 0.0008)	-0.0010 (-0.0020, -0.0001)*
18	0.0005 (-0.0013, 0.0024)	0.0010 (-0.0015, 0.0035)	0.0005 (-0.0007, 0.0016)
19	-0.0022 (-0.0039, -0.0005)**	-0.0020 (-0.0043, 0.0004)	-0.0009 (-0.0020, 0.0003)
Stratified by standing height (cm)			
Q1 (132.9-160.2)	-0.0003 (-0.0013, 0.0007)	-0.0001 (-0.0016, 0.0014)	0.0004 (-0.0002, 0.0011)
Q2 (160.3-168.7)	-0.0009 (-0.0019, 0.0001)	0.0004 (-0.0010, 0.0017)	-0.0003 (-0.0009, 0.0003)
Q3 (168.8-190.9)	-0.0013 (-0.0023, -0.0004)**	-0.0012 (-0.0025, 0.0001)	-0.0009 (-0.0015, -0.0002)**
Stratified by race			
White people	-0.0017 (-0.0027, -0.0006)**	-0.0008 (-0.0023, 0.0007)	-0.0007 (-0.0014, -0.0000)*
Black people	-0.0003 (-0.0015, 0.0009)	0.0004 (-0.0013, 0.0021)	-0.0003 (-0.0010, 0.0004)
Mexican American	-0.0016 (-0.0030, -0.0002)*	-0.0023 (-0.0040, -0.0005)*	-0.0004 (-0.0013, 0.0005)
Other race	0.0018 (0.0007, 0.0030)**	0.0015 (-0.0000, 0.0030)	0.0010 (0.0002, 0.0017)*

All factors were adjusted. In the subgroup analysis, not adjusted for the stratification variable itself. *P < 0.05, **P < 0.01.

4 Discussion

We investigated the association between dietary FA and BMD using data from adolescents aged 12-19 in the NHANES dataset. This study ultimately comprised 3440 participants for data analysis. To assess the relationship between dietary FA and BMD at a deeper level and to make full use of these data, we stratified the total BMD according to quartiles. At the same time, we modeled the three FAs (SFA, MUFA, and PUFA) and BMD separately and performed subgroup analysis according to FA intake, age, gender, standing height, and race stratification to better assess the correlation between FA intake and BMD. Our analysis demonstrated that SFA was positively correlated with total BMD, left arm BMD, total BMC, and left arm BMC. Concurrently, MUFA intake was positively associated with BMC in several body regions, though its relationship with bone density did not achieve statistical significance. Importantly, PUFA intake was inversely correlated with BMD and BMC across most body areas. Subgroup analysis further revealed that variables such as age, sex, height, and ethnicity significantly impacted the relationship between dietary FA intake and BMD. In adolescents, significant variations in hormone levels influence bone growth and development. Families with higher economic status often have access to a healthier and more balanced diet, contributing to optimal nutritional status and improved bone health. Additionally, genetic factors play a significant role in bone development.

Short-chain fatty acids (SCFAs), which are saturated fatty acids comprising 1 to 6 carbon atoms, are generally associated with positive impacts on BMD. Lucas et al. (18) found that propionate or butyrate can protect bone health by regulating whole-body bone mass and preventing pathological bone loss. This phenomenon could be attributed to the suppression of gene expression, culminating in osteoclast differentiation and conferring protection against bone loss. Additionally, studies have indicated that adherence to the Mediterranean diet is linked to a reduced likelihood of experiencing fractures and an increased overall BMD. This association may be attributed, at least in part, to the production of short- chain fatty acids resulting from the fermentation of the diet's abundant dietary fiber by intestinal microorganisms (24, 25). In another study, Carvalho et al. (23) found that diabetic mice fed a low-fat diet had a lower BMC than C57BL/6 mice fed a high-fat diet high in medium-chain fatty acids. These results support our research to some extent. In another study, the researchers assessed the risk of fractures by constructing a COX proportional hazards model combined with questionnaires, and the results showed that proper intake of PUFA and MUFA is beneficial to reduce the risk of total fractures (26). Macri et al. (27) studied the effects of high-MUFA diets on the bones of growing hypercholesterolemic rats and showed that replacing saturated fat with a high-MUFA diet improved bone mass and BMD. In a study from two-sample Mendelian Randomization, some MUFAs (such as palmitoleic acid, oleic acid, etc.) were positively associated with lower fracture risk, which seems to be the same conclusion as previous studies (28). However, in our study, it seems that inconsistent results have been obtained. In a specific population, the intake of MUFA has different effects on BMD in different parts. The specific mechanism must be explored further in the future. It is worth noting that there are generally positive effects between MUFA intake and BMC in different parts of the body, which appears to be consistent with previous research.

After reviewing a large amount of literature, it was found that the association between PUFA and bone health has garnered considerable attention among researchers, and the research conclusions are inconsistent or controversial. In a cross-sectional study from Spain, the results showed that serum Omega-3 levels were positively correlated with spine BMD and femoral neck BMD in postmenopausal women (29). Another Mendelian randomization (MR) analysis also found that alpha-linolenic acid and linoleic acid have a positive genetic causal relationship with estimated BMD and a negative genetic causal relationship with fracture risk (30). Nevertheless, the findings of a longitudinal study conducted over a period of 5 years revealed a negative correlation between increased intake of PUFA and BMD, specifically in the femoral neck region (31). Furthermore, Wang et al. (19) recently conducted a two-sample MR study, and the findings revealed a negative correlation between omega-6 PUFA and total body BMD. Notably, a systematic review and meta-analysis of randomized controlled trials showed that omega-3 PUFA supplementation may not significantly influence BMD and bone metabolism markers (32). However, they might offer potential short-term benefits for postmenopausal women's health. It is evident that the conclusions of these studies are conflicting and controversial, partly because the researchers primarily investigated the association between overall BMD and FA, and insufficient sample sizes. Additionally, differences in race, sex, age, and other demographic factors introduced variability. Consequently, we utilized large-scale datasets to assess the correlation between PUFA and BMD, as well as BMC, across different body regions, accounting for potential confounders.

FA exhibits diverse roles in bone health. Research (33) indicates that SCFAs not only influence bone metabolism directly but also modulate immune and inflammatory responses, significantly enhancing bone formation. Specifically, butyrate has been shown to indirectly regulate Wnt10B, a key ligand in bone synthesis, via modulation of regulatory T cells, which suppress immune responses (34). Experimental studies reveal that butyrate, propionate, or acetate supplementation in drinking water increases bone mass in normal female mice and mitigates hormone-dependent bone loss in estrogen-deficient mice (18). Conversely, omega-6 PUFA adversely affects bone metabolism by inhibiting osteoblast genesis and promoting adipogenesis through mesenchymal stem cells (MSCs), mediated by alterations in the OPG/RANKL expression and PPARγ pathways (35, 36). Specifically, arachidonic acid and prostaglandin E2 exacerbate this effect by enhancing COX-2 expression, which leads to reduced osteogenesis (37). A lower Omega-6/Omega-3 PUFA ratio significantly improves bone density, highlighting the complex interactions of fatty acids with BMD (38). Understanding these intricate mechanisms of fatty acid metabolism and their

impact on bone cell differentiation and homeostasis is essential for osteoporosis prevention and bone health preservation.

To our knowledge, this is the initial investigation into the association between fatty acid intake and BMD in adolescents. We examined the relationship of three specific FA with BMD using weighted multiple linear regression models. The analysis was stratified by gender, age, race, among other factors. Additionally, we explored the inherent correlations between FA and BMD. Crucially, the adequate sample size supports the development of strategic interventions for adolescent bone health. However, we acknowledge several limitations inherent in this research. Firstly, this is a cross-sectional study, which can only provide objective clinical evidence and cannot explain the intrinsic link between FA and BMD. Secondly, the investigation did not account for the current or recent use of medications by the participants, including but not limited to lipid-lowering agents and glucocorticoids, which are known to influence bone metabolism (39, 40). Finally, the NHANES database lacks data on specific FA classifications, including Omega-3 and Omega-6, precluding analysis of their individual relationships with BMD. Future studies should prioritize prospective, large-scale randomized controlled trials to establish robust, evidence-based conclusions regarding the effects of fatty acids on BMD. Moreover, the role of omega-3 PUFA in bone metabolism and health remains debated and warrants further investigation as a potential focal point in addressing clinical challenges.

In conclusion, our study reveals a significant positive correlation between the consumption of SFA and both total BMD as well as BMD in the left arm. In contrast, intake of PUFA demonstrated a significant negative correlation with these BMD indices. Notably, the association between MUFA consumption and BMD appeared to be influenced by variables such as specific body regions, age, gender, and ethnicity, yielding variable results. These findings underscore the intricate nature of bone metabolism. Based on our results, we recommend a balanced intake of dietary fatty acids among adolescents to optimize bone mass and ensure skeletal health.

Data availability statement

Publicly available datasets were analyzed in this study. This data can be found here: www.cdc.gov/nchs/nhanes/.

Ethics statement

The studies involving humans were approved by The National Center for Health Statistics' Research Ethics Review Board. The studies were conducted in accordance with the local legislation and institutional requirements. Written informed consent for participation in this study was provided by the participants' legal guardians/next of kin.

Author contributions

Z-gW: Methodology, Supervision, Writing – original draft, Writing – review & editing. Z-bF: Software, Supervision, Writing – review & editing. X-LX: Funding acquisition, Supervision, Writing – review & editing.

Funding

The author(s) declare that no financial support was received for the research, authorship, and/or publication of this article.

Acknowledgments

The authors extend their gratitude towards the NHANES study's staff and participants for their indispensable contributions.

Conflict of interest

The authors declare that the research was conducted in the absence of any commercial or financial relationships that could be construed as a potential conflict of interest.

Publisher's note

References

1. Compston JE, McClung MR, Leslie WD. Osteoporosis. *Lancet*. (2019) 393:364–76. doi: 10.1016/S0140-6736(18)32112-3

2. Song S, Guo Y, Yang Y, Fu D. Advances in pathogenesis and therapeutic strategies for osteoporosis. *Pharmacol Ther*. (2022) 237:108168. doi: 10.1016/j.pharmthera.2022.108168

3. Clynes MA, Westbury LD, Dennison EM, Kanis JA, Javaid MK, Harvey NC, et al. Bone densitometry worldwide: a global survey by the ISCD and IOF. *Osteoporos Int*. (2020) 31:1779–86. doi: 10.1007/s00198-020-05435-8

4. Burge R, Dawson-Hughes B, Solomon DH, Wong JB, King A, Tosteson A. Incidence and economic burden of osteoporosis-related fractures in the United States, 2005-2025. *J Bone Miner Res*. (2007) 22:465–75. doi: 10.1359/jbmr.061113

5. Aibar-Almazán A, Voltes-Martínez A, Castellote-Caballero Y, Afanador-Restrepo DF, Carcelén-Fraile M del C, López-Ruiz E. Current status of the diagnosis and management of osteoporosis. *IJMS*. (2022) 23:9465. doi: 10.3390/ijms23169465

6. Camacho PM, Petak SM, Binkley N, Diab DL, Eldeiry LS, Farooki A, et al. American association of clinical endocrinologists/american college of endocrinology clinical practice guidelines for the diagnosis and treatment of postmenopausal osteoporosis—2020 update. *Endocrine Pract*. (2020) 26:1–46. doi: 10.4158/GL-2020-0524SUPPL

7. Hartl F, Tyndall A, Kraenzlin M, Bachmeier C, Gückel C, Senn U, et al. Discriminatory ability of quantitative ultrasound parameters and bone mineral density in a population-based sample of postmenopausal women with vertebral fractures+. *J Bone Miner Res*. (2002) 17:321–30. doi: 10.1359/jbmr.2002.17.2.321

8. da Costa GG, da Conceição Nepomuceno G, da Silva Pereira A, Simões BFT. Worldwide dietary patterns and their association with socioeconomic data: an ecological exploratory study. *Int Libr Eth Law New*. (2022) 18:31. doi: 10.1186/s12992-022-00820-w

9. Merlo CL. Dietary and physical activity behaviors among high school students — Youth risk behavior survey, United States, 2019. *MMWR Suppl*. (2020) 69:64–76. doi: 10.15585/mmwr.su6901a8

10. Proia P, Amato A, Drid P, Korovljev D, Vasto S, Baldassano S. The impact of diet and physical activity on bone health in children and adolescents. *Front Endocrinol*. (2021) 12:704647. doi: 10.3389/fendo.2021.704647

11. Lopes KG, Rodrigues EL, da Silva Lopes MR, do Nascimento VA, Pott A, Guimarães R de CA, et al. Adiposity metabolic consequences for adolescent bone health. *Nutrients*. (2022) 14:3260. doi: 10.3390/nu14163260

12. Weaver CM, Peacock M, Johnston CCJr. Adolescent nutrition in the prevention of postmenopausal osteoporosis. *J Clin Endocrinol Metab*. (1999) 84:1839–43. doi: 10.1210/jcem.84.6.5668

13. Omer M, Ali H, Orlovskaya N, Ballesteros A, Cheong VS, Martyniak K, et al. Omega-9 modifies viscoelasticity and augments bone strength and architecture in a high-fat diet-fed murine model. *Nutrients*. (2022) 14. doi: 10.3390/nu14153165

14. Feehan O, Magee PJ, Pourshahidi LK, Armstrong DJ, Slevin MM, Allsopp PJ, et al. Associations of long chain polyunsaturated fatty acids with bone mineral density and bone turnover in postmenopausal women. *Eur J Nutr*. (2022) 62:95–104. doi: 10.1007/s00394-022-02933-9

15. Bischoff-Ferrari HA, Vellas B, Rizzoli R, Kressig RW, Da SJ, Blauth M, et al. Effect of vitamin D supplementation, omega-3 fatty acid supplementation, or a strength-training exercise program on clinical outcomes in older adults: the DO-HEALTH randomized clinical trial. *JAMA*. (2020) 324:1855–68. doi: 10.1001/jama.2020.16909

16. Bao M, Zhang K, Wei Y, Hua W, Gao Y, Li X, et al. Therapeutic potentials and modulatory mechanisms of fatty acids in bone. *Cell Prolif*. (2020) 53. doi: 10.1111/cpr.12735

17. Saini RK, Keum Y-S. Omega-3 and omega-6 polyunsaturated fatty acids: Dietary sources, metabolism, and significance — A review. *Life Sci*. (2018) 203:255–67. doi: 10.1016/j.lfs.2018.04.049

18. Lucas S, Omata Y, Hofmann J, Böttcher M, Iljazovic A, Sarter K, et al. Short-chain fatty acids regulate systemic bone mass and protect from pathological bone loss. *Nat Commun*. (2018) 9:55. doi: 10.1038/s41467-017-02490-4

19. Wang L, Zhang C, Liang H, Zhou N, Huang T, Zhao Z, et al. Polyunsaturated fatty acids level and bone mineral density: A two-sample mendelian randomization study. *Front Endocrinol (Lausanne)*. (2022) 13:858851. doi: 10.3389/fendo.2022.858851

20. the PUFAH Group, Abdelhamid A, Hooper L, Sivakaran R, Hayhoe RPG, Welch A. The relationship between omega-3, omega-6 and total polyunsaturated fat and musculoskeletal health and functional status in adults: A systematic review and meta-analysis of RCTs. *Calcif Tissue Int*. (2019) 105:353–72. doi: 10.1007/s00223-019-00584-3

21. Bostock EL, Morse CI, Winwood K, McEwan IM, Onambélé GL. Omega-3 fatty acids and vitamin D in immobilization: part A- modulation of appendicular mass content, composition and structure. *J Nutr Health Aging*. (2017) 21:51–8. doi: 10.1007/s12603-016-0710-5

22. Wu Y-L, Zhang C-H, Teng Y, Pan Y, Liu N-C, Liu P-X, et al. Propionate and butyrate attenuate macrophage pyroptosis and osteoclastogenesis induced by CoCrMo alloy particles. *Mil Med Res*. (2022) 9:46. doi: 10.1186/s40779-022-00404-0

23. Carvalho AL, DeMambro VE, Guntur AR, Le P, Nagano K, Baron R, et al. High fat diet attenuates hyperglycemia, body composition changes, and bone loss in male streptozotocin-induced type 1 diabetic mice. *J Cell Physiol*. (2018) 233:1585–600. doi: 10.1002/jcp.26062

24. Ahluwalia N, Dwyer J, Terry A, Moshfegh A, Johnson C. Update on NHANES dietary data: focus on collection, release, analytical considerations, and uses to inform public policy. *Adv Nutr*. (2016) 7:121–34. doi: 10.3945/an.115.009258

25. Hsieh CI, Zheng K, Lin C, Mei L, Lu L, Li W, et al. Automated bone mineral density prediction and fracture risk assessment using plain radiographs *via* deep learning. *Nat Commun*. (2021) 12:5472. doi: 10.1038/s41467-021-25779-x

26. Orchard TS, Cauley JA, Frank GC, Neuhouser ML, Robinson JG, Snetselaar L, et al. Fatty acid consumption and risk of fracture in the Women's Health Initiative. *Am J Clin Nutr*. (2010) 92:1452–60. doi: 10.3945/ajcn.2010.29955

27. Macri EV, Lifshitz F, Alsina E, Juiz N, Zago V, Lezón C, et al. Monounsaturated fatty acids-rich diets in hypercholesterolemic-growing rats. *Int J Food Sci Nutr*. (2015) 66:400–8. doi: 10.3109/09637486.2015.1025719

28. Yuan S, Lemming EW, Michaëlsson K, Larsson SC. Plasma phospholipid fatty acids, bone mineral density and fracture risk+. *Clin Nutr*. (2020) 39:2180–6. doi: 10.1016/j.clnu.2019.09.005

29. Roncero-Martín R, Aliaga I, Moran JM, Puerto-Parejo LM, Rey-Sánchez P, de la Luz Canal-Macías M, et al. Plasma fatty acids and quantitative ultrasound, DXA and pQCT derived parameters in postmenopausal spanish women. *Nutrients*. (2021) 13:1454. doi: 10.3390/nu13051454

30. Yuan S, Lemming EW, Michaëlsson K, Larsson SC. Plasma phospholipid fatty acids, bone mineral density and fracture risk: Evidence from a Mendelian randomization study. *Clin Nutr*. (2020) 39:2180–6. doi: 10.1016/j.clnu.2019.09.005

31. Macdonald HM, New SA, Golden MH, Campbell MK, Reid DM. Nutritional associations with bone loss during the menopausal transition: evidence of a beneficial effect of calcium, alcohol, and fruit and vegetable nutrients and of a detrimental effect of fatty acids. *Am J Clin Nutr*. (2004) 79:155–65. doi: 10.1093/ajcn/79.1.155

32. Gao J, Xie C, Yang J, Tian C, Zhang M, Lu Z, et al. The effects of n-3 PUFA supplementation on bone metabolism markers and body bone mineral density in adults: A systematic review and meta-analysis of RCTs. *Nutrients*. (2023) 15:2806. doi: 10.3390/nu15122806

33. Koh A, Vadder FD, Kovatcheva-Datchary P, Bäckhed F. From dietary fiber to host physiology: short-chain fatty acids as key bacterial metabolites. *Cell*. (2016) 165:1332–45. doi: 10.1016/j.cell.2016.05.041

34. Tyagi AM, Yu M, Darby TM, Vaccaro C, Li J-Y, Owens JA, et al. The microbial metabolite butyrate stimulates bone formation *via* T regulatory cell-mediated regulation of WNT10B expression. *Immunity*. (2018) 49:1116–1131.e7. doi: 10.1016/j.immuni.2018.10.013

35. Zhan Q, Tian Y, Han L, Wang K, Wang J, Xue C. The opposite effects of Antarctic krill oil and arachidonic acid-rich oil on bone resorption in ovariectomized mice. *Food Funct*. (2020) 11:7048–60. doi: 10.1039/D0FO00884B

36. Casado-Díaz A, Santiago-Mora R, Dorado G, Quesada-Gómez JM. The omega-6 arachidonic fatty acid, but not the omega-3 fatty acids, inhibits osteoblastogenesis and induces adipogenesis of human mesenchymal stem cells: potential implication in osteoporosis. *Osteoporos Int*. (2013) 24:1647–61. doi: 10.1007/s00198-012-2138-z

37. Martyniak K, Wei F, Ballesteros A, Meckmongkol T, Calder A, Gilbertson T, et al. Do polyunsaturated fatty acids protect against bone loss in our aging and osteoporotic population? *Bone*. (2021) 143:115736. doi: 10.1016/j.bone.2020.115736

38. Montes Chañi EM, Pacheco SOS, Martínez GA, Freitas MR, Ivona JG, Ivona JA, et al. Long-term dietary intake of chia seed is associated with increased bone mineral content and improved hepatic and intestinal morphology in sprague-dawley rats. *Nutrients*. (2018) 10:922. doi: 10.3390/nu10070922

39. Mosti MP, Ericsson M, Erben RG, Schüler C, Syversen U, Stunes AK. The PPARα Agonist fenofibrate improves the musculoskeletal effects of exercise in ovariectomized rats. *Endocrinology*. (2016) 157:3924–34. doi: 10.1210/en.2016-1114

40. Jackson RD. Topical corticosteroids and glucocorticoid-induced osteoporosis—Cumulative dose and duration matter. *JAMA Dermatol*. (2021) 157:269–70. doi: 10.1001/jamadermatol.2020.4967

frontiers | Frontiers in Endocrinology

TYPE Original Research
PUBLISHED 03 September 2024
DOI 10.3389/fendo.2024.1439255

OPEN ACCESS

EDITED BY
Sandeep Kumar,
University of Alabama at Birmingham, United States

REVIEWED BY
Shengfeng Bai,
Air Force Medical University, China
Surbhi Gahlot,
University of Texas Southwestern Medical Center, United States

*CORRESPONDENCE
Xinlei Luo
963160870@qq.com
Lirong Yang
ylr13769899918.163.com
Zhengchang Yang
532490651@qq.com

RECEIVED 27 May 2024
ACCEPTED 21 August 2024
PUBLISHED 03 September 2024

CITATION
Liu J, Jiang J, Li Y, Chen Q, Yang T, Lei Y, He Z, Wang X, Na Q, Lao C, Luo X, Yang L and Yang Z (2024) Effects of FGF21 overexpression in osteoporosis and bone mineral density: a two-sample, mediating Mendelian analysis. *Front. Endocrinol.* 15:1439255. doi: 10.3389/fendo.2024.1439255

Effects of FGF21 overexpression in osteoporosis and bone mineral density: a two-sample, mediating Mendelian analysis

Jingjing Liu[1], Jun Jiang[1], Yunjia Li[1], Qiaojun Chen[1], Ting Yang[1], Yanfa Lei[1], Zewei He[1], Xiaowei Wang[1], Qiang Na[2], Changtao Lao[2], Xinlei Luo[1*], Lirong Yang[3*] and Zhengchang Yang[1*]

[1]Department of Spinal Surgery, Southern Central Hospital of Yunnan Province, Honghe, China, [2]Department of Spinal Surgery, The Sixth Affiliated Hospital of Kunming Medical University, Yuxi, China, [3]Department of Oncology, Southern Central Hospital of Yunnan Province, Honghe, China

Objective: Fibroblast growth factor 21 (FGF21) is a secreted protein that regulates body metabolism. In recent years, many observational studies have found that FGF21 is closely related to bone mineral density and osteoporosis, but the causal relationship between them is still unclear. Therefore, this study used two-sample, mediated Mendelian randomization (MR) analysis to explore the causal relationship between FGF21 and osteoporosis and bone mineral density.

Methods: We conducted a two-sample, mediator MR Analysis using genetic data from publicly available genome-wide association studies (GWAS) that included genetic variants in the inflammatory cytokine FGF21, and Total body bone mineral density, Heel bone mineral density, Forearm bone mineral density, Femoral neck bone mineral density, osteoporosis. The main analysis method used was inverse variance weighting (IVW) to investigate the causal relationship between exposure and outcome. In addition, weighted median, simple median method, weighted median method and MR-Egger regression were used to supplement the explanation, and sensitivity analysis was performed to evaluate the reliability of the results.

Results: MR Results showed that FGF21 overexpression reduced bone mineral density: Total body bone mineral density (OR=0.920, 95%CI: 0.876-0.966), P=0.001), Heel bone mineral density (OR=0.971, 95%CI (0.949-0.993); P=0.01), Forearm bone mineral density (OR=0.882, 95%CI(0.799-0.973); P=0.012), Femoral neck bone mineral density (OR=0.952, 95%CI(0.908-0.998), P=0.039); In addition, it also increased the risk of osteoporosis (OR=1.003, 95%CI (1.001-1.005), P=0.004). Sensitivity analysis supported the reliability of these results. The effect of FGF21 overexpression on osteoporosis may be mediated by type 2 diabetes mellitus and basal metabolic rate, with mediating effects of 14.96% and 12.21%, respectively.

Conclusions: Our study suggests that the overexpression of FGF21 may lead to a decrease in bone mineral density and increase the risk of osteoporosis, and the

effect of FGF21 on osteoporosis may be mediated through type 2 diabetes and basal metabolic rate. This study can provide a reference for analyzing the potential mechanism of osteoporosis and is of great significance for the prevention and treatment of osteoporosis.

KEYWORDS

fibroblast growth factor 21, osteoporosis, GWAS, Mendelian randomization, bone mineral density

1 Introduction

Osteoporosis is a disease characterized by low bone mass, deterioration of bone tissue and destruction of bone microarchitecture, which can lead to impaired bone strength and increased risk of fracture (1). As a chronic disease of bone metabolism, it is the result of an imbalance between osteoblasts and osteoclasts (2, 3) and is ranked as one of the most serious diseases affecting health, being the second most common disease after heart disease. With the change of diet and lifestyle, the incidence of osteoporosis is increasing year by year, showing the characteristics of more and more young people. According to surveys, the prevalence of osteoporosis in adults over the age of 12 in the United States can reach 6.50%, which brings a huge economic and health burden to the affected population (4). It is expected that the related cost of osteoporosis will increase to 25.3 billion US dollars by 2025 (5). Fracture is an associated clinical complication of osteoporosis. The most common fractures are vertebrae (spine), proximal femur (hip), and distal forearm (wrist), which are also one of the main factors contributing to the increased risk of death in the affected population (6). The formation and development of osteoporosis are related to many factors, such as estrogen deficiency, age, and chemical agents. In addition, inflammation, oxidative stress and other factors can also accelerate the progression of osteoporosis (7, 8). Various signaling pathways, such as RANK/RANKL/OPG, Wnt/β-catenin, and estrogen signaling pathways, are also critical for regulating osteoclast and osteoblast activity (9). At present, osteoporosis has been highly valued and extensively studied by the society, and its treatment is mainly carried out for osteogenesis and osteoclast, such as vitamin D, diphosphonate, and selective estrogen receptor modulators (SERMs) (10). Cutting off the pathogenic factors and pathways of osteoporosis is also an effective way to prevent and treat osteoporosis, and there are many studies to explore this issue.

Fibroblast growth factor 21 is a secreted protein that regulates the metabolism of the body, but does not have the activity of promoting fibroblast growth and does not specifically bind to heparin (11). It can play a role in various tissues and organs such as brain, heart, skeletal muscle, kidney and intestine (12). FGF21 is upregulated in some tissues when subjected to different stimuli. In different organs, FGF21 expression is mainly induced by fasting, ketogenic and high-carbohydrate diets, free fatty acids, nuclear receptor agonists and other factors. In humans and animals, fasting strongly induces FGF21 expression. As an endocrine hormone, FGF21 acts on various organs mainly through FGF receptors. In liver, the physiological effect of FGF21 is mainly manifested in promoting fatty acid oxidation. In the muscles and pancreas, it increases insulin sensitivity and promotes glucose uptake. Its regulatory role in the brain increases energy expenditure for appetite suppression. In WAT, FGF21 is an effective inducer of mitochondrial brown fat uncoupling protein 1 (UCP1), which stimulates glucose uptake in WAT and BAT while promoting lipolysis and reducing body weight. Recent studies have confirmed that FGF21 may become one of the effective targets for the prevention and rehabilitation of metabolic diseases, and is widely used in the prevention and rehabilitation of metabolic diseases such as liver lipid, glucose and lipid metabolism. With the deepening of the research on FGF21, its role has been continuously excavated. Some scholars have found that FGF21 is closely related to bone mineral density and osteoporosis. Although observational studies have proved this view, the causal relationship between them is still unclear. Therefore, this study used two-sample, mediated Mendelian randomization (MR) analysis to explore the causal relationship between FGF21 and bone mineral density and osteoporosis, so as to provide reference for the prevention and treatment of osteoporosis.

2 Methods

2.1 Study design

In this study, Total body bone mineral density, Heel bone mineral density, Forearm bone mineral density, Femoral neck bone mineral density, osteoporosis as outcome variable, Single nucleotide polymorphisms (SNPs) significantly associated with FGF21 were selected as instrumental variables, and the causal relationship between exposure and outcome was analyzed by two-sample, mediated Mendelian randomization analysis. In order to verify the reliability of the results, heterogeneity test, pleiotropy analysis and sensitivity analysis were used to exclude the bias of the results. This study met the following three key assumptions: ① Strong correlations between instrumental variables and exposure factors; ② The instrumental variables were not correlated with any confounding factors associated with the outcome variables of

exposure factors; ③ Instrumental variables can only affect outcomes through their association with exposure factors.

2.2 Data source

Analyses of MR Utilized publicly available GWAS summary data.FGF21 genetic data from the study of Zhao, including 14743 samples, 12957980 SNPs (13). Genetic data on osteoporosis were obtained from the UK Biobank with a sample size of 462,933 including 7547 cases and 455,386 controls. Through the IEU database (https://gwas.mrcieu.ac.uk/) to obtain the Total body bone mineral density (56284 samples, 16162733 SNPs), Heel bone mineral density (142,487 samples, 16,959,184 SNPs), Forearm bone mineral density (8143 samples, 9,955,366 SNPs),Femoral neck bone mineral density (32735 samples, 10586900 SNPs) four bone mineral density data were used as outcome variables. In order to avoid confounding factors due to racial differences, the genetic background of the study population was selected as European ethnicity.

2.3 Instrumental variable

We selected single nucleotide polymorphisms (SNPs) with strong and independent associations with exposure as instrumental variables (IV), and SNPs with $P < 5\times10^{-8}$ as outcome variables. However, due to the limited number of SNPs with FGF21 as exposure, We adopted a less stringent threshold (5×10^{-6}) to capture more SNPs (14). The r^2 threshold was set as 0.001 and 10000 kb to exclude linkage disequilibrium (LD), and the selected SNPs met F > 10. Studies show that eating and physical activity levels, body weight, BMI, gender is a risk factor for osteoporosis, in order to avoid confounding factors influence on the result, we identify and eliminate the SNPS associated with potential confounding factors.

2.4 Statistical analysis

Inverse variance weighting (IVW) was used as the main analysis method to assess the causal relationship between exposure factors and outcomes. weighted median, simple median method, weighted median method and MR-Egger regression were used to evaluate the reliability of IVW results, P<0. 05 was considered statistically significant. An F-value of >10 means that there is no weak instrumental variable bias. In this study, IVW method and MR-Egger method were used for heterogeneity test. When P>0. 05, there was no heterogeneity between SNPs. Sensitivity analysis was performed by Leave-one-out method and the results were visualized. Single SNP was excluded to observe whether it had an impact on the final results. The analysis of pleiotropy was performed by MR-PRESSO method. When P>0. 05, it was indicated that there was no pleiotropy.

2.5 Mediation Mendelian analysis

A two-step MR Analysis was performed to determine the mediating effect of type 2 diabetes and basal metabolic rate on the relationship between FGF21 and osteoporosis. We obtained data on type 2 diabetes (655,666 samples, 5030,727 SNPs) and basal metabolic rate (454,874 samples, 9851867 SNPs) as mediators through the IEU database. The proportion of type 2 diabetes and basal metabolic rate in the total effect was estimated by dividing the indirect effect by the total effect ($\beta1 \times \beta2/\beta3$), where β1 represents the effect of FGF21 on type 2 diabetes and basal metabolic rate, β2 represents the effect of type 2 diabetes and basal metabolic rate on osteoporosis, and β3 represents the effect of FGF21 on osteoporosis.

3 Results

3.1 Instrumental variable

After removing IVs with linkage disequilibrium from FGF21 genetic data, a total of 24 SNPs were included in this study, and the basic information of SNPs is shown in Table 1. The corresponding F values of single SNP in this study were all >10, there was no weak instrumental variable bias, and the results were reliable.

3.2 Results of Mendelian randomization analysis

IVW method showed that there was a genetic causal relationship between FGF21 and osteoporosis, and the overexpression of FGF21 increased the risk of osteoporosis (OR=1.003, 95%CI (1.001-1.005), P=0.004). Meanwhile, FGF21 overexpression reduced bone mineral density: Total body bone mineral density (OR=0.920, 95%CI: 0.876-0.966), P=0.001), Heel bone mineral density (OR=0.971, 95%CI (0.949-0.993); P=0.01), Forearm bone mineral density (OR=0.882, 95%CI (0.799-0.973); P=0.012), Femoral neck bone mineral density (OR=0.952, 95%CI(0.908-0.998), P=0.039), (Figure 1).

TABLE 1 Basic information on SNPs of FGF21.

SNPs	CHR	Position	EA	OA	β	EAF	P
rs191790209	1	40125467	T	C	0.6298	0.0084	5.10E-07
rs145127946	1	203746507	A	G	-0.1747	0.037	1.22E-06
rs10495032	1	216837226	T	G	-0.1557	0.0383	9.77E-07

(Continued)

10.3389/fendo.2024.1439255

TABLE 1 Continued

SNPs	CHR	Position	EA	OA	β	EAF	P
rs536853985	2	1715685	C	G	1.0018	0.9979	8.85E-07
rs1260326	2	27730940	T	C	0.1323	0.3977	1.03E-28
rs7610704	3	11689679	T	C	-0.0568	0.4644	2.21E-06
rs185983693	3	80482685	T	C	0.3206	0.9895	1.83E-06
rs139290229	4	68860848	A	G	0.4402	0.9878	3.27E-06
rs146695032	5	16215858	A	T	-0.6864	0.9947	1.19E-06
rs4700382	5	55882435	T	C	-0.063	0.2698	3.62E-06
rs60277384	5	84356011	T	C	-0.0881	0.8922	3.54E-06
rs116778481	6	14709576	T	C	-1.2617	0.0017	2.18E-06
rs13229619	7	73030175	A	G	-0.1609	0.1297	6.13E-20
rs7012637	8	9173209	A	G	-0.0605	0.4812	4.61E-07
rs80354499	8	60950348	T	C	-0.3503	0.0133	5.40E-07
rs188758663	10	127847758	A	G	-0.3801	0.0104	3.88E-07
rs12290350	11	76480255	T	C	-0.0689	0.2168	2.02E-06
rs2429473	12	47198899	A	C	-0.0812	0.795	3.32E-08
rs535578156	17	43242054	A	G	0.9528	0.0025	4.39E-06
rs532049578	18	41779892	T	C	0.5721	0.0098	4.33E-07
rs190083220	18	43914604	T	G	0.7527	0.9953	2.66E-06
rs72965996	18	72826607	A	G	-0.2215	0.031	6.08E-07
rs838131	19	49260677	A	C	0.1627	0.501	6.15E-36
rs142603673	21	33860969	T	C	-0.2352	0.0232	2.35E-07

Position and CHR: Location of genes and chromosomal information; EA, effect_allele; OA, other_allele; β, Allele effect size; EAF, effect allele frequency.

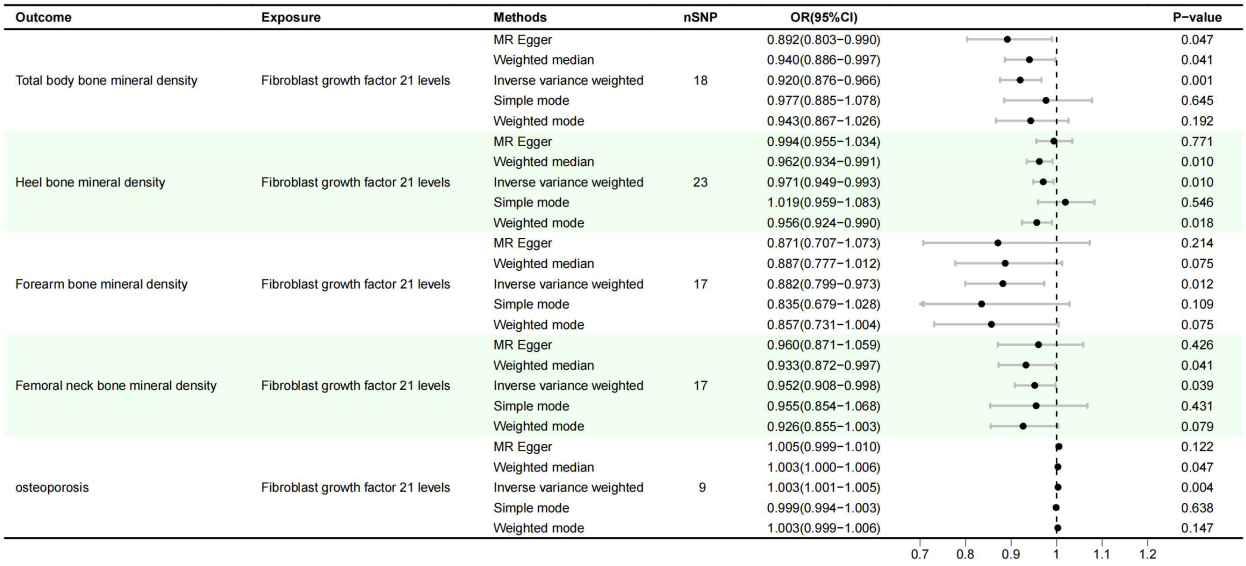

FIGURE 1
Results of MR Analysis of FGF21 and osteoporosis.

3.3 Sensitivity analysis

IVW and MR-Egger results showed no heterogeneity between FGF21 and outcome variables (P >0.05), and MR-PRESSO results showed no pleiotropy between FGF21 and outcome variables (P>0.05) (Figures 2, 3). Leave-one-out results showed that excluding each SNPs in turn had no significant effect on the results, which further verified the robustness of the results of this study (Figure 4).

3.4 Results of mediation analysis

Mediation analysis showed that FGF21 was associated with an increased risk of osteoporosis (OR=1.003, 95%CI (1.001-1.005), P=0.0037). Direct effects indicate that FGF21 has a causal relationship with Type 2 diabetes (OR=0.787, 95%CI (0.646-0.960), P=0.0179) and Basal metabolic rate (OR=0.962, 95%CI (0.935-0.990), P=0.0091). Indirect effect indicated that Type 2 diabetes (OR=0.998, 95%CI(0.997-0.999), P=0.0025) and Basal metabolic rate (OR=0.990, 95%CI(0.987-0.993), P=6.40E-11) also had causal relationship with osteoporosis. In the causal relationship between FGF21 and osteoporosis, the mediating effects of Type 2 diabetes and Basal metabolic rate were 14.96% and 12.21%, respectively (Table 2).

4 Discussion

The aim of this study was to explore the causal relationship between FGF21 and osteoporosis by two-sample, mediated Mendelian randomization method. MR Analysis showed that FGF21 was negatively correlated with Total body bone mineral density, Heel bone mineral density, Forearm bone mineral density, Femoral neck bone mineral density, and positively correlated with osteoporosis (P<0.05). This suggests FGF21 can decrease the bone mineral density, thus increasing the risk of osteoporosis, which is consistent with the predecessors' research results (15). Fibroblast growth factor 21 (FGF21) is a protein mainly secreted by the liver and regulated by a variety of physiological conditions and factors (16). Prolonged starvation, overnutrition, and glucagon all upregulated FGF21 expression (17–19), while insulin may inhibit FGF21 expression in the liver (20). In recent years, the relationship between FGF21 and osteoporosis has been continuously explored, and studies have shown that FGF21 is closely related to bone resorption and bone formation. Xu found a negative correlation between serum FGF21 content and PINP in patients with diabetic nephropathy through a cross-sectional study, suggesting that FGF21 may have a certain negative regulatory effect on bone formation (21). Hao collected and analyzed clinical data of more than 700 subjects and found that plasma FGF21 levels were negatively correlated with femoral neck BMD and hip Ward's

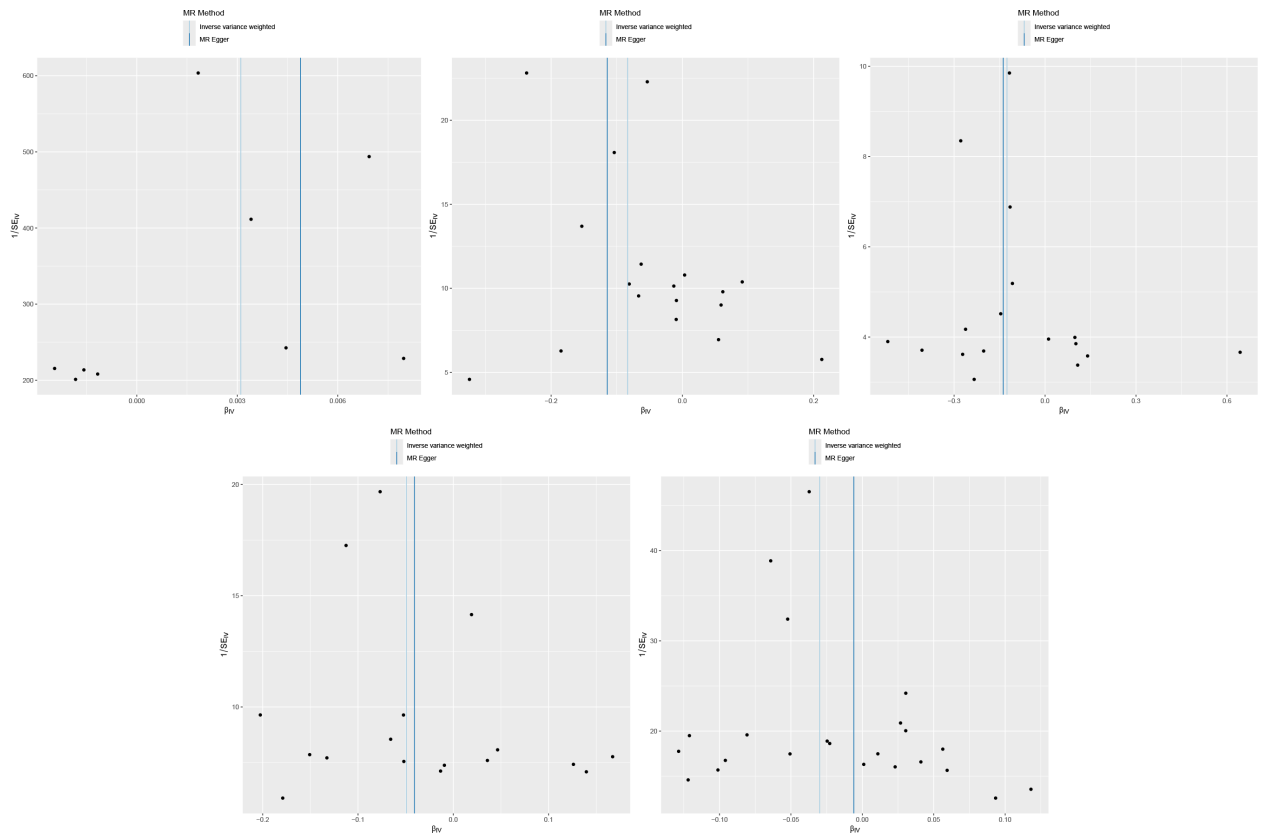

FIGURE 2
Scatter plot (From left to right, FGF21 and osteoporosis, Total body bone mineral density, Forearm bone mineral density, Femoral neck bone mineral density, Heel bone mineral density).

triangle BMD (22). Interestingly, FGF21 variant (rs490942) was significantly associated with increased hip Ward triangle BMD in the total cohort and the female cohort, and increased neck BMD in the female cohort. Zhou found that FGF21 levels in the liver and plasma were significantly increased in the osteoporosis rat model after ovariectomy (23). And Wei found FGF21 transgenic mice and FGF21 knockout mice were characterized by low bone mass and bone mass phenotypes (24). Some scholars believe that FGF21 can mediate and enhance the activity of peroxisome proliferator-activated receptorγ(PPAR-γ), thereby inhibiting the formation of osteoblasts and stimulating the adipogenesis of bone marrow mesenchymal stem cells, leading to increased bone fragility (25). Other studies have shown that FGF21 can promote the secretion of hepatic hormone, which binds to osteoclast precursors and promotes osteoclast differentiation, thereby aggravating osteoporosis (26). In addition, Zhou suggested that FGF-21 may mediate osteoclast bone resorption through RANKL/RANK/NFATc1 signaling pathway (23). Although previous studies have proposed the mechanism of FGF21 regulating bone homeostasis from both direct and indirect aspects, more studies are still needed for further investigation.

The results of mediating MR Analysis showed that the causal relationship between FGF21 and osteoporosis was mediated by Type 2 diabetes and Basal metabolic rate, and the proportion of mediating effect was 14.96% and 12.21%, respectively. As an endocrine protein, FGF-21 can regulate liver secretion, glucose and lipid metabolism and other processes. FGF-21 has the ability to inhibit glucagon receptors and improve insulin resistance. It plays an important role in the process of ketogenesis, gluconeogenesis and insulin synthesis, and is a potential therapeutic agent for metabolic diseases such as diabetes (27). In addition, FGF21 also has a certain therapeutic effect on diabetic neuropathy by reducing neuroinflammation and oxidative stress, and enhancing the protection of neuronal mitochondria, thereby alleviating diabetic neurodegeneration (28). Studies have shown that FGF-21 can reduce cell death induced by oxidative stress and autophagy, which is beneficial to remyelination and nerve regeneration after peripheral nerve injury and plays an important role in diabetes (29).Cheng's study showed that type II diabetes had a protective effect on osteoporosis, and for each additional case of type II diabetes, the incidence of osteoporosis decreased by 0.15% (30). This indicates that type 2 diabetes and osteoporosis are reverse causation, consistent with my results. The relationship between FGF21 and basal metabolic rate has not been reported at present, which may be related to the reduced risk of type 2 diabetes caused by overexpression of FGF21, and more studies are needed to clarify it in the future.

Interestingly, Hao's study showed that the correlation between FGF21 levels and Neck-BMD was significant, but the relationship was not significant when grouped by gender. At the same time, the

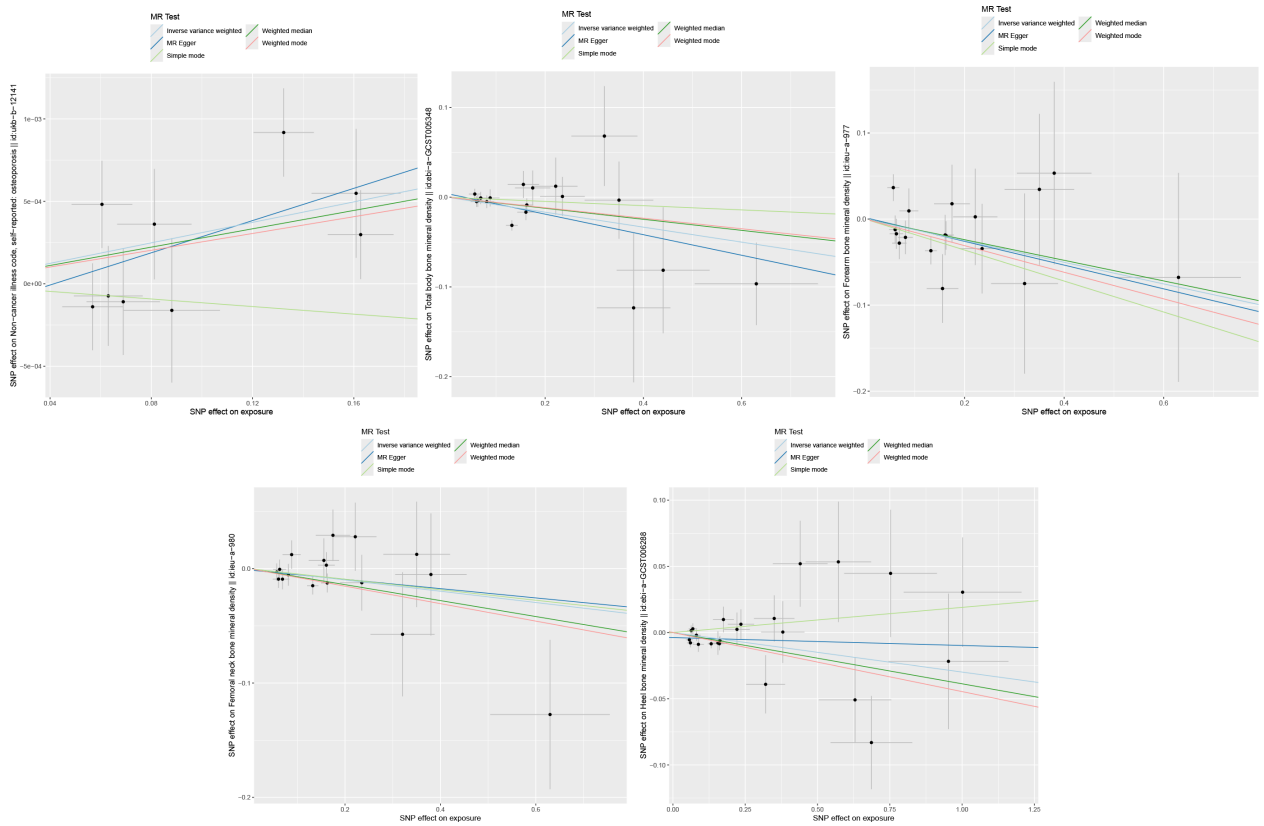

FIGURE 3
Funnel plot (From left to right, FGF21 and osteoporosis, Total body bone mineral density, Forearm bone mineral density, Femoral neck bone mineral density, Heel bone mineral density).

10.3389/fendo.2024.1439255

TABLE 2 Results of mediation analysis.

Exposure	Mediator	Outcome	Total effect			Direct effect a			Direct effect β			Mediation effect	
			Beta	SE	P	Beta	SE	P	Beta	SE	P	Beta	Proportion
FGF21	Type 2 diabetes	osteoporosis	0.0031	0.0011	0.0037	-0.2393	0.1011	0.0179	-0.0019	0.0006	0.0025	0.0005	14.96%
	Basal metabolic rate					-0.0385	0.0148	0.0091	-0.0099	0.0015	6.40E-11	0.0004	12.21%

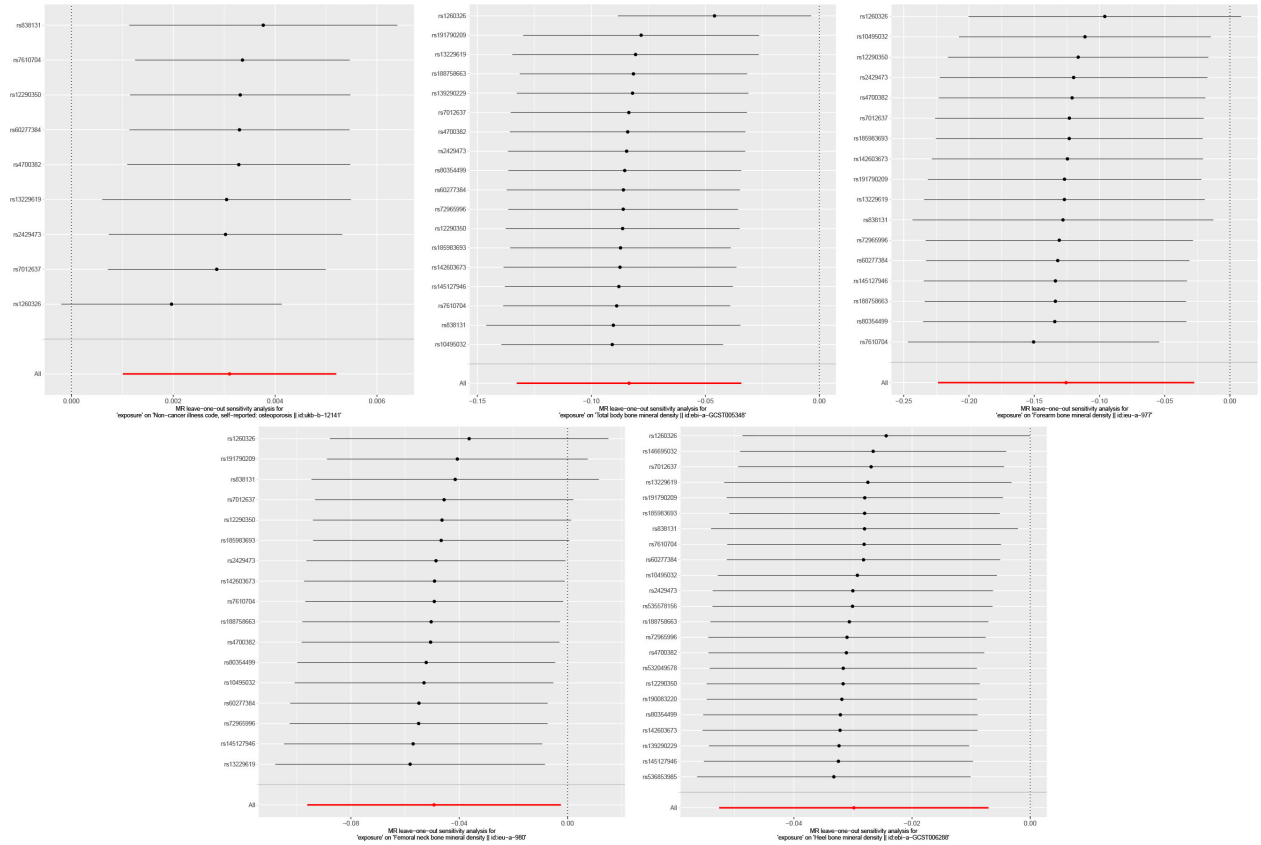

FIGURE 4
Leave-one-out analysis result (From left to right, FGF21 and osteoporosis, Total body bone mineral density, Forearm bone mineral density, Femoral neck bone mineral density, Heel bone mineral density).

correlation between FGF21 and Ward's BMD was significant in women, while the P-value of men was close to the significance threshold, indicating that men and women were equally prone to be affected by FGF21, and there was no sex specificity (22).However, Lee's study showed no significant correlation between FGF21 and total BMD and spinal BMD in men. But there was a significant positive correlation in women (31). Whether the effects of FGF21 on bone mineral density and osteoporosis are influenced by gender is still controversial, and more studies are needed to clarify.

5 Conclusions

Our study suggests that the increased expression of FGF21 may lead to the decrease of bone mineral density and increase the risk of osteoporosis, while type 2 diabetes and basal metabolic rate may play a mediating role in the relationship between FGF21 and osteoporosis. This study can provide a reference for analyzing the potential mechanism of osteoporosis and is of great significance for the prevention and treatment of osteoporosis.

Data availability statement

The original contributions presented in the study are included in the article/Supplementary Material. Further inquiries can be directed to the corresponding authors.

Author contributions

JL: Conceptualization, Writing – original draft, Writing – review & editing. JJ: Investigation, Methodology, Writing – review & editing. YuL: Supervision, Validation, Writing – review & editing. QC: Data curation, Writing – review & editing. TY: Software, Writing – review & editing. YaL: Project administration, Writing – review & editing. ZH: Formal Analysis, Writing – review & editing. XW: Visualization, Writing – review & editing. QN: Funding acquisition, Writing – review & editing. CL: Funding acquisition, Writing – review & editing. XL: Conceptualization, Data curation, Formal Analysis, Funding acquisition, Investigation, Methodology, Project administration, Resources, Software, Supervision, Validation, Visualization, Writing – review & editing. LY: Investigation, Methodology, Project administration, Writing – review & editing. ZY: Formal Analysis, Visualization, Writing – review & editing.

Funding

The author(s) declare that financial support was received for the research, authorship, and/or publication of this article. Scientific Research Fund of Yunnan Education Department (No:2023Y0956); Yunnan Talents Support Program (No: YNWR-MY-2020-033).

Acknowledgments

We thank each author for his contribution to this manuscript and the funds and other support provided by their subordinate units.

Conflict of interest

The authors declare that the research was conducted in the absence of any commercial or financial relationships that could be construed as a potential conflict of interest.

Publisher's note

All claims expressed in this article are solely those of the authors and do not necessarily represent those of their affiliated organizations, or those of the publisher, the editors and the reviewers. Any product that may be evaluated in this article, or claim that may be made by its manufacturer, is not guaranteed or endorsed by the publisher.

References

1. Sözen T, Özışık L, Başaran NÇ. An overview and management of osteoporosis. *Eur J Rheumatol.* (2017) 4:46–56. doi: 10.5152/eurjrheumatol.

2. Guo S, Wu Y, Chia W, Hsu P, Wang H, Wang Y, et al. Hypermethylation of the ALOX12 and CBS promoters in osteoporosis: Potential biomarkers for early diagnosis. *Genes Dis.* (2023) 11:30–3. doi: 10.1016/j.gendis.2023.03.005

3. Wang L, Pan Y, Liu M, Sun J, Yun L, Tu P, et al. Wen-Shen-Tong-Luo-Zhi-Tong Decoction regulates bone-fat balance in osteoporosis by adipocyte-derived exosomes. *Pharm Biol.* (2023) 61:568–80. doi: 10.1080/13880209.2023.2190773

4. Qaseem A, Mount CA, Campos K, McLean RM, Tierney S, Cross JTJr, et al. Quality indicators for osteoporosis in adults: A review of performance measures by the American college of physicians. *Ann Intern Med.* (2023) 176:1386–91. doi: 10.7326/M23-1291

5. Patel D, Gorrell C, Norris J, Liu J. A narrative review of the pharmaceutical management of osteoporosis. *Ann Jt.* (2023) 8:25. doi: 10.21037/aoj

6. Cosman F, de Beur SJ, LeBoff MS, Lewiecki EM, Tanner B, Randall S, et al. Clinician's guide to prevention and treatment of osteoporosis. *Osteoporos Int.* (2014) 25:2359–81. doi: 10.1007/s00198-014-2794-2

7. Yu B, Wang CY. Osteoporosis and periodontal diseases - An update on their association and mechanistic links. *Periodontol 2000.* (2022) 89:99–113. doi: 10.1111/prd.12422

8. Kimball JS, Johnson JP, Carlson DA. Oxidative stress and osteoporosis. *J Bone Joint Surg Am.* (2021) 103:1451–61. doi: 10.2106/JBJS.20.00989

9. Dong Q, Ren G, Li Y, Hao D. Network pharmacology analysis and experimental validation to explore the mechanism of kaempferol in the treatment of osteoporosis. *Sci Rep.* (2024) 14:7088. doi: 10.1038/s41598-024-57796-3

10. Wang MY, An MF, Fan MS, Zhang SS, Sun ZR, Zhao YL, et al. FAEE exerts a protective effect against osteoporosis by regulating the MAPK signalling pathway. *Pharm Biol.* (2022) 60:467–78. doi: 10.1080/13880209.2022.2039216

11. Jiang L, Yin Q, Yang M, Li M, Pan M, Han Y, et al. Fibroblast growth factor 21 predicts and promotes vascular calcification in haemodialysis patients. *Kidney Dis (Basel).* (2021) 7:227–40. doi: 10.1159/000512750

12. Zhu L, Li M, Zha Q, Yang M, Yu J, Pan M, et al. Fibroblast growth factor 21 (FGF21) is a sensitive marker of osteoporosis in haemodialysis patients: a cross-sectional observational study. *BMC Nephrol.* (2021) 22:183. doi: 10.1186/s12882-021-02393-z

13. Zhao JH, Stacey D, Eriksson N, Macdonald-Dunlop E, Hedman ÅK, Kalnapenkis A, et al. Genetics of circulating inflammatory proteins identifies drivers of immune-mediated disease risk and therapeutic targets. *Nat Immunol.* (2023) 24:1540–51. doi: 10.1038/s41590-023-01588-w

14. Burgess S, Butterworth A, Thompson SG. Mendelian randomization analysis with multiple genetic variants using summarized data. *Genet Epidemiol.* (2013) 37:658–65. doi: 10.1002/gepi.21758

15. Paranthaman M, Angu Bala Ganesh KSV, Silambanan S. Linking bone marrow fat with decreased bone mineral density among Indian patients with osteoporotic fracture. *Bioinformation.* (2024) 20:49–54. doi: 10.6026/bioinformation

16. Erickson A, Moreau R. The regulation of FGF21 gene expression by metabolic factors and nutrients. *Horm Mol Biol Clin Investig.* (2016) 30(1). doi: 10.1515/hmbci-2016-0016

17. Fazeli PK, Lun M, Kim SM, Bredella MA, Wright S, Zhang Y, et al. FGF21 and the late adaptive response to starvation in humans. *J Clin Invest.* (2015) 125:4601–11. doi: 10.1172/JCI83349

18. Zhang X, Yeung DC, Karpisek M, Stejskal D, Zhou ZG, Liu F, et al. Serum FGF21 Levels are increased in obesity and are independently associated with the metabolic syndrome in humans. *Diabetes.* (2008) 57:1246–53. doi: 10.2337/db07-1476

19. Habegger KM, Stemmer K, Cheng C, Müller TD, Heppner KM, Ottaway N, et al. Fibroblast growth factor 21 mediates specific glucagon actions. *Diabetes.* (2013) 62:1453–63. doi: 10.2337/db12-1116

20. Adams AC, Astapova I, Fisher FM, Badman MK, Kurgansky KE, Flier JS, et al. Thyroid hormone regulates hepatic expression of fibroblast growth factor 21 in a PPARalpha-dependent manner. *J Biol Chem.* (2010) 285:14078–82. doi: 10.1074/jbc.C110.107375

21. Xu L, Niu M, Yu W, Xia W, Gong F, Wang O. Associations between FGF21, osteonectin and bone turnover markers in type 2 diabetic patients with albuminuria. *J Diabetes Complications*. (2017) 31:583–8. doi: 10.1016/j.jdiacomp.2016.11.012

22. Hao RH, Gao JL, Li M, Huang W, Zhu DL, Thynn HN, et al. Association between fibroblast growth factor 21 and bone mineral density in adults. *Endocrine*. (2018) 59:296–303. doi: 10.1007/s12020-017-1507-y

23. Zhou L, Song HY, Gao LL, Yang LY, Mu S, Fu Q. MicroRNA−100−5p inhibits osteoclastogenesis and bone resorption by regulating fibroblast growth factor 21. *Int J Mol Med*. (2019) 43:727–38. doi: 10.3892/ijmm.2018.4017

24. Wei W, Dutchak PA, Wang X, Ding X, Wang X, Bookout AL, et al. Fibroblast growth factor 21 promotes bone loss by potentiating the effects of peroxisome proliferator-activated receptor γ. *Proc Natl Acad Sci U S A*. (2012) 109:3143–8. doi: 10.1073/pnas.1200797109

25. Zhao J, Lei H, Wang T, Xiong X. Liver-bone crosstalk in non-alcoholic fatty liver disease: Clinical implications and underlying pathophysiology. *Front Endocrinol (Lausanne)*. (2023) 14:1161402. doi: 10.3389/fendo.2023.1161402

26. Wu YT, Hsu BG, Wang CH, Lin YL, Lai YH, Kuo CH. Lower serum fibroblast growth factor 21 levels are associated with normal lumbar spine bone mineral density in hemodialysis patients. *Int J Environ Res Public Health*. (2020) 17:1938. doi: 10.3390/ijerph17061938

27. Liang YC, Jia MJ, Li L, Liu DL, Chu SF, Li HL. Association of circulating inflammatory proteins with type 2 diabetes mellitus and its complications: a bidirectional Mendelian randomization study. *Front Endocrinol (Lausanne)*. (2024) 15:1358311. doi: 10.3389/fendo.2024.1358311

28. Kang K, Xu P, Wang M, Chunyu J, Sun X, Ren G, et al. FGF21 attenuates neurodegeneration through modulating neuroinflammation and oxidant-stress. *BioMed Pharmacother*. (2020) 129:110439. doi: 10.1016/j.biopha.2020.110439

29. Lu Y, Li R, Zhu J, Wu Y, Li D, Dong L, et al. Fibroblast growth factor 21 facilitates peripheral nerve regeneration through suppressing oxidative damage and autophagic cell death. *J Cell Mol Med*. (2019) 23:497–511. doi: 10.1111/jcmm.13952

30. Cheng L, Wang S, Tang H. Type 2 diabetes mellitus plays a protective role against osteoporosis –mendelian randomization analysis. *BMC Musculoskelet Disord*. (2023) 24:444. doi: 10.1186/s12891-023-06528-1

31. Lee P, Linderman J, Smith S, Brychta RJ, Perron R, Idelson C, et al. Fibroblast growth factor 21 (FGF21) and bone: is there a relationship in humans? *Osteoporos Int*. (2013) 24:3053–7. doi: 10.1007/s00198-013-2464-9

frontiers | Frontiers in Endocrinology

TYPE Review
PUBLISHED 11 September 2024
DOI 10.3389/fendo.2024.1465816

OPEN ACCESS

EDITED BY
Sandeep Kumar,
University of Alabama at Birmingham, United States

REVIEWED BY
Surbhi Gahlot,
University of Texas Southwestern Medical Center, United States
Shivmurat Yadav,
University of Oklahoma Health Sciences Center, United States
Sanjukta Majumder,
Connecticut Children's Medical Center, United States

*CORRESPONDENCE
Chengcheng Liao
lcc_950330@163.com
Jian Yang
jerryyang114@163.com
Liang Zhang
liangzhang@scu.edu.cn

RECEIVED 16 July 2024
ACCEPTED 23 August 2024
PUBLISHED 11 September 2024

CITATION
Huang J, Liao C, Yang J and Zhang L (2024) The role of vascular and lymphatic networks in bone and joint homeostasis and pathology. *Front. Endocrinol.* 15:1465816. doi: 10.3389/fendo.2024.1465816

The role of vascular and lymphatic networks in bone and joint homeostasis and pathology

Jingxiong Huang[1], Chengcheng Liao[2,3]*, Jian Yang[2]* and Liang Zhang[1,2,4]*

[1]Center of Stomatology, West China Xiamen Hospital of Sichuan University, Xiamen, Fujian, China, [2]State Key Laboratory of Oral Diseases & National Center for Stomatology & National Clinical Research Center for Oral Diseases, West China Hospital of Stomatology, Sichuan University, Chengdu, Sichuan, China, [3]Department of Orthodontics II, Affiliated Stomatological Hospital of Zunyi Medical University, Guizhou, Zunyi, China, [4]Department of Oral Implantology, West China Hospital of Stomatology, Sichuan University, Chengdu, Sichuan, China

The vascular and lymphatic systems are integral to maintaining skeletal homeostasis and responding to pathological conditions in bone and joint tissues. This review explores the interplay between blood vessels and lymphatic vessels in bones and joints, focusing on their roles in homeostasis, regeneration, and disease progression. Type H blood vessels, characterized by high expression of CD31 and endomucin, are crucial for coupling angiogenesis with osteogenesis, thus supporting bone homeostasis and repair. These vessels facilitate nutrient delivery and waste removal, and their dysfunction can lead to conditions such as ischemia and arthritis. Recent discoveries have highlighted the presence and significance of lymphatic vessels within bone tissue, challenging the traditional view that bones are devoid of lymphatics. Lymphatic vessels contribute to interstitial fluid regulation, immune cell trafficking, and tissue repair through lymphangiocrine signaling. The pathological alterations in these networks are closely linked to inflammatory joint diseases, emphasizing the need for further research into their co-regulatory mechanisms. This comprehensive review summarizes the current understanding of the structural and functional aspects of vascular and lymphatic networks in bone and joint tissues, their roles in homeostasis, and the implications of their dysfunction in disease. By elucidating the dynamic interactions between these systems, we aim to enhance the understanding of their contributions to skeletal health and disease, potentially informing the development of targeted therapeutic strategies.

KEYWORDS

vascular system, lymphatic system, bone, joint, homeostasis, disease

1 Introduction

Mammals possess two crucial vascular systems that support essential life functions. The first is the blood vessel system, responsible for delivering oxygen and nutrients to tissues and cells while removing metabolic waste. The second is the lymphatic vessel system, which manages the drainage of interstitial fluid and immune regulation. Though these systems develop independently, they are functionally and structurally interrelated. Their coordinated interaction is vital for maintaining the microcirculatory environment's homeostasis. Recent studies have highlighted that blood and lymphatic vessels in bones and joints play multiple roles in maintaining the skeletal system's homeostasis under both physiological and pathological conditions (1–5).

A specific subtype of blood vessels, known as type H blood vessels, is crucial for bone homeostasis. Characterized by high expression of CD31 and endomucin, these vessels support osteoprogenitors by coupling angiogenesis and osteogenesis (6, 7). Additionally, endothelial cells in type H blood vessels facilitate bone tissue homeostasis and regeneration through paracrine signaling (8, 9). Conversely, interruptions in blood flow and ischemia in the subchondral bone can impede nutrient diffusion to articular cartilage, resulting in bone cell death, joint damage, and conditions like arthritis (5, 10). Recent advancements have elucidated the functional role of the lymphatic network in the skeletal system. Studies have identified a lymphatic network in bones and the role of lymphangiocrine signaling in repairing radiation-induced bone injuries (2, 11, 12). Increasing evidence also points to the critical role of lymphatic vessels in maintaining joint homeostasis, with their pathological changes closely linked to the onset and progression of inflammatory joint diseases (4, 13). Consequently, the interest in the role of lymphatic vessels in tissue injury has grown. As research continues to evolve, the significance of the vascular-lymphatic network in bone tissue repair and joint diseases is increasingly recognized. This network maintains tissue homeostasis and controls disease progression by regulating local inflammatory activity, facilitating material exchange, and releasing paracrine signals from vascular and lymphatic secretions. Despite their importance, review on the holistic role of these networks in bone and joint homeostasis and related diseases remains limited.

In this review, we provide a comprehensive overview of the current knowledge on the structural and functional aspects of blood and lymphatic vessels in bone and joint. We summarize the regulatory effects of angiogenesis and endothelial secretory signals, as well as lymphogenesis and lymphatic secretory signals, on the homeostasis of bone and joint tissues under specific conditions. Additionally, we review the interactions and co-regulatory mechanisms of the vascular and lymphatic networks in these tissues. Finally, we examine the changes and potential regulatory mechanisms of these networks under pathological conditions.

2 Blood and lymphatic vessels in bone and joint

2.1 Blood vessels in bone and joint

The skeleton contains a complex vascular network essential for tissue oxygenation and metabolism. Blood vessels in bone play multiple roles in maintaining bone homeostasis under both physiological and pathological conditions. Studies have revealed diverse vascular subtypes and a specialized vascular microenvironment within bone.

Bone tissue features a unique type of blood vessel known as type H vessels. Predominant in the metaphysis and endosteum, these capillaries are characterized by high expression of CD31 (platelet and endothelial cell adhesion molecule 1) and endomucin (Emcn) (6, 7). These columnar vessels are interconnected at their distal ends near the growth plate in the metaphysis by structures termed loops or arches (7, 14, 15). Within the bone marrow cavity, there is a highly branched and relatively irregular sinusoidal vasculature with low expression of CD31 and Emcn, referred to as type L vessels (7, 16, 17). The base of the type H capillary columns in the metaphysis connects to the bone marrow vasculature at the metaphyseal–diaphyseal interface, linking the metaphysis to the diaphysis (15, 18). Sinusoidal and columnar vessels are interconnected, forming a single vascular network (Figure 1).

Type H vessels are less abundant than type L vessels due to their limited distribution and the large area of the bone marrow cavity (7). Fed directly by arterioles, type H vessels exhibit higher partial pressure of oxygen and blood flow than type L vessels (15, 19, 20). The lower permeability of type H vessels and nearby arterioles creates an environment low in reactive oxygen species (ROS) (16, 21). Conversely, the lower blood flow in sinusoidal type L vessels promotes the transendothelial migration of blood cells and the trafficking of leukocytes (21–23). Type L vessels in the bone marrow play crucial roles in hematopoietic cell trafficking and serve as vascular niches for myelopoiesis.

The differing properties of type H and type L vessels have significant functional consequences for tissue microenvironments. Type H and type L vessels also have distinct gene expression profiles, supporting different perivascular cell types and further impacting the local microenvironment (7). At the protein and transcriptome levels, in addition to CD31 and Emcn, type H vessels express various growth factors, including fibroblast growth factor 1 (FGF1), platelet-derived growth factor A (PDGF-A), and PDGF-B (7, 24). Endothelial cell transcripts that highly express CD31 and Emcn also express bone morphogenetic protein (BMP) family members BMP1, BMP4, and BMP6, known to promote bone formation (24). This may explain the presence of osteoprogenitor cells around type H capillaries. Type H vessels are closely associated with osteoprogenitor cells, contributing significantly to bone remodeling and regeneration. The Notch ligand DLL4, an important regulator of angiogenesis, is also highly expressed in type H vessels adjacent to the growth plate (6). Given

10.3389/fendo.2024.1465816

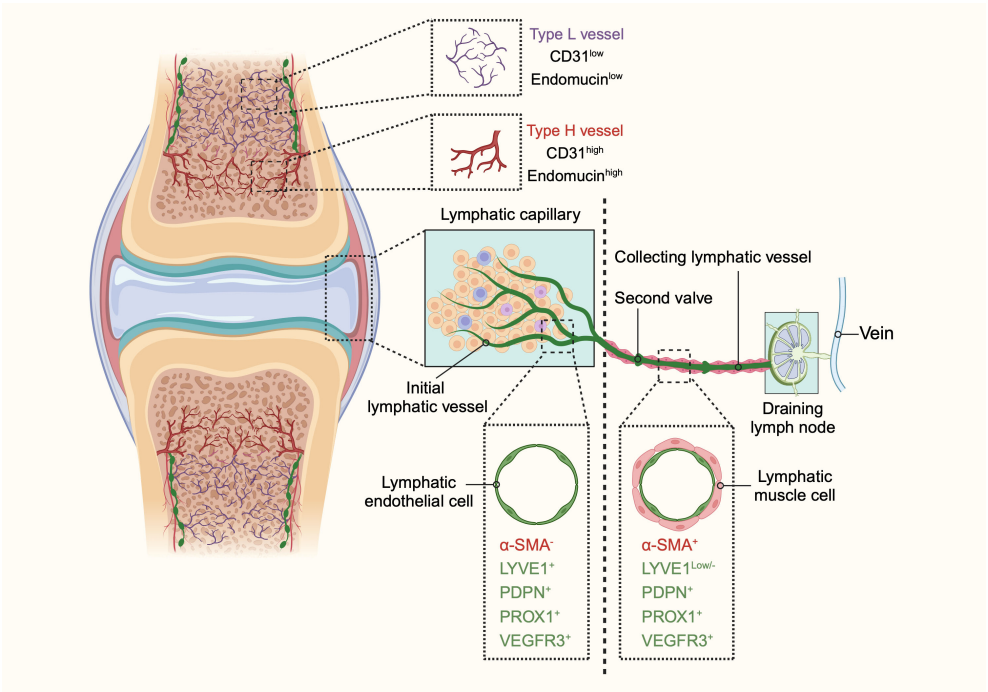

FIGURE 1
The schematic diagram illustrating the structure and distribution of blood vessels and lymphatic vessels in bones and joints. In bones, two distinct types of blood vessels are identified: type H and type L. Type H vessels, characterized by high expression of endomucin (Emcn) and cluster of differentiation 31 (CD31), are organized in a columnar manner with arterial connections and are primarily found in the metaphysis. Conversely, type L vessels, with lower levels of Emcn and CD31, are sinusoidal and located in the diaphysis. The identification of these vascular subtypes enhances our understanding of the heterogeneity of bone vasculature and its potential role in bone function in both health and disease. The lymphatic system in bones and joints also displays a hierarchical structure. Lymphatic vessels are present in the cortical regions and bone marrow cavity, with a higher concentration in the cortical areas. In joints, the lymphatic system begins with lymphatic capillaries, also known as initial lymphatic vessels. These vessels collect lymph and direct it towards collecting lymphatics equipped with anti-flowback valves. The lymph is then transported to draining lymph nodes before entering the venous system. Initial lymphatic vessels consist of a single layer of lymphatic endothelial cells (LECs) with a discontinuous basal lamina. In contrast, collecting lymphatic vessels are composed of tightly connected LECs, forming zipper-like junctions, and are surrounded by lymphatic muscle cells (LMCs) that facilitate lymph movement through contractions. Initial lymphatic vessels are marked by positive expression of lymphatic vessel endothelial hyaluronan receptor 1 (LYVE1), podoplanin (PDPN), prospero homeobox 1 (PROX1), and vascular endothelial growth factor receptor 3 (VEGFR3), but do not contain α-smooth muscle actin (α-SMA)-positive muscle cells. Collecting lymphatic vessels, however, exhibit lower levels of LYVE1 and positive expression of α-SMA, PDPN, PROX1, and VEGFR3. This differentiation between initial and collecting lymphatic vessels highlights their distinct roles and structures within the lymphatic system of bones and joints. (This figure is supported by Biorender).

their functional nature and gene expression profile, type H endothelial cells likely contribute to the coupling of angiogenesis and osteogenesis in bone development.

2.2 Lymphatic vessels in bone and joint

The lymphatic system plays a crucial role in regulating interstitial fluid homeostasis, waste clearance, and immune cell surveillance (25, 26). Through a network of initial lymphatic capillaries and collecting lymphatic vessels, the system transports interstitial fluid from peripheral tissues to lymph nodes, enters the right lymphatic duct and thoracic duct, draining into the subclavian veins and returning to the blood circulation (27–29).

Initial lymphatic capillaries are lined by a single layer of lymphatic endothelial cells connected by specialized button-like junctions, which are highly permeable to solutes and macromolecules (30–32). When external compressive forces exceed the interluminal fluid pressure, interstitial fluid is pushed into the initial lymphatic capillaries and becomes lymph. Lymphatic endothelial cells overlap to form primary valves that prevent lymph backflow. These initial lymphatics converge to form larger collecting lymphatic vessels, which are connected by adjacent lymphatic endothelial cells through tight zipper-like junctions, making them less permeable than initial lymphatics (29, 31–34). Collecting lymphatic vessels are surrounded by one or more layers of lymphatic muscle cells (LMCs), which facilitate vessel contraction to propel lymph forward (35). These vessels also contain secondary bicuspid valves to prevent backflow (36). After collection by the lymphatic vessels, lymph traverses the afferent lymphatics to reach the draining lymph nodes (DLNs). The lymphatic sinuses within DLNs are highly organized structures containing immune cells, where adaptive immune responses are generated (37). Finally, lymph exits the nodes via efferent lymphatic vessels and reenters the circulatory system (Figure 1).

Lymphatic vessels are reported not to be present in several tissues, including the brain and eye (38, 39). The presence of lymphatics in bone has been a topic of considerable controversy.

Traditionally, it was believed that bones and bone marrow lack lymphatic vessels, and that the growth of lymphatic vessels in bone could be detrimental, as observed in Gorham-Stout disease, a rare bone disorder characterized by the abnormal growth of lymphatic vessels in bones (40–42). Lymphatics in bone are not typically visible on routine lymphangiograms in humans, possibly due to the rare connections between deep and superficial lymphatics. Some historical studies, however, suggest a different conclusion. Injection of radio-opaque agents or macromolecular markers, such as ferritin and horseradish peroxidase, into the bone marrow has been shown to reach the periosteal surface of the bone (43–46). These findings imply the potential presence of lymphatic channels in bone. These results indicate that if macromolecules flow from the bone marrow to the periosteal surface, as some fluid transport studies suggest, this may occur through an alymphatic system or involve matrix prelymphatics and perivascular prelymphatics lacking an endothelial lining, similar to those described in the eye and brain (45, 47). It could be argued that, due to the relatively large gaps between the pseudopodial processes of endothelial cells in bone sinusoids, the free movement of macromolecules and newly formed blood cells between the extravascular and intravascular compartments is possible, negating the need for a lymphatic system for fluid transport in bone. However, recent research has revealed the presence of lymphatic vessels in long bones, the dura mater of the mouse brain, and the spinal vertebral column (12, 48, 49). Notably, Biswas et al., using high-resolution light-sheet imaging and cell-specific mouse genetics, demonstrated the presence of lymphatic vessels in mouse and human bones and further validated the importance of lymphatic endothelial cell-derived secretory proteins for bone regeneration (2). In addition, it has been found that lymphatic vessels were identified within the stratified connective tissues surrounding the fetal cartilaginous knee joint tissues in the fetus and adult mice, but not detected in cartilage tissues (50–52). Moreover, lymphatic vessels have been identified within the periosteum of long bones (52). Therefore, lymphatic vessels are extensively distributed throughout the various tissues of the bone and joint, excluding articular cartilage (Figure 1).

3 The dynamic interplay of vascular and lymphatic endothelial cells in development

The vascular-lymphatic network is essential for maintaining fluid homeostasis, supporting tissue repair, and facilitating immune cell trafficking. Understanding the biology of endothelial cells (ECs), which form the lining of blood and lymphatic vessels, is fundamental to these interactions. EC populations are regulated by a complex network of signaling pathways that govern their spatial and temporal organization during critical events in development, growth, and regeneration.

Both blood endothelial cells (BECs) and lymphatic endothelial cells (LECs) originate from primitive vascular endothelial progenitor cells derived from the mesoderm (53, 54). This common origin gives rise to BECs through the process of vasculogenesis, driven by key factors such as ETS variant transcription factor 2 (ETV2), fibroblast growth factor 2 (FGF2), bone morphogenetic protein 4 (BMP4), and Indian hedgehog signaling molecule (IHH) (55–59). Angioblasts formed through these pathways further mature via vasculogenesis or angiogenesis, with vascular endothelial growth factor A (VEGFA) playing a significant role in promoting the sprouting of new vessels (60).

The differentiation of these progenitor cells into either BECs or LECs is governed by distinct yet overlapping signaling mechanisms. In the early stages of development, ECs undergo arterial-venous specification, where arterial and venous fates are distinguished by the expression of EFNB2 and EPH receptor B4 (EPHB4), respectively (61). The VEGFA-VEGFR2 signaling pathway is crucial for promoting arterial phenotypes while inhibiting venous characteristics (62, 63). The Notch signaling pathway, activated by VEGF, enhances arterial gene expression and suppresses venous patterning, with Wnt signaling regulating arterial specification upstream of Notch through β-catenin and Delta-like 4 (DLL4) expression (64–69). Conversely, the acquisition of the venous phenotype involves nuclear receptor subfamily 2 (NR2F2, also known as COUP transcription factor 2, COUP-TFII), which suppresses Notch signaling and, along with VEGFA-VEGFR2 interactions, supports venous specification (65, 70–72). The mitogen-activated protein kinase (MAPK) pathway promotes arterial specification under VEGFR2 activation, while VEGFR2 also activates phosphoinositide-3-kinase (PI3K)/AKT to facilitate venous specification (73).

LECs primarily originate from venous ECs through transdifferentiation, though non-venous ECs also contribute (27). During embryonic development, venous ECs in the dorsolateral region of the cardinal vein sprout to initiate lymphangiogenesis, regulated by a network of signals including NR2F2. Deficiency in NR2F2 disrupts lymphangiogenesis and leads to edema, indicating its critical role in lymphatic specification (74, 75). Prospero homeobox protein 1 (PROX1), a classical marker for LECs, is essential for initiating lymphatic specification. In venous ECs, NR2F2 maintains the venous phenotype by suppressing Notch signaling, while in LECs, the NR2F2-PROX1 heterodimer reverses this suppression (76). SRY-related HMG-box 18 (SOX18) also enhances PROX1 transcription, driving LEC specification through a positive feedback loop (77). VEGFC, working alongside transcription factors such as SOX7 and MAFB (musculoaponeurotic fibrosarcoma oncogene homolog B), further promotes lymphatic specification by upregulating multiple LEC markers, including PROX1 (78, 79).

During the life cycle, ECs exhibit phenotypic plasticity, undergoing transdifferentiation under specific conditions. This adaptability is exemplified in the development of capillaries and the transdifferentiation of venous ECs into arterial ECs and LECs. Such transitions are regulated by signaling pathways like VEGF, Notch, and Wnt, which orchestrate the formation and specialization of blood and lymphatic networks. Understanding the dynamic interplay between these networks is crucial for developing targeted therapies. While the blood and lymphatic systems are relatively independent, they regulate and promote each other's development. Disruption in this mutual regulation can lead to developmental abnormalities, underscoring the

importance of their interdependent signaling mechanisms during growth and regeneration.

4 Vascular-lymphatic network in skeletal healing

4.1 Angiogenesis and angiocrine modulation in skeletal healing

The significant changes in BECs during tissue repair closely resemble those observed in development. Angiogenesis is the primary mechanism for new blood vessel formation in response to injury. Unlike the homeostatic state, repair in the context of injury has distinct characteristics. This shift is linked to increased local inflammation following injury, which activates angiogenesis to aid in vascular network regeneration (80). In bone, a unique form of angiogenesis, termed vessel bulging angiogenesis, is prominent, with type H vessels playing a crucial role. These vessels facilitate revascularization in hard tissue injuries, including spinal fusion surgeries (81), tooth extraction wounds (82), and diabetic osteoporosis (83). Type H vessels form by merging vascular buds from opposite ends, and although typical tip cells are not observed in bone angiogenesis, ECs display tip cell-like features such as filopodia and directional migration along VEGF gradients (6, 84, 85). Notably, Notch signaling is strongly activated during bone vascular regeneration, contrasting with its inhibitory role in vessel sprouting in other tissues. The intensity of Notch signaling correlates with blood flow rate and restoring blood flow in aging individuals promotes bone healing (7, 15). The new vascular network invades the injury site, restores blood supply, and provides channels for osteoblast precursors, coupling angiogenesis with osteogenesis (86).

BECs also release angiocrine factors, influencing vascular modulation during injury (87). In the skeletal system, type H vessels release factors like Noggin, which regulate skeletal morphology and ossification (88). Additionally, type H ECs release matrix metallopeptidases (MMPs) to remodel the extracellular matrix (ECM), essential for cartilage resorption during bone remodeling (89, 90). Various pro-angiogenic and angiocrine factors, including VEGFA, FGF2, and FGF9, are involved in inducing vascularization and bone growth during repair. VEGFA promotes bone repair, while VEGFR1 negatively regulates blood vessel growth and fracture repair (91, 92). Placental growth factor (PIGF), a VEGFR1 ligand, facilitates bone healing (81, 93). FGF signaling, particularly FGF2 and FGF9, stimulates angiogenesis and osteogenesis during bone repair (6, 83, 84). Transforming growth factor beta (TGFβ), BMP-2, BMP-7, and growth differentiation factor (GDF) also enhance angiogenesis and osteogenesis during healing (86, 87). Angiocrine crosstalk via Notch signaling promotes fracture repair, as evidenced by reduced hematopoietic stem cell (HSC) regeneration following endothelial-specific deletion of the Notch ligand Jag1 (88, 90). ECs also upregulate factors like FGF2, BMP4, Insulin-like growth factor-binding protein 2 (IGFBP2), and Angiopoietin1, expanding hematopoietic stem progenitor cells (HSPCs) and contributing to hematopoietic recovery and bone repair after acute bone marrow injury, such as chemotherapy and irradiation (89, 94).

4.2 Lymphangiogenesis and lymphangiocrine modulation in skeletal healing

The lymphatic system is primarily responsible for transporting body fluids and immune cells. Beyond these canonical functions, lymphatic vessels are implicated in diverse physiological roles across various organs and tissues. Recent research highlights the correlation between the integrity of lymphatic vessels and several metabolic phenotypes, including insulin resistance, cardiovascular diseases, lipid absorption, and liver injuries (95–98). Notably, LECs are now recognized for their role in regulating metabolic homeostasis through the secretion of various proteins, referred to as lymphangiocrine signals.

Lymphangiogenesis, or the formation of new lymphatic vessels from existing ones, is especially important for bone and joint health. Research shows that lymphangiocrine signals significantly impact the aging process. Biswas et al. discovered lymphatic vessels within bones, confirming their role in bone regeneration (2). Advanced imaging revealed these vessels at a single-cell level, expanding in response to stress in a manner dependent on the inflammatory cytokine Interleukin 6 (IL-6). LECs were found to secrete C-X-C motif chemokine 12 (CXCL12), a chemokine that regulates blood cell production and bone healing. Remarkably, injecting LECs from young mice into aged mice restored both bone and blood cell regeneration, highlighting the crucial role of lymphangiocrine signals in aging (2). The results of study highlight the importance of lymphangiocrine signals for metabolic homeostasis.

The lymphatic system also plays a vital role in managing inflammation, particularly in conditions like rheumatoid arthritis (RA), which is marked by chronic joint inflammation and progressive damage. In RA, inflammatory cytokines such as TNF-α, IL-1, and IL-6 trigger synovial inflammation, leading to joint pain, swelling, and functional impairment (99–101). Lymphatic vessels are crucial for clearing these inflammatory cells and mediators from the inflamed synovium. Studies using animal models of RA have shown that the VEGF-C/VEGFR3 signaling pathway is vital for lymphangiogenesis in arthritis. VEGF-C and its receptors, VEGFR3 and VEGFR2, are highly expressed in arthritic synovial tissue, promoting the growth and migration of LECs (102–104). Macrophages in the inflamed environment also express VEGF-C and VEGFR3, further supporting lymphangiogenesis (105).

4.3 Co-regulation of blood and lymphatic endothelial cells: VEGF and BMP signaling pathways

The co-regulation of BECs and LECs by shared signaling pathways underscores their interdependence. This knowledge has

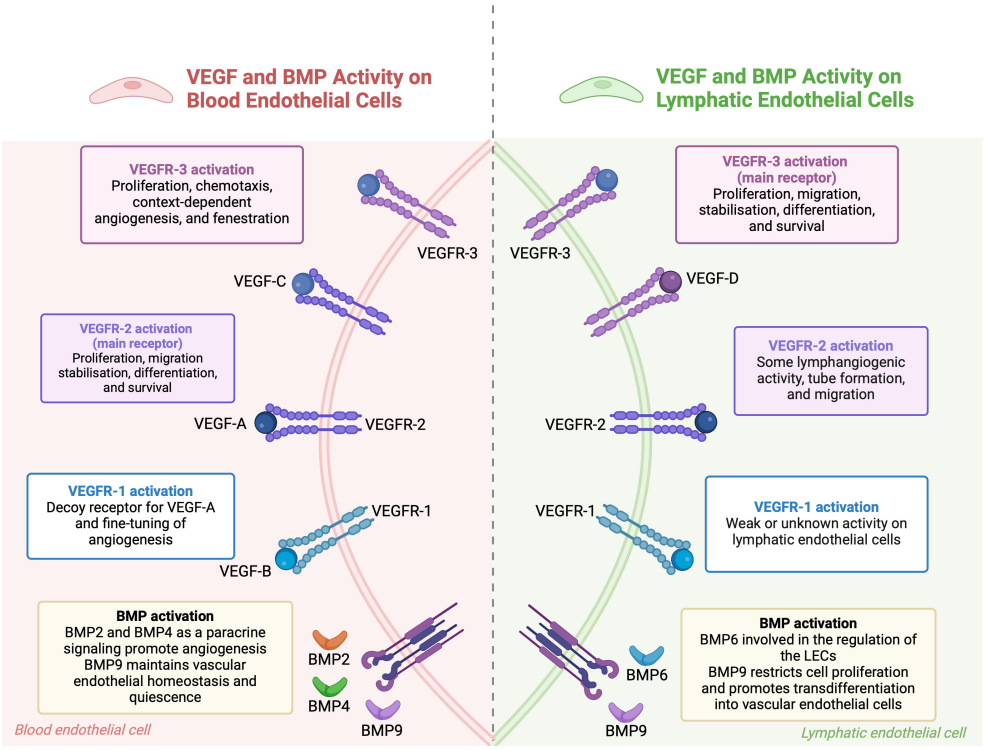

FIGURE 2
The combined roles of VEGF and BMP pathways in regulating endothelial cells. In blood endothelial cells, VEGF-A binds to VEGFR-1 and VEGFR-2 receptors. VEGFR-1 modulates angiogenesis, while VEGFR-2 promotes cell growth, movement, stabilization, differentiation, and survival. BMP signaling, through BMP2, BMP4, and BMP9, supports blood vessel formation and maintains vascular stability. In lymphatic endothelial cells, VEGF-C and VEGF-D primarily activate VEGFR-3, leading to cell growth and movement, while VEGFR-2 also aids in lymphatic vessel formation. BMP6 and BMP9 regulate lymphatic endothelial cells, with BMP9 encouraging their transformation into blood vessel cells. BMP signaling pathways interact with VEGF pathways to maintain endothelial cell function and regulate angiogenesis. (This figure is supported by Biorender).

clinical potential, especially in precision medicine, where manipulating these pathways could lead to novel treatments for vascular and lymphatic disorders. VEGF and BMP are key regulators of both blood and lymphatic vessels, orchestrating their development, function, and homeostasis (106, 107) (Figure 2).

The VEGF family is central to the repair and regeneration of the vascular-lymphatic network post-injury. VEGFA-VEGFR2 and VEGFC-VEGFR3 are primary signals for BECs and LECs, respectively, driving their migration, proliferation, and participation in regeneration. However, VEGFR2 can also be expressed in LECs, and VEGFC can bind to VEGFR2 in BECs, indicating the complexity of VEGF signaling in this network. VEGFC not only induces lymphangiogenesis but also stabilizes blood and lymphatic capillaries by regulating PDGF-B expression, which recruits pericytes and lymphatic smooth muscle cells to the vessels (108, 109). Complementary mechanisms refine vascular-lymphatic network regulation. For example, receptor activity-modifying protein 1 (RAMP1) has been shown to promote both angiogenesis and lymphangiogenesis in skin wounds, with its absence leading to impaired wound healing due to reduced VEGFA and VEGFC levels (110). Additionally, Ras homolog family member B (RHOB) and vascular endothelial zinc finger 1 (VEZF1) have opposing roles in vessel growth. RHOB inhibits blood vessel growth while promoting lymphatic vessel growth (111). VEGFR1, previously considered a decoy receptor, has been found to promote angiogenesis and lymphangiogenesis by modulating the secretome of pro-inflammatory macrophages in diabetes-related delayed wound healing models (60, 112, 113). Hemostasis also couples blood-lymphatic vessels post-injury by releasing coagulation proteases that cleave VEGFC and VEGFD, promoting LEC proliferation. Activated platelets further facilitate VEGFC-VEGFR3 binding by upregulating VEGFR3 expression in LECs (114). Angiopoietins also play a role in co-regulation, promoting angiogenesis and lymphangiogenesis at wound margins and influencing vascular-lymphatic remodeling during inflammation, though their effects can vary depending on the context (115, 116).

BMPs are crucial regulators of both blood and lymphatic vessels. In the blood vasculature, BMP2, BMP4, BMP9, and BMP10 play crucial roles. BMP2 and BMP4 are produced locally and act as paracrine signals, promoting angiogenesis. In contrast, BMP9 and BMP10 circulate systemically and inhibit sprouting (117, 118). BMP9 and BMP10 are particularly important for vessel stabilization and quiescence, inhibiting excessive sprouting and maintaining endothelial homeostasis (119, 120). In the lymphatic system, BMP6 and BMP9, circulating in the systemic bloodstream, signal to LECs. BMP9 is especially crucial for the maturation of lymphatic vessels and the formation of lymphatic valves. BMP9

knockout mice exhibit defects such as dilated lymphatic vessels and a reduced number of valves. BMP9, through the ALK1 receptor, regulates key genes like Lyve1, Foxc2, Connexin37, Ephrin-b2, and Neuropilin1, which are essential for lymphatic valve development (121, 122). Moreover, BMP9 downregulates PROX1 in LECs, leading to restricted cell proliferation and a trans-differentiation of lymphatic endothelial cells to blood endothelial cells (123, 124). BMP2 also plays a role in the lymphatic system by negatively regulating lymphatic vessel development. It inhibits PROX1 expression and induces miR-31 and miR-181a, which target Prox1 and impede lymphatic endothelium specification (125).

5 Maladaptation of vascular-lymphatic network in skeletal disease

5.1 Inflammation

Under inflammatory stress, the vasculature in the bone marrow is crucial for supporting bone remodeling. ECs express BMP-2, promoting bone formation, and release osteoprotegerin (OPG) to reduce osteoclastogenesis during diabetes (126, 127). Additionally, multiple cytokines such as IL-6, TNF-α, and IFN-γ are produced by ECs under inflammatory conditions. These cytokines activate Nuclear factor kappa-light-chain-enhancer of activated B cells (NF-κB) signaling, which regulates hematopoietic stem and progenitor cell (HSPC) functions. Inhibiting the endothelial NF-κB pathway improves HSPC proliferation and hematopoietic recovery following myelosuppressive injury (128). IL-33, a pro-inflammatory cytokine produced by CD105-expressing ECs, promotes the differentiation of bone marrow-derived stromal cells into osteoblasts and enhances calcium deposition (129).

Recent studies highlight the connection between lymphangiocrine signaling and inflammation. Under inflammatory conditions, lymphatic vessels within the bone undergo significant changes, including increased lymphangiogenesis and elevated expression of specific cytokines and growth factors that support this expansion and associated immune responses (2). IL-6 drives lymphangiogenesis in bones, and the secretion of CXCL12 from proliferating LECs is critical for hematopoietic and bone regeneration. Moreover, lymphangiocrine CXCL12 triggers the expansion of mature Myh11+ CXCR4+ pericytes, which differentiate into bone cells and contribute to bone and hematopoietic regeneration. In aged animals, this expansion of lymphatic vessels and Myh11-positive cells in response to genotoxic stress is impaired (2). The increased presence of lymphatic vessels and activated LECs significantly impacts bone regeneration and repair processes.

5.2 Osteoarthritis

OA is a common joint disorder characterized by the degeneration of articular cartilage and inflammation of surrounding tissues due to aging-related mechanical degradation and subchondral bone disorders (130, 131). Synovial cells play a crucial role in OA by releasing inflammatory mediators that stimulate the production of inflammatory cytokines and matrix-degrading enzymes like MMPs and ADAMTS (a disintegrin and metalloproteinase with thrombospondin motifs) proteins in chondrocytes, leading to cartilage destruction (132, 133). Immunohistochemical analysis of synovial specimens from OA patients reveals increased lymphatic vessels infiltrated by inflammatory cells, indicating their involvement in OA pathogenesis (134). Transmission electron microscopy has shown dysfunction in microcirculation and lymphatic drainage in OA patients (135). Post-mortem analysis of knee synovium sections from OA patients shows reduced lymphatic vessel density, negatively correlated with synovial effusion, suggesting impaired lymphatic drainage exacerbates joint inflammation (136). Dynamic changes in lymphatic structure and function may significantly impact OA progression, warranting further investigation. In a mice model of meniscal-ligamentous injury (MLI)-induced OA, increased capillary lymphatics and decreased collecting lymphatic vessels were observed (50). Although lymphatic capillaries increased, their drainage function declined due to a leaky phenotype. This led to impaired lymphatic pumping and accumulation of pro-inflammatory factors in OA-affected knees, supported by findings in human OA samples (52, 137). These results indicate impaired synovial lymphatic drainage during OA progression.

Macrophages also play a significant role in joint inflammation and bone destruction in OA, potentially through interaction with lymphatic vessels (138, 139). Macrophages can be categorized into pro-inflammatory M1 and anti-inflammatory M2 phenotypes, accumulating and polarizing within the synovium and articular cavity during OA progression. Early-stage OA shows synovitis and M1 macrophage accumulation near lymphatic vessels, with M1 macrophages promoting destructive processes by regulating inflammatory mediators like TNF, IL-1, and iNOS (140). Itch, a negative regulator of the NF-κB pathway, suppresses pro-inflammatory macrophage polarization and IL-1α release (141, 142). Knockout of itch in mice results in severe OA phenotypes and impaired lymphatic drainage due to M1 macrophage-induced inflammation (143). Decreased FGFR3 expression in OA patient monocytes, and conditional FGFR3 knockout in macrophages exacerbates joint destruction through synovitis and macrophage accumulation via CXCL12/CXCR7-dependent chemotaxis (144). Since CXCL12 from LECs is crucial for tissue regeneration post-injury, further research is needed on the interplay between synovial macrophages and lymphatic vessels in OA.

5.3 Rheumatoid arthritis

RA is a chronic autoimmune disorder primarily affecting the joints, leading to persistent inflammation and progressive damage. This inflammation triggers the release of inflammatory mediators and activates immune cells, further worsening the condition. Inflamed joints in RA patients exhibit a significant increase in activated and infiltrated immune cells, such as macrophages,

lymphocytes, and plasma cells. These cells are crucial in the progression of joint inflammation as they produce and release various mediators, including cytokines, chemokines, and enzymes (100, 101). Key cytokines involved in RA pathogenesis include tumor necrosis factor TNF-α, IL-1, and IL-6. These cytokines induce synovial inflammation and vasodilation, resulting in joint pain, swelling, and functional impairment (99). RA is also characterized by increased angiogenesis and vessel density in non-calcified articular cartilage regions. Lymphocyte infiltration and active ECs are essential for the trafficking of leukocytes into the joint during RA progression (145). Intercellular adhesion molecule-1 (ICAM-1), vascular cell adhesion protein 1 (VCAM-1), and E-selectin expressed by ECs promote the migration of leukocytes and fibroblasts into RA joints (146). Specifically, endothelial Notch3 signaling drives the differentiation of synovial fibroblasts, which acquire an invasive phenotype during the disease (147). This invasive behavior of synovial fibroblasts contributes to the overall joint damage and functional decline observed in RA patients.

Clinical studies and animal models indicate that lymphatic vessels likely play a crucial role in clearing inflammatory cells and mediators from the inflamed synovium. The VEGF family comprises key regulators in angiogenesis and lymphangiogenesis, including VEGF-A, VEGF-B, VEGF-C, VEGF-D, VEGF-E, VEGF-F, and placenta growth factor (PIGF) (104). These VEGF ligands activate signaling pathways by binding to tyrosine kinase receptors known as vascular endothelial growth factor receptors (VEGFRs), which have three subtypes: VEGFR1, VEGFR2, and VEGFR3. While VEGFR1 and VEGFR2 primarily regulate angiogenesis, VEGFR3 signaling is central to lymphangiogenesis (102). The downstream signaling pathways activated by VEGF-C/VEGFR3 include mitogen-activated protein kinase/extracellular signal-related kinase (MAPK/ERK), phosphatidylinositol 3-kinase/protein kinase B (PI3k/AKT), and Jun N-terminal kinase1/2 (JNK1/2) pathways (148, 149). Activation of these pathways leads to the proliferation, survival, and migration of LECs and the remodeling of lymphatic vessels. Previous studies have shown high expression of VEGF-C and its receptors, VEGFR2 and VEGFR3, in the synovial tissues of arthritis patients compared to healthy controls. Macrophages also exhibit high expression of VEGF-C and VEGFR3. Additionally, significantly elevated levels of VEGF-C have been observed in the synovial fluid of patients with RA, showing a strong positive correlation with TNF-α levels (150).

5.4 Bone metastasis

Bone metastasis is a frequent complication of several primary tumors, where disseminated tumor cells (DTCs) can remain dormant for extended periods before reactivation and metastatic growth (151, 152). The process of reactivation and metastasis is intricately linked to the vascular and lymphatic networks within the bone microenvironment.

ECs in the bone marrow play crucial roles in both supporting and regulating DTC behavior. They produce thrombospondin-1, inducing DTC quiescence, and express molecules like Von Willebrand factor (VWF) and vascular cell adhesion molecule 1 (VCAM-1), which affect DTC interaction with the perivascular niche and chemotherapy sensitivity (153, 154). Moreover, ADAM17-regulated CX3CL1 expression by bone marrow ECs promotes specific types of metastases, such as spinal metastasis from hepatocellular carcinoma (155). The vascular structure within bones also influences metastatic progression. Sinusoids and low blood flow facilitate interactions between tumor cells and ECs, while type H vessels with higher blood flow and oxygen supply support tumor cell survival and resistance to therapies (154). Reduction in blood flow diminishes type H vessels and inhibits pericyte expansion, thereby rendering DTCs more susceptible to treatment (156).

Tumors undergo phenotypic changes through accumulated genetic mutations, fostering polyclonal cell populations. Epithelial-mesenchymal transition (EMT) enhances cancer cell motility and invasiveness, mediated by cytokines like TGF-β, FGF, and others. EMT also reduces E-cadherin expression and promotes mesenchymal markers like vimentin and N-cadherin, enhancing malignant traits and chemotherapy resistance (157, 158). In the context of lymphatic involvement, tumor cells invade lymphatic vessels primarily from the peritumoral regions rather than from within the tumor itself due to high interstitial pressure (159). TGF-β signaling and ALK5 inhibitors play significant roles in tumor lymphangiogenesis in tumor xenografts (160, 161). Studies suggest that TGF-β influences tumor metastasis by regulating the structure and function of newly formed tumor lymphatic vessels. Secondary lymphedema, a common complication of cancer treatment, often involves increased TGF-β1 levels. In mouse models, inhibition of TGF-β1 has been demonstrated to mitigate the severity of lymphedema (162). Thus, targeting TGF-β could potentially effectively inhibit lymphatic metastasis and reduce lymphedema.

Several studies emphasize the significant role of bone marrow mesenchymal stem cells (BM-MSCs) in cancer progression, particularly through their impact on lymphangiogenesis (163–165). Human BM-MSCs contribute to tumor growth and metastasis by promoting both neovascularization and the formation of lymphatic vessels (164). Research shows that BM-MSCs and their conditioned medium not only support tumor growth but also facilitate lymph vessel formation in metastatic environments by increasing the expression of lymph-associated markers and enhancing tube formation in lymphatic endothelial cells and specific tumor cell lines (165). However, there are concerns about the potential for these processes to awaken dormant tumors through lymphangiogenesis. Additionally, both human and murine BM-MSCs have demonstrated the ability to adopt a lymphatic phenotype and stimulate lymphatic vessel formation by secreting factors like VEGF-A (163). This factor activates the VEGFR-2 pathway in lymphatic endothelial cells (LECs), leading to increased LEC proliferation, migration, and tube formation, which, in turn, enhances lymphatic vessel density within tumors and promotes metastasis (163). While these findings suggest promising therapeutic applications of MSCs in regenerative medicine, they also highlight the need to consider their role in cancer-related lymphangiogenesis when developing cancer treatment strategies.

Overall, understanding the maladaptation of the vascular-lymphatic network in bone metastasis involves deciphering complex interactions between tumor cells, endothelial cells, and the lymphatic system. Therapeutic strategies targeting these

interactions hold promise for improving outcomes in patients with metastatic bone disease, necessitating further research into the precise molecular mechanisms driving vascular and lymphatic dysregulation in this context.

6 Targeting the vascular-lymphatic network as a potential therapeutic strategy

The vascular and lymphatic networks play crucial roles in maintaining tissue homeostasis and responding to pathological conditions in bone and joint disorders. Given their involvement in inflammation, tissue regeneration, and disease progression, targeting these networks presents a promising therapeutic approach. By modulating angiogenesis and lymphangiogenesis, it is possible to address the underlying mechanisms of various bone and joint diseases, potentially leading to more effective treatments and improved patient outcomes.

Angiogenesis, the process of blood vessel formation, is essential for bone tissue engineering and regeneration. Strategies to enhance vascularization in engineered bone tissues have shown significant promise, particularly through the delivery of angiogenic growth factors such as VEGF, Angiogenin (ANG), and PDGF (166–169). For instance, the incorporation of VEGF into bone scaffolds has been demonstrated to promote neovascularization and bone healing, as evidenced by advanced bone regeneration in animal models (167). Additionally, the sustained release of these growth factors, facilitated by sophisticated delivery systems, ensures prolonged therapeutic effects, making them superior to bolus injections (166). Given the coupling of angiogenesis and osteogenesis, these strategies hold great potential for improving the success rates of bone tissue engineering and addressing bone-related pathologies.

The lymphatic network, particularly lymphangiogenesis and lymphatic drainage, also offers potential therapeutic targets, especially in conditions like RA and OA. The VEGF-C/VEGFR3 signaling pathway has emerged as a key regulator of lymphangiogenesis and lymphatic function. In RA, enhancing lymphatic drainage through intra-articular administration of VEGF-C has been shown to reduce joint damage by promoting local lymphatic function (170). Similarly, in OA, impaired lymphatic drainage has been linked to disease progression, and targeting VEGF-C/VEGFR3 signaling has demonstrated the potential to enhance lymphatic function and mitigate tissue damage (137, 171). Despite these promising findings, further research is necessary to fully understand the long-term effects and safety of such treatments, particularly in chronic conditions like arthritis.

VEGF serves as a crucial common regulator, linking both the vascular and lymphatic networks. VEGF not only drives angiogenesis, essential for blood vessel formation and bone regeneration, but also plays a significant role in lymphangiogenesis through its interaction with VEGF-C and the VEGFR3 signaling pathway (172–174). This dual role of VEGF highlights its importance as a therapeutic target that can simultaneously influence both blood and lymphatic vessel dynamics. By modulating VEGF activity, it may be possible to achieve coordinated regulation of these two networks, offering a unified approach to treating complex bone and joint disorders where both vascular and lymphatic dysfunctions are involved.

7 Conclusion and perspective

The intricate interplay between blood and lymphatic networks is vital for maintaining bone and joint homeostasis and responding to pathological conditions. Type H blood vessels play a crucial role in coupling angiogenesis with osteogenesis, while emerging evidence highlights the significance of lymphatic vessels in bone support regeneration after injury. These networks work synergistically to regulate bone homeostasis and facilitate bone repair. Understanding these interactions provides a comprehensive view of skeletal biology and offers insights into the mechanisms underlying bone and joint diseases. Future research should focus on elucidating the specific molecular pathways and signaling mechanisms driving these interactions, which could pave the way for novel therapeutic strategies. Additionally, integrating recent advancements in vascular and lymphatic biology will enhance our ability to develop targeted treatments for bone and joint diseases, ultimately improving patient outcomes. This evolving field holds promise for significant breakthroughs in both basic science and clinical applications.

Research on lymphatic vessels in bone tissue lags behind the more extensive studies on blood vessels in bones and joints. While it's known that lymphatic vessels are present in bones and play roles in fluid transport and immune surveillance, their drainage pathways within bones remain unexplored. Identifying these drainage routes is crucial for a deeper understanding of bone physiology, the specific functions of lymphatic vessels in bone, and potential drug interventions. Further research using advanced techniques such as single-cell sequencing and lineage tracing is necessary to identify the key cell subsets and molecular characteristics of lymphatic vessels, particularly in disease conditions. Understanding how lymphatic vessels change and function during different stages of diseases like RA, OA, and aging could help pinpoint the optimal timing for clinical interventions. We anticipate that future research will lead to better strategies for regulating lymphatic vessels in joints, ultimately improving the treatment and outcomes of inflammatory joint diseases.

Author contributions

JH: Writing – review & editing, Writing – original draft, Validation, Conceptualization. CL: Writing – review & editing, Resources, Funding acquisition. JY: Writing – review & editing, Supervision, Conceptualization. LZ: Writing – review & editing, Supervision.

Funding

The author(s) declare financial support was received for the research, authorship, and/or publication of this article. This study is funded by the Zunyi Science and Technology Bureau and Zunyi

Medical University Science and Technology Joint Fund (QianShiKeHe HZ Zi (2022) No.393).

Conflict of interest

The authors declare that the research was conducted in the absence of any commercial or financial relationships that could be construed as a potential conflict of interest.

Publisher's note

References

1. Meng YM, Jiang X, Zhao X, Meng Q, Wu S, Chen Y, et al. Hexokinase 2-driven glycolysis in pericytes activates their contractility leading to tumor blood vessel abnormalities. *Nat Commun*. (2021) 12:6011. doi: 10.1038/s41467-021-26259-y

2. Biswas L, Chen J, De Angelis J, Singh A, Owen-Woods C, Ding Z, et al. Lymphatic vessels in bone support regeneration after injury. *Cell*. (2023) 186:382–397.e24. doi: 10.1016/j.cell.2022.12.031

3. Peng Y, Kenney HM, de Mesy Bentley KL, Xing L, Ritchlin CT, Schwarz EM. Distinct mast cell subpopulations within and around lymphatic vessels regulate lymph flow and progression of inflammatory-erosive arthritis in TNF-transgenic mice. *Front Immunol*. (2023) 14:1275871. doi: 10.3389/fimmu.2023.1275871

4. Zhou S, Zhao G, Chen R, Li Y, Huang J, Kuang L, et al. Lymphatic vessels: roles and potential therapeutic intervention in rheumatoid arthritis and osteoarthritis. *Theranostics*. (2024) 14:265–82. doi: 10.7150/thno.90940

5. Tuckermann J, Adams RH. The endothelium-bone axis in development, homeostasis and bone and joint disease. *Nat Rev Rheumatol*. (2021) 17:608–20. doi: 10.1038/s41584-021-00682-3

6. Ramasamy SK, Kusumbe AP, Wang L, Adams RH. Endothelial Notch activity promotes angiogenesis and osteogenesis in bone. *Nature*. (2014) 507:376–80. doi: 10.1038/nature13146

7. Kusumbe AP, Ramasamy SK, Adams RH. Coupling of angiogenesis and osteogenesis by a specific vessel subtype in bone. *Nature*. (2014) 507:323–8. doi: 10.1038/nature13145

8. Liu X, Zhang P, Gu Y, Guo Q, Liu Y. Type H vessels: functions in bone development and diseases. *Front Cell Dev Biol*. (2023) 11:1236545. doi: 10.3389/fcell.2023.1236545

9. Xu Z, Kusumbe AP, Cai H, Wan Q, Chen J. Type H blood vessels in coupling angiogenesis-osteogenesis and its application in bone tissue engineering. *J BioMed Mater Res B Appl Biomater*. (2023) 111:1434–46. doi: 10.1002/jbm.b.35243

10. Wang M, Wu Y, Li G, Lin Q, Zhang W, Liu H, et al. Articular cartilage repair biomaterials: strategies and applications. *Mater Today Bio*. (2024) 24:100948. doi: 10.1016/j.mtbio.2024.100948

11. McCarter AL, Khalid A, Yi Y, Monroy M, Zhao H, Rios JJ, et al. Bone development and fracture healing is normal in mice that have a defect in the development of the lymphatic system. *Lymphology*. (2020) 53:162–71.

12. Jacob L, Boisserand LSB, Geraldo LHM, de Brito Neto J, Mathivet T, Antila S, et al. Anatomy and function of the vertebral column lymphatic network in mice. *Nat Commun*. (2019) 10:4594. doi: 10.1038/s41467-019-12568-w

13. Bouta EM, Bell RD, Rahimi H, Xing L, Wood RW, Bingham CO, et al. Targeting lymphatic function as a novel therapeutic intervention for rheumatoid arthritis. *Nat Rev Rheumatol*. (2018) 14:94–106. doi: 10.1038/nrrheum.2017.205

14. Acar M, Kocherlakota KS, Murphy MM, Peyer JG, Oguro H, Inra CN, et al. Deep imaging of bone marrow shows non-dividing stem cells are mainly perisinusoidal. *Nature*. (2015) 526:126–30. doi: 10.1038/nature15250

15. Ramasamy SK, Kusumbe AP, Schiller M, Zeuschner D, Bixel MG, Milia C, et al. Blood flow controls bone vascular function and osteogenesis. *Nat Commun*. (2016) 7:13601. doi: 10.1038/ncomms13601

16. Filipowska J, Tomaszewski KA, Niedźwiedzki Ł, Walocha JA, Niedźwiedzki T. The role of vasculature in bone development, regeneration and proper systemic functioning. *Angiogenesis*. (2017) 20:291–302. doi: 10.1007/s10456-017-9541-1

17. Kusumbe AP, Ramasamy SK, Itkin T, Mäe MA, Langen UH, Betsholtz C, et al. Age-dependent modulation of vascular niches for haematopoietic stem cells. *Nature*. (2016) 532:380–4. doi: 10.1038/nature17638

18. Sivaraj KK, Adams RH. Blood vessel formation and function in bone. *Development*. (2016) 143:2706–15. doi: 10.1242/dev.136861

19. Arnett TR. Acidosis, hypoxia and bone. *Arch Biochem Biophys*. (2010) 503:103–9. doi: 10.1016/j.abb.2010.07.021

20. Spencer JA, Ferraro F, Roussakis E, Klein A, Wu J, Runnels JM, et al. Direct measurement of local oxygen concentration in the bone marrow of live animals. *Nature*. (2014) 508:269–73. doi: 10.1038/nature13034

21. Itkin T, Gur-Cohen S, Spencer JA, Schajnovitz A, Ramasamy SK, Kusumbe AP, et al. Distinct bone marrow blood vessels differentially regulate haematopoiesis. *Nature*. (2016) 532:323–8. doi: 10.1038/nature17624

22. Bixel MG, Kusumbe AP, Ramasamy SK, Sivaraj KK, Butz S, Vestweber D, et al. Flow dynamics and HSPC homing in bone marrow microvessels. *Cell Rep*. (2017) 18:1804–16. doi: 10.1016/j.celrep.2017.01.042

23. Lo Celso C, Lin CP, Scadden DT. *In vivo* imaging of transplanted hematopoietic stem and progenitor cells in mouse calvarium bone marrow. *Nat Protoc*. (2011) 6:1–14. doi: 10.1038/nprot.2010.168

24. Langen UH, Pitulescu ME, Kim JM, Enriquez-Gasca R, Sivaraj KK, Kusumbe AP, et al. Cell–matrix signals specify bone endothelial cells during developmental osteogenesis. *Nat Cell Biol*. (2017) 19:189–201. doi: 10.1038/ncb3476

25. Zawieja D. Lymphatic biology and the microcirculation: past, present and future. *Microcirculation*. (2005) 12:141–50. doi: 10.1080/10739680590900003

26. Petrova TV, Koh GY. Biological functions of lymphatic vessels. *Science*. (2020) 369:eaax4063. doi: 10.1126/science.aax4063

27. Srinivasan RS, Dillard ME, Lagutin OV, Lin FJ, Tsai S, Tsai MJ, et al. Lineage tracing demonstrates the venous origin of the mammalian lymphatic vasculature. *Genes Dev*. (2007) 21:2422–32. doi: 10.1101/gad.1588407

28. Skandalakis JE, Skandalakis LJ, Skandalakis PN. Anatomy of the lymphatics. *Surg Oncol Clin N Am*. (2007) 16:1–16. doi: 10.1016/j.soc.2006.10.006

29. Yang Y, Oliver G. Development of the mammalian lymphatic vasculature. *J Clin Invest*. (2014) 124:888–97. doi: 10.1172/JCI71609

30. Tammela T, Alitalo K. Lymphangiogenesis: molecular mechanisms and future promise. *Cell*. (2010) 140:460–76. doi: 10.1016/j.cell.2010.01.045

31. Breslin JW, Yang Y, Scallan JP, Sweat RS, Adderley SP, Murfee WL. Lymphatic vessel network structure and physiology. In: *Comprehensive Physiology*. John Wiley & Sons, Ltd (2018). p. 207–99. doi: 10.1002/cphy.c180015

32. Schulte-Merker S, Sabine A, Petrova TV. Lymphatic vascular morphogenesis in development, physiology, and disease. *J Cell Biol*. (2011) 193:607–18. doi: 10.1083/jcb.201012094

33. Zawieja DC. Contractile physiology of lymphatics. *Lymphat Res Biol*. (2009) 7:87–96. doi: 10.1089/lrb.2009.0007

34. Baluk P, Fuxe J, Hashizume H, Romano T, Lashnits E, Butz S, et al. Functionally specialized junctions between endothelial cells of lymphatic vessels. *J Exp Med*. (2007) 204:2349–62. doi: 10.1084/jem.20062596

35. Chakraborty S, Davis MJ, Muthuchamy M. Emerging trends in the pathophysiology of lymphatic contractile function. *Semin Cell Dev Biol*. (2015) 38:55–66. doi: 10.1016/j.semcdb.2015.01.005

36. Aspelund A, Robciuc MR, Karaman S, Makinen T, Alitalo K. Lymphatic system in cardiovascular medicine. *Circ Res*. (2016) 118:515–30. doi: 10.1161/CIRCRESAHA.115.306544

37. Padera TP, Meijer EFJ, Munn LL. The lymphatic system in disease processes and cancer progression. *Annu Rev BioMed Eng*. (2016) 18:125–58. doi: 10.1146/annurev-bioeng-112315-031200

38. Wu Y, Seong YJ, Li K, Choi D, Park E, Daghlian GH, et al. Organogenesis and distribution of the ocular lymphatic vessels in the anterior eye. *JCI Insight*. (2020) 5:e135121, 135121. doi: 10.1172/jci.insight.135121

39. Kizhatil K, Ryan M, Marchant JK, Henrich S, John SWM. Schlemm's canal is a unique vessel with a combination of blood vascular and lymphatic phenotypes that forms by a novel developmental process. *PloS Biol*. (2014) 12:e1001912. doi: 10.1371/journal.pbio.1001912

40. Monroy M, McCarter AL, Hominick D, Cassidy N, Dellinger MT. Lymphatics in bone arise from pre-existing lymphatics. *Dev Camb Engl*. (2020) 147:dev184291. doi: 10.1242/dev.184291

41. Wang W, Wang H, Zhou X, Li X, Sun W, Dellinger M, et al. Lymphatic endothelial cells produce M-CSF, causing massive bone loss in mice. *J Bone Miner Res Off J Am Soc Bone Miner Res*. (2017) 32:939–50. doi: 10.1002/jbmr.3077

42. Hominick D, Silva A, Khurana N, Liu Y, Dechow PC, Feng JQ, et al. VEGF-C promotes the development of lymphatics in bone and bone loss. *eLife*. (2018) 7:e34323. doi: 10.7554/eLife.34323

43. Edwards JR, Williams K, Kindblom LG, Meis-Kindblom JM, Hogendoorn PCW, Hughes D, et al. Lymphatics and bone. *Hum Pathol*. (2008) 39:49–55. doi: 10.1016/j.humpath.2007.04.022

44. Dillaman RM. Movement of ferritin in the 2-day-old chick femur. *Anat Rec*. (1984) 209:445–53. doi: 10.1002/ar.1092090404

45. Montgomery RJ, Sutker BD, Bronk JT, Smith SR, Kelly PJ. Interstitial fluid flow in cortical bone. *Microvasc Res*. (1988) 35:295–307. doi: 10.1016/0026-2862(88)90084-2

46. Vittas D, Hainau B. Lymphatic capillaries of the periosteum: do they exist? *Lymphology*. (1989) 22:173–7.

47. Casley-Smith JR, Földi-Börsök E, Földi M. The prelymphatic pathways of the brain as revealed by cervical lymphatic obstruction and the passage of particles. *Br J Exp Pathol*. (1976) 57:179–88.

48. Louveau A, Herz J, Alme MN, Salvador AF, Dong MQ, Viar KE, et al. CNS lymphatic drainage and neuroinflammation are regulated by meningeal lymphatic vasculature. *Nat Neurosci*. (2018) 21:1380–91. https://pubmed.ncbi.nlm.nih.gov/30224810/.

49. Aspelund A, Antila S, Proulx ST, Karlsen TV, Karaman S, Detmar M, et al. A dural lymphatic vascular system that drains brain interstitial fluid and macromolecules. *J Exp Med*. (2015) 212:991–9. doi: 10.1084/jem.20142290

50. Shi JX, Liang QQ, Wang YJ, Mooney RA, Boyce BF, Xing L. Use of a whole-slide imaging system to assess the presence and alteration of lymphatic vessels in joint sections of arthritic mice. *Biotech Histochem Off Publ Biol Stain Commun*. (2013) 88:428–39. doi: 10.3109/10520295.2012.729864

51. Melrose J, Little CB. Immunolocalization of lymphatic vessels in human fetal knee joint tissues. *Connect Tissue Res*. (2010) 51:289–305. doi: 10.3109/03008200903318287

52. Shi J, Liang Q, Zuscik M, Shen J, Chen D, Xu H, et al. Distribution and alteration of lymphatic vessels in knee joints of normal and osteoarthritic mice. *Arthritis Rheumatol Hoboken NJ*. (2014) 66:657–66. doi: 10.1002/art.38278

53. Proulx K, Lu A, Sumanas S. Cranial vasculature in zebrafish forms by angioblast cluster-derived angiogenesis. *Dev Biol*. (2010) 348:34–46. doi: 10.1016/j.ydbio.2010.08.036

54. Marziano C, Genet G, Hirschi KK. Vascular endothelial cell specification in health and disease. *Angiogenesis*. (2021) 24:213–36. doi: 10.1007/s10456-021-09785-7

55. Kim TM, Lee RH, Kim MS, Lewis CA, Park C. ETV2/ER71, the key factor leading the paths to vascular regeneration and angiogenic reprogramming. *Stem Cell Res Ther*. (2023) 14:41. doi: 10.1186/s13287-023-03267-x

56. Lee D, Park C, Lee H, Lugus JJ, Kim SH, Arentson E, et al. ER71 acts downstream of BMP, Notch, and Wnt signaling in blood and vessel progenitor specification. *Cell Stem Cell*. (2008) 2:497–507. doi: 10.1016/j.stem.2008.03.008

57. Kelly MA, Hirschi KK. Signaling hierarchy regulating human endothelial cell development. *Arterioscler Thromb Vasc Biol*. (2009) 29:718–24. doi: 10.1161/ATVBAHA.109.184200

58. Sumanas S, Lin S. Ets1-related protein is a key regulator of vasculogenesis in zebrafish. *PloS Biol*. (2006) 4:e10. doi: 10.1371/journal.pbio.0040010

59. Marcelo KL, Goldie LC, Hirschi KK. Regulation of endothelial cell differentiation and specification. *Circ Res*. (2013) 112:1272–87. doi: 10.1161/CIRCRESAHA.113.300506

60. Simons M, Gordon E, Claesson-Welsh L. Mechanisms and regulation of endothelial VEGF receptor signalling. *Nat Rev Mol Cell Biol*. (2016) 17:611–25. doi: 10.1038/nrm.2016.87

61. Wang HU, Chen ZF, Anderson DJ. Molecular distinction and angiogenic interaction between embryonic arteries and veins revealed by ephrin-B2 and its receptor Eph-B4. *Cell*. (1998) 93:741–53. doi: 10.1016/S0092-8674(00)81436-1

62. Fang JS, Coon BG, Gillis N, Chen Z, Qiu J, Chittenden TW, et al. Shear-induced Notch-Cx37-p27 axis arrests endothelial cell cycle to enable arterial specification. *Nat Commun*. (2017) 8:2149. doi: 10.1038/s41467-017-01742-7

63. Masumura T, Yamamoto K, Shimizu N, Obi S, Ando J. Shear stress increases expression of the arterial endothelial marker ephrinB2 in murine ES cells via the VEGF-Notch signaling pathways. *Arterioscler Thromb Vasc Biol*. (2009) 29:2125–31. doi: 10.1161/ATVBAHA.109.193185

64. Becker PW, Sacilotto N, Nornes S, Neal A, Thomas MO, Liu K, et al. An intronic flk1 enhancer directs arterial-specific expression via RBPJ-mediated venous repression. *Arterioscler Thromb Vasc Biol*. (2016) 36:1209–19. doi: 10.1161/ATVBAHA.116.307517

65. Casie Chetty S, Rost MS, Enriquez JR, Schumacher JA, Baltrunaite K, Rossi A, et al. Vegf signaling promotes vascular endothelial differentiation by modulating etv2 expression. *Dev Biol*. (2017) 424:147–61. doi: 10.1016/j.ydbio.2017.03.005

66. Iso T, Maeno T, Oike Y, Yamazaki M, Doi H, Arai M, et al. Dll4-selective Notch signaling induces ephrinB2 gene expression in endothelial cells. *Biochem Biophys Res Commun*. (2006) 341:708–14. doi: 10.1016/j.bbrc.2006.01.020

67. Hasan SS, Fischer A. Notch signaling in the vasculature: angiogenesis and angiocrine functions. *Cold Spring Harb Perspect Med*. (2023) 13:a041166. doi: 10.1101/cshperspect.a041166

68. Corada M, Nyqvist D, Orsenigo F, Caprini A, Giampietro C, Taketo MM, et al. The Wnt/beta-catenin pathway modulates vascular remodeling and specification by upregulating Dll4/Notch signaling. *Dev Cell*. (2010) 18:938–49. doi: 10.1016/j.devcel.2010.05.006

69. García-Pascual CM, Zimmermann RC, Ferrero H, Shawber CJ, Kitajewski J, Simón C, et al. Delta-like ligand 4 regulates vascular endothelial growth factor receptor 2-driven luteal angiogenesis through induction of a tip/stalk phenotype in proliferating endothelial cells. *Fertil Steril*. (2013) 100:1768–76. doi: 10.1016/j.fertnstert.2013.08.034

70. Jahnsen ED, Trindade A, Zaun HC, Lehoux S, Duarte A, Jones EAV. Notch1 is pan-endothelial at the onset of flow and regulated by flow. *PloS One*. (2015) 10:e0122622. doi: 10.1371/journal.pone.0122622

71. You LR, Lin FJ, Lee CT, DeMayo FJ, Tsai MJ, Tsai SY. Suppression of Notch signalling by the COUP-TFII transcription factor regulates vein identity. *Nature*. (2005) 435:98–104. doi: 10.1038/nature03511

72. Swift MR, Weinstein BM. Arterial-venous specification during development. *Circ Res*. (2009) 104:576–88. doi: 10.1161/CIRCRESAHA.108.188805

73. Hong CC, Peterson QP, Hong JY, Peterson RT. Artery/vein specification is governed by opposing phosphatidylinositol-3 kinase and MAP kinase/ERK signaling. *Curr Biol CB*. (2006) 16:1366–72. doi: 10.1016/j.cub.2006.05.046

74. Lin FJ, Chen X, Qin J, Hong YK, Tsai MJ, Tsai SY. Direct transcriptional regulation of neuropilin-2 by COUP-TFII modulates multiple steps in murine lymphatic vessel development. *J Clin Invest*. (2010) 120:1694–707. doi: 10.1172/JCI40101

75. Srinivasan RS, Geng X, Yang Y, Wang Y, Mukatira S, Studer M, et al. The nuclear hormone receptor Coup-TFII is required for the initiation and early maintenance of Prox1 expression in lymphatic endothelial cells. *Genes Dev*. (2010) 24:696–707. doi: 10.1101/gad.1859310

76. Aranguren XL, Beerens M, Coppiello G, Wiese C, Vandersmissen I, Lo Nigro A, et al. COUP-TFII orchestrates venous and lymphatic endothelial identity by homo- or hetero-dimerisation with PROX1. *J Cell Sci*. (2013) 126:1164–75. doi: 10.1242/jcs.116293

77. François M, Caprini A, Hosking B, Orsenigo F, Wilhelm D, Browne C, et al. Sox18 induces development of the lymphatic vasculature in mice. *Nature*. (2008) 456:643–7. doi: 10.1038/nature07391

78. Chiang IKN, Graus MS, Kirschnick N, Davidson T, Luu W, Harwood R, et al. The blood vasculature instructs lymphatic patterning in a SOX7-dependent manner. *EMBO J*. (2023) 42:e109032. doi: 10.15252/embj.2021109032

79. Dieterich LC, Klein S, Mathelier A, Sliwa-Primorac A, Ma Q, Hong YK, et al. DeepCAGE transcriptomics reveal an important role of the transcription factor MAFB in the lymphatic endothelium. *Cell Rep*. (2015) 13:1493–504. doi: 10.1016/j.celrep.2015.10.002

80. Moreira HR, Marques AP. Vascularization in skin wound healing: where do we stand and where do we go? *Curr Opin Biotechnol*. (2022) 73:253–62. doi: 10.1016/j.copbio.2021.08.019

81. Xu X, Wang F, Yang Y, Zhou X, Cheng Y, Wei X, et al. LIPUS promotes spinal fusion coupling proliferation of type H microvessels in bone. *Sci Rep*. (2016) 6:20116. doi: 10.1038/srep20116

82. Yan ZQ, Wang XK, Zhou Y, Wang ZG, Wang ZX, Jin L, et al. H-type blood vessels participate in alveolar bone remodeling during murine tooth extraction healing. *Oral Dis*. (2020) 26:998–1009. doi: 10.1111/odi.13321

83. Chen W, Jin X, Wang T, Bai R, Shi J, Jiang Y, et al. Ginsenoside Rg1 interferes with the progression of diabetic osteoporosis by promoting type H angiogenesis modulating vasculogenic and osteogenic coupling. *Front Pharmacol*. (2022) 13:1010937. doi: 10.3389/fphar.2022.1010937

84. Owen-Woods C, Kusumbe A. Fundamentals of bone vasculature: Specialization, interactions and functions. *Semin Cell Dev Biol*. (2022) 123:36–47. doi: 10.1016/j.semcdb.2021.06.025

85. Gerber HP, Vu TH, Ryan AM, Kowalski J, Werb Z, Ferrara N. VEGF couples hypertrophic cartilage remodeling, ossification and angiogenesis during endochondral bone formation. *Nat Med*. (1999) 5:623–8. doi: 10.1038/9467

86. Zhang J, Pan J, Jing W. Motivating role of type H vessels in bone regeneration. *Cell Prolif*. (2020) 53:e12874. doi: 10.1111/cpr.12874

87. Rafii S, Butler JM, Ding BS. Angiocrine functions of organ-specific endothelial cells. *Nature*. (2016) 529:316–25. doi: 10.1038/nature17040

88. Ramasamy SK, Kusumbe AP, Adams RH. Regulation of tissue morphogenesis by endothelial cell-derived signals. *Trends Cell Biol*. (2015) 25:148–57. doi: 10.1016/j.tcb.2014.11.007

89. Romeo SG, Alawi KM, Rodrigues J, Singh A, Kusumbe AP, Ramasamy SK. Endothelial proteolytic activity and interaction with non-resorbing osteoclasts mediate bone elongation. *Nat Cell Biol*. (2019) 21:430–41. doi: 10.1038/s41556-019-0304-7

90. Maes C, Kobayashi T, Selig MK, Torrekens S, Roth SI, Mackem S, et al. Osteoblast precursors, but not mature osteoblasts, move into developing and fractured bones along with invading blood vessels. *Dev Cell*. (2010) 19:329–44. doi: 10.1016/j.devcel.2010.07.010

91. Moya IM, Umans L, Maas E, Pereira PNG, Beets K, Francis A, et al. Stalk cell phenotype depends on integration of Notch and Smad1/5 signaling cascades. *Dev Cell*. (2012) 22:501–14. doi: 10.1016/j.devcel.2012.01.007

92. Pitulescu ME, Schmidt I, Giaimo BD, Antoine T, Berkenfeld F, Ferrante F, et al. Dll4 and Notch signalling couples sprouting angiogenesis and artery formation. *Nat Cell Biol*. (2017) 19:915–27. doi: 10.1038/ncb3555

93. Hasan SS, Tsaryk R, Lange M, Wisniewski L, Moore JC, Lawson ND, et al. Endothelial Notch signalling limits angiogenesis via control of artery formation. *Nat Cell Biol*. (2017) 19:928–40. doi: 10.1038/ncb3574

94. Wilgus TA, Ferreira AM, Oberyszyn TM, Bergdall VK, Dipietro LA. Regulation of scar formation by vascular endothelial growth factor. *Lab Investig J Tech Methods Pathol*. (2008) 88:579–90. doi: 10.1038/labinvest.2008.36

95. Han YH, Onufer EJ, Huang LH, Sprung RW, Davidson WS, Czepielewski RS, et al. Enterically derived high-density lipoprotein restrains liver injury through the portal vein. *Science*. (2021) 373:eabe6729. doi: 10.1126/science.abe6729

96. Cao E, Watt MJ, Nowell CJ, Quach T, Simpson JS, De Melo Ferreira V, et al. Mesenteric lymphatic dysfunction promotes insulin resistance and represents a potential treatment target in obesity. *Nat Metab*. (2021) 3:1175–88. doi: 10.1038/s42255-021-00457-w

97. Liu X, Cui K, Wu H, Li KS, Peng Q, Wang D, et al. Promoting lymphangiogenesis and lymphatic growth and remodeling to treat cardiovascular and metabolic diseases. *Arterioscler Thromb Vasc Biol*. (2023) 43:e1–10. doi: 10.1161/ATVBAHA.122.318406

98. Zhang F, Zarkada G, Han J, Li J, Dubrac A, Ola R, et al. Lacteal junction zippering protects against diet-induced obesity. *Science*. (2018) 361:599–603. doi: 10.1126/science.aap9331

99. Bartok B, Firestein GS. Fibroblast-like synoviocytes: key effector cells in rheumatoid arthritis. *Immunol Rev*. (2010) 233:233–55. doi: 10.1111/j.0105-2896.2009.00859.x

100. Smolen JS. Rheumatoid arthritis Primer - behind the scenes. *Nat Rev Dis Primer*. (2020) 6:32. doi: 10.1038/s41572-020-0168-y

101. McInnes IB, Schett G. The pathogenesis of rheumatoid arthritis. *N Engl J Med*. (2011) 365:2205–19. doi: 10.1056/NEJMra1004965

102. Carmeliet P, Jain RK. Molecular mechanisms and clinical applications of angiogenesis. *Nature*. (2011) 473:298–307. https://pubmed.ncbi.nlm.nih.gov/21593862/.

103. Shibuya M, Claesson-Welsh L. Signal transduction by VEGF receptors in regulation of angiogenesis and lymphangiogenesis. *Exp Cell Res*. (2006) 312:549–60. https://pubmed.ncbi.nlm.nih.gov/16336962/.

104. Melincovici CS, Boşca AB, Şuşman S, Mărginean M, Mihu C, Istrate M, et al. Vascular endothelial growth factor (VEGF) - key factor in normal and pathological angiogenesis. *Romanian J Morphol Embryol Rev Roum Morphol Embryol*. (2018) 59:455–67. https://pubmed.ncbi.nlm.nih.gov/30173249/.

105. Bouta EM, Kuzin I, de Mesy Bentley K, Wood RW, Rahimi H, Ji RC, et al. Brief report: treatment of tumor necrosis factor-transgenic mice with anti-tumor necrosis factor restores lymphatic contractions, repairs lymphatic vessels, and may increase monocyte/macrophage egress. *Arthritis Rheumatol Hoboken NJ*. (2017) 69:1187–93. doi: 10.1002/art.40047

106. Ponomarev LC, Ksiazkiewicz J, Staring MW, Luttun A, Zwijsen A. The BMP pathway in blood vessel and lymphatic vessel biology. *Int J Mol Sci*. (2021) 22:6364. doi: 10.3390/ijms22126364

107. Renò F, Sabbatini M. Breaking a vicious circle: lymphangiogenesis as a new therapeutic target in wound healing. *Biomedicines*. (2023) 11:656. doi: 10.3390/biomedicines11030656

108. Wang Y, Jin Y, Mäe MA, Zhang Y, Ortsäter H, Betsholtz C, et al. Smooth muscle cell recruitment to lymphatic vessels requires PDGFB and impacts vessel size but not identity. *Dev Camb Engl*. (2017) 144:3590–601. doi: 10.1242/dev.147967

109. Onimaru M, Yonemitsu Y, Fujii T, Tanii M, Nakano T, Nakagawa K, et al. VEGF-C regulates lymphangiogenesis and capillary stability by regulation of PDGF-B. *Am J Physiol Heart Circ Physiol*. (2009) 297:H1685–1696. doi: 10.1152/ajpheart.00015.2009

110. Kurashige C, Hosono K, Matsuda H, Tsujikawa K, Okamoto H, Majima M. Roles of receptor activity-modifying protein 1 in angiogenesis and lymphangiogenesis during skin wound healing in mice. *FASEB J Off Publ Fed Am Soc Exp Biol*. (2014) 28:1237–47. doi: 10.1096/fj.13-238998

111. Gerald D, Adini I, Shechter S, Perruzzi C, Varnau J, Hopkins B, et al. RhoB controls coordination of adult angiogenesis and lymphangiogenesis following injury by regulating VEZF1-mediated transcription. *Nat Commun*. (2013) 4:2824. doi: 10.1038/ncomms3824

112. Naiche LA, Villa SR, Kitajewski JK. Endothelial cell fate determination: A top notch job in vascular decision-making. *Cold Spring Harb Perspect Med*. (2022) 12:a041183. doi: 10.1101/cshperspect.a041183

113. Okizaki SI, Ito Y, Hosono K, Oba K, Ohkubo H, Kojo K, et al. Vascular endothelial growth factor receptor type 1 signaling prevents delayed wound healing in diabetes by attenuating the production of IL-1β by recruited macrophages. *Am J Pathol*. (2016) 186:1481–98. doi: 10.1016/j.ajpath.2016.02.014

114. Lim L, Bui H, Farrelly O, Yang J, Li L, Enis D, et al. Hemostasis stimulates lymphangiogenesis through release and activation of VEGFC. *Blood*. (2019) 134:1764–75. doi: 10.1182/blood.2019001736

115. Tabata M, Kadomatsu T, Fukuhara S, Miyata K, Ito Y, Endo M, et al. Angiopoietin-like protein 2 promotes chronic adipose tissue inflammation and obesity-related systemic insulin resistance. *Cell Metab*. (2009) 10:178–88. doi: 10.1016/j.cmet.2009.08.003

116. Cho CH, Sung HK, Kim KT, Cheon HG, Oh GT, Hong HJ, et al. COMP-angiopoietin-1 promotes wound healing through enhanced angiogenesis, lymphangiogenesis, and blood flow in a diabetic mouse model. *Proc Natl Acad Sci U S A*. (2006) 103:4946–51. doi: 10.1073/pnas.0506352103

117. Hiepen C, Mendez PL, Knaus P. It takes two to tango: endothelial TGFβ/BMP signaling crosstalk with mechanobiology. *Cells*. (2020) 9:1965. doi: 10.3390/cells9091965

118. Goumans MJ, Zwijsen A, Ten Dijke P, Bailly S. Bone morphogenetic proteins in vascular homeostasis and disease. *Cold Spring Harb Perspect Biol*. (2018) 10:a031989. doi: 10.1101/cshperspect.a031989

119. Morrell NW, Bloch DB, ten Dijke P, Goumans MJTH, Hata A, Smith J, et al. Targeting BMP signalling in cardiovascular disease and anaemia. *Nat Rev Cardiol*. (2016) 13:106–20. doi: 10.1038/nrcardio.2015.156

120. García de Vinuesa A, Abdelilah-Seyfried S, Knaus P, Zwijsen A, Bailly S. BMP signaling in vascular biology and dysfunction. *Cytokine Growth Factor Rev*. (2016) 27:65–79. doi: 10.1016/j.cytogfr.2015.12.005

121. Subileau M, Merdzhanova G, Ciais D, Collin-Faure V, Feige JJ, Bailly S, et al. Bone morphogenetic protein 9 regulates early lymphatic-specified endothelial cell expansion during mouse embryonic stem cell differentiation. *Stem Cell Rep*. (2019) 12:98–111. doi: 10.1016/j.stemcr.2018.11.024

122. Levet S, Ciais D, Merdzhanova G, Mallet C, Zimmers TA, Lee SJ, et al. Bone morphogenetic protein 9 (BMP9) controls lymphatic vessel maturation and valve formation. *Blood*. (2013) 122:598–607. doi: 10.1182/blood-2012-12-472142

123. Chen H, Brady Ridgway J, Sai T, Lai J, Warming S, Chen H, et al. Context-dependent signaling defines roles of BMP9 and BMP10 in embryonic and postnatal development. *Proc Natl Acad Sci U S A*. (2013) 110:11887–92. doi: 10.1073/pnas.1306074110

124. Yoshimatsu Y, Lee YG, Akatsu Y, Taguchi L, Suzuki HI, Cunha SI, et al. Bone morphogenetic protein-9 inhibits lymphatic vessel formation via activin receptor-like kinase 1 during development and cancer progression. *Proc Natl Acad Sci U S A*. (2013) 110:18940–5. doi: 10.1073/pnas.1310479110

125. Dunworth WP, Cardona-Costa J, Bozkulak EC, Kim JD, Meadows S, Fischer JC, et al. Bone morphogenetic protein 2 signaling negatively modulates lymphatic development in vertebrate embryos. *Circ Res*. (2014) 114:56–66. doi: 10.1161/CIRCRESAHA.114.302452

126. de Ciriza CP, Lawrie A, Varo N. OPG expression on endothelial cells and modulation by IL-1B, PDGF, insulin, and glucose. *Biochem Physiol Open Access*. (2015) 4:1. doi: 10.4172/2168-9652

127. Basic-Jukic N, Gulin M, Hudolin T, Kastelan Z, Katalinic L, Coric M, et al. Expression of BMP-2 in vascular endothelial cells of recipient may predict delayed graft function after renal transplantation. *Kidney Blood Press Res*. (2016) 41:781–93. doi: 10.1159/000450568

128. Poulos MG, Ramalingam P, Gutkin MC, Kleppe M, Ginsberg M, Crowley MJP, et al. Endothelial-specific inhibition of NF-κB enhances functional haematopoiesis. *Nat Commun*. (2016) 7:13829. doi: 10.1038/ncomms13829

129. Kenswil KJG, Jaramillo AC, Ping Z, Chen S, Hoogenboezem RM, Mylona MA, et al. Characterization of endothelial cells associated with hematopoietic niche formation in humans identifies IL-33 as an anabolic factor. *Cell Rep*. (2018) 22:666–78. doi: 10.1016/j.celrep.2017.12.070

130. Dainese P, Wyngaert KV, De Mits S, Wittoek R, Van Ginckel A, Calders P. Association between knee inflammation and knee pain in patients with knee osteoarthritis: a systematic review. *Osteoarthritis Cartilage*. (2022) 4):516–34. doi: 10.1016/j.joca.2021.12.003

131. Sanchez-Lopez E, Coras R, Torres A, Lane NE, Guma M. Synovial inflammation in osteoarthritis progression. *Nat Rev Rheumatol*. (2022) 18:258–75. doi: 10.1038/s41584-022-00749-9

132. Yang CY, Chanalaris A, Troeberg L. ADAMTS and ADAM metalloproteinases in osteoarthritis - looking beyond the 'usual suspects'. *Osteoarthritis Cartilage*. (2017) 25:1000–9. doi: 10.1016/j.joca.2017.02.791

133. Grillet B, Pereira RVS, Van Damme J, Abu El-Asrar A, Proost P, Opdenakker G. Matrix metalloproteinases in arthritis: towards precision medicine. *Nat Rev Rheumatol*. (2023) 19:363–77. doi: 10.1038/s41584-023-00966-w

134. Xu H, Edwards J, Banerji S, Prevo R, Jackson DG, Athanasou NA. Distribution of lymphatic vessels in normal and arthritic human synovial tissues. *Ann Rheum Dis*. (2003) 62:1227–9. doi: 10.1136/ard.2003.005876

135. Borodin II, Liubarskiĭ MS, Bgatova NP, Mustafaev NR, Dremov EI. Morphological criteria of the state of the microcirculation and the lymphatic drainage in the synovial membrane of the knee joint under normal and pathological conditions. *Morfol St Petersburg Russ*. (2008) 133:51–5.

136. Walsh DA, Verghese P, Cook GJ, McWilliams DF, Mapp PI, Ashraf S, et al. Lymphatic vessels in osteoarthritic human knees. *Osteoarthritis Cartilage*. (2012) 20:405–12. doi: 10.1016/j.joca.2012.01.012

137. Lin X, Bell RD, Catheline SE, Takano T, McDavid A, Jonason JH, et al. Targeting synovial lymphatic function as a novel therapeutic intervention for age-related osteoarthritis in mice. *Arthritis Rheumatol Hoboken NJ*. (2023) 75:923–36. doi: 10.1002/art.42441

138. Wu CL, Harasymowicz NS, Klimak MA, Collins KH, Guilak F. The role of macrophages in osteoarthritis and cartilage repair. *Osteoarthritis Cartilage*. (2020) 28:544–54. doi: 10.1016/j.joca.2019.12.007

139. Thomson A, Hilkens CMU. Synovial macrophages in osteoarthritis: the key to understanding pathogenesis? *Front Immunol*. (2021) 12:678757. doi: 10.3389/fimmu.2021.678757

140. Wang W, Lin X, Xu H, Sun W, Bouta EM, Zuscik MJ, et al. Attenuated joint tissue damage associated with improved synovial lymphatic function following treatment with bortezomib in a mouse model of experimental posttraumatic osteoarthritis. *Arthritis Rheumatol Hoboken NJ*. (2019) 71:244–57. doi: 10.1002/art.40696

141. Lin X, Zhang H, Boyce BF, Xing L. Ubiquitination of interleukin-1α is associated with increased pro-inflammatory polarization of murine macrophages deficient in the E3 ligase ITCH. *J Biol Chem*. (2020) 295:11764–75. doi: 10.1074/jbc.RA120.014298

142. Lin X, Wang W, McDavid A, Xu H, Boyce BF, Xing L. The E3 ubiquitin ligase Itch limits the progression of post-traumatic osteoarthritis in mice by inhibiting macrophage polarization. *Osteoarthritis Cartilage*. (2021) 29:1225–36. doi: 10.1016/j.joca.2021.04.009

143. Wang W, Xu H, Sun W, Wang H, Zuscik M, Xing L. Mice deficient in the NF-κB negative regulator, itch, develop severe osteoarthritis and reduced synovial lymphatic drainage due to m1 macrophages-induced lymphatic endothelial cell inflammation. *Osteoarthritis Cartilage*. (2016) 24:S31–2. doi: 10.1016/j.joca.2016.01.083

144. Kuang L, Wu J, Su N, Qi H, Chen H, Zhou S, et al. FGFR3 deficiency enhances CXCL12-dependent chemotaxis of macrophages via upregulating CXCR7 and aggravates joint destruction in mice. *Ann Rheum Dis*. (2020) 79:112–22. doi: 10.1136/annrheumdis-2019-215696

145. Walsh DA, McWilliams DF, Turley MJ, Dixon MR, Fransès RE, Mapp PI, et al. Angiogenesis and nerve growth factor at the osteochondral junction in rheumatoid arthritis and osteoarthritis. *Rheumatol Oxf Engl*. (2010) 49:1852–61. doi: 10.1093/rheumatology/keq188

146. Zimmermann-Geller B, Köppert S, Kesel N, Hasseli R, Ullrich S, Lefèvre S, et al. Interactions between rheumatoid arthritis synovial fibroblast migration and endothelial cells. *Immunol Cell Biol*. (2019) 97:178–89. doi: 10.1111/imcb.12208

147. Wei K, Korsunsky I, Marshall JL, Gao A, Watts GFM, Major T, et al. Notch signalling drives synovial fibroblast identity and arthritis pathology. *Nature*. (2020) 582:259–64. doi: 10.1038/s41586-020-2222-z

148. Salameh A, Galvagni F, Bardelli M, Bussolino F, Oliviero S. Direct recruitment of CRK and GRB2 to VEGFR-3 induces proliferation, migration, and survival of endothelial cells through the activation of ERK, AKT, and JNK pathways. *Blood*. (2005) 106:3423–31. doi: 10.1182/blood-2005-04-1388

149. Xu Y, Yuan L, Mak J, Pardanaud L, Caunt M, Kasman I, et al. Neuropilin-2 mediates VEGF-C-induced lymphatic sprouting together with VEGFR3. *J Cell Biol*. (2010) 188:115–30. doi: 10.1083/jcb.200903137

150. Cha HS, Bae EK, Koh JH, Chai JY, Jeon CH, Ahn KS, et al. Tumor necrosis factor-alpha induces vascular endothelial growth factor-C expression in rheumatoid synoviocytes. *J Rheumatol*. (2007) 34:16–9.

151. Virk MS, Lieberman JR. Tumor metastasis to bone. *Arthritis Res Ther*. (2007) 9 Suppl 1:S5. doi: 10.1186/ar2169

152. Kusumbe AP. Vascular niches for disseminated tumour cells in bone. *J Bone Oncol*. (2016) 5:112–6. doi: 10.1016/j.jbo.2016.04.003

153. Carlson P, Dasgupta A, Grzelak CA, Kim J, Barrett A, Coleman IM, et al. Targeting the perivascular niche sensitizes disseminated tumour cells to chemotherapy. *Nat Cell Biol*. (2019) 21:238–50. doi: 10.1038/s41556-018-0267-0

154. Ghajar CM, Peinado H, Mori H, Matei IR, Evason KJ, Brazier H, et al. The perivascular niche regulates breast tumour dormancy. *Nat Cell Biol*. (2013) 15:807–17. doi: 10.1038/ncb2767

155. Sun C, Hu A, Wang S, Tian B, Jiang L, Liang Y, et al. ADAM17-regulated CX3CL1 expression produced by bone marrow endothelial cells promotes spinal metastasis from hepatocellular carcinoma. *Int J Oncol*. (2020) 57:249–63. doi: 10.3892/ijo

156. Singh A, Veeriah V, Xi P, Labella R, Chen J, Romeo SG, et al. Angiocrine signals regulate quiescence and therapy resistance in bone metastasis. *JCI Insight*. (2019) 4:e125679, 125679. doi: 10.1172/jci.insight.125679

157. Heldin CH, Vanlandewijck M, Moustakas A. Regulation of EMT by TGFβ in cancer. *FEBS Lett*. (2012) 586:1959–70. doi: 10.1016/j.febslet.2012.02.037

158. Brabletz T, Kalluri R, Nieto MA, Weinberg RA. EMT in cancer. *Nat Rev Cancer*. (2018) 18:128–34. doi: 10.1038/nrc.2017.118

159. Padera TP, Stoll BR, Tooredman JB, Capen D, di Tomaso E, Jain RK. Pathology: cancer cells compress intratumour vessels. *Nature*. (2004) 427:695. doi: 10.1038/427695a

160. Pak KH, Park KC, Cheong JH. VEGF-C induced by TGF- β1 signaling in gastric cancer enhances tumor-induced lymphangiogenesis. *BMC Cancer*. (2019) 19:799. doi: 10.1186/s12885-019-5972-y

161. Oka M, Iwata C, Suzuki HI, Kiyono K, Morishita Y, Watabe T, et al. Inhibition of endogenous TGF-beta signaling enhances lymphangiogenesis. *Blood*. (2008) 111:4571–9. doi: 10.1182/blood-2007-10-120337

162. Baik JE, Park HJ, Kataru RP, Savetsky IL, Ly CL, Shin J, et al. TGF-β1 mediates pathologic changes of secondary lymphedema by promoting fibrosis and inflammation. *Clin Transl Med*. (2022) 12:e758. doi: 10.1002/ctm2.758

163. Maertens L, Erpicum C, Detry B, Blacher S, Lenoir B, Carnet O, et al. Bone marrow-derived mesenchymal stem cells drive lymphangiogenesis. *PloS One*. (2014) 9:e106976. doi: 10.1371/journal.pone.0106976

164. Conrad C, Niess H, Huss R, Huber S, von Luettichau I, Nelson PJ, et al. Multipotent mesenchymal stem cells acquire a lymphendothelial phenotype and enhance lymphatic regeneration in *vivo*. *Circulation*. (2009) 119:281–9. doi: 10.1161/CIRCULATIONAHA.108.793208

165. Zhan J, Li Y, Yu J, Zhao Y, Cao W, Ma J, et al. Culture medium of bone marrow-derived human mesenchymal stem cells effects lymphatic endothelial cells and tumor lymph vessel formation. *Oncol Lett*. (2015) 9:1221–6. doi: 10.3892/ol.2015.2868

166. Chen RR, Silva EA, Yuen WW, Mooney DJ. Spatio-temporal VEGF and PDGF delivery patterns blood vessel formation and maturation. *Pharm Res*. (2007) 24:258–64. doi: 10.1007/s11095-006-9173-4

167. Kent Leach J, Kaigler D, Wang Z, Krebsbach PH, Mooney DJ. Coating of VEGF-releasing scaffolds with bioactive glass for angiogenesis and bone regeneration. *Biomaterials*. (2006) 27:3249–55. doi: 10.1016/j.biomaterials.2006.01.033

168. Quinlan E, López-Noriega A, Thompson EM, Hibbitts A, Cryan SA, O'Brien FJ. Controlled release of vascular endothelial growth factor from spray-dried alginate microparticles in collagen-hydroxyapatite scaffolds for promoting vascularization and bone repair. *J Tissue Eng Regener Med*. (2017) 11:1097–109. doi: 10.1002/term.2013

169. Kim BS, Kim JS, Yang SS, Kim HW, Lim HJ, Lee J. Angiogenin-loaded fibrin/bone powder composite scaffold for vascularized bone regeneration. *Biomater Res*. (2015) 19:18. doi: 10.1186/s40824-015-0040-4

170. Zhou Q, Guo R, Wood R, Boyce BF, Liang Q, Wang YJ, et al. Vascular endothelial growth factor C attenuates joint damage in chronic inflammatory arthritis by accelerating local lymphatic drainage in mice. *Arthritis Rheumatol*. (2011) 63:2318–28. doi: 10.1002/art.30421

171. Joukov V, Kumar V, Sorsa T, Arighi E, Weich H, Saksela O, et al. A recombinant mutant vascular endothelial growth factor-C that has lost vascular endothelial growth factor receptor-2 binding, activation, and vascular permeability activities. *J Biol Chem*. (1998) 273:6599–602. doi: 10.1074/jbc.273.12.6599

172. Yin S, Zhang W, Zhang Z, Jiang X. Recent advances in scaffold design and material for vascularized tissue-engineered bone regeneration. *Adv Healthc Mater*. (2019) 8:e1801433. doi: 10.1002/adhm.201801433

173. Orlandini M, Spreafico A, Bardelli M, Rocchigiani M, Salameh A, Nucciotti S, et al. Vascular endothelial growth factor-D activates VEGFR-3 expressed in osteoblasts inducing their differentiation. *J Biol Chem*. (2006) 281:17961–7. doi: 10.1074/jbc.M600413200

174. Hartiala P, Suominen S, Suominen E, Kaartinen I, Kiiski J, Viitanen T, et al. Phase 1 lymfactin® Study: short-term safety of combined adenoviral VEGF-C and lymph node transfer treatment for upper extremity lymphedema. *J Plast Reconstr Aesthetic Surg JPRAS*. (2020) 73:1612–21. doi: 10.1016/j.bjps.2020.05.009

frontiers | Frontiers in Endocrinology

TYPE Original Research
PUBLISHED 02 October 2024
DOI 10.3389/fendo.2024.1412872

OPEN ACCESS

EDITED BY
Giuseppina Storlino,
University of Foggia, Italy

REVIEWED BY
Biagio Barone,
ASL Napoli 1 Centro, Italy
Silvia Capuani,
National Research Council (CNR), Italy

*CORRESPONDENCE
Xiangdong Lu
wallforever@sohu.com

RECEIVED 05 April 2024
ACCEPTED 16 September 2024
PUBLISHED 02 October 2024

CITATION
Wang S, Zhao X, Zhou R, Jin Y, Wang X, Ma X and Lu X (2024) The influence of adult urine lead exposure on bone mineral densit: NHANES 2015-2018.
Front. Endocrinol. 15:1412872.
doi: 10.3389/fendo.2024.1412872

The influence of adult urine lead exposure on bone mineral densit: NHANES 2015-2018

Shaokang Wang, Xiaofeng Zhao, Runtian Zhou, Yuanzhang Jin, Xiaonan Wang, Xiaotian Ma and Xiangdong Lu*

Department of Orthopedics, the Second Hospital of Shanxi Medical University, Taiyuan, Shanxi, China

Introduction: Previous studies have indicated that exposure to heavy metals related to bone health is primarily limited to some common harmful metals, and the impact of lead has not been fully understood. This study aims to explore the relationship between urine lead exposure and bone density.

Methods: 1,310 adults were included from the NHANES database (2015-2018), and through generalized linear regression analysis and constrained cubic spline models, the association between lead levels and total bone density as well as lumbar spine bone density was explored. The study also examined the impact of combined exposure to lead and cadmium on bone density.

Results and conclusions: Urinary lead levels were significantly negatively correlated with total bone mineral density (β: −0.015; 95%CI: −0.024, −0.007) and lumbar spine bone mineral density (β: −0.019; 95%CI: −0.031, −0.006). Compared to the lowest three quartiles of lead levels, the adjusted odds ratios for T3 changes in total bone mineral density and lumbar spine bone mineral density were 0.974 (95%CI: 0.959, 0.990) and 0.967 (95%CI: 0.943, 0.991), indicating a significant negative trend. Further analysis with constrained cubic spline models revealed a non-linear decreasing relationship between urinary lead and total bone mineral density as well as lumbar spine bone mineral density. Stratified analyses suggested that the relationship between urinary lead levels and bone mineral density might be significantly influenced by age, while gender showed no significant impact on the relationship. Moreover, combined exposure to lead and cadmium was found to be associated with decreased bone mineral density, emphasizing the potential synergistic effects between lead and cadmium on bone health. However, the specific mechanisms of lead and its effects on different populations require further comprehensive research. This study provides valuable insights for further exploration and development of relevant public health policies.

KEYWORDS

bone mineral density, urinary lead, national health and nutrition examination survey (NHANES), lead exposure, combined exposure

1 Background

Osteoporosis is a metabolic bone disease characterized by changes in bone microstructure and decreased bone mineral density (BMD) (1). Bone density is an important indicator for evaluating bone health, with the two most common sites for measuring bone density being the whole body and the lumbar spine (2). Factors leading to decreased bone density include genetics (3), metabolism (4), and nutrition (5). According to recent evidence, decreased bone density may be related to environmental toxin exposure (6, 7), and heavy metals such as lead (Pb) may be associated with osteoporosis and related fractures (8, 9).

As a typical heavy metal, lead has received much attention due to its harmful effects on human health. The role of lead exposure in human biology is intricate and far-reaching, impacting not only the endocrine system by disrupting thyroid and sex hormone levels but also exerting significant effects on the nervous, immune systems, and reproductive health. As an endocrine-disrupting compound (EDC), lead binds to estrogen and androgen receptors, mimicking estrogenic effects and obstructing androgen actions, thus disturbing hormonal balance (10). This action is not only linked to thyroid dysfunction but also to reproductive health issues, particularly in males, where the association between lead exposure and infertility is increasingly evident. Lead exposure further damages reproductive capabilities through the induction of reactive oxygen species (ROS), cell apoptosis, local necrosis, immunosuppression, and mutagenic stimulation, negatively impacting the male reproductive system and potentially leading to azoospermia (11).

Moreover, lead exposure significantly impairs cognitive and behavioral development in children, correlating with decreased IQ, alterations in neurotransmitter levels, and reduced cognitive and behavioral scores (12–15). In terms of immune function, lead exposure is associated with altered levels of pro-inflammatory cytokines in children, potentially triggering a cascade of health issues spanning neurological, respiratory, cardiovascular, reproductive, and renal systems (16). More alarmingly, lead and its compounds are classified by the International Agency for Research on Cancer (IARC) as probable human carcinogens, indicating a potential cancer risk associated with long-term lead exposure (17). Although the organ toxicity of lead has been widely studied, research on the impact of lead on human bone health is limited.

More than 90% of lead in the human body is found in the bones (18). Lead has strong cytotoxicity, affecting osteoblasts, osteoclasts, and chondrocytes (19). An vitro studies have shown that lead can replace calcium in hydroxyapatite crystals and has a higher affinity for bone sialoprotein than calcium (20). Many animal studies have reported that lead exposure is associated with pathological processes in bone, resulting in decreased bone density and strength (21). In the United States, studies on elderly individuals have shown a significant negative correlation between blood lead levels and osteoporosis, particularly among Caucasian subjects (22). Furthermore, a study conducted in Taiwan found that adults, especially females, with higher urinary lead levels may have an increased risk of osteopenia and osteoporosis (23). Other studies have indicated that lead exposure is associated with femoral and spinal bone density in premenopausal women in the United States (24, 25), and lead and manganese exposure have been found to have a synergistic effect on bone density (8). The toxic effects of lead on bone density in different bone sites vary among children and adolescents, and there are differences in various age groups, genders, and levels of exposure (26). Overall, the research on the effects of normal lead exposure on bone density in adults is still limited, and further systematic studies are needed to obtain accurate conclusions.Therefore, we utilized data from the 2015-2018 National Health and Nutrition Examination Survey (NHANES) database to investigate the correlation between urinary lead levels and bone density in a representative sample of adults aged 20 and above in the United States.

2 Subjects and methods

2.1 Design

The research data is derived from the NHANES database and is a cross-sectional study. All analyses were performed under logarithmic transformation and statistical analysis was conducted using multiplicative interaction models and generalized linear regression models. For other continuous variables, differences between groups were calculated using generalized linear regression models. Weighted chi-square tests were used for categorical variables.

2.2 Time and Location

The study selected information from the US NHANES database from January 2015 to December 2018, and the samples were taken from the general population of the United States.

2.3 Subjects

The data for the study was derived from the US NHANES database. The NHANES database collects nutritional and health information from the general population of the United States and is a cross-sectional study. The NHANES database uses a large-scale, multi-stage complex sampling method, with non-repetitive sampling population, abundant sample size, and good representativeness. The study was approved by the Ethics Review Committee of the National Center for Health Statistics (NCHS), with ethics protocol numbers Continuation of Protocol #2011-17 (2013-2016) and Protocol #2018-01 (2017-2020), and written informed consent was obtained from each participant. The study subjects were selected from data spanning four years, from 2015 to 2018. Among the participants who underwent urinary metal testing from 2015 to 2018, a total of 6102 individuals were included. After excluding individuals with missing data on urine lead, bone density, renal insufficiency, or age less than 20 years (n=4565), 1537

participants were selected. Further exclusions were made for individuals with missing information on basic covariates including poverty-income ratio, body mass index, serum cotinine, and serum 25(OH)D (n=227), resulting in a final analytical sample of 1310 participants, as shown in Figure 1.

2.4 Methods

The selection of covariates is based on previous literature (27). The final covariates include age, gender (male and female), race/ethnicity (Mexican American, Other Hispanic, Non-Hispanic White, Non-Hispanic Black, Other), body mass index (kg/m2), poverty income ratio (<1, ≥1), education level (less than high school, high school or equivalent, higher than high school), serum cotinine (≥10ng/mL, 1-9.9ng/mL, and <1ng/mL), physical activity (<10 minutes/week and ≥10 minutes/week), serum 25(OH)D, thyroid disease (yes or no), diabetes (yes or no), and hypertension (yes or no).

Urine metal determination: Urine samples were collected and stored at -70°C, then transported to the National Center for Environmental Health for testing. Urine lead concentration was measured using inductively coupled plasma mass spectrometry (ICPMS). The laboratory procedures are described in detail on the NHANES website. The metals included in this study were detectable in over 99% of the participants. The metal levels in urine were calibrated with urine creatinine and expressed as μg/g creatinine.At a dedicated mobile examination center, total bone density and lumbar spine bone density were measured using the Hologic QDR 4500A fan-beam dual-energy X-ray absorptiometry (Hologic, Inc., Bedford, Massachusetts). For more detailed information on bone density assessment, please visit the NHANES website.

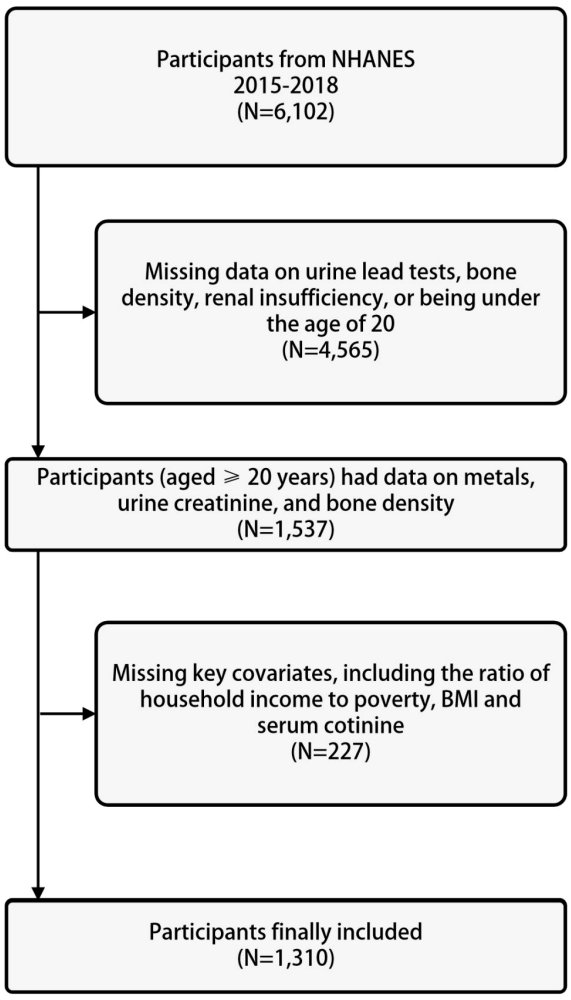

FIGURE 1
Baseline characteristics of participants.

2.5 Statistical analysis

Due to skewed distributions, both bone density and urine lead concentration underwent natural logarithm (ln) transformation. Descriptive analysis was conducted on the participants' basic demographic characteristics and bone density. Continuous variables were expressed as means and standard deviations (± s) or percentiles, while categorical variables were expressed as frequencies (proportions).

Generalized linear regression was used to evaluate the correlation between individual urine lead and bone density, treating each metal as a continuous exposure variable. The transformed regression coefficient represents the percentage change in bone density with a doubling of urine metal levels, using the following formula: $(e(\ln 2 \times \beta) - 1) \times 100\%$. To further explore the relationship between urine lead and bone density, the generalized linear regression model treated urine lead concentration as tertiles. The percentage change in bone density associated with urine metal tertiles was estimated as $(eOR - 1) \times 100\%$. Restricted cubic splines (RCS) were used to assess the dose-response relationship between urine lead and bone density. The RCS model included three knots: the 25th, 50th, and 75th percentiles of the transformed metal concentration.

Stratified analysis by gender and age was conducted, followed by multiplicative interaction analysis. Generalized linear regression was used to further evaluate the combined effect of urine lead and urine cadmium exposure. Participants were divided into low exposure and high exposure groups based on the median levels of the metals. The group with low exposure to both metals was considered as the reference group. The percentage change in bone density for the exposed group was estimated as $(eOR - 1) \times 100\%$.

All analyses were performed using R (version 4.2.3), with statistical significance set at $P<0.05$ (two-tailed). Generalized linear regression analysis and RCS models were implemented using the "ggplot2" and "rms" packages, respectively.

3 Results

3.1 Baseline characteristics

The study included a total of 1310 subjects, with mean ages and body mass indexes of 39.5 ± 11.2 years and 29.0 ± 6.9 kg/m^2 ,

respectively. Among the study population, 642 individuals (49.0%) were male, 777 individuals (59.3%) had received higher education (beyond high school), 388 individuals (29.6%) were non-Hispanic white, 1069 individuals (81.6%) were at or above the poverty line, 915 individuals (69.8%) were non-smokers, 86 individuals (6.6%) were informed of thyroid issues, 101 individuals (7.7%) had diabetes, and 275 individuals (21.0%) had hypertension. The median serum 25(OH)D, total bone density, and lumbar spine bone density were 56.7 (42.0, 73.7) nmol/L, 1.11 (1.04, 1.18) g/cm^2, and 1.02 (0.93, 1.12) g/cm^2, respectively. See Table 1 for details.

3.2 Distribution of urinary lead levels

The geometric mean of urine lead concentration corrected for urinary creatinine was 3.918 μg/g creatinine. The median urine lead concentration was 2.826 μg/g creatinine, with an interquartile range (IQR) of 1.785-4.580 μg/g creatinine, and the standard deviation of urine lead was 4.0927 μg/g creatinine.

3.3 Correlation between urinary lead exposure and bone density

In the fully adjusted model, a significant negative correlation was observed between urinary lead levels and total bone density (β: -0.015; 95%CI: -0.024, -0.007) as well as lumbar spine bone density (β: -0.019; 95%CI: -0.031, -0.006). Furthermore, in the multivariable adjusted model, compared with the lowest tertile of lead level, the odds ratios (ORs) (95%CI) of total bone density at T2 and T3 levels were 0.997 (0.982, 1.011) and 0.974 (0.959, 0.990), respectively, when introducing the tertiles of urinary lead concentration. Similarly, compared with the lowest tertile of lead level, the ORs (95%CI) of lumbar spine bone density at T2 and T3 levels were 0.999 (0.978, 1.021) and 0.967 (0.943, 0.991) (Table 2), respectively. This indicates a significant negative correlation between total bone density and lumbar spine bone density at the highest tertile of urinary lead concentration. It is worth noting that the relationship between these bone density indicators and moderate levels of urinary lead concentration was not significant. This result emphasizes the different effects of urinary lead concentrations on bone density at different levels. A restricted cubic spline showed a nonlinear relationship between urinary lead and total bone density as well as lumbar spine bone density (Figure 2).

In a multivariable adjusted model, gender-stratified analysis revealed that the β values (95% CI) of urinary lead levels and total bone density in men and women were −0.012 (−0.025, 0.0004) and −0.021 (−0.033, −0.010), with corresponding P values of 0.059 and <0.001, respectively. For women, there was a significant negative correlation between urinary lead levels and total bone density, with a β value of −0.021, a 95% CI not including zero, and P value <0.001. However, in men, although the β value was negative, the P value did not reach significance. As for the relationship between urinary lead levels and lumbar bone density, the β values (95% CI) in men and women were −0.021 (−0.033, −0.010) and −0.022

TABLE 1 Characteristics of included participants from NHANES 2015–2018 (N = 1310).

Characteristics	Means ± SDs/N (%)/median (25th, 75th)
Age	39.5± 11.2
Sex	
Male	642 (49.0)
Female	668 (51.0)
Race/ethnicity	
Mexican American	226(17.3)
Other Hispanic	156(11.9)
Non-Hispanic White	388(29.6)
Non-Hispanic Black	259(19.8)
Other Race	281(21.5)
BMI(kg/m^2)	29.0 ± 6.9
Family PIR	
<1	241(18.4)
≥1	1069(81.6)
Education	
Under high school	238(18.2)
High school or equivalent	295 (22.5)
Above high school	777(59.3)
Serum cotinine (ng/mL)	
<1.0 ng/mL	915 (69.8)
1.0-9.9 ng/mL	43(3.3)
≥10 ng/mL	352(26.9)
Physical activity (n/%)	
<10 minutes/week	987 (75.3)
≥10 minutes/week	323(24.7)
Thyroid disease (n/%)	
Yes	86 (6.6)
No	1224 (93.4)
Hypertension (n/%)	
Yes	275 (21.0)
No	1035(79.0)
Diabetes (n/%)	
Yes	101 (7.7)
No	1209(92.3)
Serum 25(OH)D (M(Q_{25},Q_{75}),nmol/L)	56.7(42.0,73.7)
Total bone density (M(Q_{25},Q_{75}),g/cm^2)	1.11(1.04,1.18)
Lumbar bone density (M(Q_{25},Q_{75}), g/cm^2)	1.02 (0.93, 1.12)

TABLE 2 Associations between urinary lead exposure and BMDs.

Urinary lead (ug/mg creatinine)	Percentage change (95% CI) in BMDs			
	Total BMD	P	Lumbar BMD	P
Per 100% increase	−0.015 (−0.024, −0.007)	<0.001	−0.019 (−0.031, −0.006)	0.004
Tertiles				
T1(< 0.216)	Reference		Reference	
T2(0.216–0.382)	0.997 (0.982, 1.011)	0.668	0.999 (0.978, 1.021)	0.946
T3(≥ 0.382)	0.974 (0.959, 0.990)	0.002	0.967 (0.943, 0.991)	0.007

These models were adjusted for factors such as age, sex, body mass index, race, family income-to-poverty ratio, education, serum cotinine levels, physical activity, serum 25(OH)D, thyroid disease, hypertension, and diabetes.

(−0.040, −0.004), with P values of 0.089 and 0.015, respectively. Urinary lead levels were significantly negatively correlated with lumbar bone density in both men and women. However, in men, the P value was 0.089, which did not reach significance, while in women, the P value was 0.015, indicating a higher level of significance (Table 3).

Overall, the relationship between urinary lead levels and total bone density as well as lumbar bone density was significant in women and tended towards a negative correlation in men but was not significant. However, the overall bone P_{int} for gender stratification was 0.241, and the lumbar bone density P_{int} was 0.380, indicating no significant interactive effects, showing that gender had no significant impact on the relationship between urinary lead levels and bone density.

Similarly, in a multivariable adjusted model, stratified analysis based on the median age (39 years) revealed that the β values (95% CI) of urinary lead levels and total bone density in the low-age and high-age groups were −0.009 (−0.021, 0.003) and −0.023 (−0.035, −0.010), with corresponding P values of 0.138 and <0.001, respectively. Regarding total bone density, the relationship between urinary lead levels and bone density was not significant in the low-age group (P value = 0.138), while in the high-age group, there was a significant negative correlation between urinary lead levels and total bone density (P value <0.001). As for the relationship between urinary lead levels and lumbar bone density, the β values (95% CI) in the low-age and high-age groups were −0.006 (−0.022, 0.011) and −0.031 (−0.051, −0.012), with P values of 0.509 and 0.001, respectively. In terms of lumbar bone density, the relationship between urinary lead levels and bone density

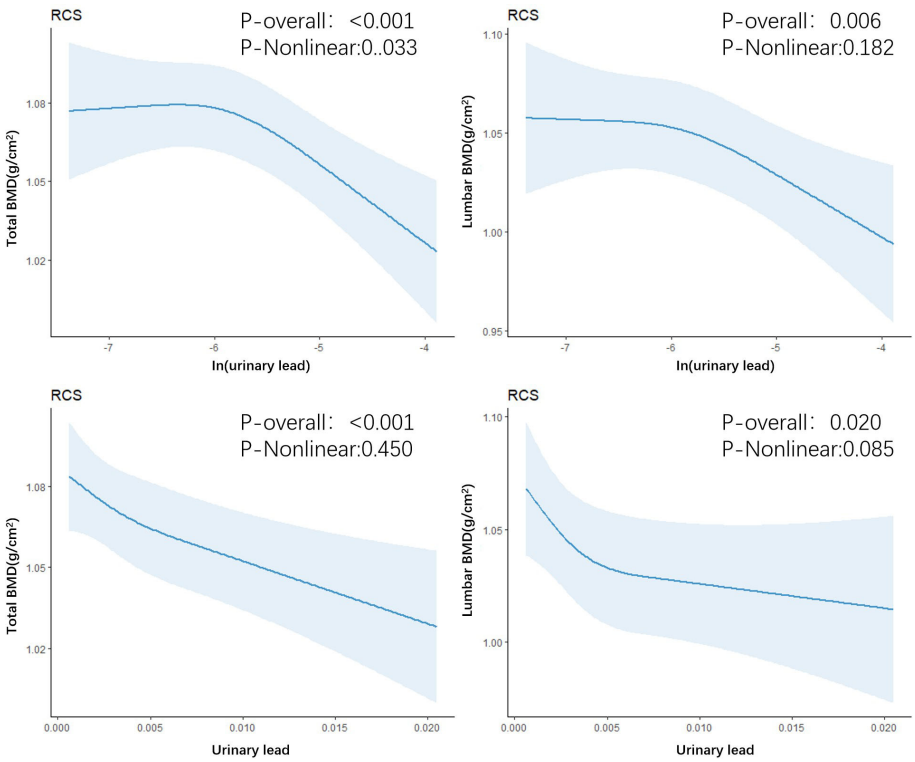

FIGURE 2
Restricted cubic spline regression of urinary lead with total bone density and lumbar spine bone density.

TABLE 3 Interaction of sex and age on the relationship between urinary lead levels and total BMD and lumbar BMD.

Urinary lead (ug/mg creatinine)	Percentage change (95% CI) in BMDs					
	Total BMD	P	P_{int}	Lumbar BMD	P	P_{int}
Sex			0.241			0.380
Male	−0.012(−0.025, 0.0004)	0.059		−0.016 (−0.034, 0.002)	0.089	
Female	−0.021 (−0.033, −0.010)	<0.001		−0.022 (−0.040, −0.004)	0.015	
Age			0.034			0.045
<39(Median)	-0.009 (-0.021, 0.003)	0.138		−0.006 (−0.022, 0.011)	0.509	
≥39(Median)	-0.023(-0.035, -0.010)	<0.001		−0.031 (−0.051, −0.012)	0.001	

These models were adjusted for factors such as age, sex, body mass index, race, family income-to-poverty ratio, education, serum cotinine levels, physical activity, serum 25(OH)D, thyroid disease, hypertension, and diabetes.

was similarly not significant in the low-age group (P value = 0.509), whereas there was a significant negative correlation between urinary lead levels and lumbar bone density in the high-age group (P value = 0.001).

Furthermore, the overall bone P_{int} for age stratification was 0.034, and the lumbar bone density P_{int} was 0.045. These data suggest that the relationship between urinary lead levels and bone density may be significantly influenced by age, and in the high-age group, there is a stronger correlation between increasing urinary lead levels and decreasing bone density.

3.4 Joint effect analysis

Further evaluates the combined effects of lead and cadmium exposure on total bone density and lumbar spine bone density. The groups with low exposure levels to both metals were considered as the reference group. The odds ratios (OR) for total bone density in the low-cadmium high-lead exposure group, high-cadmium low-lead exposure group, and high-cadmium high-lead exposure group were 0.991 (0.976, 1.008), 1.002 (0.985, 1.020), and 0.984 (0.968, 1.001) respectively, with p-values of 0.337, 0.806, and 0.071. The odds ratios (OR) for lumbar spine bone density in the low-cadmium high-lead exposure group, high-cadmium low-lead exposure group, and high-cadmium high-lead exposure group were 0.989 (0.966, 1.014), 1.000 (0.975, 1.026), and 0.968 (0.945, 0.993) respectively, with p-values of 0.387, 0.999, and 0.012 (Table 4). Through the high-cadmium high-lead exposure group, it is demonstrated that the combined exposure to cadmium and lead has a negative impact on bone density, and this effect is statistically significant.

4 Discussion

In this study, we investigated the relationship between urinary lead exposure and bone density during the NHANES survey period from 2015 to 2018. Overall, our study results showed that urinary lead exposure was associated with reduced total bone density and lumbar spine bone density. In stratified analysis, it was also found that urinary lead levels were correlated with decreased bone density, and the relationship between urinary lead levels and bone density may be significantly influenced by age with no significant gender effect observed. The combined effect of lead and cadmium was found to be related to decreased bone density.

The results of this study showed a negative correlation between urinary lead exposure levels and bone density. To our knowledge, this is the largest epidemiological research report on lead exposure and bone density across a wide age range. Lead is highly toxic and lead poisoning can cause damage to the nervous system and brain function. There have been few studies on the impact of lead on bone health. A report from Sweden found no association between adult lead exposure and bone density (28). The potential mechanism by which elevated lead levels cause bone disease is not clear. *In vitro* studies have shown that lead can exchange calcium in hydroxyapatite crystals, with higher affinity for osteocalcin than calcium (20), and inhibit the activation of vitamin D and dietary calcium absorption (29). However, more investigations are needed to validate our research results and elucidate the specific mechanisms behind the reduction of bone density with lead exposure.

Plasma lead concentration is difficult to accurately measure because of its low concentration and susceptibility to contamination (30). Whole blood lead levels are usually used as a biological marker of lead exposure because over 99% of lead is bound to red blood cells. However, due to the saturation effect of lead-binding sites in red blood cells, male blood lead levels are higher than female levels, while urinary lead levels show no significant difference between genders (24). Urinary lead is considered an alternative indicator reflecting plasma lead levels, as lead is mainly filtered through the glomerulus and excreted in urine. To accurately reflect urinary lead excretion, adjustments for urine dilution need to be considered. This study used urinary lead as a biological marker of lead exposure.

One finding in our study is the non-linear negative correlation between urinary lead levels in adults and total bone density and lumbar bone density. We found a stronger association between increasing urinary lead levels and decreasing bone density in the older age group (≥39 years old). This differs from previous studies in adults (8), but the reasons are still unclear. It could be due to variations in hormone levels at different ages. Further research is needed to investigate the differences in bone remodeling, absorption, and formation capabilities in different bone sites under various levels of lead exposure and in different age groups.

TABLE 4 The impact of lead and cadmium combined exposure on BMDs.

Metals	N	Total BMD Percent change (95% CI)	P	Lumbar BMD Percent change (95% CI)	P
cadmium - lead					
Low Cd + low Pb	427	Reference		Reference	
Low Cd + high Pd	228	0.991(0.976,1.008)	0.337	0.989(0.966,1.014)	0.387
High Cd + low Pb	228	1.002(0.985,1.020)	0.806	1.000(0.975,1.026)	0.999
High Cd + high Pd	427	0.984(0.968,1.001)	0.071	0.968(0.945,0.993)	0.012

These models have been adjusted for factors such as age, gender, body mass index, race, family income to poverty ratio, education, serum cotinine levels, physical activity, serum 25(OH)D, thyroid disorders, hypertension, and diabetes.

We found that urinary lead concentration has different effects on bone density at different levels, and as urinary lead concentration increases, the decrease in bone density shows an initial rapid decline followed by a slower decline. The differences in lead's impact on bone density may be attributed to the complex mechanisms of lead metabolism in bone at different levels. Previous studies have found that long-term lead exposure at low levels (blood levels <10μg/dL) inhibits the Wnt signaling pathway and leads to decreased bone density in adult rats, while increased bone mass has been observed in mice exposed to high levels of lead, which inhibits the ability of osteoclasts to reabsorb bone mass (31). This may suggest the need for greater attention to the effects of lead exposure on bone health in older age groups.

In our study, there was a significant relationship between urinary lead levels and total bone density and lumbar bone density in females, while in males, the correlation tended to be negative but not significant. In gender-stratified analyses, the P interaction values were 0.241 for total bone density and 0.380 for lumbar bone density, indicating that gender does not significantly affect the relationship between urinary lead levels and bone density. The negative association between lead exposure levels and bone density in adult women is consistent with previous studies, which found an association between lead exposure and decreased bone density in premenopausal women (32). However, another study of 50-70-year-old women also found a non-significant correlation (33). Even at low levels, lead can affect follicles in mice (34), which are the primary source of endogenous estrogen. Due to the decrease in estrogen, women experience rapid bone loss in the first 5-10 years after menopause (35). Therefore, we speculate that lead exposure induces a decrease in bone density by suddenly lowering estrogen levels. No association between lead concentration and bone density was observed in postmenopausal women because their ovaries no longer produce endogenous estrogen. The lack of significant correlation in males may be due to the fact that males have higher peak bone mass than females in early adulthood.

In this study, the combined exposure of cadmium and lead has a negative impact on bone density, and this impact is statistically significant, emphasizing a potential synergistic effect of these two metals on bone density. The production of reactive oxygen species induced oxidative stress is an important mechanism of lead and cadmium toxicity, which may be crucial for bone metabolism (36). In the real world, humans are simultaneously exposed to multiple heavy metals, which interact with each other. Further research is needed to validate this finding and explore its potential mechanisms in the future.

The relationship between urinary lead exposure and bone density is intricate, encompassing interactions with bone metabolism, endocrine regulation, oxidative stress, and interplays with age, gender, and metabolic status. When evaluating bone density risk, a holistic consideration of multiple risk factors, including urinary lead levels, elements of metabolic syndrome (e.g., abdominal obesity, hypertension, glucose abnormalities), and demographic factors, is essential. The potential interplay between urinary lead exposure and components of metabolic syndrome deserves attention (37). For example, certain aspects of metabolic syndrome may influence the body's lead handling, affecting lead's absorption, distribution, and excretion, and thus altering the lead burden in the body, which can have implications for bone density. Concurrently, lead exposure could exacerbate metabolic syndrome risks through its impacts on metabolic functions, such as insulin resistance and lipid metabolism, indirectly affecting bone health (38).

This study has several key strengths. First, it reports an epidemiological study of the maximum range of age groups with a negative correlation between lead exposure and bone density. Additionally, objectively measured urinary lead levels were used as a biomarker reflecting lead status. Furthermore, this study also conducted stratified analyses, yielding more stable results. However, the study also has some limitations. First, our study is a cross-sectional study, and further longitudinal research is needed to investigate more accurate causal relationships. Second, potential residual confounding factors such as genetics, diet, and other environmental chemicals were not fully considered. Lastly, during the continuous physiological process of bone remodeling, nearly 10% of bone is rebuilt each year (39), which this study cannot reflect in long-term bone health.

Our study has unveiled a nonlinear negative correlation between urinary lead exposure and bone density, along with variations in this association across different age and gender groups. This finding holds significant implications for clinical practice and public health interventions. At the clinical level, healthcare professionals should recognize lead exposure as a potential risk factor for osteoporosis, particularly in older women. Public health strategies should encompass educating the public on measures to reduce lead exposure, such as abstaining from lead-containing products, ensuring the safety of drinking water, and enforcing stricter regulations on industrial emissions, all aimed at safeguarding public bone health.

Data availability statement

The original contributions presented in the study are included in the article/supplementary material. Further inquiries can be directed to the corresponding author.

Ethics statement

All NHANES protocols were approved by the NCHS Ethics Review Board. The studies were conducted in accordance with the local legislation and institutional requirements. Written informed consent for participation was not required from the participants or the participants' legal guardians/next of kin in accordance with the national legislation and institutional requirements.

Author contributions

SW: Writing – original draft. XZ: Writing – review & editing. RZ: Writing – review & editing. YJ: Writing – review & editing. XW: Writing – review & editing. XM: Writing – review & editing. XL: Writing – review & editing.

Funding

The author(s) declare financial support was received for the research, authorship, and/or publication of this article. The current research was funded by Shanxi Provincial Basic Research Program Plan Project (202203021221274).

Conflict of interest

The authors declare that the research was conducted in the absence of any commercial or financial relationships that could be construed as a potential conflict of interest.

Publisher's note

References

1. Hipps D, Dobson PF, Warren C, McDonald D, Fuller A, Filby A, et al. Detecting respiratory chain defects in osteoblasts from osteoarthritic patients using imaging mass cytometry. *Bone*. (2022) 158:116371. doi: 10.1016/j.bone.2022.116371

2. Medina-Gomez C, Kemp JP, Trajanoska K, Luan J, Chesi A, Ahluwalia TS, et al. Life-course genome-wide association study meta-analysis of total body BMD and assessment of age-specific effects. *Am J Hum Genet*. (2018) 102(1):88–102. doi: 10.1016/j.ajhg.2017.12.005

3. Hou R, Cole SA, Graff M, Haack K, Laston S, Comuzzie AG, et al. Genetic variants affecting bone mineral density and bone mineral content at multiple skeletal sites in Hispanic children. *Bone*. (2020) 132:115175. doi: 10.1016/j.bone.2019.115175

4. Lupsa BC, Insogna K. Bone health and osteoporosis. *Endocrinol Metab Clin North Am*. (2015) 44(3):517–30. doi: 10.1016/j.ecl.2015.05.002

5. Rizzoli R, Biver E, Brennan-Speranza TC. Nutritional intake and bone health. *Lancet Diabetes Endocrinol*. (2021) 9(9):606–21. doi: 10.1016/S2213-8587(21)00119-4

6. Gu L, Wang Z, Pan Y, Wang H, Sun L, Liu L, et al. Associations between mixed urinary phenols and parabens metabolites and bone mineral density: Four statistical models. *Chemosphere*. (2023) 311(Pt 2):137065. doi: 10.1016/j.chemosphere.2022.137065

7. Zhao X, Lin JY, Dong WW, Tang ML, Yan SG. Per- and polyfluoroalkyl substances exposure and bone mineral density in the U.S. population from NHANES 2005-2014. *J Expo Sci Environ Epidemiol*. (2023) 33(1):69–75. doi: 10.1038/s41370-022-00452-7

8. Wei MH, Cui Y, Zhou HL, Song WJ, Di DS, Zhang RY, et al. Associations of multiple metals with bone mineral density: A population-based study in US adults. *Chemosphere*. (2021) 282:131150. doi: 10.1016/j.chemosphere.2021.131150

9. Scimeca M, Feola M, Romano L, Rao C, Gasbarra E, Bonanno E, et al. Heavy metals accumulation affects bone microarchitecture in osteoporotic patients. *Environ Toxicol*. (2017) 32(4):1333–42. doi: 10.1002/tox.22327

10. Liu D, Shi Q, Liu C, Sun Q, Zeng X. Effects of endocrine-disrupting heavy metals on human health. *Toxics*. (2023) 11(4):322. doi: 10.3390/toxics11040322

11. Crocetto F, Risolo R, Colapietro R, Bellavita R, Barone B, Ballini A, et al. Heavy metal pollution and male fertility: an overview on adverse biological effects and socio-economic implications. *Endocr Metab Immune Disord Drug Targets*. (2023) 23(2):129–46. doi: 10.2174/1871530322666220627141651

12. Liu L, Zhang B, Lin K, Zhang Y, Xu X, Huo X. Thyroid disruption and reduced mental development in children from an informal e-waste recycling area: A mediation analysis. *Chemosphere*. (2018) 193:498–505. doi: 10.1016/j.chemosphere.2017.11.059

13. Zeng X, Xu C, Xu X, Zhang Y, Huang Y, Huo X. Elevated lead levels in relation to low serum neuropeptide Y and adverse behavioral effects in preschool children with e-waste exposure. *Chemosphere*. (2021) 269:129380. doi: 10.1016/j.chemosphere.2020.129380

14. Axelrad DA, Coffman E, Kirrane EF, Klemick H. The relationship between childhood blood lead levels below 5 μg/dL and childhood intelligence quotient (IQ): Protocol for a systematic review and meta-analysis. *Environ Int*. (2022) 169:107475. doi: 10.1016/j.envint.2022.107475

15. Santa Maria MP, Hill BD, Kline J. Lead (Pb) neurotoxicology and cognition. *Appl Neuropsychol Child*. (2019) 8(3):272–93. doi: 10.1080/21622965.2018.1428803

16. Zhang Y, Huo X, Lu X, Zeng Z, Faas MM, Xu X. Exposure to multiple heavy metals associate with aberrant immune homeostasis and inflammatory activation in preschool children. *Chemosphere*. (2020) 257:127257. doi: 10.1016/j.chemosphere.2020.127257

17. Pearce N, Blair A, Vineis P, Ahrens W, Andersen A, Anto JM, et al. IARC monographs: 40 years of evaluating carcinogenic hazards to humans. *Environ Health Perspect*. (2015) 123(6):507–14. doi: 10.1289/ehp.1409149

18. Li X, Li R, Yan J, Song Y, Huo J, Lan Z, et al. Co-exposure of cadmium and lead on bone health in a southwestern Chinese population aged 40-75 years. *J Appl Toxicol*. (2020) 40(3):352–62. doi: 10.1002/jat.3908

19. Liu XB, Gong ZL, Zhang Y, Zhang HD, Wang J, Tan HX, et al. A comparative study of blood lead levels in urban children in China: the China nutrition and health survey (CNHS) 2002 and 2012. *BioMed Environ Sci*. (2023) 36(4):376–80. doi: 10.3967/bes2023.044

20. Dowd TL, Rosen JF, Mints L, Gundberg CM. The effect of Pb(2+) on the structure and hydroxyapatite binding properties of osteocalcin. *Biochim Biophys Acta*. (2001) 1535(2):153–63. doi: 10.1016/s0925-4439(00)00094-6

21. Ronis MJ, Aronson J, Gao GG, Hogue W, Skinner RA, Badger TM, et al. Skeletal effects of developmental lead exposure in rats. *Toxicol Sci*. (2001) 62(2):321–9. doi: 10.1093/toxsci/62.2.321

22. Campbell JR, Auinger P. The association between blood lead levels and osteoporosis among adults–results from the third national health and nutrition examination survey (NHANES III). *Environ Health Perspect*. (2007) 115(7):1018–22. doi: 10.1289/ehp.9716

23. Tsai TL, Pan WH, Chung YT, Wu TN, Tseng YC, Liou SH, et al. Association between urinary lead and bone health in a general population from Taiwan. *J Expo Sci Environ Epidemiol*. (2016) 26(5):481–7. doi: 10.1038/jes.2015.30

24. Wang WJ, Wu CC, Jung WT, Lin CY. The associations among lead exposure, bone mineral density, and FRAX score: NHANES, 2013 to 2014. *Bone*. (2019) 128:115045. doi: 10.1016/j.bone.2019.115045

25. Lu J, Lan J, Li X, Zhu Z. Blood lead and cadmium levels are negatively associated with bone mineral density in young female adults. *Arch Public Health*. (2021) 79 (1):116. doi: 10.1186/s13690-021-00636-x

26. Li T, Xie Y, Wang L, Huang G, Cheng Y, Hou D, et al. The association between lead exposure and bone mineral density in childhood and adolescence: results from NHANES 1999-2006 and 2011-2018. *Nutrients*. (2022) 14(7):1523. doi: 10.3390/nu14071523

27. Tang P, Liao Q, Huang H, Chen Q, Liang J, Tang Y, et al. Effects of urinary barium exposure on bone mineral density in general population. *Environ Sci pollut Res Int*. (2023) 30(48):106038–46. doi: 10.1007/s11356-023-29791-0

28. Alfvén T, Järup L, Elinder CG. Cadmium and lead in blood in relation to low bone mineral density and tubular proteinuria. *Environ Health Perspect*. (2002) 110 (7):699–702. doi: 10.1289/ehp.110-1240916

29. Silbergeld EK, Schwartz J, Mahaffey K. Lead and osteoporosis: mobilization of lead from bone in postmenopausal women. *Environ Res*. (1988) 47(1):79–94. doi: 10.1016/s0013-9351(88)80023-9

30. Tsaih SW, Schwartz J, Lee ML, Amarasiriwardena C, Aro A, Sparrow D, et al. The independent contribution of bone and erythrocyte lead to urinary lead among middle-aged and elderly men: the normative aging study. *Environ Health Perspect*. (1999) 107(5):391–6. doi: 10.1289/ehp.99107391

31. Beier EE, Holz JD, Sheu TJ, Puzas JE. Elevated lifetime lead exposure impedes osteoclast activity and produces an increase in bone mass in adolescent mice. *Toxicol Sci*. (2016) 149(2):277–88. doi: 10.1093/toxsci/kfv234

32. Lim HS, Lee HH, Kim TH, Lee BR. Relationship between heavy metal exposure and bone mineral density in korean adult. *J Bone Metab*. (2016) 23(4):223–31. doi: 10.11005/jbm.2016.23.4.223

33. Theppeang K, Glass TA, Bandeen-Roche K, Todd AC, Rohde CA, Links JM, et al. Associations of bone mineral density and lead levels in blood, tibia, and patella in urban-dwelling women. *Environ Health Perspect*. (2008) 116(6):784–90. doi: 10.1289/ehp.10977

34. Junaid M, Chowdhuri DK, Narayan R, Shanker R, Saxena DK. Lead-induced changes in ovarian follicular development and maturation in mice. *J Toxicol Environ Health*. (1997) 50(1):31–40. doi: 10.1080/009841097160582

35. Wang X, Ding N, Harlow SD, Randolph JF, Mukherjee B, Gold EB, et al. Exposure to heavy metals and hormone levels in midlife women: The Study of Women's Health Across the Nation (SWAN). *Environ pollut*. (2023) 317:120740. doi: 10.1016/j.envpol.2022.120740

36. Lopes ACBA, Peixe TS, Mesas AE, Paoliello MMB. Lead exposure and oxidative stress: A systematic review. *Rev Environ Contam Toxicol*. (2016) 236:193–238. doi: 10.1007/978-3-319-20013-2_3

37. Rendina D, D'Elia L, Evangelista M, De Filippo G, Giaquinto A, Abate V, et al. Metabolic syndrome is associated to an increased risk of low bone mineral density in free-living women with suspected osteoporosis. *J Endocrinol Invest*. (2021) 44(6):1321–6. doi: 10.1007/s40618-020-01428-w

38. Rendina D, D'Elia L, De Filippo G, Abate V, Evangelista M, Giaquinto A, et al. Metabolic syndrome is not associated to an increased risk of low bone mineral density in men at risk for osteoporosis. *J Endocrinol Invest*. (2022) 45(2):309–15. doi: 10.1007/s40618-021-01638-w

39. Hendrickx G, Boudin E, Van Hul W. A look behind the scenes: the risk and pathogenesis of primary osteoporosis. *Nat Rev Rheumatol*. (2015) 11(8):462–74. doi: 10.1038/nrrheum.2015.48

frontiers | Frontiers in Endocrinology

TYPE Original Research
PUBLISHED 29 October 2024
DOI 10.3389/fendo.2024.1436203

OPEN ACCESS

EDITED BY
Sandeep Kumar,
University of Alabama at Birmingham, United States

REVIEWED BY
Surbhi Gahlot,
University of Texas Southwestern Medical Center, United States
Amit Kumar Madeshiya,
The University of Texas Health Science Center at San Antonio, United States

*CORRESPONDENCE
Daguang Zhang
zhangdg@jlu.edu.cn
Qiushi Wei
weiqshi@126.com

†These authors have contributed equally to this work and share last authorship

RECEIVED 21 May 2024
ACCEPTED 26 September 2024
PUBLISHED 29 October 2024

CITATION
Yang D, Li Z, Jiang Z, Mei X, Zhang D and Wei Q (2024) Causal relationship between sarcopenia and rotator cuff tears: a Mendelian randomization study. *Front. Endocrinol.* 15:1436203. doi: 10.3389/fendo.2024.1436203

Causal relationship between sarcopenia and rotator cuff tears: a Mendelian randomization study

Dongmei Yang[1,2], Zheng Li[1], Ziqing Jiang[3], Xianzhong Mei[1], Daguang Zhang[4*†] and Qiushi Wei[5,6*†]

[1]Department of Orthopedics, Shenzhen Pingle Orthopedics Hospital(Pingshan District Hospital of Traditional Chinese Medicine, Shenzhen, Guangdong, China, [2]The Third Clinical Medical College, Guangzhou University of Chinese Medicine, Guangzhou, Guangdong, China, [3]School of Traditional Chinese Medicine, Southern Medical University, Guangzhou, Guangdong, China, [4]Department of Orthopedics, The First Bethune Hospital of Jilin University, Changchun, Jilin, China, [5]Traumatology & Orthopaedics Institute, Guangzhou University of Chinese Medicine, Guangzhou, Guangdong, China, [6]Department of Orthopedics, The Third Affiliated Hospital, Guangzhou University of Traditional Chinese Medicine, Guangzhou, Guangdong, China

Background: Sarcopenia and rotator cuff tears are common among elderly patients. However, the role of sarcopenia in the management of rotator cuff tears has been often overlooked. This study aimed to elucidate the effects of sarcopenia-related traits on rotator cuff tears.

Methods: Two-sample Mendelian randomization (MR) analyses based on genome-wide association study data were used to evaluate the causal relationships among appendicular lean mass (ALM), usual walking pace, low hand grip strength, and rotator cuff tears. Multivariate Mendelian randomization (MVMR) analyses were used to evaluate the direct effects of each muscle trait on the causal relationship.

Results: Univariate MR analysis showed that ALM and usual walking pace were causally related to rotator cuff tears (odds ratio (OR) = 0.895; 95% confidence interval (CI), 0.758-0.966, P<0.001 and OR = 0.458, 95% CI, 0.276-0.762, P = 0.003, respectively), and there was no evidence of causality between low hand grip strength and rotator cuff tears (OR = 1.132, 95% CI, 0.913-1.404, P = 0.26). MVMR analysis confirmed the causal effects of ALM and walking pace on rotator cuff tears (OR = 0.918, 95% CI, 0.851-0.990, P = 0.03 and OR = 0.476, 95% CI, 0.304-0.746, P = 0.001, respectively).

Conclusion: A causal genetic relationship exists between sarcopenia and rotator cuff tears. Sarcopenia-related traits including low muscle mass and physical function, increase the risk of rotator cuff tears. These findings provide new clinical insights and evidence-based medicine to optimize management of rotator cuff tears.

KEYWORDS

causal relationship, rotator cuff tears, sarcopenia, genetic epidemiology, skeletal muscle disease

1 Introduction

The rotator cuff is an important dynamic anatomical complex that maintains shoulder stability and provides precise spatial positional control to achieve shoulder torque balance. Therefore, it is prone to injury during daily activities and upper limb movements, resulting in varying degrees of pain and functional impairment, which seriously affect patients' quality of life. Rotator cuff tears account for 13–41% of shoulder disorders (1, 2) and have a linear correlation with ageing, with a morbidity rate of 13% in people aged >50 years and 20% for those aged >60 years (3, 4). With an increasingly ageing population worldwide, rotator cuff diseases have become a progressively serious social health problem with enormous medical expenses (5). Early identification of related risk factors and timely interventions have an important clinical value for the management of rotator cuff tears. Previous studies have shown that the occurrence of rotator cuff disease is accompanied by tendon cell atrophy and fat infiltration, with some genetic susceptibility (6).

Sarcopenia is a geriatric syndrome characterized by age-related loss of skeletal muscle mass, muscle strength, or physical function (7). It is estimated that approximately 50 million people worldwide suffer from this condition, with a prevalence rate of 10–27% in patients aged >60 years (8). With the increasing global aging population, the number of sarcopenia cases is expected to reach 500 million by 2050 (9). The European Working Group on Sarcopenia in Older People 2(EWGSOP2) has identified muscle strength, muscle mass, and physical function as the main criteria for diagnosing sarcopenia (10). Despite being formally incorporated into the World Health Organization's International Classification of Diseases (ICD) in 2016, sarcopenia may be underdiagnosed due to its insidious onset (11).

Sarcopenia increases the risk of falls, fractures, motor dysfunction, physical disability, and mortality. An observational study (12) showed no significant difference in the incidence of sarcopenia between the rotator cuff tears and normal control groups, indicating that sarcopenia cannot be used as a risk factor for rotator cuff tears. However, Kara et al. (13) obtained the opposite results and found that probable sarcopenia was a risk prediction factor for rotator cuff tears, which occurred in 18.6% of 1448 postmenopausal women. A relevant animal study has confirmed a correlation between sarcopenia and rotator cuff tears, which can occur before the onset of rotator cuff disease (14). However, due to the lack of consistency in the conclusions of existing studies, the causal relationship between sarcopenia and rotator cuff diseases is not clear. At the same time, based on case-control and cross-sectional observational studies, and considering the limitations of small sample size and insufficient follow-up, more powerful research designs are needed to further verify the causal relationship between sarcopenia and rotator cuff tears (15).

Mendelian randomization (MR) is a genetic analysis method (16) that uses single nucleotide polymorphisms (SNPs) as instrumental variables (IVs) to evaluate the causal relationships between exposure to relevant phenotypic characteristics and outcome factors. Due to the random allocation of individual genes at conception, resulting in the inheritance of a trait being independent of other traits and exhibiting randomness. Therefore, it is unlikely for the genotype of offspring to be influenced by lifestyle or environmental confounders (17). In comparison to observational studies, MR can more effectively mitigate confounding variables and reverse causality (18). With advancements in biological genetics, genome-wide association studies (GWAS) utilizing large sample sizes have identified multiple gene loci represented by SNPs that are closely associated with sarcopenia-related muscle characteristics, providing a valuable basis for causal investigation (19).

As a recently proposed disease concept, it is challenging to locate GWAS summary data for sarcopenia. According to the EWGSOP2 consensus, low muscle mass and strength (specifically grip strength and physical function) serve as primary indicators for measuring sarcopenia. Therefore, we have selected appendicular lean mass (ALM), low grip strength, and walking speed as exposure phenotypes (19). Utilizing validated SNPs and publicly available GWAS datasets, MR analysis was employed to investigate the causal relationship between traits related to sarcopenia and the development of rotator cuff tears. This study aims to provide clinical evidence-based support for managing sarcopenia in individuals with rotator cuff tears.

2 Materials and methods

2.1 Study design

MR requires three major assumptions (17): association, independence, and exclusion restriction, meaning that the SNPs used as IVs should have a robust association with the exposure factor and be independent of confounding factors, and that the outcome factor can only be influenced by the exposure factor. Multivariate MR (MVMR) analysis was used to evaluate the direct effects of various muscle characteristics on the causal relationship (20). The study flowchart is shown in Figure 1.

2.2 Data sources

To ensure the rigor and validity of the findings, we adhered to the following criteria in selecting the sarcopenia and rotator cuff tear datasets. Firstly, we selected the datasets covering disease phenotypes. Secondly, we screened statistics datasets from large-scale genetic biobanks and public summary data to ensure data undergo rigorous quality control and collation. Thirdly, we utilized the most up-to-date datasets to maintain the cutting-edge nature of our research. At the same time, datasets with a large sample size were preferable chosen to ensure the power of the statistical analysis and to reduce the potential for weak instrument bias.

All exposure and outcome genetic tools were obtained from different public gene datasets. The relevant characteristics of sarcopenia were obtained from the public gene database 'IEU

10.3389/fendo.2024.1436203

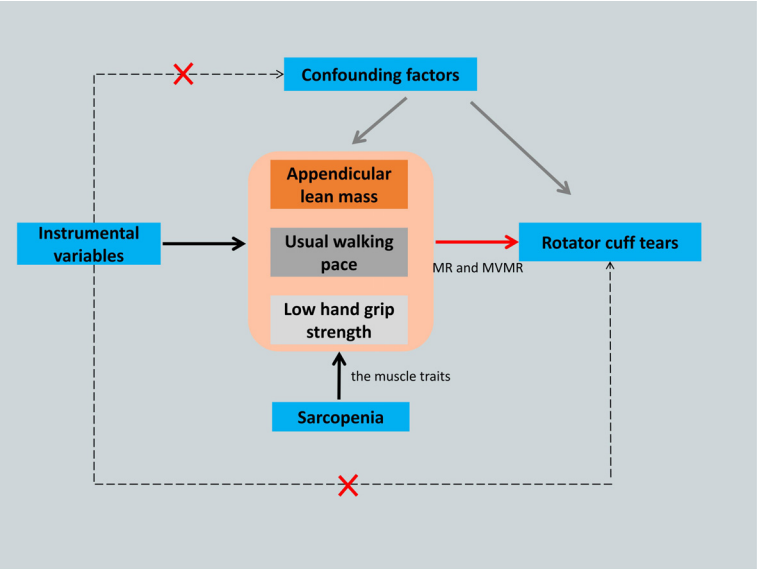

FIGURE 1
The framework flowchart of the Mendelian randomization study. Dotted arrow: Instrumental variables are not associated with any known or unknown confounding factors and influence rotator cuff tears not through any direct causal pathway. Black arrow: Instrumental variables reliably associated with the sarcopenia- related traits. Red arrow: Instrumental variables affect the rotator cuff tears only through appendicular lean mass, usual walking pace and low hand grip strength by using Mendelian randomization and Multivariate Mendelian randomization. MR, Mendelian randomization; MVMR, Multivariate Mendelian randomization.

GWAS' (https://gwas.mrcieu.ac.uk/datasets/), while the data on rotator cuff tears were obtained from the FinnGen database (https://www.finngen.fi). Detailed information for obtaining the exposure and outcome factors from GWAS is listed in Table 1. All data used were open to the public and did not require separate ethical reviews or informed consent.

Low skeletal muscle mass and strength (hand grip strength and physical function) are the primary indicators of sarcopenia, code ICD-10(M62.84) (11). The GWAS data for ALM were obtained from a pooled dataset of 450 243 participants aged 48-73 years (21). ALM was measured using bioelectrical impedance analysis. The low hand grip strength GWAS data were obtained from a pooled dataset of 256 523 participants (48 596 with low grip strength and 207 927 with normal grip strength) aged ≥60 years from the EWGSOP alliance (22). The maximum grip strength was recorded in kg, and low grip strength was defined as a grip strength of <30 kg in males and <20 kg in females. The GWAS data for walking speeds were obtained from the UK Biobank and included 459 915 participants of European ancestry with walking speed classified into three levels: slow, steady, or brisk (23).

We obtained summary data on SNPs related to rotator cuff tears as outcome factors from the FinnGen consortium database (26 376 cases and 299 606 non-cases), code ICD-10(M75.1). The FinnGen study is a large-scale genomics initiative that has analyzed over 500,000 Finnish biobank samples and correlated genetic variation with health data to understand disease mechanisms and predispositions (24). The FinnGen data used in this study were obtained from the whole-genome analysis results released in FinnGen R10, with participants having an average age of 55.57 years and an observation period spanning 1985 to 2022. Individuals with unclear sex and high missing/heterozygosity rates (>5%) were also excluded. To avoid population-specific bias, all participants were of European ancestry.

TABLE 1 Data sources and description.

Phenotype	Consortium	Participants	Ancestry	GWAS ID	Year of publication
ALM*	UKB	450 243	European	ebi-a-GCST90000025	2020
Low hand grip strength	EWGSOP	48 596 cases and 207 927 controls	European	ebi-a-GCST90007526	2021
Usual walking pace	UKB	459 915	European	ukb-b-4711	2018
Rotator cuff tears	Finngen	26 376 cases and 299 606 controls	European	finn-b-M13_ROTATORCUFF	2023

*ALM, Appendicular lean mass.

2.3 IV selection

To ensure the robustness and replicability of MR results, we selected SNPs that were significantly associated with the exposure factor from the pooled GWAS data as IVs ($P < 5\times10^{-8}$). Removal of linkage disequilibrium (LD) reduced the non-random bias of IVs, and strict criteria were used to evaluate the independence of the SNPs (r^2, 0.001; clump, 10 000kb) in order to select independent SNPs as IVs (25). The F-values of the selected IVs were calculated through univariate regression analysis for each IV and exposure phenotype (sarcopenia-related traits). The formula of calculating the IV's F-statistic is as follows. IVs with an F-value ≤ 10 were eliminated to ensure sufficient explanatory power, thereby reducing the risk of weak instrumental variable bias (26).

$$R2 = 2^{*}(1 - MAF)^{*}MAF^{*}\beta 2,$$

$$2F = (N - \kappa - 1/\kappa)^{*}(R2/1 - R2)$$

2.4 Data analysis

All MR data analyses were conducted using the 'TwoSampleMR' (v.0.5.7), 'MendelianRandomization (27) (v.0.9.0), 'MRPRESSO' (v.1.0), 'MVMR (28)' (v.0.4), and 'forestplot' (v.3.1.3) packages in R software (version 4.3.1; R Foundation for Statistical Computing, Vienna, Austria).

In MR, the inverse-variance weighted (IVW) method is the main statistical analysis and can merge the Wald ratio estimates for each IV in the causal estimate (29). Both MR-Egger regression and the weighted median estimator (WME) were utilized for sensitivity analysis, to verify the reliability of the results (30, 31). The advantage of the weighted median method is that it can provide effective results, even if the number of effective IVs is reduced by at least half during the analysis. MR-Egger regression has the advantage of providing an effective causal effect evaluation, even when all SNPs are ineffective. We considered the consistent direction of the results from these three methods to indicate a relatively stable causal association. We used a forest plot to visualize the causal effect values of each IV and of the overall exposure on the outcome effect size.

We used the Cochran's Q test to evaluate heterogeneity; $P < 0.05$ indicated the presence of heterogeneity, and the IVW random-effects model was applied (32). Conversely, $P > 0.05$ indicated no heterogeneity, and the IVW fixed-effects model was used. Funnel plots were used to visualize the results.

We used the MR-Egger regression intercept to conduct pleiotropy testing, ensuring that the selected IVs did not affect the outcomes through confounding factors (33). $P > 0.05$ for the intercept indicated the absence of horizontal pleiotropy, while $P<0.05$ indicated that the causal relationship between the exposure and outcome did not hold. The MR pleiotropy residual sum and outlier (MR-PRESSO) test was used to detect outliers and correct the pleiotropy. Outliers were removed, and the remaining gene IVs were reanalyzed (34). We conducted a leave-one-out analysis of each SNP by gradually removing IVs to observe their direct impact on the results. We also used a function to graphically visualize the results.

Univariate MR was used to evaluate the "total effect" of sarcopenia-related traits on the causal relationship of rotator cuff tears. Then, the MVMR evaluated the "direct effect" of each trait on rotator cuff tears. $P<0.05$ indicated a statistically significant difference (20).

3 Results

3.1 IVs

Based on the selection criteria for IVs, we selected 690 SNPs with genome-wide significance as IVs for ALM, 16 for low hand grip strength, and 57 for usual walking pace. After removing palindromic sequences in the MR analysis, 536 SNPs were finally included for ALM, 14 for low hand grip strength, and 50 for usual walking pace. All F-values of the instrumental variables for the evaluation indicators of sarcopenia were >10, indicating that all three sets of IVs were strong indicators. The results are shown in Supplementary Tables 1-3.

3.2 MR analysis

MR analysis based on the IVW method showed that genetically determined sarcopenia-related traits were causally associated with rotator cuff tears, as demonstrated in Figure 2. Scatter plots (Figure 3) were used to visualize the causal effect. ALM and usual walking pace were significantly associated with rotator cuff tears (odds ratio (OR) = 0.895, 95% confidence interval (CI), 0.758-0.966, $P<0.001$ and OR = 0.458, 95% CI, 0.276-0.762, $P = 0.003$, respectively), while there was no evidence to support a relationship between low hand grip strength and rotator cuff tears (OR = 1.132, 95% CI, 0.913-1.404, $P = 0.26$).

In the analysis of WME and MR-Egger, the beta value of sarcopenia muscle traits and rotator cuff tear was consistent with the IVW results. Moreover, the MR-Egger intercept term test of each trait was P>0.05, there was no horizontal pleiotropy, and the results were reliable (Supplementary Table 4).

Cochran's Q heterogeneity test showed the presence of heterogeneity among the sarcopenia-related traits, which may be influenced by differences in the sample population or sequencing methods. Nevertheless, the results of the random-effects IVW method were reliable. The funnel plot exhibits a symmetric distribution (Supplementary Figure 1). Using the MR-PRESSO method, we found one outlier for ALM and low hand grip strength and two outliers for usual walking pace. After removing potential outliers, the random-effects IVW method remained stable (Supplementary Table 4).

The leave-one-out method was used to explore whether each SNP had a significant impact on the final result. Removing each SNP demonstrated that SNPs that did not introduce excessive bias to the results (Supplementary Figure 2).

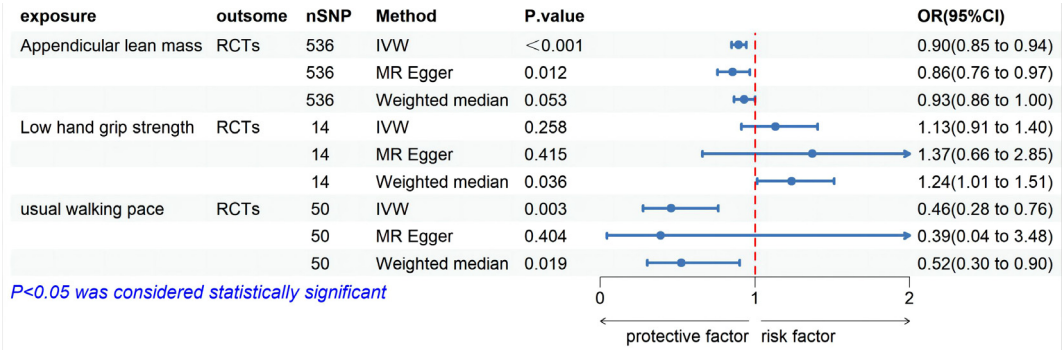

FIGURE 2
Forest plot of MR analysis estimates for the association between sarcopenia-related muscle traits and rotator cuff tears. OR, odds ratio; 95%CI, 95% confidence interval; IVW, inverse variance weighted random; RCTs, rotator cuff tears.

In the MVMR analysis, genetic predictions of skeletal muscle mass and gait speed were found to have a causal effect on rotator cuff tears after excluding the influence of other exposure factors (OR = 0.918, 95% CI, 0.851-0.990, P = 0.03 and OR = 0.476, 95% CI, 0.304-0.746, P = 0.001, respectively) (Figure 2). However, the direct causal effect of the adjusted ALM on rotator cuff tears was reduced. Moreover, horizontal pleiotropy was not found in the multivariate analysis results (P = 0.10), which was consistent with the univariate analysis results (Table 2).

4 Discussion

Research on the genetic causal association between sarcopenia and rotator cuff tears is lacking. In this study, we used MR analysis to analyze GWAS data, including single and joint effects, and found a causal relationship between sarcopenia and rotator cuff tears. The results showed that ALM and usual walking pace had a negative linear correlation with rotator cuff tears, which were protective factors for the latter. However, no evidence supported a genetic causal relationship between muscle strength and rotator cuff tears.

As a newly recognized muscle disease, sarcopenia was proposed in 2010. Initially, only skeletal muscle mass was used as the sole diagnostic criterion due to the lack of specific manifestations. With further clinical exploration, research on the correlation between sarcopenia and other musculoskeletal diseases has become more comprehensive. Han et al. (35) discovered that patients with sarcopenia exhibited a higher prevalence of shoulder pain, mucoid degeneration, and disordered muscle bundles in the supraspinatus tendon through musculoskeletal ultrasound comparison. Histopathological examination demonstrated varying degrees of fat infiltration and loss of muscle fibers, resulting in secondary strength loss and limb dysfunction (36). Chung et al. (37) compared the prevalence of sarcopenia between patients with rotator cuff injury and healthy individuals; they found that those with injuries had a higher likelihood of low muscle mass and strength which correlated with tendon tear size. The present study's findings align with those results, suggesting a causal association between sarcopenia and rotator cuff tears where low muscle mass or physical function increases susceptibility to such injuries. Surprisingly though, this study did not establish a causal relationship between low grip strength and rotator cuff injuries. A prospective study examining grip strength before and after rotator cuff repair reached similar conclusions (38). Their founding indicated that grip strength was not related to shoulder dysfunction.

As key regulators of muscle homeostasis, fibro-adipogenic progenitors (FAPs) are widely distributed in skeletal muscle and tendinous tissues with bipotency (39). They play a crucial role in

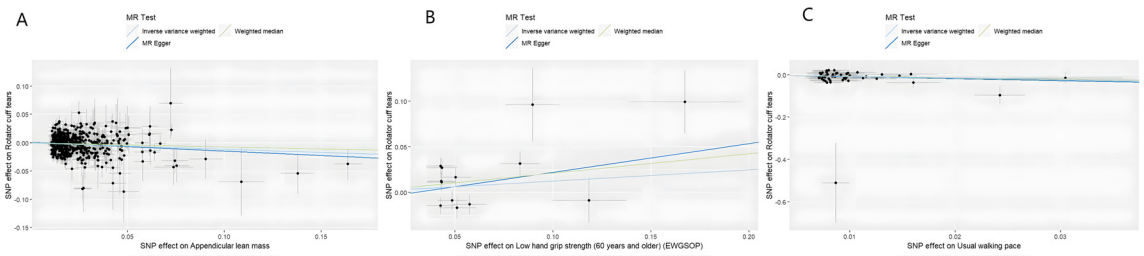

FIGURE 3
Scatter plots of univariate MR analysis. The horizontal coordinate is the effect of SNP on exposure, and the vertical coordinate is the effect of SNP on outcome. The horizontal and vertical lines on the dots are the confidence intervals of SNP for exposure effect and SNP for outcome effect, respectively. The colored lines correspond to the output of the MR analytical methods. **(A)** The causal association appendicular lean mass on rotator cuff tears. **(B)** The causal association of low hand grip strength on rotator cuff tears. **(C)** The causal association of usual walking pace on rotator cuff tears.

TABLE 2 Causal effects of sarcopenia-related traits on rotator cuff tears using MVMR[#].

Exposure	nSNP[||]	MVMR Methods	beta	se**	P value	OR[†](95%CI)[† †]	MR Egger p-intercept
ALM*	497	MVMR IVW[##]	-0.085	0.038	0.03	0.92 (0.85-0.99)	
	497	MVMR MR-Egger	-0.177	0.068	0.01	0.84 (0.73-0.96)	0.104
Low hand grip strength	497	MVMR IVW[##]	-0.029	0.056	0.61	0.97 (0.87-1.08)	
	497	MVMR MR-Egger	-0.037	0.057	0.51	0.96 (0.86-1.08)	0.104
Usual walking pace	497	MVMR IVW[##]	-0.743	0.229	0.001	0.48 (0.3-0.75)	
	497	MVMR MR-Egger	-0.805	0.232	0.001	0.45 (0.28-0.7)	0.104

[#]MVMR, Multivariate Mendelian randomization; || SNP, single nucleotide polymorphisms; **SE, standard error; [†]OR, odds ratio; [† †]95%CI, 95% confidence interval; *ALM, Appendicular lean mass; [##]IVW, inverse-variance weighted random.

promoting the proliferation and differentiation of satellite cells, which are specific muscle stem cells, thereby enhancing skeletal muscle regeneration capacity and compensating for muscle fiber atrophy and functional decline (40). Additionally, FAPs exhibit inherent adipogenic and fibrogenic potential, leading to pathological aggregation. The expression of fibrogenic/adipogenic markers in FAPs was significantly elevated in the massive rotator cuff tear group, indicating an irreversible trend. Low muscle mass serves as the initial factor contributing to sarcopenia, characterized by varying degrees of fat infiltration and loss of type II muscle fibers (41). Studies have confirmed that mitochondrial dysfunction and immune response can induce skeletal muscle mass loss and disrupt muscular homeostasis. Mitochondria function as cellular energy communicators, regulating intracellular calcium concentration and cell proliferation, thereby playing a crucial role in muscle health, function, and homeostasis (42). In chronic muscle injury diseases, mitochondria can activate nuclear factor kappa B to trigger the NLRP3 inflammasome, which leads to the expression of tumor necrosis factor-α, interleukin (IL)-1β, and other inflammatory factors. This process enhances both local and systemic inflammatory responses and immune reactions while promoting ectopic fat accumulation (43). Consequently, it results in a decline in muscle function. IL-1β induces fibroblast activation along with the extracellular matrix of tendinous tissue. This chronic inflammatory response causes structural changes and disarrangement in tendons. Moreover, IL-1β interferes with the proliferation and adipogenic differentiation of FAPs (44). In addition to the effects of inflammatory factors on myofibers, mechanical stimulation also influences the number of FAPs. Exercise training has been shown to reduce muscle fiber loss (45).

Sarcopenia and rotator cuff tears are prevalent conditions among the elderly population. By investigating the causal association between sarcopenia and rotator cuff tears, have shown that sarcopenia-related muscle characteristics increasing the risk of rotator cuff tears. This study emphasizes the public health significance of restoring skeletal muscle mass and physical function in the prevention and acceleration of rehabilitation after rotator cuff tears. The functional repair of tendon and tendon-bone interface healing poses significant challenges in the treatment of rotator cuff tears. Although surgical or nonsurgical treatments (such as physical therapy and local or systemic pharmacotherapy) can restore normal anatomy and alleviate symptoms (46), 20%-25% of patients still experience tendon nonunion or progressive muscle atrophy, which significantly impacts their quality of life (47). Currently, there are numerous drug studies on sarcopenia; however, direct evidence supporting clinical efficacy and safety is lacking (48, 49). The primary treatment involves nutritional support combined with exercise intervention. For instance, elderly patients treated with whey protein supplements along with leucine and vitamin D have shown improvements in physical function (50). In addition to nutritional support, moderate intensity resistance exercise has been found to effectively enhance body composition and physical function (51). Relevant studies have also demonstrated that progressive resistance exercise or trunk block chain training for patients with rotator cuff tears can better alleviate pain caused by non-traumatic rotator cuff tears while influencing clinical outcomes positively (52, 53). However, no systematic study has reported on the effect of nutritional support on rotator cuff tears.

To our knowledge, this is the first MR study to investigate the association between sarcopenia and the risk of rotator cuff tears. Compared with the traditional observational studies, it has the advantages of reducing the risk of residual confounding and artificial bias. Our study highlights the predictive role of sarcopenia in the risk of rotator cuff tears and provides further insights and research directions to improve clinical recovery rates and optimize clinical disease management for rotator cuff tears. In addition, through sensitivity analysis and causal estimation, this study eliminated the biological effects of related risk factors such as lifestyle, age, and comorbidities on rotator cuff tears, verifying the robustness of the results. In the future, further exploration of the pathophysiological mechanisms involving bone, tendon-bone interface, and muscle tissue associated with sarcopenia and rotator cuff tears can be conducted, along with exploring therapeutic strategies for rotator cuff tears at a cellular or molecular level from the perspective of restoring skeletal muscle homeostasis. Additionally, increasing research on the combined intervention effects of exercise and nutritional support on outcomes of rotator cuff tear is warranted.

However, this study had some limitations. First, despite employing multiple analyses to ensure the robustness of the results, there may still exist unknown or unmeasured environmental and biological factors associated with sarcopenia

or rotator cuff tears that could introduce confounding bias, such as exercise habits, external trauma factors and occupational exposure. Second, due to the utilization of the public gene datasets with the lack of sex- or age-stratified in this study, thereby failing to account for sex or age differences in the causal association between exposure and outcome. Nevertheless, as more GWAS studies are conducted with larger sample sizes, it becomes feasible to perform subgroup analyses based on age or sex. Third, The data of all associated exposure SNPs in the resulting GWAS were exclusively collected from European populations, thereby limiting their applicability in explaining the causal association of disease in Asian or other ethnic populations. Consequently, the causal association between sarcopenia and rotator cuff injury remains unknown in these non-European populations. Furthermore, selection bias may occur if those with a higher genetic liability to rotator cuff tears and a specific trait (e.g., higher upper extremity movements or the porter of physical activity) are more likely to participate in the study. This could induce an association between genetic liability for rotator cuff tears and the traits in our study. Finally, MR estimates lifelong rather than acute effects. Compared to short-term exposure, lifelong exposure usually has a greater impact on outcomes. This is because most exposures have a cumulative effect on the outcome over time; therefore, they cannot be extrapolated to study potential therapeutic effects in clinical settings. Our understanding of this topic remains limited, particularly regarding the age-related differences in disease development.

5 Conclusion

This MR study provides evidence of a genetic causal relationship between sarcopenia and rotator cuff tears. The evidence supports a negative correlation between ALM, usual walking pace, and the occurrence of rotator cuff tears. This confirms that sarcopenia-related muscle characteristics, including low skeletal muscle mass and physical function, may increase the risk of rotator cuff tears. However, no association was found between genetically predicted low hand grip strength and rotator cuff tears.

Data availability statement

The datasets presented in this study can be found in online repositories. The names of the repository/repositories and accession number(s) can be found below: https://gwas.mrcieu.ac.uk/datasets/ebi-a-GCST90000025/, ebi-a-GSCT90000025 https://ftp.ebi.ac.uk/pub/databases/gwas/summary_statistics/GCST90007001-GCST90008000/GCST90007526/, ebi-a-GCST90007526 https://gwas.mrcieu.ac.uk/datasets/ukb-4711/, Ukb-b-4711; https://r10.finngen.fi/pheno/M13_ROTATORCUFF, finn-b-M13_ROTATORCUFF.

Author contributions

DY: Writing – original draft, Funding acquisition, Formal Analysis, Conceptualization. ZL: Writing – original draft, Supervision, Resources, Methodology, Funding acquisition. ZJ: Writing – original draft, Software, Methodology, Formal Analysis, Data curation, Conceptualization. XM: Writing – original draft, Visualization, Validation, Software. DZ: Writing – review & editing, Supervision. QW: Writing – review & editing, Project administration.

Funding

The author(s) declare that financial support was received for the research, authorship, and/or publication of this article. This work was financially supported by the Scientific Research Project of Health System in Pingshan District of Shenzhen (202103) and the foundation of School Management Project of Fujian University of Traditional Chinese Medicine (XB2023222).

Acknowledgments

We want to acknowledge the participants and investigators of the FinnGen study and we would like to acknowledge all the study and databases that made GWAS summary data available.

Conflict of interest

The authors declare that the research was conducted in the absence of any commercial or financial relationships that could be construed as a potential conflict of interest.

Publisher's note

Supplementary material

The Supplementary Material for this article can be found online at: https://www.frontiersin.org/articles/10.3389/fendo.2024.1436203/full#supplementary-material

References

1. Patel S, Gualtieri AP, Lu HH, Levine WN. Advances in biologic augmentation for rotator cuff repair. *Ann N Y Acad Sci*. (2016) 1383:97–114. doi: 10.1111/nyas.13267

2. Jeong JJ, Park SE, Ji JH, Lee HH, Jung SH, Choi BS. Trans-tendon suture bridge rotator cuff repair with tenotomized pathologic biceps tendon augmentation in high-grade PASTA lesions. *Arch Orthop Trauma Surg*. (2020) 140:67–76. doi: 10.1007/s00402-019-03285-6

3. American Academy of Orthopedic Surgeons. Management of rotator cuff injuries clinical practice guideline [A/OL] (2019). Available online at: https://www.aaos.org/rotatorcuffinjuriescpg.

4. Viswanath A, Monga P. Trends in rotator cuff surgery: Research through the decades. *J Clin Orthop Trauma*. (2021) 19:105–13. doi: 10.1016/j.jcot.2021.04.011

5. Zhao J, Pan J, Zeng LF, Wu M, Yang W, Liu J. Risk factors for full-thickness rotator cuff tears: a systematic review and meta-analysis. *EFORT Open Rev*. (2021) 6:1087–96. doi: 10.1302/2058-5241.6.210027

6. Melis B, DeFranco MJ, Chuinard C, Walch G. Natural history of fatty infiltration and atrophy of the supraspinatus muscle in rotator cuff tears. *Clin Orthop Relat Res*. (2010) 468:1498–505. doi: 10.1007/s11999-009-1207-x

7. Inouye SK, Studenski S, Tinetti ME, Kuchel GA. Geriatric syndromes: clinical, research, and policy implications of a core geriatric concept. *J Am Geriatr Soc*. (2007) 55 (5):780–91. doi: 10.1111/j.1532-5415.2007.01156.x

8. Petermann-Rocha F, Balntzi V, Gray SR, Lara J, Ho FK, Pell JP, et al. Global prevalence of sarcopenia and severe sarcopenia: a systematic review and meta-analysis. *J Cachexia Sarcopenia Muscle*. (2022) 13(1):86–99. doi: 10.1002/jcsm.12783

9. Cui H, Wang Z, Wu J, Liu Y, Zheng J, Xiao W, et al. Chinese expert consensus on prevention and intervention for elderly with sarcopenia. *Ageing Med*. (2023) 6(2):104–15. doi: 10.1002/agm2.12245

10. Cruz-Jentoft AJ, Bahat G, Bauer J, Boirie Y, Bruyère O, Cederholm T, et al. Writing Group for the European Working Group on Sarcopenia in Older People 2 (EWGSOP2), and the Extended Group for EWGSOP2. Sarcopenia: revised European consensus on definition and diagnosis. *Age Ageing*. (2019) 48(4):16–31. doi: 10.1093/ageing/afy169

11. Anker SD, Morley JE, von Haehling S. Welcome to the ICD-10 code for sarcopenia. *J Cachexia Sarcopenia Muscle*. (2016) 7:512–4. doi: 10.1002/jcsm.12147

12. Atala NA, Bongiovanni SL, Galich AM, Bruchmann MG, Rossi LA, Tanoira I, et al. Is sarcopenia a risk factor for rotator cuff tears? *J Shoulder Elbow Surg*. (2021) 30 (8):1851–5. doi: 10.1016/j.jse.2020.10.001

13. Kara M, Kara Ö, Durmuş ME, Analay P, Şener FE, Çıtır BN, et al. The relationship among probable SARCopenia, osteoporosis and SuprasPinatus tendon tears in postmenopausal women: the SARCOSP study. *Calcif Tissue Int*. (2024) 114 (4):340–7. doi: 10.1007/s00223-024-01183-7

14. Meyer GA, Shen KC. A unique sarcopenic progression in the mouse rotator cuff. *J Cachexia Sarcopenia Muscle*. (2022) 13:561–73. doi: 10.1002/jcsm.12808

15. Arsenault BJ. From the garden to the clinic: how Mendelian randomization is shaping up atherosclerotic cardiovascular disease prevention strategies. *Eur Heart J*. (2022) 43:4447–9. doi: 10.1093/eurheartj/ehac394

16. Emdin CA, Khera AV, Kathiresan S. Mendelian randomization. *JAMA*. (2017) 318:1925–6. doi: 10.1001/jama.2017.17219

17. Neeland IJ, Kozlitina J. Mendelian randomization: using natural genetic variation to assess the causal role of modifiable risk factors in observational studies. *Circulation*. (2017) 135:755–8. doi: 10.1161/CIRCULATIONAHA.117.026857

18. Smith GD, Ebrahim S. Mendelian randomization: prospects, potentials, and limitations. *Int J Epidemiol*. (2004) 33:30–42. doi: 10.1093/ije/dyh132

19. Liu M, Chen P, Yang C, Sun G. Standardizing trait selection in Mendelian randomization studies concerning sarcopenia. *J Cachexia Sarcopenia Muscle*. (2024) 15:1220–1. doi: 10.1002/jcsm.13463

20. Sanderson E. Multivariable Mendelian randomization and mediation. *Cold Spring Harb Perspect Med*. (2021) 11:a038984. doi: 10.1101/cshperspect.a038984

21. Pei YF, Liu YZ, Yang XL, Zhang H, Feng GJ, Wei XT, et al. The genetic architecture of appendicular lean mass characterized by association analysis in the uk biobank study. *Commun Biol*. (2020) 3:608. doi: 10.1038/s42003-020-01334-0

22. Jones G, Trajanoska K, Santanasto AJ, Stringa N, Kuo CL, Atkins JL, et al. Genome-wide meta-analysis of muscle weakness identifies 15 susceptibility loci in older men and women. *Nat Commun*. (2021) 12(1):654. doi: 10.1038/s41467-021-20918-w

23. Mitchell REEB, Mitchell R, Raistrick CA, Paternoster L, Hemani G, Gaunt TR. Univ Bristol (2019). doi: 10.5523/bris.pnoat8cxo0u52p6ynfaekeigi. MRC IEU UK Biobank GWAS pipeline version 2.

24. Kurki MI, Karjalainen J, Palta P, Sipilä TP, Kristiansson K, Donner KM, et al. FinnGen provides genetic insights from a well-phenotyped isolated population. *Nature*. (2023) 613(7944):508–18. doi: 10.1038/s41586-022-05473-8

25. Burgess S, Davey Smith G, Davies NM, Dudbridge F, Gill D, Glymour MM, et al. Guidelines for performing mendelian randomization investigations. *Wellcome Open Res*. (2019) 4:186. doi: 10.12688/wellcomeopenres.15555.3

26. Pierce BL, Ahsan H, Vanderweele TJ. Power and instrument strength requirements for mendelian randomization studies using multiple genetic variants. *Int J Epidemiol*. (2011) 40:740–52. doi: 10.1093/ije/dyq151

27. Yavorska OO, Burgess S. MendelianRandomization: an R package for performing Mendelian randomization analyses using summarized data. *Int J Epidemiol*. (2017) 46:1734–9. doi: 10.1093/ije/dyx034

28. Rasooly D, Peloso GM. Two-sample multivariable mendelian randomization analysis using R. *Curr Protoc*. (2021) 1:e335. doi: 10.1002/cpz1.335

29. Hung RJ, Zheng W, Gunter MJ, Davey Smith G, Relton C, Martin RM, et al. Design and quality control of large-scale two-sample Mendelian randomization studies. *Int J Epidemiol*. (2023) 52:1498–521. doi: 10.1093/ije/dyad018

30. Bowden J, Del Greco MF, Minelli C, Davey Smith G, Sheehan NA, Thompson JR. Assessing the suitability of summary data for two-sample Mendelian randomization analyses using MR-Egger regression: the role of the I2 statistic. *Int J Epidemiol*. (2016) 45(6):1961–74. doi: 10.1093/ije/dyw220

31. Bowden J, Davey Smith G, Haycock PC, Burgess S. Consistent estimation in Mendelian randomization with some invalid instruments using a weighted median estimator. *Genet Epidemiol*. (2016) 40:304–14. doi: 10.1002/gepi.21965

32. Burgess S, Bowden J, Fall T. et al: Sensitivity analyses for robust causal inference from mendelian randomization analyses with multiple genetic variants. *Epidemiology*. (2017) 28:30–42. doi: 10.1097/EDE.0000000000000559

33. Bowden J, Davey Smith G, Burgess S. Mendelian randomization with invalid instruments: effect estimation and bias detection through Egger regression. *Int J Epidemiol*. (2015) 44:512–25. doi: 10.1093/ije/dyv080

34. Verbanck M, Chen CY, Neale B, Do R. Detection of widespread horizontal pleiotropy in causal relationships inferred from Mendelian randomization between complex traits and diseases. *Nat Genet*. (2018) 50(5):693–8. doi: 10.1038/s41588-018-0099-7

35. Han DS, Wu WT, Hsu PC, Chang HC, Huang KC, Chang KV. Sarcopenia is associated with increased risks of rotator cuff tendon diseases among community-dwelling elders: A cross-sectional quantitative ultrasound study. *Front Med (Lausanne)*. (2021) 8:630009. doi: 10.3389/fmed.2021.630009

36. Yamaguchi K, Ditsios K, Middleton WD, Hildebolt CF, Galatz LM, Teefey SA. The demographic and morphological features of rotator cuff disease. A comparison of asymptomatic ansd symptomatic shoulders. *J Bone Joint Surg Am*. (2006) 88(8):1699–704. doi: 10.2106/JBJS.E.00835

37. Chung SW, Yoon JP, Oh KS, Kim HS, Kim YG, Lee HJ, et al. Rotator cuff tear and sarcopenia: are these related? *J Shoulder Elbow Surg*. (2016) 25(9):e249–55. doi: 10.1016/j.jse.2016.02.008

38. Manske RC, Jones DW, Dir CE, LeBlanc HK, Reddy MA, Straka MA, et al. Grip and shoulder strength correlation with validated outcome instruments in patients with rotator cuff tears. *J Shoulder Elbow Surg*. (2021) 30:1088–94. doi: 10.1016/j.jse.2020.07.041

39. Farup J, Madaro L, Puri PL, Mikkelsen UR. Interactions between muscle stem cells, mesenchymal-derived cells and immune cells in muscle homeostasis, regeneration and disease. *Cell Death Dis*. (2015) 6:e1830. doi: 10.1038/cddis.2015.198

40. Loomis T, Smith LR. Thrown for a loop: fibro-adipogenic progenitors in skeletal muscle fibrosis. *Am J Physiol Cell Physiol*. (2023) 325:C895–906. doi: 10.1152/ajpcell.00245.2023

41. Feeley BT, Liu M, Ma CB, Agha O, Aung M, Lee C, et al. Human rotator cuff tears have an endogenous, inducible stem cell source capable of improving muscle quality and function after rotator cuff repair. *Am J Sports Med*. (2020) 48:2660–8. doi: 10.1177/0363546520935855

42. Ferri E, Marzetti E, Calvani R, Picca A, Cesari M, Arosio B. Role of age-related mitochondrial dysfunction in sarcopenia. *Int J Mol Sci*. (2020) 21(15):5236. doi: 10.3390/ijms21155236

43. Lemos DR, Babaeijandaghi F, Low M, Chang CK, Lee ST, Fiore D, et al. Nilotinib reduces muscle fibrosis in chronic muscle injury by promoting TNF-mediated apoptosis of fibro/adipogenic progenitors. *Nat Med*. (2015) 21(7):786–94. doi: 10.1038/nm.3869

44. Dakin SG, Buckley CD, Al-Mossawi MH, Hedley R, Martinez FO, Wheway K, et al. Persistent stromal fibroblast activation is present in chronic tendinopathy. *Arthritis Res Ther*. (2017) 19:16. doi: 10.1186/s13075-016-1218-4

45. Pagano AF, Brioche T, Arc-Chagnaud C, Demangel R, Chopard A, Py G. Short-term disuse promotes fatty acid infiltration into skeletal muscle. *J Cachexia Sarcopenia Muscle*. (2018) 9:335–47. doi: 10.1002/jcsm.12259

46. Weber S, Chahal J. Management of rotator cuff injuries. *J Am Acad Orthop Surg*. (2020) 28:e193–201. doi: 10.5435/JAAOS-D-19-00463

47. Hong S-Y, Lee S-J, Hahm H-B, Chang J-W, Hyun Y-S. Onlay patch augmentation in rotator cuff repair for moderate to large tears in elderly patients: Clinical and radiologic outcomes. *Clin Shoulder Elb*. (2023) 26:71–81. doi: 10.5397/cise.2022.01382

48. Zhong W, Jia H, Zhu H, Tian Y, Huang W, Yang Q. Sarcopenia is attenuated by mairin in SAMP8 mice via the inhibition of FAPs fibrosis through the AMPK-TGF-β-SMAD axis. *Gene*. (2024) 931:148873. doi: 10.1016/j.gene.2024.148873

49. Xu H, Piekarz KM, Brown JL, Bhaskaran S, Smith N, Towner RA, et al. Neuroprotective treatment with the nitrone compound OKN-007 mitigates age-related muscle weakness in aging mice. *Geroscience*. (2024) 46:4263–73. doi: 10.1007/s11357-024-01134-y

50. Lin CC, Shih MH, Chen CD, Yeh SL. Effects of adequate dietary protein with whey protein, leucine, and vitamin D supplementation on sarcopenia in older adults: An open-label, parallel-group study. *Clin Nutr*. (2021) 40:1323–9. doi: 10.1016/j.clnu.2020.08.017

51. Hsu KJ, Liao CD, Tsai MW, Chen CN. Effects of exercise and nutritional intervention on body composition, metabolic health, and physical performance in adults with sarcopenic obesity: A meta-analysis. *Nutrients*. (2019) 11:2163. doi: 10.3390/nu11092163

52. Yörükoğlu AÇ, Şavkın R, Büker N, Alsayani KYA. Is there a relation between rotator cuff injury and core stability? *J Back Musculoskelet Rehabil*. (2019) 32:445–52. doi: 10.3233/BMR-170962

53. Richardson E, Lewis JS, Gibson J, Morgan C, Halaki M, Ginn K, et al. Role of the kinetic chain in shoulder rehabilitation: does incorporating the trunk and lower limb into shoulder exercise regimes influence shoulder muscle recruitment patterns? Systematic review of electromyography studies. *BMJ Open Sport Exerc Med*. (2020) 6 (1):e000683. doi: 10.1136/bmjsem-2019-000683

frontiers | Frontiers in Endocrinology

TYPE Original Research
PUBLISHED 06 November 2024
DOI 10.3389/fendo.2024.1467769

OPEN ACCESS

EDITED BY
Sandeep Kumar,
University of Alabama at Birmingham, United States

REVIEWED BY
Surbhi Gahlot,
University of Texas Southwestern Medical Center, United States
Sonal Kale,
National Institute of Allergy and Infectious Diseases (NIH), United States
Reena Kumari,
University of Alabama at Birmingham, United States

*CORRESPONDENCE
Jianhua Zeng
zengjianhua0411@163.com
Kai Guo
2014guokai@tongji.edu.cn
Haihong Zhao
2131171@tongji.edu.cn

†These authors have contributed equally to this work

RECEIVED 20 July 2024
ACCEPTED 09 October 2024
PUBLISHED 06 November 2024

CITATION
Yan L, Zhang J, Wang X, Zhou Q, Wen J, Zhao H, Guo K and Zeng J (2024) Efficacy of acupuncture for lumbar disc herniation: changes in paravertebral muscle and fat infiltration – a multicenter retrospective cohort study. *Front. Endocrinol.* 15:1467769. doi: 10.3389/fendo.2024.1467769

Efficacy of acupuncture for lumbar disc herniation: changes in paravertebral muscle and fat infiltration – a multicenter retrospective cohort study

Liang Yan[1†], Jiliang Zhang[2†], Xianliang Wang[3†], Qinming Zhou[4], Jingdong Wen[5], Haihong Zhao[6*], Kai Guo[6*] and Jianhua Zeng[6*]

[1]Department of Orthopaedic Surgery, The Third Hospital of Nanchang, Nanchang People's Hospital, Nanchang, Jiangxi, China, [2]Department of Rehabilitation Medicine, Xingguo Hospital Affiliated with Gannan Medical University, Ganzhou, Jiangxi, China, [3]Department of Acupuncture Rehabilitation, Ganzhou Hospital of Traditional Chinese Medicine, Ganzhou, Jiangxi, China, [4]Department of Orthopaedic Surgery, Ganxian District Hospital of Traditional Chinese Medicine, Ganzhou, Jiangxi, China, [5]Department of Traditional Chinese Medicine, Ganzhou Hospital of Guangdong Provincial People's Hospital, Ganzhou City Hospital, Ganzhou, Jiangxi, China, [6]Department of Spine Surgery, Shanghai East Hospital, School of Medicine, Tongji University, Shanghai, China

Objective: This study seeks to elucidate the dynamic alterations in the multifidus, erector spinae, and psoas major muscles, along with their fatty infiltration, in patients diagnosed with lumbar disc herniation treated through acupuncture. Concurrently, the Visual Analogue Scale (VAS) and Japanese Orthopedic Association (JOA) scores are employed to evaluate modifications in lumbar and leg pain and the enhancement in lumbar functionality.

Methods: A retrospective multi-center cohort study enrolled 332 adult LDH patients. Participants were divided into acupuncture and rehabilitation therapy groups. The acupuncture cohort received targeted treatments at specific acupuncture points, while the rehabilitation group received traditional rehabilitative therapy. Magnetic Resonance Imaging (MRI) gauged muscle cross-sectional areas (Sm, Se, Sp) and their ratios to vertebral area (Sm/Sv, Se/Sv, Sp/Sv), and fatty infiltration areas (Sfm, Sfe, Sfp) and their ratios (Sfm/Sv, Sfe/Sv, Sfp/Sv). Pain and function were assessed using Visual Analogue Scale (VAS) and Japanese Orthopedic Association (JOA) scores pre-treatment, 2-weeks, and 3-months post-intervention.

Results: A total of 332 patients were enrolled for analysis. Post-treatment, the acupuncture group exhibited increased Sm, Se, Sp and their ratios and reduced fatty infiltration areas and their ratios ($P<0.05$) compared to rehabilitation. Both treatments decreased VAS scores and enhanced JOA scores at both intervals ($P<0.05$). Intriguingly, no significant disparities were observed between the acupuncture and rehabilitation groups concerning pain and JOA scores at the 2-week follow-up ($p>0.05$); however, 3 months post-treatment, the acupuncture group significantly outperformed the rehabilitation group in both pain and JOA scores ($p<0.05$).

Conclusion: This study demonstrates that acupuncture treatment is significantly more effective than traditional rehabilitation therapy in improving paraspinal

muscle function, reducing muscle fat infiltration, and alleviating lumbar and leg pain in patients with lumbar disc herniation (LDH). Specifically, acupuncture significantly increases the cross-sectional areas (Sm, Se, Sp) of the paraspinal muscles and reduces muscle fat infiltration, showing superior long-term results in pain relief and functional improvement. Future research should further explore the long-term effects of acupuncture on the function and structure of paraspinal muscles, assess its potential in preventing the recurrence of LDH, and delve deeper into how acupuncture affects paraspinal muscles at the molecular level, to better understand its therapeutic mechanisms and enhance its clinical application.

KEYWORDS

acupuncture, lumbar disc herniation, paraspinal muscles, fat infiltration, VAS Score

Introduction

Lumbar disc herniation (LDH) is a prevalent degenerative disorder characterized by lower back pain, radiating pain in the lower extremities, and cauda equina syndrome. It stands as a common etiology for lower back discomfort, neurological dysfunction, and pain in the buttock/leg region (1), Consequently, LDH can significantly compromise the quality of life of affected individuals, posing a considerable economic strain on both families and the broader healthcare system (2). Epidemiological studies suggest that globally, around 80% of individuals will experience low back pain at least once in their lifetimes, with a significant portion attributed to disc herniation (3–5). Owing to shifts in lifestyle and work patterns, such as prolonged sitting and overweight issues, the prevalence of this ailment has been escalating among younger populations (6).

In clinical settings, it is often observed that radiological findings do not consistently align with the clinical presentation of patients. Notably, certain patients with MRI/CT scans indicating disc protrusion or extrusion may only exhibit mild symptoms, while others with minimal herniation present with pronounced manifestations (5). This suggests that symptoms stemming from LDH aren't solely associated with spinal canal compression and inflammation. A comprehensive prospective study illuminated various determinants of early disc herniation resorption, identifying that nearly a quarter of LDH patients experienced early absorption (7). In recent years, the role of paraspinal muscles in maintaining spinal stability has garnered increasing attention. As one of the most vital muscles surrounding the spine, paraspinal muscles are essential for preserving spinal stability and dynamic function (8). The paraspinal group includes the multifidus and the erector spinae muscles, the latter of which is further divided into the spinalis, longissimus, and iliocostalis (9). The quantity and quality of these muscles directly impact lumbar health. The quantity of paraspinal muscles is typically quantified by measuring the cross-sectional area (CSA) of the multifidus, erector spinae, and iliocostalis via MRI, which helps assess the extent of muscle atrophy (10). The quality of paraspinal muscles involves evaluating muscle composition, particularly the proportion of fatty tissue within the muscles assessed through MRI imaging, reflecting the health and functional status of the muscles (11). Changes in the quality and quantity of paraspinal muscles have significant clinical implications for lumbar health (8, 12): Specifically, the atrophy of muscles, particularly the multifidus, is associated with spinal instability, potentially leading to or exacerbating lower back pain and spinal functional impairments (12). Moreover, the degeneration of paraspinal muscles, such as fat infiltration and muscle atrophy, is often linked to symptoms of lower back pain (11, 13). The ability to predict and treat these symptoms is crucial clinically, as strengthening paraspinal muscles can effectively alleviate pain and enhance functionality. Therefore, a deeper understanding of changes in paraspinal muscles can assist physicians in developing more effective rehabilitation plans, including targeted physical therapy and exercises to restore or improve muscle function. In young LDH patients with unilateral neurological symptoms, bilateral MF atrophy is more likely to induce lower back pain (14). When paraspinal muscles undergo atrophy, stiffness, or dysregulation, lumbar stability is compromised, leading to uneven stress distribution on the intervertebral discs and disruption of the intervertebral cushioning system, subsequently impacting the disc's workload. A meta-analysis focusing on muscle fiber size, distribution, and overall muscle lateral differences highlighted that LDH patients had more pronounced fat infiltration and atrophy in the MF compared to a control group. These alterations could further influence post-treatment pain and recovery outcomes (15). Another prospective study using MRI assessed isokinetic back muscle strength and both the quantity and quality of paraspinal muscles. The findings indicated that degeneration of paraspinal muscles might expedite lumbar deterioration (16). Factors such as prolonged sitting, excessive loading, and poor posture contribute to lumbar muscle strain, leading

to functional imbalances and a reduction in spinal stability. In summary, assessing the quality and quantity of paraspinal muscles is vital for diagnosing and treating muscle functional degradation in patients with lumbar disc herniation (15). Hence, the health status of lumbar paraspinal muscles, such as asymmetry in muscle area, atrophy, fat infiltration, and functional imbalances, could be pivotal factors influencing the symptoms of LDH.

While ultrasonography and CT scans have traditionally been employed to assess the morphology of paraspinal muscles (17–19), these modalities exhibit reduced capacity to differentiate muscle tissues and are prone to larger errors. In contrast, MRI emerges as a superior diagnostic tool due to its non-invasive nature, repeatability, and high-resolution imaging capabilities. MRI not only enables precise determination of vertebral segment levels and identification of intraspinal pathological conditions but also enables accurate measurement of the density and area of paraspinal muscles and the extent of intermuscular fat infiltration (20), Clinically, MRI is extensively utilized for the observation and diagnosis of neurological and musculoskeletal soft tissues.

While the majority of current treatments for LDH remain non-surgical, studies indicate that appropriate non-operative interventions can alleviate symptoms in 85%-90% of patients. These approaches primarily aim to enhance paraspinal muscle function and regulate spinal biomechanical balance. Prevalent clinical treatments encompass conservative therapies, minimally invasive interventions, and surgical procedures (21). Among these, conservative therapies like acupuncture, physical therapy, and exercise rehabilitation have been widely adopted in clinical practice. Notably, acupuncture has been demonstrated to effectively treat musculoskeletal soft tissue injuries (22–24), By stimulating structures such as myofascia, tendons, and muscles, it can enhance local micro-circulation and blood supply, and has been established as a safe procedure (25, 26). Compared to other conservative treatments, acupuncture has shown unique advantages in improving the quality of paravertebral muscles and alleviating pain (27). The choice of acupuncture as the treatment modality in our study is based on the traditional applications of Traditional Chinese Medicine (TCM) theory, as well as the effects demonstrated in modern research (28–30). Specific acupuncture points have been shown to directly improve lower back and leg pain by regulating the natural healing processes of lumbar disc herniation and pain perception (31). Furthermore, rehabilitation therapy, diverse in methods and easy to administer, has been widely utilized in the clinic, with satisfactory short-term results (32, 33), Thus, in this study, we chose rehabilitation therapy as the comparative treatment.

While acupuncture has shown significant efficacy in treating lumbar disc herniation, scant research has employed MRI to assess the specific impacts of acupuncture on paraspinal muscles and fat infiltration. In this vein, our study aims to delve into the effects of acupuncture on the structural changes of paraspinal muscles and fat infiltration in patients with LDH using MRI. Concurrently, we will evaluate the influence of acupuncture on patients' VAS and JOA scores, comparing these outcomes to those undergoing rehabilitation therapy. In this study, we hypothesize that acupuncture treatment can significantly improve the cross-sectional area of paraspinal muscles (Sm, Se, Sp) and reduce muscle fat infiltration in patients with lumbar disc herniation (LDH). Through these improvements, acupuncture is expected to alleviate lumbar and leg pain, thereby enhancing overall quality of life. Compared to conventional rehabilitation therapy, we predict that acupuncture will show significant increases in the cross-sectional area of paraspinal muscles, significant reductions in muscle fat infiltration, and significant improvements in Visual Analogue Scale (VAS) and Japanese Orthopaedic Association (JOA) scores at 2 weeks and 3 months post-treatment. Specifically, acupuncture is expected to exhibit superior long-term effects in pain relief and functional improvement. Through this research, we aspire to gain a more comprehensive understanding of the underlying mechanisms of acupuncture in the context of LDH.

Materials and methods

We conducted a multi-center retrospective cohort study across 6 hospitals in China, in strict adherence to the principles of the Declaration of Helsinki. The research protocol received thorough review and approved by the ethics committees of several respected institutions: Shanghai East Hospital, Ganzhou Hospital of Traditional Chinese Medicine in Jiangxi Province, Ganzhou Hospital of Guangdong Provincial People's Hospital, Xingguo Hospital affiliated with Gannan Medical College, The Third Hospital of Nanchang, and Ganxian District Hospital of Traditional Chinese Medicine, Jiangxi Province. All participants, after receiving comprehensive education regarding the study, provided their informed consent in writing. They were also informed of their right to withdraw from the study at any time without repercussion. From June 2020 to June 2023, we gathered 332 patients diagnosed with Lumbar Disc Herniation (LDH) from acupuncture outpatient rehabilitation departments and rehabilitation medicine center wards. The cohort was divided into two groups: 166 patients received acupuncture treatment and 166 underwent rehabilitation therapy. The study collected data on age, gender, Body Mass Index (BMI), medical history, clinical diagnosis, affected areas, and side of pain. Additionally, Japanese Orthopaedic Association (JOA) scores, Visual Analogue Scale (VAS) scores for back pain and leg pain were recorded both before and after the treatment to assess the therapeutic effects. The diagnostic criteria for LDH are based on the expert consensus and related literature of the 2014 revised Guidelines of the North American Spine Association (8, 14, 15, 34, 35). Inclusion Criteria: 1.Patients diagnosed with Lumbar Disc Herniation (LDH) without indications for surgical intervention. 2. Duration of the condition not exceeding three months, with no recurrent symptoms. 3. Age between 18 to 70 years, irrespective of gender. 4. Radiological findings consistent with the symptoms and signs of the corresponding spinal segment. 5. Patients who refuse pharmacological treatment and opt for acupuncture or rehabilitation therapy. Exclusion Criteria: 1. Patients exhibiting progressive symptoms of neurological damage. 2. Patients diagnosed with cauda equina syndrome. 3. Presence of lumbar instability, lumbar injury, or spinal tumors. 4. Symptoms and signs involving more than two vertebral segments. 5. Patients with systemic infectious diseases

(such as osteomyelitis, systemic lupus erythematosus, ankylosing spondylitis, rheumatoid arthritis), severe hematologic diseases, infectious diseases, skin lesions, allergic constitution, or mental disorders. 6. Patients with severe heart disease, severe diabetes, or Parkinson's disease, or other serious chronic conditions. 7. Patients non-compliant with treatment or follow-up procedures. We established strict screening criteria for participants, explicitly excluding those with chronic conditions such as heart disease, severe diabetes, or Parkinson's disease that might affect the study outcomes. Throughout the study, we regularly monitored the patients' blood pressure, blood sugar, and other relevant health indicators to ensure they remained within acceptable limits. By ensuring comparability in baseline characteristics such as age, gender, Body Mass Index (BMI), and duration of illness, we enhanced the scientific rigor and fairness of the research (36, 37). The work used the CONSORT reporting guidelines (38).

Treatment method

In the acupuncture group, acupoints such as Shen Shu (BL 23), Yao Yang Guan (GV 3), Da Chang Shu (BL 25), Zhi Bian (BL 54), Wei Zhong (BL 40), Cheng Shan (BL 57), Yang Ling Quan (GB 34), and Kun Lun (BL 60) were selected for treatment. Prior to each needle insertion, the skin was thoroughly disinfected with alcohol. We employed fine needles of dimensions0.3 x 40mm(Ring handle needle 0197, Suzhou Hualun Medical Supplies Co., LTD, China), inserting them vertically into the skin until a sensation of 'De Qi' or the arrival of qi was achieved. Once the needles were accurately positioned into the designated acupoints, they were retained for 20 minutes (Figure 1). Treatments were administered daily for a continuous period of 20 days. Conversely, Patients in the rehabilitation treatment group underwent lumbar rehabilitation therapy (Figure 2), which included plank exercises, low frequency electron pulse therapy(G6805-2B,Shanghai Huayi Medical Instrument Co., LTD,China), and iliolumbar muscle stretching exercises. The intensity of the rehabilitation regimen was adjusted based on patient tolerance. Each session lasted 20 minutes, conducted once daily for a duration of 20 days. All lumbar MRI evaluations were performed using a 3.0T magnetic resonance imaging system(Siemens, Germany). The study involved T1-weighted and T2-weighted scans, with each type of scan calibrated for specific diagnostic requirements(PACS System, Fujifilm (China) Investment Co., LTD). Lumbar MRI examinations were conducted prior to treatment to establish baseline data, and then repeated three months after treatment to assess therapeutic outcomes.

Outcome measurements and data collection

In our study, we employed a comprehensive approach to meticulously evaluate the therapeutic outcomes of lumbar spine disorders. Our holistic assessment encompassed the cross-sectional areas (CSA) of MF, ES, and PM(*Sm, Se, and Sp* respectively), and their relative proportions to the vertebral area (*Sv*), given by ratios *Sm/Sv, Se/Sv*, and *Sp/Sv*. Additionally, we evaluated the fat infiltration areas (*Sfm, Sfe, Sfp*) and their respective ratios to the vertebral CSA (*Sfm/Sv, Sfe/Sv, Sfp/Sv*). Specifically, we chose T2-weighted images (T2WI) of the L3/4, L4/5, and L5/S1 vertebrae (Figure 3A) and utilized ImageJ software to measure the CSA of the aforementioned muscles and the vertebral body (Figure 3B). By configuring an appropriate threshold within the software, fatty tissue within the muscles was delineated in red (Figure 3C), facilitating the computation of its area. The area of each muscle and its fatty infiltration was calculated based on the average values obtained from both the left and right sides. Subsequently, we discerned the ratios of these muscle areas and fatty infiltration areas to the vertebral CSA, shedding light on the degree of paraspinal muscle atrophy and the extent of fatty infiltration. A smaller muscle ratio indicated pronounced muscle atrophy, whereas a higher fatty ratio denoted a substantial fatty infiltration within the muscles. Additionally, the study employed the Visual Analog Scale (VAS) and Japanese Orthopaedic Association (JOA) scores to assess pain and functional outcomes pre-treatment, at two weeks post-treatment, and after three months. The VAS scoring system was employed to gauge the effectiveness of the treatment, with a score of 0 representing an absence of pain and a score of 10 signifying the most intense pain. To provide a comprehensive overview of the

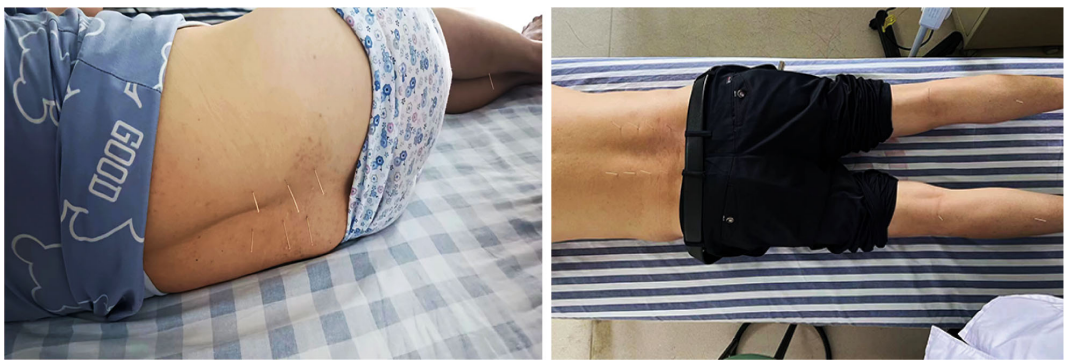

FIGURE 1
Acupuncture treatment diagram for patients with lumbar disc herniation.

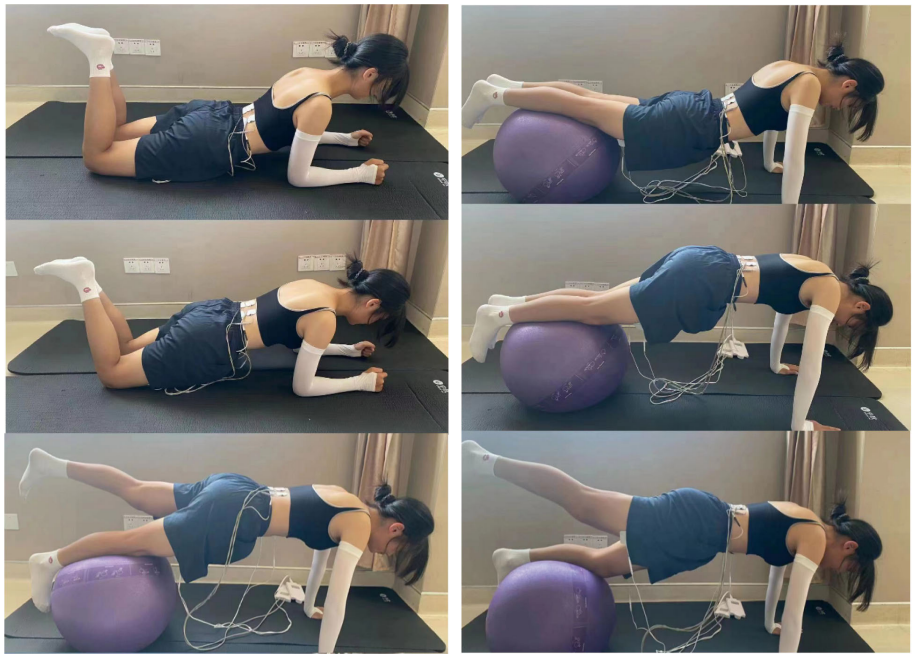

FIGURE 2
Rehabilitation Diagram: Plank, Bridge Exercise, and Iliopsoas Stretch.

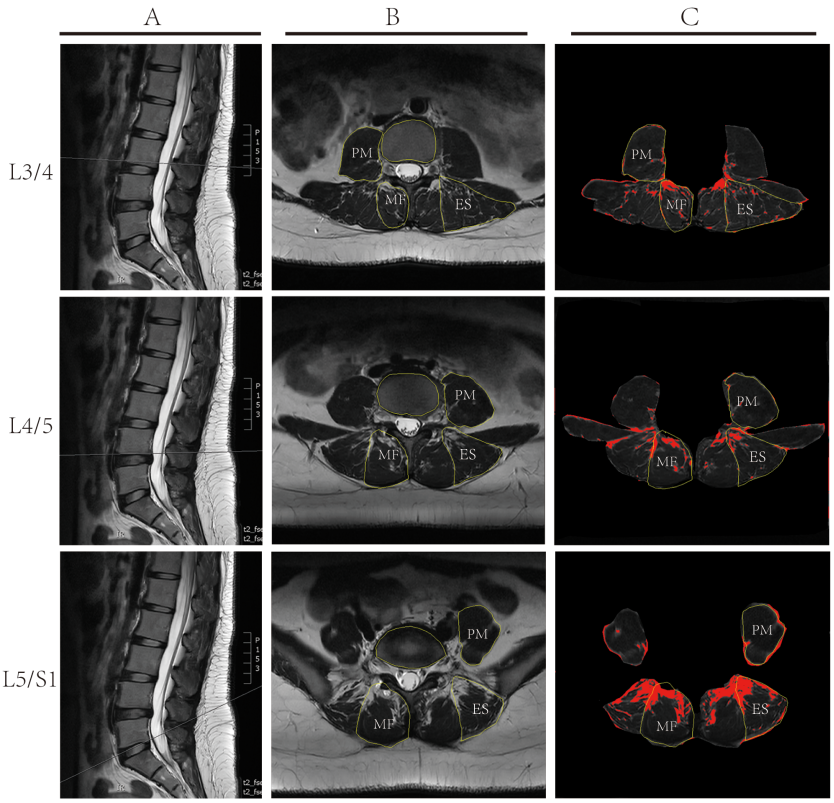

FIGURE 3
Illustrative Depiction of Lumbar MRI Measurement Techniques: **(A)** Sagittal T2 weighted MRI Imaging of the lumbar spine, depicting measurement planes for L3/4, L4/5, and L5/S1; **(B)** Cross-sectional Analysis using ImageJ software to delineate the multifidus muscle (MF), erector spinae (ES), psoas major muscle (PM), and vertebral contours. **(C)** Using ImageJ software and based on set thresholds, the fatty tissues within the muscles are marked in red, and the area of the fat is calculated.

patients' quality of life, we also utilized the JOA scoring questionnaire. This tool examines the effects on various aspects such as pain intensity, daily care activities, weight lifting, ambulation, postural transitions between sitting and standing, and sleep patterns. A heightened JOA score denotes a more severe medical condition and evident functional limitations.

Statistical analysis

Data analysis was performed using SPSS 20.0 statistical software. Quantitative data were expressed as mean ± standard deviation (X ± SD). For data conforming to normal distribution and homogeneity of variance, paired sample t-tests were used for within-group comparisons, and independent sample t-tests for between-group comparisons. For data with unequal variances, t' tests were utilized. Count data were represented as counts and percentages (%), analyzed using the $\chi 2$ test. In chi-square tests, if the total sample size was $n \geq 40$ but the expected frequency in any cell $1 \leq T < 5$, a continuity correction chi-square test was applied; if $T < 1$ or total sample size was $n < 40$, Fisher's exact test was used. All statistical tests were two-tailed, with a significance level set at $P < 0.05$.

Results

Baseline data characteristics

In this study, we included a total of 332 patients with single-segment LDH. Table 1 offers a comprehensive overview of the baseline characteristics of the patients. Participants were divided into the acupuncture group (n=166) and the rehabilitation treatment group (n=166). Out of the entire cohort, there were 160 males and 172 females. The average age for patients in the acupuncture group was 46.67 ± 15.29 years, while it was 45.61 ± 16.14 years for the rehabilitation group. The acupuncture group had a mean BMI of 28.84 ± 2.47kg/m^2, while the rehabilitation group presented with a mean BMI of 23.41 ± 2.62kg/m^2. The duration of the disease for the acupuncture and rehabilitation groups was 4.85 ± 2.51 months and 4.49 ± 2.16 months, respectively. Concerning the lumbar disc herniation segments, the acupuncture group comprised 20, 86, and 60 patients with L3/4, L4/5, and L5/S1 LDH, respectively. In contrast, the rehabilitation group had 27, 89, and 50 patients with L3/4, L4/5, and L5/S1 LDH, respectively. The distribution of left and right-sided pain in the acupuncture group was 84 and 82 cases, respectively, while in the rehabilitation group, it was 77 and 89 cases, respectively. Pre-treatment assessment scores for the acupuncture group were: lumbar VAS pain score of 4.18 ± 0.90, leg VAS pain score of 4.16 ± 0.98, and a JOA score of 19.01 ± 1.54. For the rehabilitation group, the scores were: lumbar VAS pain score of 4.10 ± 0.94, leg VAS pain score of 4.17 ± 1.05, and a JOA score of 18.86 ± 1.61. The two patient groups showed no statistically significant differences in terms of age, gender, Body Mass Index (BMI), affected segments, side of pain, pre-treatment JOA scores, and pre-treatment VAS scores for back and leg pain (all P values >0.05). This ensures the comparability of baseline data between the two groups prior to treatment.

Analysis of paraspinal muscle CSA ratios before and after treatment

In this study, Multifidus (MF), Erector Spinae (ES), and Psoas Major (PM) were selected as research subjects, with vertebral body cross-sectional area (CSA) as a reference. T2-weighted imaging (T2WI) muscle CSA measurements at the lower edges of the L3, L4, and L5 vertebrae were conducted pre- and post-treatment, as shown in Table 2. The ratios of MF CSA to vertebral CSA *(Sm/Sv)* were calculated. Pre-treatment ratios at L3/4, L4/5, L5/S1 for acupuncture and rehabilitation groups were (0.74 ± 0.22, 0.71 ± 0.28, p=0.279), (0.82 ± 0.17, 0.80 ± 0.18, p=0.499), and (0.87 ± 0.17, 0.85 ± 0.18, p=0.551) respectively, showing no significant differences (P>0.05), ensuring comparability of baseline data. Post-treatment, the Sm/Sv ratios showed significant improvements in both groups: (0.80 ± 0.23, 0.73 ± 0.29, p=0.028), (0.87 ± 0.17, 0.83 ± 0.19, p=0.041), and (0.91 ± 0.16, 0.87 ± 0.19, p=0.041), with the acupuncture group

TABLE 1 Baseline characteristics of lumbar disc herniation patients.

Parameter	Acupuncture Group	Rehabilitation Therapy Group	Statistical value	*p*-value
Age (years)	46.67 ± 15.29	45.61 ± 16.14	0.618	0.537
Gender (M/F)	86/80	74/92	1.737	0.187
BMI (kg/m^2)	23.52 ± 2.27	23.41 ± 2.64	0.417	0.677
Duration (months)	4.85 ± 2.51	4.49 ± 2.16	1.408	0.160
Side (Left/Right)	84/82	77/89	0.591	0.442
Level (L3/4, L4/5, L5/S1)	20/86/60	27/89/50	2.003	0.367
JOA Score	19.01 ± 1.54	18.86 ± 1.61	0.871	0.385
Lumbar Pain VAS Score	4.18 ± 0.90	4.10 ± 0.94	0.836	0.404
Leg Pain VAS Score	4.16 ± 0.98	4.17 ± 1.05	0.108	0.914

M/F, Male/Female; VAS, Visual Analog Scale; JOA, Japanese Orthopedic Association.

TABLE 2 Primary outcomes for the acupuncture group and the rehabilitation therapy group *(SpA/Sv)*.

Variables	L3			L4			L5		
	Pre-treatment	Post-treatment	t	Pre-treatment	Post-treatment	t	Pre-treatment	Post-treatment	t
S_m/S_v									
Acupuncture	0.74 ± 0.22	0.80 ± 0.23	46.76***	0.82 ± 0.17	0.87 ± 0.17	141.50***	0.87 ± 0.17	0.91 ± 0.16	60.26***
Rehabilitation Therapy	0.71 ± 0.28	0.73 ± 0.29	31.23***	0.80 ± 0.18	0.83 ± 0.19	96.23***	0.85 ± 0.18	0.87 ± 0.19	36.45***
T	1.085	2.213*		0.677	2.051*		0.597	2.055*	
P	0.279	0.028		0.499	0.041		0.551	0.041	、
Se/Sv									
Acupuncture	1.09 ± 0.16	1.14 ± 0.15	118.20***	1.10 ± 0.19	1.18 ± 0.20	331.00***	0.82 ± 0.22	0.89 ± 0.21	110.63***
Rehabilitation Therapy	1.06 ± 0.15	1.08 ± 0.15	43.42***	1.11 ± 020	1.14 ± 0.21	43.22***	0.82 ± 0.23	0.84 ± 0.24	73.05***
T	1.511	3.149**		0.117	2.028*		0.067	2.218*	
P	0.132	0.002		0.907	0.043		0.947	0.034	
Sp/Sv									
Acupuncture	0.78 ± 0.18	0.82 ± 0.19	63.11***	1.13 ± 0.18	1.14 ± 0.19	117.84***	0.88 ± 0.18	0.90 ± 0.20	3.74*
Rehabilitation Therapy	0.77 ± 0.19	0.79 ± 0.18	72.7***	1.14 ± 0.22	1.15 ± 0.21	143.01***	0.85 ± 0.23	0.88 ± 0.24	4.08*
t	0.584	1.413		0.396	0.471		1.412	0.475	
p	0.56	0.159		0.693	0.638		0.159	0.635	

Sv, Vertebral Area; *SpA*, Paraspinal Muscle Cross-Sectional Area; *Sm*, Multifidus Cross-Sectional Area; *Se*, Erector Spinae Cross-Sectional Area; *Sp*, Psoas Major Cross-Sectional Area; *SpA/Sv*, Paraspinal Muscle Cross-Sectional Area to vertebral area ratio; *Sm/Sv*, Multifidus muscle cross-sectional Area to vertebral area ratio; *Se/Sv*, Erector spinae muscle cross-sectional Area to vertebral area ratio; *Sp/Sv*, Psoas major muscle cross-sectional Area to vertebral area ratio. ***p<0.001, **p<0.01, *p<0.05.

exhibiting notably greater enhancements(P<0.05).Within-group analyses further revealed significant improvements post-treatment in both groups (P<0.001).For the ES CSA to vertebral CSA ratio *(Se/Sv)*, pre-treatment ratios at L3/4, L4/5, L5/S1 for acupuncture and rehabilitation groups were (1.09 ± 0.16, 1.06 ± 0.15, p=0.132), (1.10 ± 0.19, 1.11 ± 0.20, p=0.907), and (0.82 ± 0.22, 0.82 ± 0.23, p=0.947) respectively, indicating no significant differences (P>0.05) and similar baselines. Post-treatment ratios were (1.14 ± 0.15, 1.08 ± 0.15, p=0.002), (1.18 ± 0.20, 1.14 ± 0.21, p=0.043), and (0.89 ± 0.21, 0.84 ± 0.24, p=0.034), showing significant increases in both groups (P<0.05), with more pronounced elevation in the acupuncture group (P<0.05). Furthermore, within-group comparisons revealed that both the acupuncture and rehabilitation groups demonstrated significant improvements compared to their pre-treatment statuses (P<0.001).

For the PM CSA to vertebral CSA ratio *(Sp/Sv)*, pre-treatment ratios at L3/4, L4/5, L5/S1 in the acupuncture and rehabilitation groups were (0.78 ± 0.18, 0.77 ± 0.19, p=0.56), (1.13 ± 0.18, 1.14 ± 0.22, p=0.693), and (0.88 ± 0.18, 0.85 ± 0.23, p=0.159) respectively, showing no significant differences between groups (P>0.05) and indicating similar baselines. Post-treatment ratios at L3/4, L4/5, L5/S1 were (0.82 ± 0.19, 0.79 ± 0.18, p=0.159), (1.14 ± 0.19, 1.15 ± 0.21, p=0.638), and (0.90 ± 0.20, 0.88 ± 0.24, p=0.635) respectively; there were no significant differences between groups post-treatment (P>0.05). However, within-group comparisons showed significant improvement in both groups compared to pre-treatment (P<0.05). In summary, acupuncture treatment showed superior results in improving the ratios of these three muscle CSA to the vertebral CSA compared to rehabilitation treatment. While both treatments notably ameliorated muscle atrophy in LDH patients, acupuncture therapy proved more effective in augmenting paravertebral muscle CSA, subsequently enhancing patients' symptoms and quality of life.

Analysis of fat infiltration in paraspinal muscles before and after treatment

In this study, we measured the fat tissue area and vertebral CSA of the ES, MF, and PM on the lumbar magnetic resonance T2WI images at the lower edges of the L3, L4, and L5 vertebrae. The ratios of each muscle's fatty tissue area to vertebral CSA (Sfm/Sv, Sfe/Sv, Sfp/Sv) were computed. Pre-treatment, the acupuncture and rehabilitation groups at L3/4, L4/5, L5/S1 showed the following ratios for *Sfm/Sv*: (0.057 ± 0.021, 0.056 ± 0.018, p=0.739), (0.071 ± 0.026, 0.066 ± 0.023, p=0.07), (0.119 ± 0.032, 0.112 ± 0.033, p=0.058), for *Sfe/Sv*: (0.075 ± 0.020, 0.076 ± 0.019, p=0.765), (0.049 ± 0.025, 0.047 ± 0.018, p=0.506), (0.122 ± 0.031, 0.120 ± 0.026, p=0.725), and for *Sfp/Sv*: (0.029 ± 0.008, 0.030 ± 0.005, p=0.614), (0.026 ± 0.005, 0.025 ± 0.004, p=0.114), (0.029 ± 0.010, 0.030 ± 0.007, p=0.400),

respectively, all with no statistical significance (P>0.05) (Table 3), ensuring baseline comparability. Post-treatment, the acupuncture and rehabilitation groups at L3/4, L4/5, L5/S1 showed the following ratios for *Sfm/Sv*: (0.047 ± 0.021, 0.053 ± 0.017, p=0.012), (0.049 ± 0.027, 0.055 ± 0.022, p=0.044), (0.089 ± 0.033, 0.104 ± 0.032, p<0.001); for *Sfe/Sv*: (0.040 ± 0.022, 0.063 ± 0.018, p<0.001), (0.035 ± 0.024, 0.041 ± 0.019, p=0.017), (0.095 ± 0.032, 0.102 ± 0.025, p=0.033); and for *Sfp/Sv*: (0.024 ± 0.008, 0.026 ± 0.004, p=0.016), (0.021 ± 0.005, 0.022 ± 0.004, p=0.013), (0.025 ± 0.010, 0.027 ± 0.006, p=0.011). The *Sfm/Sv*, *Sfe/Sv*, *and Sfp/Sv* for MF, ES, and PM at L3/4, L4/5, and L5/S1 decreased significantly compared to pre-treatment (P<0.05). This indicates that acupuncture treatment demonstrates evident efficacy in reducing muscular fat infiltration. In contrast, the ratio changes in the rehabilitation group were not as pronounced as those in the acupuncture group, indicating that the therapeutic effects of rehabilitation were not as significant as those of acupuncture (P<0.05).Within-group comparisons showed significant improvements in both groups compared to pre-treatment (P<0.001).

Analysis of VAS and JOA scores before and after treatment

This study utilized the Visual Analogue Scale (VAS) to assess pain levels and the Japanese Orthopaedic Association (JOA) score to evaluate the quality of life in patients (Table 4). Pre-treatment, the VAS scores for back pain in the acupuncture and rehabilitation groups were (4.18 ± 0.90, 4.10 ± 0.94, p=0.404) and for leg pain were (4.16 ± 0.98, 4.17 ± 1.05, p=0.914). The JOA scores for the acupuncture and rehabilitation groups were (19.01 ± 1.54, 18.86 ± 1.61, p=0.385). There were no significant differences in VAS scores for back and leg pain or JOA scores between the groups (P>0.05), indicating comparable baselines for pain and quality of life. Two weeks post-treatment, the VAS scores for back pain in the acupuncture and rehabilitation groups decreased to (0.27 ± 0.44, 0.32 ± 0.47, p=0.278), and for leg pain to (0.41 ± 0.49, 0.46 ± 0.62, p=0.433). The JOA scores were (25.39 ± 1.14, 25.18 ± 1.21, p=0.113). At this stage, inter-group comparisons revealed no significant differences in VAS and JOA scores (P>0.05), indicating a comparable level of therapeutic effectiveness between the groups during the initial treatment phase. However, there was a significant improvement in these scores compared to pre-treatment (P<0.05), reflecting a considerable decrease in pain and enhancement in quality of life post-treatment. Three months post-treatment, the acupuncture and rehabilitation groups reported VAS scores for back pain as (0.15 ± 0.36, 0.28 ± 0.45, p=0.003) and for leg pain as (0.11 ± 0.32, 0.32 ± 0.47, p<0.001) respectively. The JOA scores were (26.75 ± 0.88, 26.55 ± 0.92, p=0.045). The acupuncture group showed more significant improvements in both VAS scores for back and leg pain and JOA scores compared to the rehabilitation

TABLE 3 Primary outcomes for the acupuncture group and the rehabilitation therapy group (*Sf/Sv*).

Variables	L3			L4			L5		
	Pre-treatment	Post-treatment	t	Pre-treatment	Post-treatment	t	Pre-treatment	Post-treatment	T
Sfm/S$_v$									
Acupuncture	0.057 ± 0.021	0.047 ± 0.021	102.13***	0.071 ± 0.026	0.049 ± 0.027	58.804***	0.119 ± 0.032	0.089 ± 0.033	249.86***
Rehabilitation Therapy	0.056 ± 0.018	0.053 ± 0.017	38.13***	0.066 ± 0.023	0.055 ± 0.022	150.07***	0.112 ± 0.033	0.104 ± 0.032	50.49***
t	0.333	2.534*		1.820	2.026*		1.904	3.955***	
p	0.739	0.012		0.070	0.044		0.058	<0.001	
Sfe/Sv									
Acupuncture	0.075 ± 0.020	0.040 ± 0.022	46.399***	0,049 ± 0.025	0.035 ± 0.024	67.228***	0.122 ± 0.031	0.095 ± 0.032	75.114***
Rehabilitation Therapy	0.076 ± 0.019	0.063 ± 0.018	49.210***	0.047 ± 0.018	0.041 ± 0.019	65.576***	0.120 ± 0.026	0.102 ± 0.025	63.508***
t	0.300	10.132***		0.666	2.396*		0.352	2.147*	
p	0.765	<0.001		0.506	0.017		0.725	0.033	
Sfp/S$_v$									
Acupuncture	0.029 ± 0.008	0.024 ± 0.008	17.095***	0.026 ± 0.005	0.021 ± 0.005	124.818***	0.029 ± 0.010	0.025 ± 0.010	38.704***
Rehabilitation Therapy	0.030 ± 0.005	0.026 ± 0.004	34.902***	0.025 ± 0.004	0.022 ± 0.004	47.755***	0.030 ± 0.007	0.027 ± 0.006	23.051***
t	0.504	2.412*		1.583	2.503*		0.842	2.588*	
p	0.614	0.016		0.114	0.013		0.400	0.011	

Sv, Vertebral Area; *Sfm*, Multifidus Fat Infiltration Area; *Sfe*, Erector Spinae Fat Infiltration Area; *Sfp*, Psoas Major Fat Infiltration Area; *Sf/Sv*, Paravertebral muscle fat infiltration Area to vertebral area ratio; *Sfm/Sv*, Multifidus muscle fat infiltration Area to vertebral area ratio; *Sfe/Sv*, Erector spinae muscle fat infiltration Area to vertebral area ratio; *Sfp/Sv*, Psoas major muscle fat infiltration Area to vertebral area ratio. ***p<0.001, *p<0.05.

TABLE 4 Secondary outcome comparisons between the acupuncture group and the rehabilitation therapy group (lumbar pain, leg pain VAS, and JOA scores).

Groups	Lumbar Pain VAS Score			Leg Pain VAS Score			JOA Score		
	Pre-treat	2w post-treat	3m post-treat	Pre-treat	2w post-treat	3m post-treat	Pre-treat	2w post-treat	3m post-treat
Acupuncture	4.18 ± 0.90	0.27 ± 0.44$^{\Delta}$	0.15 ± 0.36▲	4.16 ± 0.98	0.41 ± 0.49$^{\Delta}$	0.11 ± 0.32▲	19.01 ± 1.54	25.39 ± 1.14$^{\Delta}$	26.75 ± 0.88▲
Rehabilitation Therapy	4.10 ± 0.94	0.32 ± 0.47❑	0.28 ± 0.45★	4.17 ± 1.05	0.46 ± 062❑	0.32 ± 0.47★	18.86 ± 1.61	25.18 ± 1.21❑	26.55 ± 0.92★
T	0.836	1.085	2.959	0.108	0.785	4.660	0.871	1.588	2.010
P	0.404	0.278	0.003	0.914	0.433	<0.001	0.385	0.113	0.045

Δ❑▲★ compared to baseline, p<0.05, the difference is statistically significant.

group, with statistical significance (P<0.05), indicating a more pronounced effect of acupuncture treatment on pain reduction and quality of life enhancement. This suggests that acupuncture therapy was more efficacious in mitigating pain and elevating patients' quality of life than the rehabilitation treatment. While the therapeutic outcomes appeared similar in the initial phase of treatment, long-term observations highlighted that acupuncture treatment yielded more significant improvements in both lumbar and leg pain, as well as in the overall quality of life.

Discussion

In the present study, we embarked on an in-depth investigation of the therapeutic efficacy of acupuncture and rehabilitation treatments for LDH, as well as their impact on paravertebral muscles and fatty infiltration. Unlike many studies that focus solely on acupuncture (27), Our findings underscored that both treatments notably enhanced patients' quality of life and ameliorated conditions of paravertebral muscles and fatty infiltration within a span of two weeks and three months post-treatment. While both treatments are effective, acupuncture shows statistically significant advantages in improving muscle indicators and pain relief over a longer term,. The association between lumbar disc protrusion and paravertebral muscles represents a nascent yet profoundly clinically relevant domain of research. Paravertebral muscles play a pivotal role in preserving spinal stability, being integral in both static and dynamic states. A well-functioning state of these muscles is imperative for maintaining spinal stability (39, 40). Muscle degeneration, manifesting as atrophy, fatty infiltration, alterations in muscle fiber types, and changes in muscle activity, can impair the biomechanics and motion of spinal units in patients with lumbar pain. Paraspinal muscles may be influenced by confounding factors such as age, gender, duration of illness, obesity, and smoking, which are prevalent in patients with Lumbar Disc Herniation (LDH). We adjusted for age, gender, ethnicity, and BMI in our model to exclude potential confounders. Recent studies suggest that muscles and bones share common genetic, nutritional, lifestyle, and hormonal determinants (41), with low muscle mass and strength depending on BMI (42), A lower BMI is associated with muscle loss, whereas a higher BMI is not (43). Exercise interventions have been shown to beneficially impact muscle quality, strength, and physical performance (44). Literature reports that hypertension, cognitive impairments, hyperlipidemia, heart disease, stroke, cancer, pain, anemia, and liver disease are not associated with an increased risk of muscle loss (43). Similarly, geographical differences relate to many important human health factors such as latitude, dietary variations, and hours of sunlight exposure. All these factors could directly or indirectly contribute to variations in muscle loss. Moreover, modifications in the structure and function of these muscles might be linked to the recurrence or chronicity of lumbar pain (45). Numerous studies have elucidated this association, with Denis's 1983 proposition of the "Three-column theory of the spine" laying the foundational theoretical framework for understanding the integral role of paravertebral muscles in spinal stability. Lumbar pain induced by LDH frequently coincides with atrophy or functional impairments in paravertebral muscles. The anterior lumbar large muscle and the posterior extensor muscle group, encompassing the ES and MF, are paramount in ensuring lumbar stability (46). However, despite evidence pointing to marked atrophy in paravertebral muscles of patients with LDH, a comprehensive understanding of its etiology and implications remains in its infancy (47).

LDH is a common degenerative spinal disease in clinical practice, primarily manifesting as lumbar pain and radiating pain in the lower extremities. These symptoms not only severely impact patients' daily activities but can occasionally lead to neurological dysfunctions, imposing significant economic burdens on families and the healthcare system (2). Recent global prevalence data indicate that the incidence of LDH is on the rise worldwide, particularly among younger populations (48–50). This trend is largely attributed to changes in modern lifestyles and work environments (51), such as prolonged sitting and lack of physical exercise. Studies suggest that approximately 80% of adults will experience at least one episode of lower back pain during their lifetime, with lower back pain being one of the most common symptoms of LDH (3, 34, 52). The socioeconomic impact of LDH is profound. Direct medical costs include surgery, medication, and physical therapy (1), but more significant are the indirect costs related to pain and functional impairments that lead to unemployment and decreased productivity (53). Chronic disability may result in long-term dependency on pain management and rehabilitation services, thus increasing the societal burden. It has been reported that lower back pain, including that caused by LDH, is one of the leading causes of

work disability, placing immense pressure on the economy (54). Acupuncture, an ancient therapeutic technique, has been empirically shown to modulate endogenous pain regulatory networks, thereby offering analgesic benefits to LDH patients with lumbar and leg pain (55). Compared to other conservative treatment modalities, acupuncture has demonstrated superior efficacy in managing LDH (56), Although rooted in traditional practices, recent research underscores its significant therapeutic impact on LDH patients, mitigating lumbar pain, leg pain, enhancing lumbar mobility, and improving overall quality of life (57). Our study corroborates these findings, underscoring the remarkable efficacy of acupuncture in LDH management. We observed a tangible reduction in pain and localized tenderness among LDH patients subjected to acupuncture. Further accentuating our results, we noted a marked alleviation in lumbar pain post-treatment, irrespective of whether patients underwent acupuncture or rehabilitative therapy. This not only emphasizes the efficacy of both modalities but also suggests the potential synergistic effects when combined, warranting further exploration in future research endeavors.

A significant correlation exists between LDH and the degeneration and fatty infiltration of paraspinal muscles. Research indicates that severe fatty infiltration is associated with neural root compression, and the severity of this infiltration can escalate in the presence of such compression (58). Moreover, there are indications that patients with advanced disc degeneration exhibit increased chances of fatty infiltration in the MF and ES (59). In younger patients with lumbar disc herniation, an increased thickness of subcutaneous fat tissue at the L1-L2 level, prolonged extended symptom duration, and more pronounced atrophy in the normal side of the MF are reported to correlate with elevated occurrences of lumbar pain (14). Lee et al. discovered through MRI assessments that patients with lumbar flatback deformity demonstrated evident atrophy of the lumbar paraspinal muscles, characterized predominantly by reduced muscle volume and conspicuous intermuscular fat infiltration (60). In our study, we evaluated the fatty tissue area's variations in the ES, MF, and PM relative to vertebral CSA pre- and post-treatment. Notably, our results indicated that the acupuncture treatment group exhibited a more pronounced reduction in muscle fat deposition compared to the rehabilitative therapy group. Acupuncture, a non-surgical intervention, involves needle insertion into muscle tissues followed by manipulative rotations. It has been substantiated to effectively ameliorate pain intensity and range of motion in LDH patients (61). Consistent with previous research, our results show significant pain relief and functional improvement three months post-treatment. Similar findings were reported by Zhong et al (26). The literature documents greater improvements with electroacupuncture and spinal manipulation in terms of pain in the lower back, buttocks, and legs, as well as associated disabilities (28, 62). However, our study further explores the timeline of these improvements, noting no significant differences at two weeks, but substantial improvements at three months, providing a more nuanced understanding of the temporal dynamics of acupuncture effects. Clinical trials have demonstrated that post-acupuncture, there's an augmentation in local blood circulation and a rise in soft tissue temperature. This facilitates inflammation resolution, alleviates muscle spasms, fosters an increase in the volume of paraspinal muscles, and diminishes the proportion of fatty infiltration between them.

Acupuncture, a traditional Chinese medicinal technique, aims to modulate the body's internal flow of Qi and blood by stimulating specific acupoints, thereby achieving therapeutic effects. The primary mechanisms underlying the localized pain of LDH originate from atrophy and excessive tension in the paraspinal muscles, combined with the occurrence of aseptic inflammation and spasms (63). These pathological changes are principally related to the diminished interaction between muscle and fascial structures, reductions in muscle quality, strength, and regenerative capacity, and the increase in fascial rigidity coupled with decreased elasticity. Furthermore, the atrophy of the motor cortex, stemming from aging, reduces its excitability and plasticity, thus accelerating the accumulation of denervated muscle fibers (64). Contemporary research has validated the efficacy of acupuncture in alleviating pain, enhancing sleep quality, and elevating overall life quality. Our study highlights the advantages of acupuncture in treating LDH and uncovers its significant role in mitigating paraspinal muscle atrophy among LDH patients. Our findings indicate an increase in the area ratio of multifidus (MF), erector spinae (ES), and psoas major (PM) relative to the vertebral body after acupuncture treatment, along with a reduction in fatty infiltration. This is consistent with literature studies (65–67), which emphasize the efficacy of electroacupuncture in enhancing muscle strength of LDH patients and reducing fat infiltration. However, our study provides additional insights into the differential responses of various muscle groups, which have not been extensively reported in earlier literature. It's noteworthy that the improvements in the PM were not as pronounced as those in the ES and MF. This discrepancy might stem from the acupuncture treatment primarily targeting the latter two muscles, bypassing direct intervention on the psoas major. Nevertheless, with enhancements in the ES and MF, we anticipate improvements in the condition of the psoas major over time. Given our study's short follow-up duration, noticeable improvements in the psoas major were not evident. Thus, our findings underscore acupuncture's potential in notably ameliorating the atrophy in the ES and MF.

Acupuncture, an age-old therapeutic modality, has demonstrated potential in addressing LDH and the associated paravertebral muscle atrophy through multiple mechanisms. Primarily, HA-19, a derivative of oleanolic acid, has demonstrated significant potential in mitigating muscle atrophy by activating the mTORC1/p70 S6K pathway to enhance protein synthesis. It also upregulates myogenic transcription factors such as Pax7 and MyoD, which are critical for the proliferation and differentiation of myoblasts, thus effectively counteracting muscle atrophy (68). Additionally, acupuncture increases the expression of neurotrophic factors, including brain-derived and glial cell-derived neurotrophic factors, which are essential for nourishing peripheral nerves. Moreover, acupuncture elevates levels of IGF-1, a potent agent for muscle regeneration, offering further resistance against muscle atrophy. It also reduces neuronal excitability within muscles, easing muscle and fibrous tissue tension. The increased localized temperature and enhanced blood flow induced by acupuncture contribute significantly to its therapeutic effects on paravertebral muscle atrophy. The selection of an optimal internal reference gene for muscle tissue continues to be a debated issue in the field. Tokłowicz

et al (69) embarked on an evaluation of 90 tissue samples from deep and superficial paravertebral muscles of the convex and concave sides of spinal curvatures. In their quest to assess the stability of 12 miRNAs, they discovered three with reference potential, while the remaining nine exhibited tissue-specific properties. While our findings bear significant clinical implications, this realm necessitates more in-depth exploration. It's pivotal to unearth the precise roles of these mechanisms and fully realize their potential in therapeutic contexts.

This study introduces a novel perspective in understanding the etiology of LDH, emphasizing the pivotal role of paravertebral muscle function. Notably, if targeted interventions for these muscles were initiated prior to the diagnosis of LDH, or even before its onset, it might present an opportunity to prevent or at least delay the progression of the condition. Consequently, future investigations should delve deeper into the causative relationship between paravertebral muscle atrophy and LDH, offering fresh avenues and evidence for preventive strategies. However, our research is not without limitations. The relatively small sample size necessitates larger and more rigorous prospective studies to ensure objectivity and accuracy. Additionally, while our participants primarily came from several hospitals in China and the acupuncture techniques and specific points used in our study are standardized, making them highly reproducible and applicable across different regions or countries, variations in the practice of acupuncture points and techniques in other regions or countries might affect our results. Moreover, the follow-up period of our study was three months, primarily to observe the short-term effects post-treatment. This brief follow-up period only allows for the assessment of short-term therapeutic effects, overlooking potential long-term treatment outcomes. Considering these factors, although our findings are useful, they underscore the need for extensive long-term studies to further validate and establish these preliminary insights. Future studies should further explore the long-term effects of acupuncture on the morphology and fat infiltration of paravertebral muscles and evaluate its effectiveness in preventing the recurrence of lumbar disc herniation (LDH). Additionally, it is advisable to conduct more randomized controlled trials to verify the effects of acupuncture across different LDH patient groups, thereby optimizing and personalizing acupuncture treatment strategies to enhance treatment efficacy and patient satisfaction. Prospective studies are also recommended to validate our findings, investigate the long-term effects of acupuncture on muscle health, and compare different acupuncture techniques. Finally, molecular mechanism studies at the cellular and molecular levels should be conducted to deeply understand how acupuncture affects paravertebral muscles at the biological level.

Conclusions

Acupuncture treatment for LDH has been shown to effectively increase the CSA of the MF, ES, and PM. Additionally, it ameliorates paravertebral muscle atrophy and reduces fat infiltration in these muscles. Concurrently, patients experience notable relief in pain across the lumbar and leg regions and exhibit a marked improvement in their overall quality of life. These findings robustly advocate for the inclusion of acupuncture in clinical practices treating such conditions.

Data availability statement

The original contributions presented in the study are included in the article/supplementary material. Further inquiries can be directed to the corresponding authors.

Ethics statement

All procedures of this study were ethically reviewed and approved by the Shanghai East Hospital of Tongji University and Xingguo Hospital Affiliated with Gannan Medical University, Ethical Review Board. Additionally, ethical approval was granted by the Medical Ethics Committee of the Ganzhou Hospital of Traditional Chinese Medicine (Approval Number: GZSZYYKYLL20230076). The studies involving humans were approved by the Medical Ethics Committee of the Ganzhou Hospital of Traditional Chinese Medicine and Xingguo Hospital Affiliated with Gannan Medical University. The studies were conducted in accordance with the local legislation and institutional requirements. The participants provided their written informed consent to participate in this study. Written informed consent was obtained from the individual(s) for the publication of any potentially identifiable images or data included in this article.

Author contributions

JHZ: Conceptualization, Data curation, Funding acquisition, Methodology, Project administration, Resources, Writing – original draft. XW: Investigation, Methodology, Software, Writing – original draft. JLZ: Investigation, Software, Supervision, Writing – original draft. LY: Formal analysis, Methodology, Writing – original draft. QZ: Formal analysis, Project administration, Writing – original draft. JW: Formal analysis, Methodology, Software, Writing – original draft. HZ: Investigation, Software, Writing – original draft. KG: Formal analysis, Methodology, Resources, Software, Writing – original draft.

Funding

The author(s) declare that no financial support was received for the research, authorship, and/or publication of this article.

Conflict of interest

The authors declare that the research was conducted in the absence of any commercial or financial relationships that could be construed as a potential conflict of interest.

Publisher's note

References

1. Zhang AS, Xu A, Ansari K, Hardacker K, Anderson G, Alsoof D, et al. Lumbar disc herniation: diagnosis and management. *Am J Med*. (2023) 136:645–51. doi: 10.1016/j.amjmed.2023.03.024

2. Yuan S, Huang C, Xu Y, Chen D, Chen L. Acupuncture for lumbar disc herniation: Protocol for a systematic review and meta-analysis. *Med (Baltimore)*. (2020) 99:e19117. doi: 10.1097/MD.0000000000019117

3. Melman A, Lord HJ, Coombs D, Zadro J, Maher CG, MaChado GC. Global prevalence of hospital admissions for low back pain: a systematic review with meta-analysis. *BMJ Open*. (2023) 13:e069517. doi: 10.1136/bmjopen-2022-069517

4. Rizzardo A, Miceli L, Bednarova R, Guadagnin GM, Sbrojavacca R, Della Rocca G. Low-back pain at the emergency department: still not being managed? *Ther Clin Risk Manag*. (2016) 12:183–7. doi: 10.2147/TCRM.S91898

5. Li Y, Fredrickson V, Resnick DK. How should we grade lumbar disc herniation and nerve root compression? A systematic review. *Clin Orthop Relat Res*. (2015) 473:1896–902. doi: 10.1007/s11999-014-3674-y

6. Battié MC, Videman T, Parent E. Lumbar disc degeneration: epidemiology and genetic influences. *Spine (Phila Pa 1976)*. (2004) 29:2679–90. doi: 10.1097/01.brs.0000146457.83240.eb

7. Hornung AL, Barajas JN, Rudisill SS, Aboushaala K, Butler A, Park G, et al. Prediction of lumbar disc herniation resorption in symptomatic patients: a prospective, multi-imaging and clinical phenotype study. *Spine journal: Off J North Am Spine Society*. (2023) 23:247–60. doi: 10.1016/j.spinee.2022.10.003

8. Shen M, Shen Z, Yang G, Tian X, Zhao H, Wang W, et al. The differences on the fatty infiltration of paraspinal muscles between single- and multiple-level intervertebral disc degeneration in patients with lumbar disc herniation. *Orthop Surg*. (2024) 16:1999–2010. doi: 10.1111/os.14101

9. Goubert D, Oosterwijck JV, Meeus M, Danneels L. Structural changes of lumbar muscles in non-specific low back pain: A systematic review. *Pain Physician*. (2016) 19:E985–e1000. doi: 10.36076/ppj/2016.19.E985

10. Huang Y, Wang L, Zeng X, Chen J, Zhang Z, Jiang Y, et al. Association of paraspinal muscle CSA and PDFF measurements with lumbar intervertebral disk degeneration in patients with chronic low back pain. *Front Endocrinol (Lausanne)*. (2022) 13:792819. doi: 10.3389/fendo.2022.792819

11. Gu H, Hong J, Wang Z, Chen J, Yuan F, Jiang Y, et al. Association of MRI findings with paraspinal muscles fat infiltration at lower lumbar levels in patients with chronic low back pain: a multicenter prospective study. *BMC Musculoskelet Disord*. (2024) 25:549. doi: 10.1186/s12891-024-07649-x

12. Seyedhoseinpoor T, Taghipour M, Dadgoo M, Sanjari MA, Takamjani IE, Kazemnejad A, et al. Alteration of lumbar muscle morphology and composition in relation to low back pain: a systematic review and meta-analysis. *Spine journal: Off J North Am Spine Society*. (2022) 22:660–76. doi: 10.1016/j.spinee.2021.10.018

13. Ranger TA, Cicuttini FM, Jensen TS, Peiris WL, Hussain SM, Fairley J, et al. Are the size and composition of the paraspinal muscles associated with low back pain? A systematic review. *Spine journal: Off J North Am Spine Society*. (2017) 17:1729–48. doi: 10.1016/j.spinee.2017.07.002

14. Zhao X, Liang H, Hua Z, Li W, Li J, Wang L, et al. The morphological characteristics of paraspinal muscles in young patients with unilateral neurological symptoms of lumbar disc herniation. *BMC Musculoskelet Disord*. (2022) 23:994. doi: 10.1186/s12891-022-05968-5

15. Stevens S, Agten A, Timmermans A, Vandenabeele F. Unilateral changes of the multifidus in persons with lumbar disc herniation: a systematic review and meta-analysis. *Spine journal: Off J North Am Spine Society*. (2020) 20:1573–85. doi: 10.1016/j.spinee.2020.04.007

16. Kim JC, Lee SU, Jung SH, Lim JY, Kim DH, Lee SY. Natural aging course of paraspinal muscle and back extensor strength in community-dwelling older adults (sarcopenia of spine, SarcoSpine): a prospective cohort study protocol. *BMJ Open*. (2019) 9:e032443. doi: 10.1136/bmjopen-2019-032443

17. Keller A, Gunderson R, Reikerås O, Brox JI. Reliability of computed tomography measurements of paraspinal muscle cross-sectional area and density in patients with chronic low back pain. *Spine (Phila Pa 1976)*. (2003) 28:1455–60. doi: 10.1097/01.BRS.0000067094.55003.AD

18. Lee SH, Park SW, Kim YB, Nam TK, Lee YS. The fatty degeneration of lumbar paraspinal muscles on computed tomography scan according to age and disc level. *Spine journal: Off J North Am Spine Society*. (2017) 17:81–7. doi: 10.1016/j.spinee.2016.08.001

19. Stokes M, Hides J, Elliott J, Kiesel K, Hodges P. Rehabilitative ultrasound imaging of the posterior paraspinal muscles. *J Orthop Sports Phys Ther*. (2007) 37:581–95. doi: 10.2519/jospt.2007.2599

20. Hides JA, Richardson CA, Jull GA. Magnetic resonance imaging and ultrasonography of the lumbar multifidus muscle. *Comparison two different modalities. Spine (Phila Pa 1976)*. (1995) 20:54–8. doi: 10.1097/00007632-199501000-00010

21. Yuan P, Shi X, Wei X, Wang Z, Mu J, Zhang H. Development process and clinical application of collagenase chemonucleolysis in the treatment of lumbar disc herniation: a narrative review in China. *Postgrad Med J*. (2023) 99:529–34. doi: 10.1136/postgradmedj-2021-141208

22. Furlan AD, van Tulder MW, Cherkin DC, Tsukayama H, Lao L, Koes BW, et al. Acupuncture and dry-needling for low back pain. *Cochrane Database Syst Rev*. (2005) 1)::Cd001351. doi: 10.1002/14651858.CD001351.pub2

23. Lewit K. The needle effect in the relief of myofascial pain. *Pain*. (1979) 6:83–90. doi: 10.1016/0304-3959(79)90142-8

24. Berman BM, Langevin HM, Witt CM, Dubner R. Acupuncture for chronic low back pain. *N Engl J Med*. (2010) 363:454–61. doi: 10.1056/NEJMct0806114

25. Deng R, Huang Z, Li X, Pei X, Li C, Zhao J. The effectiveness and safety of acupuncture in the treatment of lumbar disc herniation: Protocol for a systematic review and meta-analysis. *Med (Baltimore)*. (2020) 99:e18930. doi: 10.1097/MD.0000000000018930

26. Zhong X, Liu J, Wang Y, Zhang L, Zhang H. Which of the acupuncture treatment regimen for lumbar disc herniation is more effective and safer: A protocol for systematic review and network meta-analysis. *Med (Baltimore)*. (2021) 100:e25199. doi: 10.1097/MD.0000000000025199

27. Minakawa Y, Miyazaki S, Waki H, Yoshida N, Iimura K, Itoh K. Trigger point acupuncture and exercise for chronic low back pain in older adult: a preliminary randomized clinical trial. *J Acupunct Meridian Stud*. (2022) 15:143–51. doi: 10.51507/j.jams.2022.15.2.143

28. Young I, Dunning J, Butts R, Bliton P, Zacharko N, Garcia J, et al. Spinal manipulation and electrical dry needling as an adjunct to conventional physical therapy in patients with lumbar spinal stenosis: a multi-center randomized clinical trial. *Spine journal: Off J North Am Spine Society*. (2024) 24:590–600. doi: 10.1016/j.spinee.2023.12.002

29. Itoh K, Katsumi Y, Kitakoji H. Trigger point acupuncture treatment of chronic low back pain in elderly patients–a blinded RCT. *Acupunct Med*. (2004) 22:170–7. doi: 10.1136/aim.22.4.170

30. Yu H, Wang D, Verville L, Southerst D, Bussières A, Gross DP, et al. Systematic review to inform a world health organization (WHO) clinical practice guideline: benefits and harms of needling therapies for chronic primary low back pain in adults. *J Occup Rehabil*. (2023) 33:661–72. doi: 10.1007/s10926-023-10125-3

31. Wei X, Liu B, He L, Yang X, Zhou J, Zhao H, et al. Acupuncture therapy for chronic low back pain: protocol of a prospective, multi-center, registry study. *BMC Musculoskelet Disord*. (2019) 20:488. doi: 10.1186/s12891-019-2894-4

32. Huang F, Xiao Z, Zhan X, Zeng P, Zhao S, Guo R, et al. Tuina combined with Adjuvant therapy for lumbar disc herniation: A network meta-analysis. *Complement Ther Clin Pract*. (2022) 49:101627. doi: 10.1016/j.ctcp.2022.101627

33. Zhang B, Xu H, Wang J, Liu B, Sun G. A narrative review of non-operative treatment, especially traditional Chinese medicine therapy, for lumbar intervertebral disc herniation. *Biosci Trends*. (2017) 11:406–17. doi: 10.5582/bst.2017.01199

34. Kreiner DS, Hwang SW, Easa JE, Resnick DK, Baisden JL, Bess S, et al. An evidence-based clinical guideline for the diagnosis and treatment of lumbar disc herniation with radiculopathy. *Spine journal: Off J North Am Spine Society*. (2014) 14:180–91. doi: 10.1016/j.spinee.2013.08.003

35. Li Z, Chen J, Yang J, Wang R, Wang W. Relationship between paraspinal muscle properties and bone mineral density based on QCT in patients with lumbar disc herniation. *BMC Musculoskelet Disord*. (2024) 25:360. doi: 10.1186/s12891-024-07484-0

36. Tian G, Wang Y, Xia J, Wen J, Li T, Li Y, et al. Correlation of multifidus degeneration with sex, age and side of herniation in patients with lumbar disc herniation. *BMC Musculoskelet Disord*. (2023) 24:652. doi: 10.1186/s12891-023-06783-2

37. Fortin M, Lazáry À, Varga PP, McCall I, Battié MC. Paraspinal muscle asymmetry and fat infiltration in patients with symptomatic disc herniation. *Eur Spine J*. (2016) 25:1452–9. doi: 10.1007/s00586-016-4503-7

38. Schulz KF, Altman DG, Moher D. CONSORT 2010 statement: updated guidelines for reporting parallel group randomised trials. *PloS Med*. (2010) 7:e1000251. doi: 10.7326/0003-4819-154-4-201102150-00016

39. Ghiasi MS, Arjmand N, Shirazi-Adl A, Farahmand F, Hashemi H, Bagheri S, et al. Cross-sectional area of human trunk paraspinal muscles before and after posterior lumbar surgery using magnetic resonance imaging. *Eur Spine J*. (2016) 25:774–82. doi: 10.1007/s00586-015-4014-y

40. Wang Z, Zhao Z, Han S, Hu X, Ye L, Li Y, et al. Advances in research on fat infiltration and lumbar intervertebral disc degeneration. *Front Endocrinol (Lausanne)*. (2022) 13:1067373. doi: 10.3389/fendo.2022.1067373

41. He H, Liu Y, Tian Q, Papasian CJ, Hu T, Deng HW. Relationship of sarcopenia and body composition with osteoporosis. *Osteoporos Int*. (2016) 27:473–82. doi: 10.1007/s00198-015-3241-8

42. Nishimoto K, Doi T, Tsutsumimoto K, Nakakubo S, Kurita S, Kiuchi Y, et al. Relationship between diabetes status and sarcopenia in community-dwelling older adults. *J Am Med Dir Assoc*. (2022) 23:1718.e7–.e12. doi: 10.1016/j.jamda.2022.07.020

43. Gao Q, Hu K, Yan C, Zhao B, Mei F, Chen F, et al. Associated factors of sarcopenia in community-dwelling older adults: A systematic review and meta-analysis. *Nutrients*. (2021) 13. doi: 10.3390/nu13124291

44. Tsekoura M, Billis E, Kastrinis A, Katsoulaki M, Fousekis K, Tsepis E, et al. The effects of exercise in patients with sarcopenia. *Adv Exp Med Biol*. (2021) 1337:281–90. doi: 10.1007/978-3-030-78771-4_31

45. Goubert D, De Pauw R, Meeus M, Willems T, Cagnie B, Schouppe S, et al. Lumbar muscle structure and function in chronic versus recurrent low back pain: a cross-sectional study. *Spine journal: Off J North Am Spine Society*. (2017) 17:1285–96. doi: 10.1016/j.spinee.2017.04.025

46. Mohammadi Y, Arjmand N, Shirazi-Adl A. Comparison of trunk muscle forces, spinal loads and stability estimated by one stability- and three EMG-assisted optimization approaches. *Med Eng Phys*. (2015) 37:792–800. doi: 10.1016/j.medengphy.2015.05.018

47. Regev GJ, Kim CW, Tomiya A, Lee YP, Ghofrani H, Garfin SR, et al. Psoas muscle architectural design, in *vivo* sarcomere length range, and passive tensile properties support its role as a lumbar spine stabilizer. *Spine (Phila Pa 1976)*. (2011) 36:E1666–74. doi: 10.1097/BRS.0b013e31821847b3

48. Kim DK, Oh CH, Lee MS, Yoon SH, Park HC, Park CO. Prevalence of lumbar disc herniation in adolescent males in seoul, korea: prevalence of adolescent LDH in seoul, korea. *Korean J Spine*. (2011) 8:261–6. doi: 10.14245/kjs.2011.8.4.261

49. Shiga Y. The essence of clinical practice guidelines for lumbar disc herniation, 2021: 1. *Epidemiol Natural Course. Spine Surg Relat Res*. (2022) 6:319–21. doi: 10.22603/ssrr.2022-0042

50. Lagerbäck T, Möller H, Gerdhem P. Lumbar disc herniation surgery in adolescents and young adults: a long-term outcome comparison. *Bone Joint J*. (2019) 101-b:1534–41. doi: 10.1302/0301-620X.101B12.BJJ-2019-0621.R1

51. Xue K, Wang X, Xiao C, Zhang N, Liu M, Fu J, et al. Clinical efficacy and safety of a modified moxibustion therapy for low back pain in lumbar disc herniation: A two-center, randomized, controlled, non-inferiority trial. *J Pain Res*. (2024) 17:1853–65. doi: 10.2147/JPR.S457724

52. Matz PG, Meagher RJ, Lamer T, Tontz WL Jr., Annaswamy TM, Cassidy RC, et al. Guideline summary review: An evidence-based clinical guideline for the diagnosis and treatment of degenerative lumbar spondylolisthesis. *Spine journal: Off J North Am Spine Society*. (2016) 16:439–48. doi: 10.1016/j.spinee.2015.11.055

53. Chen L, Sun Q, Chou R, Anderson DB, Shi B, Chen Y, et al. Low back pain-driven inpatient stays in the United States: a nationwide repeated cross-sectional analysis. *Int J Surg*. (2024) 110:1411–9. doi: 10.1097/JS9.0000000000000951

54. Liu W, Liu L, Pan Z, Gu E. Percutaneous endoscopic interlaminar discectomy with patients' participation: better postoperative rehabilitation and satisfaction. *J orthopaedic Surg Res*. (2024) 19:547. doi: 10.1186/s13018-024-05043-w

55. Ye Y, Liu B. Analgesic effects of balanced acupuncture versus body acupuncture in low-back and leg pain patients with lumbar disc herniation, as assessed by resting-state functional magnetic resonance imaging. *Neural regeneration Res*. (2012) 7:1624–9. doi: 10.3969/j.issn 1673-5374.2012.21.004

56. Tang S, Mo Z, Zhang R. Acupuncture for lumbar disc herniation: a systematic review and meta-analysis. *Acupunct Med*. (2018) 36:62–70. doi: 10.1136/acupmed-2016-011332

57. Kim E, Kim SY, Kim HS, Jeong JK, Jung SY, Han CH, et al. Effectiveness and safety of acupotomy for lumbar disc herniation: a study protocol for a randomized, assessor-blinded, controlled pilot trial. *Integr Med Res*. (2017) 6:310–6. doi: 10.1016/j.imr.2017.07.005

58. Yazici A, Yerlikaya T. The relationship between the degeneration and asymmetry of the lumbar multifidus and erector spinae muscles in patients with lumbar disc herniation with and without root compression. *J orthopaedic Surg Res*. (2022) 17:541. doi: 10.1186/s13018-022-03444-3

59. Özcan-Ekşi EE, Ekşi M, Akçal MA. Severe Lumbar Intervertebral Disc Degeneration Is Associated with Modic Changes and Fatty Infiltration in the Paraspinal Muscles at all Lumbar Levels, Except for L1-L2: A Cross-Sectional Analysis of 50 Symptomatic Women and 50 Age-Matched Symptomatic Men. *World Neurosurg*. (2019) 122:e1069–e77. doi: 10.1016/j.wneu.2018.10.229

60. Lee JC, Cha JG, Kim Y, Kim YI, Shin BJ. Quantitative analysis of back muscle degeneration in the patients with the degenerative lumbar flat back using a digital image analysis: comparison with the normal controls. *Spine (Phila Pa 1976)*. (2008) 33:318–25. doi: 10.1097/BRS.0b013e318162458f

61. Jeong JK, Kim E, Yoon KS, Jeon JH, Kim YI, Lee H, et al. Acupotomy versus Manual Acupuncture for the Treatment of Back and/or Leg Pain in Patients with Lumbar Disc Herniation: A Multicenter, Randomized, Controlled, Assessor-Blinded Clinical Trial. *J Pain Res*. (2020) 13:677–87. doi: 10.2147/JPR.S234761

62. Shen Y, Zhou Q, Zhang L, Gao L, Zhang D, Wang X, et al. Electroacupuncture for lumbar disc herniation: A protocol for systematic review and meta-analysis. *Med (Baltimore)*. (2020) 99:e19867. doi: 10.1097/MD.0000000000019867

63. Ferrando AA. Effects of inactivity and hormonal mediators on skeletal muscle during recovery from trauma. *Curr Opin Clin Nutr Metab Care*. (2000) 3:171–5. doi: 10.1097/00075197-200005000-00002

64. Zullo A, Fleckenstein J, Schleip R, Hoppe K, Wearing S, Klingler W. Structural and functional changes in the coupling of fascial tissue, skeletal muscle, and nerves during aging. *Front Physiol*. (2020) 11:592. doi: 10.3389/fphys.2020.00592

65. Zhong YX, Ding Y, Fu BS, Ma GH, Cui HP, Chen TT, et al. Effect of acupotomy on the fat infiltration degree of lumbar multifidus muscle in patients with lumbar disc herniation after percutaneous transforaminal endoscopic discectomy. *Zhongguo Zhen Jiu*. (2023) 43:153–7. doi: 10.13703/j.0255-2930.20220628-k0002

66. Lv Y, Dai DC, Jiang HN, Wang L. Effect of electroacupuncture on lumbar disc herniation with different multifidus fatty infiltration rates. *Zhongguo Zhen Jiu*. (2021) 41:593–7. doi: 10.13703/j.0255-2930.20200817-k0006

67. Lv Y, Dai DC, Jiang HN, Shen XM, Lu JC. Effect of electroacupuncture on the multifidus muscle in patients with lumbar disc herniation. *Zhongguo Zhen Jiu*. (2022) 42:1103–7. doi: 10.13703/j.0255-2930.20220215-k0006

68. Cui W, Liu CX, Zhang YC, Shen Q, Feng ZH, Wang J, et al. A novel oleanolic acid derivative HA-19 ameliorates muscle atrophy via promoting protein synthesis and preventing protein degradation. *Toxicol Appl Pharmacol*. (2019) 378:114625. doi: 10.1016/j.taap.2019.114625

69. Tokłowicz M, Żbikowska A, Janusz P, Kotwicki T, Andrusiewicz M, Kotwicka M. MicroRNA expression profile analysis in human skeletal muscle tissue: Selection of critical reference. *BioMed Pharmacother*. (2023) 162:114682. doi: 10.1016/j.biopha.2023.114682

frontiers | Frontiers in Endocrinology

TYPE Original Research
PUBLISHED 24 December 2024
DOI 10.3389/fendo.2024.1477257

OPEN ACCESS

EDITED BY
Giuseppina Storlino,
University of Foggia, Italy

REVIEWED BY
Graziana Colaianni,
University of Bari Aldo Moro, Italy
Ciro Menale,
University of Naples Federico II, Italy

*CORRESPONDENCE
Martina Rauner
Martina.rauner@ukdd.de

RECEIVED 07 August 2024
ACCEPTED 10 December 2024
PUBLISHED 24 December 2024

CITATION
Daamouch S, Diendorfer A, Hackl M, Christoffel G, Hofbauer LC and Rauner M (2024) Exploratory miRNA profiling from serum and bone tissue of mice with T1D-induced bone loss. *Front. Endocrinol.* 15:1477257. doi: 10.3389/fendo.2024.1477257

Exploratory miRNA profiling from serum and bone tissue of mice with T1D-induced bone loss

Souad Daamouch[1], Andreas Diendorfer[2], Matthias Hackl[2], Gabriele Christoffel[3], Lorenz C. Hofbauer[1] and Martina Rauner[1]*

[1]Department of Medicine III and Center for Healthy Aging, Technische Universität Dresden, Dresden, Germany, [2]TAmiRNA, Vienna, Austria, [3]Qiagen, Hilden, Germany

Type 1 diabetes (T1D) represents a significant health burden worldwide, with associated complications including bone fragility. Current clinical methods and biomarkers for assessing bone health and predicting fracture risk in T1D are limited and lack accuracy. MicroRNAs (miRNAs) have emerged as potential biomarkers for predicting T1D-induced bone loss, although comprehensive profiling studies are lacking. Previous investigations have indicated a link between dysregulated miRNA expression levels and impaired bone health in T1D. Therefore, in this study, we explored differential miRNA expression levels in serum and bone tissue of mice with T1D-induced bone loss using Next Generation Sequencing (NGS). T1D was induced using streptozotocin in male wild-type mice. Serum and bone tissues were analyzed at 14 weeks of age, following the prior characterization of bone loss in this mouse model. MiRNA profiling was conducted using two-independent NGS analyses and validated through quantitative RT-PCR. NGS profiling identified differential expression of miRNAs in serum and bone tissue of T1D mice compared to controls. The first NGS analysis revealed 24 differentially expressed miRNAs in serum and 13 in bone tissue. Especially, miR-136-3p was consistently downregulated in both serum and bone tissue. However, the second NGS analysis presented a distinct set of dysregulated miRNAs, with miR-206-3p overlapping in both tissues but exhibiting differential expression patterns. Surprisingly, miR-144-5p, miR-19a-3p, and miR-21a-5p displayed contrasting regulatory patterns between NGS and qPCR analyses. Finally, gene network analysis identified associations between dysregulated miRNAs and pathways involved in bone physiology, including TGF-beta, PI3-Akt signaling, and osteoclast differentiation in humans. In conclusion, our study offers initial insights into dysregulated miRNAs associated with T1D-induced bone loss, but also highlights the lack of consistency in the results obtained from miRNA sequencing in different cohorts. Thus, further investigation is needed to better understand the complexities of miRNA analyses before they can be established as reproducible biomarkers for predicting bone health in T1D.

KEYWORDS

miRNAs, T1D, serum, bone, NGS, RT-PCR

1 Introduction

Type 1 diabetes (T1D) is a chronic condition triggered by an autoimmune response that hinders the body's natural regulation of blood glucose levels. While this disease is frequently diagnosed in childhood, with 80% of beta cells typically already destroyed by that time (1, 2), the International Diabetes Federation reported in 2022 that 64% of individuals with T1D fall within the 20-59 age group. Thus, not only the incidence of T1D is increasing worldwide, but also the proportion of older individuals suffering from T1D. Due to the chronic nature of the disease, long-term T1D is associated with several complications that impact human health, including cardiomyopathy (3, 4), nephropathy (5, 6), and bone fragility (7, 8). Individuals with T1D have a six-fold higher risk of hip fractures compared to the general population, highlighting the need for a better understanding of the underlying pathomechanisms of bone fragility as well as the development of better prediction tools to assess patients at risk for fracture (9, 10).

Current clinical methods employed to assess bone fragility in T1D, such as bone turnover markers (BTMs), dual-energy X-ray absorptiometry (DXA), the fracture risk assessment tool (FRAX), and trabecular bone score (TBS) fall short in predicting fracture risk and present various limitations. Given the global burden of T1D and diabetic osteoporosis, there is an urgent need for affordable and innovative methods to overcome current limitations and more accurately predict fracture risk in T1D. Recent investigations have provided promising insights into the potential use of miRNAs. MiRNAs, small non-coding RNAs with a length of 19-22 nucleotides, play a crucial role as post-transcriptional gene regulators (11, 12). While limited studies have explored the role of miRNAs in bone diseases associated with T1D (13), evidence of dysregulated miRNAs, such as miR-148a-3p and miR-21-5p has been reported, showing a negative correlation with bone mineral density (BMD) in the serum of 15 patients with T1D compared to 14 matched non-diabetic subjects (14). In another study, miRNA expression patterns were assessed in 58 diabetic rats and 58 non-diabetic rats during the fracture healing process on days 5 and 11 within femurs. This study observed the dysregulation of five miRNAs (miR-140-3p, miR-140-5p, miR-181a-1-3p, miR-210-3p, and miR-222-3p), which were previously reported as dysregulated in the context of impaired fracture healing in diabetic rats (15). These findings provide evidence that specific miRNAs are dysregulated in T1D and highlight miRNAs as potential biomarkers for bone fragility in T1D. To date, only pre-defined panels of miRNAs have been studied in the context of T1D bone disease. However, untargeted approaches to assess the regulation of miRNAs in total in T1D are warranted and may be beneficial to identify novel miRNA targets or miRNA signatures that may serve as novel biomarkers to enhance fracture risk assessment in T1D.

The aim of this study was to perform an unbiased miRNA profiling approach from bone tissue and serum of mice with T1D-induced bone loss to assess local *vs.* systemic miRNA regulations using Next Generation Sequencing (NGS). A second aim was to assess the reproducibility of these findings in two independent mouse cohorts. To achieve this, we conducted two independent miRNA profiling analyses on bone and serum samples, employing two independent mouse cohorts and two different library preparation methods. Our investigations revealed first, minor overlap between miRNAs regulated in bone tissue vs. serum and second, variability in dysregulated miRNAs between both NGS profiling experiments. Thus, when evaluating miRNAs or miRNA signatures resulting from NGS experiments as potential biomarkers for disease prediction or monitoring, validation procedures are clearly needed before they can be applied as biomarkers.

2 Materials and methods

2.1 STZ-induced T1D mouse model

In order to establish the T1D mouse model, we administered streptozotocin (STZ) via intra-peritoneal injections at a dose of 45 mg/kg to 10-week-old male C57BL/6J mice. This treatment was repeated for five consecutive days. The control group received injections with citrate buffer (CB) (16). One week after the STZ or CB injections, we assessed blood glucose levels obtained from the tail vein. The onset of diabetes was defined with blood glucose levels reaching 250 mg/dl. Over the course of the study, we monitored blood glucose levels and body weight on a weekly basis, up to week 14, at which point all the mice were euthanized. To ensure uniform conditions, all mice were given standard diets and had continuous access to water. They were housed in groups of four or five per cage, maintained at room temperature, and adhered to a 12-hour light/dark cycle. Ethical approval for all procedures involving mice was obtained from the Landesdirektion Sachsen (TVV 18/2020) and the institutional animal care committee.

2.2 Glucose tolerance test

To assess the glycemic state of T1D mice, a glucose tolerance test (GTT) was carried out following an overnight fasting period. Blood glucose levels were assessed at intervals of 15, 30, 60, 90, and 180 minutes after intraperitoneal administration of a 2 g/l glucose solution, utilizing a glucometer (ACCU CHEK Aviva III; Roche Diabetes Care, Mannheim, Germany).

2.3 Bone microarchitecture analysis

We employed micro-computed tomography (microCT) to assess the bone mass and microarchitecture of the distal femur. The microCT scans were conducted ex vivo using a vivaCT 40 scanner manufactured by Scanco Medical in Brüttisellen, Switzerland. These scans were performed with an energy level of 70 kVp with a resolution of 10.5 µm isotropic voxel size (utilizing 114 mA and an integration time of 200 msec). A total of one hundred slices from the distal femur were subjected to analysis using Scanco Medical's standard protocols. This analysis was carried out to assess trabecular bone parameters, which include bone trabecular thickness (Tb.Th) and trabecular bone mineral density (Tb. BMD). Additional MicroCT parameters were assessed in our previous study (17).

2.4 MiRNA isolation, cDNA synthesis and quantitative RT-PCR

The extraction of total RNA from bone tissue was carried out using TRIzol reagent (Invitrogen, Darmstadt, Germany) in accordance with the provided manufacturer's guidelines. Subsequently, the RNA concentration was assessed using a Nanodrop ND-1000 spectrophotometer (Thermo Scientific/PEQLAB, Erlangen, Germany). Post-mortem, the bones were collected and flushed out with PBS before the RNA extraction process. For miRNA reverse transcription, 5 nanograms of total RNA were employed and reverse-transcribed using the miRCURY LNA RT Kit (#339340; Qiagen, Hilden, Germany). Following this step, the resulting cDNA samples were diluted at a 1:40 ratio. Quantitative real-time PCR was performed using miRCURY LNA SYBR Green (#339345; Qiagen, Hilden, Germany). The PCR conditions consisted of an initial denaturation at 95°C for 2 minutes, followed by denaturation at 95°C for 10 seconds, and annealing/extension at 56°C for 60 seconds, repeated for 40 cycles. To normalize the data, the miRNA expression levels were compared to those of the 5S housekeeping gene, employing the ΔΔCT method, and the results are presented as fold changes (x-fold). All procedures adhered to the manufacturer's instructions.

2.5 NGS miRNA profiling using Illumina sequencing

We performed total RNA extraction from bone tissue of T1D and control mice and subsequently employed the RealSeq-Biofluids Plasma/Serum miRNA Library kit for Illumina sequencing (RealSeq Biosciences) in accordance with the manufacturer's protocol (17). In this study, two independent NGS analyses were conducted on bone and serum samples from both T1D and non-diabetic mice. The purpose was to evaluate the reproducibility of the findings.

Prior to library preparation, we assessed RNA quality using the Agilent Bioanalyzer DNA 1000 kit and associated reagents (Agilent Technologies, Waldbronn, Germany). Only samples with a RIN over 6 were taken for further analyses. The NGS Illumina sequencing process is based on the "sequencing by synthesis" method, which aims to produce sequence reads of approximately 32-40 base pairs by simultaneously sequencing tens of millions of surface-amplified DNA fragments (18). The library preparation involves a sequence of six consecutive steps: adapter ligation, surface attachment, bridge amplification, denaturation, clustering, and single base extension.

In our study, two library preparation protocols were employed as per institutional methods. Serum and bone samples RNA underwent library preparations using RealSeq Biosciences and QIAseq miRNA Library Kit following manufacturer protocols, with 8.5 µl and 4 µl RNA input, respectively. Amplification steps comprised 18-23 cycles. Initial library quality control utilized the Agilent DNA 1000 kit to evaluate fragment distribution. Subsequently, libraries were equimolarly pooled and subjected to size-selection using the BluePippin system with a 3% agarose cassette (100-250 kb) to eliminate DNA fragments outside the desired range. A second library quality check was performed using the Agilent high sensitivity DNA kit. Finally, libraries were sequenced on an Illumina NextSeq550, following manufacturer instructions.

2.6 Statistical analysis

Data are given as mean ± SD. A two-sided, unpaired Student's t test was used in statistical analyses to compare two groups. Graphs were generated using GraphPad Prism 9.0 (GraphPad, La Jolla, CA, USA). Statistical significance was defined as a P value of less than 0.05. The analysis of RNA-Seq data was conducted using MiND, a software package for data analysis that produces comprehensive QC data, unsupervised clustering analysis, normalized miRNA count matrices, and differential expression analysis from raw NGS data (19, 20). Assessment of the overall quality of next-generation sequencing data involved both automatic and manual evaluations using fastQC v0.11.9 and multiQC v1.10.

To increase robustness of the false discovery rate (FDR) correction and eliminate low-abundance miRNAs, the independent filtering method of DESeq2 was modified for compatibility with edgeR. Volcano plots were employed to visually represent the relationship between logFC and the statistical significance of observed miRNA level changes. Consequently, miRNAs displaying significant differential expression with an FDR below 0.05 are highlighted in green.

3 Results

3.1 MiRNA profile in serum and bone tissue of T1D mice with bone loss

3.1.1 Characterization of STZ-induced T1D and bone loss in male mice

We used the well-established STZ-induced T1D mouse model and characterized its metabolic and bone phenotype at 14 weeks of age, 4 weeks after T1D induction. The results were reported elsewhere (17). Briefly, and consistent with previous studies (21, 22), we observed a significant decrease in the body weight, impaired glucose tolerance, and bone loss with low bone formation and high bone resorption in T1D compared to non-diabetic mice in both cohorts. Thus, this T1D mouse model exhibited a consistent and validated profile for further investigations. To provide additional characterization, we assessed several metabolic and bone parameters at the end of the experiment (14 weeks of age). A detailed summary of these findings is presented in our previous manuscript (17). These results highlight the significant metabolic and skeletal alterations induced by T1D, supporting the robustness of this model.

3.1.2 NGS volcano plots of serum and bone

We next performed an exploratory miRNA profiling from serum and femoral bone samples collected from T1D versus control mice. Therefore, we conducted two separate NGS

analyses, each using three samples per tissue type (serum and femur) from T1D and non-diabetic mice.

In the first NGS analysis, we identified 24 differentially expressed miRNAs in serum samples, in contrast to 13 in bone tissue. Specifically, in bone tissue, we observed 3 upregulated miRNAs (miR-144-3p, miR-144-5p and miR-451a) and 10 downregulated miRNAs (miR-133a-5p, miR-133b-3p, miR-133a-3p, miR-378d, miR-378b, miR-378a-5p, miR-181a-2-3p, miR-434-3p, miR-22-3p and miR-136-3p) (Figure 1A NGS-1 from bone). In serum samples, we found 12 upregulated and 12 downregulated miRNAs when comparing T1D and control mice (Figure 1B NGS-1 from serum).

Intriguingly, the second NGS analysis conducted in another independent cohort, presented a different set of dysregulated miRNAs. While bone tissue displayed 3 up-regulated miRNAs (miR-206-3p, miR-1a-3p and miR-196a-5p) when comparing T1D and non-diabetic mice (Figure 1C NGS-2 from bone), serum data exhibited 12 up- and 12 down-regulated miRNAs (Figure 1D NGS-2 from serum), None of the up- or down-regulated miRNAs overlapped with the results from the first NGS analysis.

3.1.3 VENN diagrams from NGS data showing overlapping miRNAs in serum and bone

Afterwards, to ascertain potential overlaps of miRNAs between serum and bone tissue using NGS data, we generated Venn diagrams based on both NGS analyses. It became evident that there were no shared miRNAs between the two NGS datasets. Interestingly, the initial NGS evaluation revealed that miR-136-3p was upregulated in serum while downregulated in bone tissue (Figure 2A). Additionally, in the second NGS analysis, a distinct miRNA, miR-206-3p, was found to overlap in both tissues but exhibited again a differential expression pattern. It was downregulated in serum but upregulated in bone tissue of T1D mice (Figure 2B).

3.2 Discrepant miRNA expression level measured between NGS and qPCR in bone tissue

The discrepancy in miRNA expression levels between serum and bone tissue underscores that tissue-based differences in miRNA transcription are not necessarily mirrored by changes in circulating miRNA levels. Given our primary interest in bone tissue, we exclusively validated miRNA candidates through further qPCR analysis using bone samples in this study. For the NGS measurements presented in panel A, only the highest-quality RNA samples (n=3 per group) were selected, based on stringent quality criteria such as a RIN between 6 and 10, as measured by the bioanalyzer. This careful selection ensured the reliability and robustness of the sequencing data by minimizing variability due to RNA integrity. Additionally, to date, no studies have directly investigated miRNA expression in bone tissue related to T1D. Thus, we proceeded with the selection of a set of miRNAs, based on our initial NGS analysis of bone tissue samples and the existing literature. The following miRNAs were chosen for additional qPCR validation: miR-144-5p, miR-19a-3p, miR-451a, miR-21a-5p, miR-133a-3p, and miR-136-3p (Figure 3). To provide an overview of their expression patterns from NGS analysis, the normalized reads per million (RPM) for these miRNAs are shown in panel A (Figure 3A). We then evaluated these miRNAs using two different approaches to validate and ensure the reproducibility of identical targets through qPCR. First, we measured miRNA levels using the same samples employed in our initial NGS analysis (Figure 3B). Secondly, we measured miRNA levels from another independent cohort of T1D mice (Figure 3C).

By using the same set of bone samples utilized in the NGS analysis, qPCR analysis confirmed a trend toward elevated levels for miR-144-5p, miR-19a-3p, and miR-451a. Similarly, miR-133a-3p displayed a declining trend, though it did not achieve statistical significance. However, miR-21a-5p exhibited contrasting regulatory patterns, while miR-136-3p, previously identified as downregulated, displayed no significant change by qPCR (Figure 3B).

Subsequent qPCR analysis using a distinct set of bone samples revealed differing outcomes concerning miRNA expression. Particularly, miR-144-5p, miR-19a-3p, and miR-21a-5p demonstrated contrasting trends in regulation. However, the downregulation patterns of miR-451a, miR-133a-3p, and miR-136-3p remained consistent with the NGS findings (Figure 3C).

3.3 Tissue-type enrichment analysis of dysregulated miRNAs

To evaluate the expression levels of these miRNA candidates under steady conditions in humans, we conducted a mapping of the top 9 highly enriched tissues for each of our six miRNAs. Additionally, we included bone tissue as our primary focus, even if it did not consistently rank among the top nine enriched tissues. These data were obtained from the miRNA Tissue Atlas database (23).

Our findings revealed that our six miRNA targets displayed differential abundance in human tissues, with the highest expression levels observed for hsa-miR-451a, hsa-miR-21a-5p, and hsa-miR-133a-3p. Interestingly, despite the dysregulation of these miRNAs observed in our NGS analysis in mouse bone tissue, they exhibited low expression in human bone. Among our three highly abundant miRNAs, we observed enriched expression in tissues such as veins, thyroid, arteries, spleen, lungs, muscles, skin, and adipocytes. Moreover, for the less abundant miRNAs, hsa-miR-144-5p was predominantly expressed in the thyroid, and hsa-miR-19a-3p in the veins. Interestingly, although generally low in expression, hsa-miR-136-3p was predominantly expressed in human bone tissue (Figure 4).

3.4 Gene network and potential signaling pathways involved in bone pathophysiology triggered by dysregulated miRNAs

To investigate the gene and pathway networks associated with these miRNA targets, we used the miRPathDB v2.0 database, which

10.3389/fendo.2024.1477257

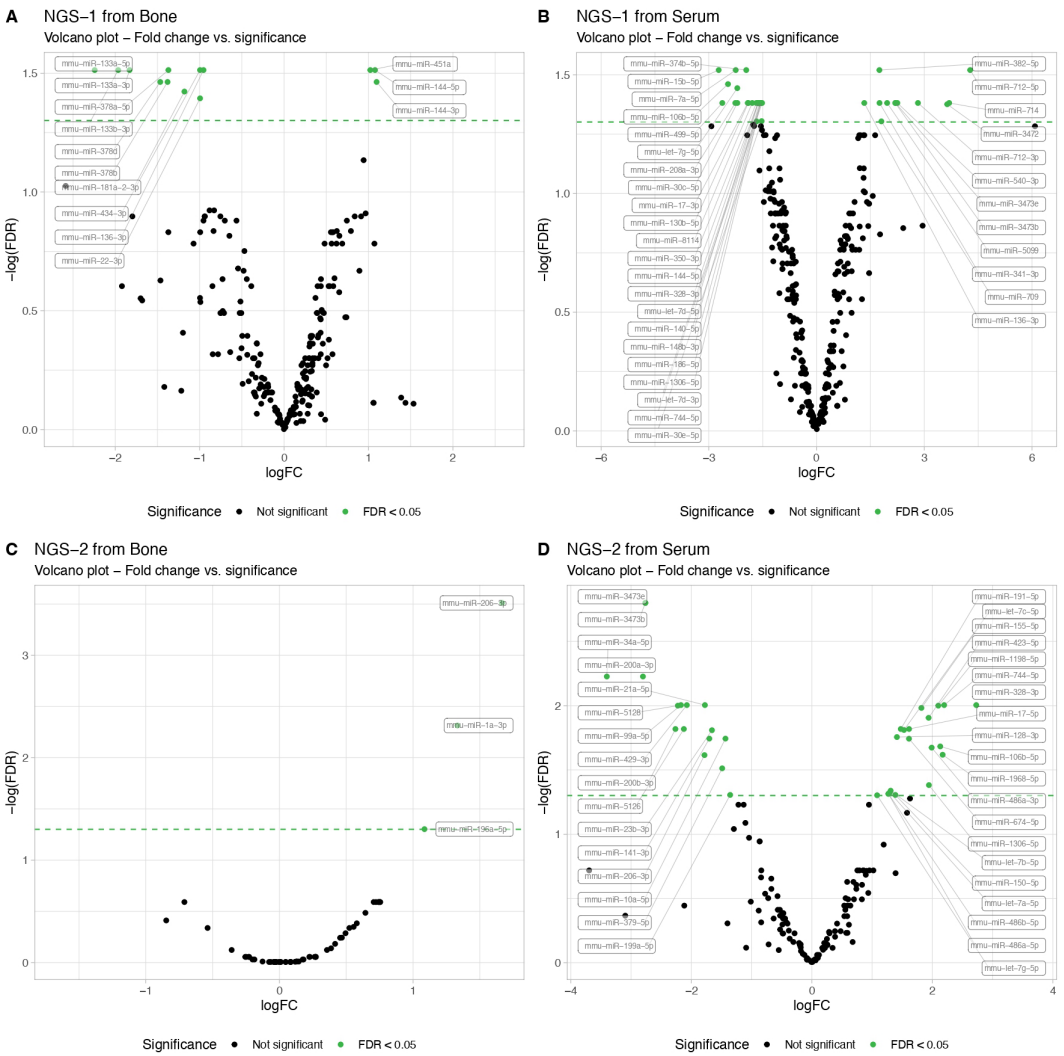

FIGURE 1
Next-Generation Sequencing (NGS) miRNA profiling in serum and femur bone from mice with T1D compared to non-diabetic mice. The NGS data results from exploratory miRNA profiling conducted on serum (N=3 per group) and femur bone (N=3 per group) of STZ-induced T1D versus non-diabetic mice, revealing differentially expressed miRNAs. Volcano plots illustrate the NGS miRNA data profiling from the first analysis, showing **(A)** serum and **(B)** bone mice samples. A second NGS analysis, performed in another independent cohort, similarly showcases **(C)** serum and **(D)** bone mice samples. MiRNA expression levels are indicated by the logarithm of fold change (logFC). All data are statistically significant with a False Discovery Rate (FDR) of less than 0.05.

is based on the KEGG database of humans. We identified significant signaling pathways that are targeted by the dysregulated miRNAs and may be involved in bone metabolism.

Our analysis revealed that the majority of our dysregulated miRNAs and their targeted genes are prominently associated with TGF-beta, PI3-Akt signaling, osteoclast differentiation, and adherens junction signaling pathways. Additionally, they exhibited connections to Wnt and TNF signaling pathways, albeit to a lesser extent compared to the previously mentioned pathways. Notably, we identified five genes targeted at least four times within these signaling pathways: SMAD4, MAPK1, MYC, TGFBR2, and AKT1 (Table 1). Taken together, this suggests the potential significance of the TGF-beta/BMP and Wnt pathways in the context of bone physiopathology in T1D (Table 1).

4 Discussion

In this study, an exploratory and unbiased miRNA profiling was conducted on serum and bone samples obtained from STZ-induced T1D male mice, with a comparative analysis against matched non-diabetic mice. The primary objective was to identify dysregulated miRNA targets potentially linked to T1D-induced bone fragility. We hypothesized that by studying bone samples in addition to serum samples from T1D mice, we could find specific miRNA candidates linked to bone fragility in T1D. To reinforce the robustness and significance of our findings, miRNA profiling was carried out on two independent mouse cohorts, which were generated through separate experiments conducted at different time points.

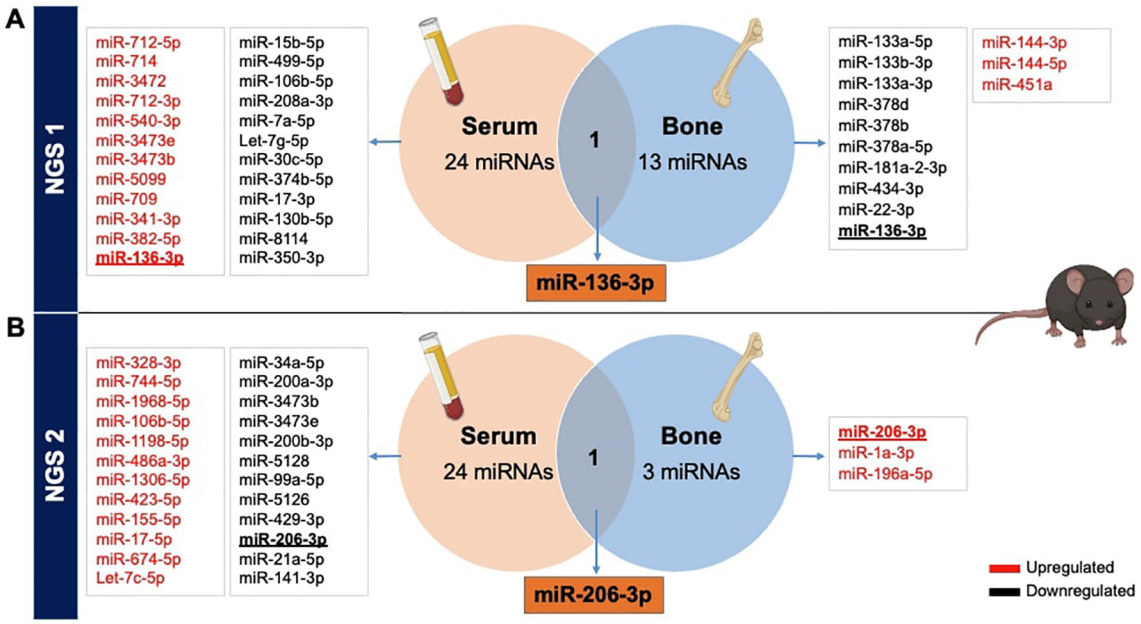

FIGURE 2
Overlapping miRNAs from NGS in serum and bone tissues of STZ-induced T1D versus non-diabetic mice. Identification of differentially expressed miRNAs obtained from serum and femoral bones, from 2 independent NGS exploratory miRNA profiling, reported in VENN diagrams. **(A)** The primary NGS detected miR-136-3p as a commonly dysregulated miRNA, while **(B)** the second NGS identified miR-206-3p between both tissues of T1DM versus non-diabetic mice.

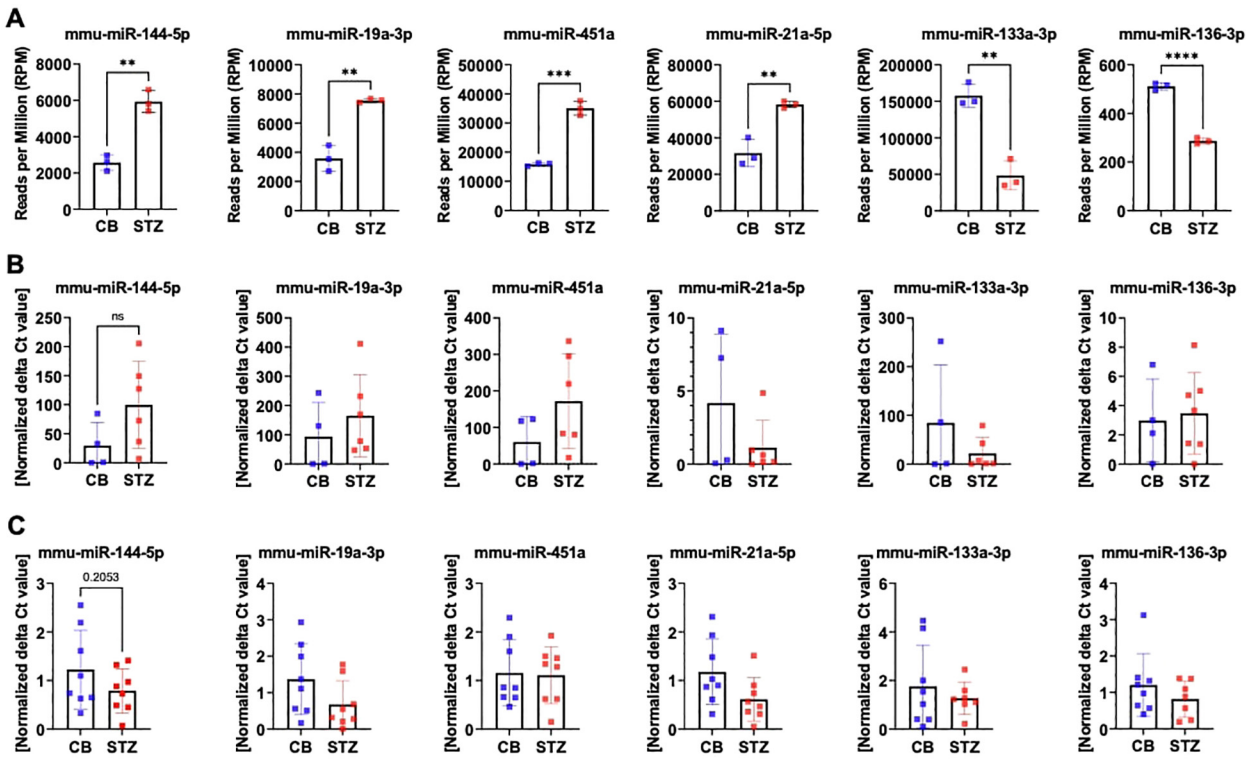

FIGURE 3
MiRNA expression level assessed by RT-PCR in mouse bone tissues. Quantification of selected miRNA targets from bone tissue of 14-week-old T1D versus non-diabetic mice was performed using NGS and RT-PCR based on the 1st NGS analysis. Panel **(A)** showcases NGS data depicting miRNA expression levels in reads per million (RPM). Panel **(B)** indicates miRNA expression levels assessed in the identical bone samples employed for NGS, while panel **(C)** illustrates miRNA expression levels assessed in bone samples from a separate cohort by RT-PCR. Data are indicated as mean ± SD (N=3-8). A Student's t-test was used for statistical analysis, and significant results were denoted as follows: **p<0.01, ***p<0.001.

10.3389/fendo.2024.1477257

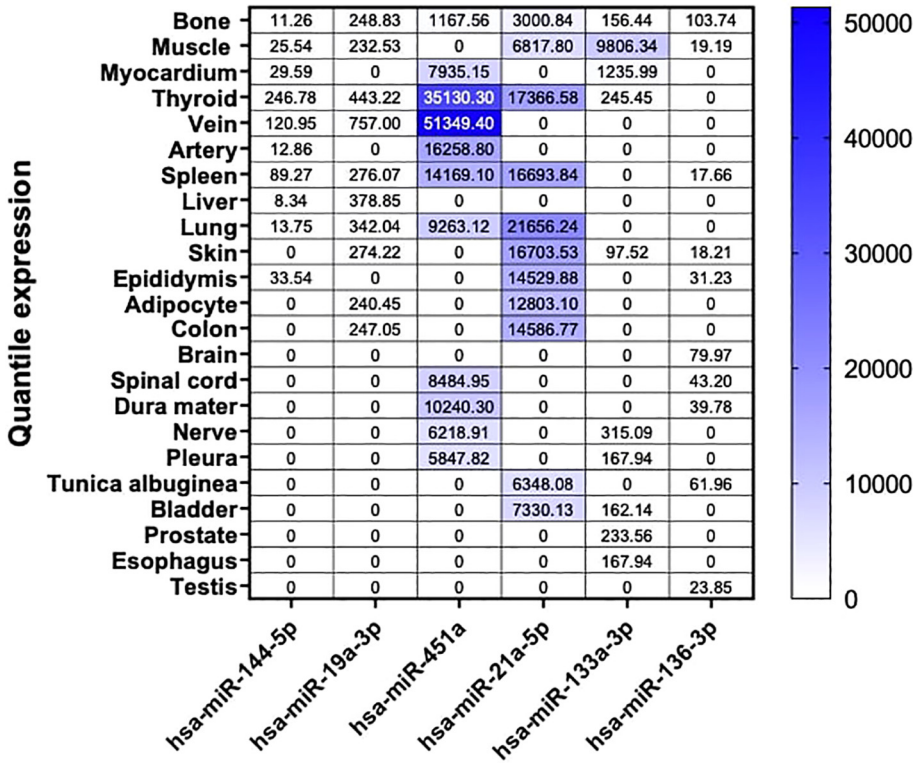

FIGURE 4
Tissue-specific miRNA enrichment analysis in Human. Custom heatmap representing an overview of bone and the top 9 highly enriched tissue from our 6 selected miRNA candidates in Human. Bone tissue is presented in this heatmap as our tissue of interest. These results are expressed in normalized quantile for each miRNA respectively. These data are extracted from the miRNA Tissue Atlas database.

We employed the STZ-induced T1D mouse model, as these mice effectively mimic T1D conditions, displaying notable decreases in body weight, elevated blood glucose levels, and impaired bone mass (17). Thus, we considered this model a well-validated platform for further exploratory miRNA profiling. Studies have previously highlighted the potential of miRNAs as biomarkers for bone fragility (24–26). Importantly, their accessibility in biofluids prevents from invasive biopsy procedures to assess disease progression. Previous research has investigated on the regulation of predefined and specific miRNAs in the circulation and sometimes even in bone biopsies of individuals with diabetic bone disease (14, 27). Nevertheless, no studies have yet conducted unbiased exploratory miRNA profiling to discover novel miRNAs signatures specific to bone tissues.

Our initial miRNA profiling revealed several miRNAs with differential regulation when comparing T1D to non-diabetic mice. This discovery aligns with prior research, contributing to the growing evidence on miRNA dysregulation in T1D (24, 28, 29). The majority of significantly dysregulated miRNAs were identified in serum samples (12 upregulated, 12 downregulated), while fewer were dysregulated in bone tissue. This may be explained by a more restricted portfolio of miRNAs in bone tissue, while in the serum, many tissues contribute to the altered miRNA profile. Across both NGS analyses, only three miRNAs were consistently upregulated in the serum. Setting aside the divergence observed in the two NGS experiments, miR-136-3p emerged as a shared miRNA target in both bone and serum during our initial NGS analysis. This miRNA exhibited downregulation in both tissues of T1D mice and suggests a potentially noteworthy dysregulation within the context of T1D in this particular mouse cohort. On the other hand, our second analysis using NGS uncovered a distinct miRNA intersection with miR-206-3p. Notably, miR-206-3p demonstrated an upregulation within the bone but exhibited downregulation at the systemic level. This finding implies the likelihood of a tissue-specific regulation of miR-206-3p, particularly concerning bone-related processes. Despite its well-documented abundance in muscle and its classification as a myomiR (30), findings from the miRPath miRNA database suggest the involvement of this miRNA in pathways related to bone, such as the Wnt signaling and calcium signaling pathways in murine models. Thus, these pieces of evidence indicate a potential influence of miR-206-3p on processes like bone remodeling and mineralization, both crucial for maintaining bone strength.

Interestingly, distinctive miRNA signatures were noted between our two NGS experiments, despite employing the same T1D mouse model in both independent cohorts. To validate the miRNAs identified in the initial NGS profiling, qPCR was conducted on distinct sets of bone samples. Nevertheless, confirmation of the expression levels for all miRNAs proved challenging with no discernible trend aligning with the NGS findings. Even though we can acknowledge the different miRNA library preparations used that may have contributed to differential outcomes, the lack of

10.3389/fendo.2024.1477257

TABLE 1 Gene network related to miRNA targets in Human.

Pathways	miRNA	Hits	P-val.	Targets
TGF-beta signaling	miR-144-5p	3	0.005	ID4, ROCK1, **SMAD4**
	miR-19a-3p	10	0.005	BAMBI, BMPR2, **MAPK1**, **MYC, SMAD4**, SMAD5, **TGFBR2**, THBS1, TNF, ZFYVE9
	miR-451a	2	0.013	**MAPK1**, **MYC**
	miR-21a-5p	9	0.015	BMPR2, GDF5, **MYC**, SMAD7, SP1, TGFB1, TGFB2, **TGFBR2**, ZFYVE16
p53 signaling	miR-144-5p	3	0.005	CCNE1, CCNE2, MDM4
	miR-19a-3p	11	6.13e-4	CCND1, CCND2, CHEK1, CHEK2, FAS, PTEN, SESN3, THBS1, TNFRSF10B, TP53, ZMAT3
	miR-21a-5p	10	0.002	APAF1, CASP8, CCNG1, CDK6, FAS, MDM4, PTEN, SERPINB5, SESN1, TNFRSF10B
	miR-133a-3p	5	0.002	CASP9, CDKN1A, IGF1, SESN2, SESN3
PI3K-Akt signaling	miR-144-5p	4	0.015	CCNE1, CCNE2, ITGA3, MET
	miR-451a	8	2.89e-6	**AKT1**, BCL2, IKBKB, IL6, IL6R, **MAPK1**, **MYC**, TSC1
	miR-21a-5p	23	0.009	AKT2, ATF2, BCL2, BRCA1, CDK6, COL4A1, COL5A2, EGFR, FASLG, FGF12, FOXO3, GNB4, IGF1R, ITGB8, **MYC**, NFKB1, PDGFD, PIK3R1, PTEN, PTK2, SGK3, TLR4, VEGFA
	miR-133a-3p	11	9.76e-4	ANGPT4, BCL2L1, CASP9, CDKN1A, COL1A1, EGFR, IGF1, IGF1R, MCL1, NGFR, THBS2
Wnt signaling	miR-144-5p	2	0.028	ROCK2, **SMAD4**
	miR-19a-3p	12	0.020	BAMBI, CCND1, CCND2, CSNK2A1, FZD6, **MYC**, PRICKLE2, PRKACB, **SMAD4**, TP53, WNT10A, WNT7B
Osteoclast differentiation	miR-19a-3p	11	0.020	**AKT1**, MAP3K14, **MAPK1**, MAPK14, PIK3CA, PIK3R3, SOCS1, SOCS3, **TGFBR2**, TNF, TNFRSF11A
	miR-451a	3	0.003	**AKT1**, IKBKB, **MAPK1**
Regulation of actin cytoskeleton	miR-144-5p	3	0.023	ITGA3, ROCK1, ROCK2
Calcium signaling	miR-133a-3p	5	0.031	CACNA1C, EGFR, ERBB2, ITPKB, PDE1A
TNF signaling	miR-451a	5	1.80e-5	**AKT1**, IKBKB, IL6, **MAPK1**, MMP9
	miR-21a-5p	15	1.56e-4	AKT2, ATF2, CASP8, CCL20, CEBPB, CXCL10, DNM1L, FAS, ICAM1, IL1B, JAG1, MAP2K3, MMP9, NFKB1, PIK3R1
Adherens junction	miR-144-5p	2	0.016	MET, **SMAD4**
	miR-19a-3p	7	0.039	ACTB, CSNK2A1, **MAPK1**, PTPRB, **SMAD4**, **TGFBR2**, WASL

Identification of significant enriched signaling pathway potentially linked to bone metabolism, using KEGG database based on experimental evidence for the 5 following miRNAs: hsa-miR-144-5p, hsa-miR-19a-3p, hsa-miR-451a, hsa-miR-21a-5p. Genes reported in bold indicate their presence among signaling pathways at least four times. Predicted targets of hsa-miR-136-3p are nor presented here. These data are extracted from miRPathDB v2.0 database.

reproducible results between the two NGS experiments and the qPCR validation in general is concerning as it shows that even small differences in experimental setups can significantly affect the outcome. This would imply that despite miRNAs being known as stable tools, a standardization in miRNA procedures including collection, storage, isolation, measurements etc. is necessary to identify true signatures that could be used as biomarkers (31). Another factor that may complicate the use of miRNA signatures as

biomarkers is their often-minor regulation, suggesting that a substantial number of replicates may be essential to replicate findings. Overall, these data argue for the necessity to better replicate miRNA findings, especially those resulting from NGS analyses.

Finally, by examining the expression patterns of dysregulated miRNAs across various human tissues using data from the miRNA Tissue Atlas database, we found intriguing insights. Despite their dysregulation in mouse bone tissue, miRNAs such as hsa-miR-451a, hsa-miR-21a-5p, and hsa-miR-133a-3p exhibited high expression levels across multiple human tissues, suggesting potential roles beyond bone physiology. Conversely, hsa-miR-136-3p, while generally low in expression across tissues, displayed predominant expression in human bone tissue, suggesting its specific relevance to bone health. Furthermore, our gene network analysis using the miRPathDB v2.0 database revealed significant associations between dysregulated miRNAs and key signaling pathways implicated in bone metabolism, including TGF-beta, PI3-Akt signaling, osteoclast differentiation, and adherens junction signaling pathways. Especially, genes targeted by dysregulated miRNAs, such as SMAD4, MAPK1, MYC, TGFBR2, and AKT1, were identified multiple times within these pathways, highlighting their potential importance in the pathophysiology of bone loss in T1D. For instance, hsa-miR-21a-5p is extensively implicated in the TGF-beta and PI3-Akt signaling pathways, targeting critical genes such as BMPR2, TGFBR2 and AKT2, which regulate osteoblast activity, matrix production, and cell survival. Similarly, hsa-miR-133a-3p, linked to the PI3K-Akt and calcium signaling pathways, targets IGF1 and CACNA1C, emphasizing its role in modulating osteoclast differentiation and bone resorption. On the other hand, hsa-miR-451a, a key player in the PI3K-Akt and TNF signaling pathways, influences genes such as MAPK1, MYC and AKT1, underscoring its involvement in inflammation and cell proliferation within the bone microenvironment. Notably, hsa-miR-19a-3p impacts multiple pathways, including TGF-beta and Wnt signaling, targeting genes such as SMAD4 and MYC, which are pivotal for bone remodeling and repair. Lastly, hsa-miR-144-5p, through its regulation of SMAD4 and ROCK1 in the adherens junction and regulation of actin cytoskeleton pathways, may influence cytoskeletal dynamics and cell adhesion in bone tissue.

While this study provides valuable insights into miRNA regulation in T1D, it does have certain limitations. Firstly, the restriction to male mice restricts the generalizability of the results to both sexes. Secondly, while the characterization of STZ-induced T1D demonstrates a robust phenotype characterized by hyperglycemia and significant bone loss compared to non-diabetic mice, it is important to acknowledge that the utilization of only three samples per group for each NGS analysis may have been insufficient to identify genuine miRNA targets associated with bone loss in T1D. Next to the costs, the challenge of obtaining adequate bone RNA quality in our mouse experiments for NGS is why a limited number of bone samples was used. Thirdly, our study employed two distinct library preparation methods for our two NGS analyses, which may have influenced miRNA expressions and could therefore account for the discrepant results observed between NGS sequencings. These discrepancies in miRNA expression align with previous investigations evaluating miRNA expressions using four different library preparation protocols (19), as well as variations in mice, albeit less pronounced than in human samples where multiple factors such as lifestyle and family history can contribute to genetic differences. Although the use of two different library preparation methods in this study did not result in the same miRNA profile, it does underscore the inconsistent findings observed among different research institutes worldwide, given the lack of standardized guidelines for identifying miRNA targets associated with T1D-induced bone loss, or any other diseases (32).

Despite these limitations, this study possesses several strengths. We utilized a well-established mouse model of T1D, providing a reliable basis for exploratory research in miRNA profiling in T1D-induced bone loss. Our study marks the first to employ an unbiased approach to miRNA profiling in serum and bone samples from a T1D mouse model. The rationale behind conducting exploratory miRNA profiling in both serum and bone was to determine if and how well the systemic and local expression of miRNAs overlap. Finally, the experiment was conducted twice for NGS profiling in serum and bone mouse samples, providing insights into the reproducibility and sensitivity of miRNA expression.

In conclusion, our investigation presents novel findings regarding the identification of miRNA signatures in the serum and bone tissue of mice with T1D-induced bone loss employing an unbiased approach through NGS. Our study demonstrates a minor overlap in miRNA signatures between serum and bone tissues. Importantly, the utilization of independent cohorts and distinct library preparation protocols revealed varying miRNA dysregulation patterns linked to T1D-related bone disease. Hence, future research should include multiple cohorts to consistently identify and validate dysregulated miRNAs associated with T1D-induced bone disease.

Data availability statement

The datasets presented in this study can be found in online repositories. The names of the repository/repositories and accession number(s) can be found in the article/supplementary material.

Ethics statement

The animal study was approved by Technische Universität Dresden. The study was conducted in accordance with the local legislation and institutional requirements.

Author contributions

SD: Conceptualization, Data curation, Formal analysis, Investigation, Methodology, Validation, Visualization, Writing – original draft, Writing – review & editing. AD: Data curation, Formal analysis, Investigation, Methodology, Writing – review & editing. MH: Conceptualization, Funding acquisition, Investigation,

Methodology, Resources, Supervision, Writing – review & editing. GC: Formal analysis, Investigation, Methodology, Resources, Writing – review & editing. LH: Conceptualization, Funding acquisition, Project administration, Resources, Supervision, Writing – review & editing. MR: Conceptualization, Funding acquisition, Project administration, Resources, Supervision, Writing – original draft, Writing – review & editing.

Funding

The author(s) declare financial support was received for the research, authorship, and/or publication of this article. This work was supported by FIDELIO, a MSCA Innovative Training Network and receives funding from the European Union's Horizon 2020 program under Grant Agreement No. 860898, and by the Elsbeth Bonhoff foundation.

Acknowledgments

This study received financial support from the MARIE SKLODOWSKA-CURIE grant agreement no. 860898 ("FIDELIO"), which is part of the European Union's Horizon 2020 research and innovation program. Also, LH received funding from the Elsbeth Bonhoff foundation.

Conflict of interest

AD and MH are employed by TAmiRNA GmbH. MH is also a shareholder of TAmiRNA GmbH. GC is employed by Qiagen.

The remaining authors declare that the research was conducted in the absence of any commercial or financial relationships that could be construed as a potential conflict of interest.

Publisher's note

References

1. Thomas NJ, Jones SE, Weedon MN, Shields BM, Oram RA, Hattersley AT. Frequency and phenotype of type 1 diabetes in the first six decades of life: a cross-sectional, genetically stratified survival analysis from UK Biobank. *Lancet Diabetes Endocrinol.* (2018) 6:122–9. doi: 10.1016/S2213-8587(17)30362-5

2. Sun H, Saeedi P, Karuranga S, Pinkepank M, Ogurtsova K, Duncan BB, et al. IDF Diabetes Atlas: Global, regional and country-level diabetes prevalence estimates for 2021 and projections for 2045. *Diabetes Res Clin Pract.* (2022) 183:109119. doi: 10.1016/j.diabres.2021.109119

3. Katsarou A, Gudbjörnsdottir S, Rawshani A, Dabelea D, Bonifacio E, Anderson BJ, et al. Type 1 diabetes mellitus. *Nat Rev Dis Primers.* (2017) 3:17016. doi: 10.1038/nrdp.2017.16

4. Miki T, Yuda S, Kouzu H, Miura T. Diabetic cardiomyopathy: pathophysiology and clinical features. *Heart Fail Rev.* (2013) 18:149–66. doi: 10.1007/s10741-012-9313-3

5. Cameron JS. The discovery of diabetic nephropathy: from small print to centre stage. *J Nephrol.* (2006) 19 Suppl 1:S75–87.

6. Reynolds L, Luo Z, Singh K. Diabetic complications and prospective immunotherapy. *Front Immunol.* (2023) 14:1219598. doi: 10.3389/fimmu.2023.1219598

7. Sellmeyer DE, Civitelli R, Hofbauer LC, Khosla S, Lecka-Czernik B, Schwartz AV. Skeletal metabolism, fracture risk, and fracture outcomes in type 1 and type 2 diabetes. *Diabetes.* (2016) 65:1757–66. doi: 10.2337/db16-0063

8. Vestergaard P. Discrepancies in bone mineral density and fracture risk in patients with type 1 and type 2 diabetes - A meta-analysis. *Osteoporosis Int.* (2007) 18:427–44. doi: 10.1007/s00198-006-0253-4

9. Janghorbani M, Feskanich D, Willett WC, Hu F. Prospective study of diabetes and risk of hip fracture: the Nurses' Health Study. *Diabetes Care.* (2006) 29:1573–8. doi: 10.2337/dc06-0440

10. Janghorbani M, Van Dam RM, Willett WC, Hu FB. Systematic review of type 1 and type 2 diabetes mellitus and risk of fracture. *Am J Epidemiol.* (2007) 166:495–505. doi: 10.1093/aje/kwm106

11. He L, Hannon GJ. MicroRNAs: small RNAs with a big role in gene regulation. *Nat Rev Genet.* (2004) 5:522–31. doi: 10.1038/nrg1379

12. Vishnoi A, Rani S. MiRNA biogenesis and regulation of diseases: an overview. *Methods Mol Biol.* (2017) 1509:1–10. doi: 10.1007/978-1-4939-6524-3_1

13. Swolin-Eide D, Forsander G, Pundziute Lyckå A, Novak D, Grillari J, Diendorfer AB, et al. Circulating microRNAs in young individuals with long-duration type 1 diabetes in comparison with healthy controls. *Sci Rep.* (2023) 13:11634. doi: 10.1038/s41598-023-38615-7

14. Grieco GE, Cataldo D, Ceccarelli E, Nigi L, Catalano G, Brusco N, et al. Serum Levels of miR-148a and miR-21-5p Are Increased in Type 1 Diabetic Patients and Correlated with Markers of Bone Strength and Metabolism. *Noncoding RNA.* (2018) 4 (4):37. doi: 10.3390/ncrna4040037

15. Takahara S, Lee SY, Iwakura T, Oe K, Fukui T, Okumachi E, et al. Altered expression of microRNA during fracture healing in diabetic rats. *Bone Joint Res.* (2018) 7:139–47. doi: 10.1302/2046-3758.72.BJR-2017-0082.R1

16. Furman BL. Streptozotocin-induced diabetic models in mice and rats. *Curr Protoc Pharmacol.* (2015) 70:5.47.1–5.47.20. doi: 10.1002/0471141755.2015.70.issue-1

17. Daamouch S, Blüher M, Vázquez DC, Hackl M, Hofbauer LC, Rauner M. MiR-144-5p and miR-21-5p do not drive bone disease in a mouse model of type 1 diabetes mellitus. *JBMR Plus.* (2024) 8(5):ziae036. doi: 10.1093/jbmrpl/ziae036

18. Mardis ER. The impact of next-generation sequencing technology on genetics. *Trends Genet.* (2008) 24:133–41. doi: 10.1016/j.tig.2007.12.007

19. Khamina K, Diendorfer AB, Skalicky S, Weigl M, Pultar M, Krammer TL, et al. A microRNA next-generation-sequencing discovery assay (miND) for genome-scale analysis and absolute quantitation of circulating microRNA biomarkers. *Int J Mol Sci.* (2022) 23(3):1226. doi: 10.3390/ijms23031226

20. Diendorfer A, Khamina K, Pultar M, Hackl M. miND (miRNA NGS Discovery pipeline): a small RNA-seq analysis pipeline and report generator for microRNA biomarker discovery studies. *F1000Res.* (2022) 11:233. doi: 10.12688/f1000research

21. Coe LM, Zhang J, McCabe LR. Both spontaneous Ins2(+/-) and streptozotocin-induced type I diabetes cause bone loss in young mice. *J Cell Physiol.* (2013) 228:689–95. doi: 10.1002/jcp.v228.4

22. Furman BL. Streptozotocin-induced diabetic models in mice and rats. *Curr Protoc.* (2021) 1:e78. doi: 10.1002/cpz1.v1.4

23. Ludwig N, Leidinger P, Becker K, Backes C, Fehlmann T, Pallasch C, et al. Distribution of miRNA expression across human tissues. *Nucleic Acids Res.* (2016) 44:3865–77. doi: 10.1093/nar/gkw116

24. Daamouch S, Emini L, Rauner M, Hofbauer LC. MicroRNA and diabetic bone disease. *Curr Osteoporos Rep.* (2022) 20(3):194-201. doi: 10.1007/s11914-022-00731-0

25. Ladang A, Beaudart C, Locquet M, Reginster JY, Bruyère O, Cavalier E. Evaluation of a panel of microRNAs that predicts fragility fracture risk: A pilot study. *Calcif Tissue Int.* (2020) 106:239–47. doi: 10.1007/s00223-019-00628-8

26. Hackl M, Heilmeier U, Weilner S, Grillari J. Circulating microRNAs as novel biomarkers for bone diseases - Complex signatures for multifactorial diseases? *Mol Cell Endocrinol.* (2016) :432:83–95. doi: 10.1016/j.mce.2015.10.015

27. Wang R, Zhang Y, Jin F, Li G, Sun Y, Wang X. High-glucose-induced miR-214-3p inhibits BMSCs osteogenic differentiation in type 1 diabetes mellitus. *Cell Death Discovery*. (2019) 5:143. doi: 10.1038/s41420-019-0223-1

28. Miao C, Chang J, Zhang G, Fang Y. MicroRNAs in type 1 diabetes: New research progress and potential directions. *Biochem Cell Biol*. (2018) 96:498–506. doi: 10.1139/bcb-2018-0027

29. Margaritis K, Margioula-Siarkou G, Giza S, Kotanidou EP, Tsinopoulou VR, Christoforidis A, et al. Micro-RNA implications in type-1 diabetes mellitus: A review of literature. *Int J Mol Sci*. (2021) 22(22):1265. doi: 10.3390/ijms222212165

30. Lu Z, Wang D, Wang X, Zou J, Sun J, Bi Z. MiR-206 regulates the progression of osteoporosis via targeting HDAC4. *Eur J Med Res*. (2021) 26:8. doi: 10.1186/s40001-021-00480-3

31. Chorley BN, Atabakhsh E, Doran G, Gautier JC, Ellinger-Ziegelbauer H, Jackson D, et al. Methodological considerations for measuring biofluid-based microRNA biomarkers. *Crit Rev Toxicol*. (2021) 51:264–82. doi: 10.1080/10408444.2021.1907530

32. Assmann TS, Recamonde-Mendoza M, De Souza BM, Crispim D. MicroRNA expression profiles and type 1 diabetes mellitus: systematic review and bioinformatic analysis. *Endocr Connect*. (2017) 6:773–90. doi: 10.1530/EC-17-0248

Frontiers in Endocrinology

Explores the endocrine system to find new therapies for key health issues

The second most-cited endocrinology and metabolism journal, which advances our understanding of the endocrine system. It uncovers new therapies for prevalent health issues such as obesity, diabetes, reproduction, and aging.

Discover the latest Research Topics

See more →

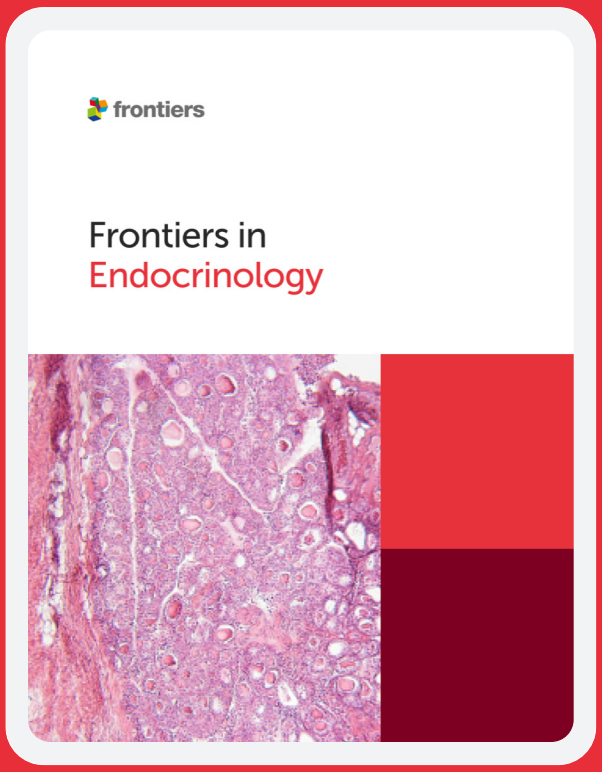

Frontiers

Avenue du Tribunal-Fédéral 34
1005 Lausanne, Switzerland
frontiersin.org

Contact us

+41 (0)21 510 17 00
frontiersin.org/about/contact